

# Sheffield Hallam University

*Development and application of capillary electrophoresis/mass spectrometry.*

PALMER, Martin.

Available from the Sheffield Hallam University Research Archive (SHURA) at:

<http://shura.shu.ac.uk/20181/>

## A Sheffield Hallam University thesis

This thesis is protected by copyright which belongs to the author.

The content must not be changed in any way or sold commercially in any format or medium without the formal permission of the author.

When referring to this work, full bibliographic details including the author, title, awarding institution and date of the thesis must be given.

Please visit <http://shura.shu.ac.uk/20181/> and <http://shura.shu.ac.uk/information.html> for further details about copyright and re-use permissions.

LEARNING CENTRE  
CITY CAMPUS, POND STREET,  
EPPING, SI 1WB

sketchmark 19689

101 651 864 1



**REFERENCE**

**Fines are charged at 50p per hour**

26 FEB 2002

9.00

- 4 JUL 2005

ProQuest Number: 10700826

All rights reserved

INFORMATION TO ALL USERS

The quality of this reproduction is dependent upon the quality of the copy submitted.

In the unlikely event that the author did not send a complete manuscript and there are missing pages, these will be noted. Also, if material had to be removed, a note will indicate the deletion.



ProQuest 10700826

Published by ProQuest LLC (2017). Copyright of the Dissertation is held by the Author.

All rights reserved.

This work is protected against unauthorized copying under Title 17, United States Code  
Microform Edition © ProQuest LLC.

ProQuest LLC.  
789 East Eisenhower Parkway  
P.O. Box 1346  
Ann Arbor, MI 48106 – 1346

**Development and Application of Capillary  
Electrophoresis / Mass Spectrometry**

*Martin Palmer*

A thesis submitted in partial fulfilment of the requirements of  
Sheffield Hallam University  
For the degree of Doctor of Philosophy

July 2000

## *Declaration*

A thesis submitted to Sheffield Hallam University for the degree of Doctor of Philosophy in the School of Science and Mathematics.

No portion of the work referred to in the thesis has been submitted in support of an application for another degree or qualification of this or any other university or other institute of learning.

Signed .....

Date 13/7/00 .....

## *Abstract*

Capillary electrophoresis is a generic term used to describe separation techniques employing high voltages. In its simplest form, capillary zone electrophoresis (CZE), separations are based on the differential migration of charged analytes under the influence of a high electric field. CZE offers several advantages over other separation techniques, such as high performance liquid chromatography (HPLC). These include higher separation efficiency, enhanced resolution and reduced analysis time. In addition, small injection volumes (nanolitres *cf.* microlitres for HPLC) and low solvent consumption make CZE an attractive alternative to HPLC. Unfortunately, CZE is not amenable to neutral species, therefore alternative electroseparation methods are employed for neutrals, *e.g.* capillary electrochromatography (CEC) and micellar electrokinetic chromatography (MEKC), so therefore CZE can be treated as a complementary technique to HPLC.

Mass spectrometry (MS) has previously been demonstrated to be a sensitive, selective and near-universal detector. Analytes must be ionised in order to be detected; thus, CZE (which also requires ions) seems an ideal separation technique for combining with MS.

CZE/MS interfacing would seem problematic; the linear flow velocity through the capillary is significantly less than that required by appropriate MS ionisation sources (*e.g.* continuous-flow fast atom bombardment and electrospray). In addition, it is necessary to provide a ground for the separation voltage within the interface. However, interfacing of CZE and MS was first reported in 1987. Since then three distinct interface designs have been developed, co-axial sheath flow, liquid junction and the use of a low flow electrospray (nanospray) interface. Co-axial sheath flow and liquid junction methods serve to increase the overall flow rate of CZE to a suitable level for MS, whereas nanospray is a low flow ionisation technique that accepts similar flow rates to those provided by CZE.

The work presented in this thesis details the off-line development of a CZE separation of a pharmaceutical product (cimetidine) and related impurities. The separation was then transferred to mass spectral detection on a commercial triple quadrupole MS instrument employing home-built co-axial sheath flow (electrospray) and nanospray interfaces and the data obtained evaluated. The separation was subsequently transferred to an orthogonal acceleration time-of-flight MS (oa-ToF) for the exact mass determination of the narrow electrophoretic peaks.

The feasibility of hydrogen / deuterium exchange via the sheath liquid for CZE/MS has been investigated using model pharmaceutical compounds and preliminary work is presented.

An application of CZE/MS for the separation of nicotine and ten of its metabolites has been developed. This method could be further developed into a quantitative assay for nicotine metabolites in biological fluids and suggestions for future work in this area are made.

## *Acknowledgements*

I would like to thank my supervisor, Dr Lee Tetler, for his continuous help and support both during and after the period of this research. My thanks also go to my colleagues in the Division of Chemistry, especially Dr Malcolm Clench and Mrs Joan Hague, both for their advice and making my time in the department more enjoyable. In addition, thanks also to all the friends I made during my time at Sheffield, especially Arnie, Dave C, D and E, Donna, Jackie, Matt, Jo, John, Steve, Chris.

I would also like to express my gratitude to Dr Christine Eckers of SmithKline Beecham Pharmaceuticals for supplying samples and guidance.

Thanks also to Dr Gwyn Lord of the Medical Research Centre for useful discussions on interfacing capillary zone electrophoresis and mass spectrometry.

My gratitude is also extended to Mike Curtis of Separation Solutions for the loan of the PrinCE 560 CE System, without which, this work would have taken a great deal longer to complete.

My thanks also go to Micromass, especially Drs Mark McDowall and David Little for the use of instrumentation, helpful advice and providing funding to present at the 15<sup>th</sup> Montreux LC/MS Symposium, 11/98, Montreux, Switzerland.

In addition, my thanks to Dr Bob Smith and Kerry Chambers of Biomedical Research Centre, SHU. For supplying the nicotine metabolites and useful discussions in the preparation of this thesis and the presentation given at 24<sup>th</sup> BMSS meeting, 9/99, Reading.

Dedicated to Claire and my parents.  
For all their love and support throughout this work.

<b>Section 1.1 Capillary Electrophoresis .....</b>	<b>2</b>
1.1.1 INTRODUCTION .....	3
1.1.2 THEORY OF MIGRATION AND ELECTROOSMOTIC FLOW .....	4
1.1.2.1 <i>Experimental Factors Controlling EOF</i> .....	7
1.1.3 DISPERSION.....	8
1.1.3.1 <i>Minor Dispersive Sources</i> .....	10
a) Joule Heating and Temperature Gradients .....	10
b) Injection Plug Length.....	12
c) Analyte-wall Interaction .....	12
d) Electrodispersion .....	13
1.1.4 RESOLUTION .....	13
1.1.5 INSTRUMENTATION .....	14
1.1.5.1 <i>Inlet / Outlet Vials</i> .....	15
1.1.5.2 <i>Fused Silica Capillary</i> .....	15
1.1.5.3 <i>Detectors</i> .....	16
1.1.5.4 <i>Power Supply</i> .....	18
1.1.6 SAMPLE INJECTION .....	19
1.1.6.1 <i>Hydrodynamic injection</i> .....	19
1.1.6.2 <i>Electrokinetic injection</i> .....	19
1.1.7 OPERATIONAL PARAMETERS.....	20
1.1.7.1 <i>Applied Voltage</i> .....	20
1.1.7.2 <i>Buffer pH</i> .....	20
1.1.7.3 <i>Buffer Concentration / Ionic Strength</i> .....	21
1.1.7.4 <i>Addition of Organic Modifiers</i> .....	22
a) Non-aqueous Capillary Zone Electrophoresis.....	22
1.1.7.5 <i>Surface Active Agents</i> .....	23
1.1.7.6 <i>Chiral Selectors</i> .....	23
1.1.7.7 <i>Temperature</i> .....	24
1.1.7.8 <i>Capillary wall modifications</i> .....	24
a) Bonded Phases .....	24
b) Dynamic Deactivation .....	25
1.1.8 MODES OF CAPILLARY ELECTROPHORESIS .....	26
1.1.8.1 <i>Capillary Electrochromatography (CEC)</i> .....	26
a) Packing Methods.....	30
b) Dispersion in CEC .....	32
1.1.8.2 <i>Micellar Electrokinetic Chromatography (MEKC)</i> .....	33
1.1.8.3 <i>Capillary Gel Electrophoresis (CGE)</i> .....	35
1.1.8.4 <i>Capillary Isoelectric Focusing (CIEF)</i> .....	35
1.1.8.5 <i>Capillary Isotachopheresis (CITP)</i> .....	36
1.1.8.6 <i>On-column Transient Isotachopheresis Preconcentration (t-ITP)</i> .....	37
REFERENCES.....	39
<b>Section 1.2 Mass Spectrometry .....</b>	<b>41</b>
1.2.1 INTRODUCTION .....	42
1.2.2 INSTRUMENTATION .....	42
1.2.2.1 <i>Inlet Systems</i> .....	43
1.2.2.2 <i>Ionisation Sources</i> .....	43
a) Atmospheric Pressure Ionisation (API).....	45
i) Electrospray Ionisation (ESI) .....	46
ii) Atmospheric Pressure Chemical Ionisation (APCI) .....	48
b) Continuous Flow Fast-atom-bombardment (cf-FAB) .....	48
1.2.2.3 <i>Mass Analysers</i> .....	49
a) Quadrupole Mass Filters .....	50
Tandem Mass Spectrometry (MS/MS) Scanning Techniques.....	53
b) Time-of-flight Analysers .....	54
i) Resolution .....	55
ii) The Reflectron.....	56
iii) Orthogonal Acceleration .....	57
1.2.2.4 <i>Ion Detectors</i> .....	59
a) Electron Multiplier.....	60
b) Photomultiplier .....	60

c) Multichannel Plate Detectors .....	60
REFERENCES.....	62
<b>Section 1.3 Methods of Interfacing Capillary Electrophoresis to Mass Spectrometry .....</b>	<b>63</b>
1.3.1 INTRODUCTION TO CE/MS INTERFACES .....	64
1.3.2 LIQUID JUNCTION INTERFACES .....	65
1.3.2.1 CZE / Liquid Junction / cf-FAB.....	66
1.3.1.2 CZE / Liquid Junction / ESI.....	68
1.3.3 CZE / CO-AXIAL SHEATH FLOW / ESI .....	70
1.3.4 NANOSPRAY CZE INTERFACES.....	82
1.3.5 ALTERNATIVE ELECTROSEPARATION TECHNIQUES / MS .....	90
1.3.5.1 Capillary Electrochromatography and Pseudo-electrochromatography.....	90
1.3.5.2 Transient Isotachopheresis (t-ITP) / CZE / MS.....	92
1.3.6 SUMMARY .....	93
REFERENCES.....	97
<b>Chapter 2 Adaptation of a VG MassLab Trio3 Thermospray Interface for Operation as an Electrospray Ionisation Interface .....</b>	<b>101</b>
2.1 INTRODUCTION .....	102
2.2 EXPERIMENTAL.....	104
2.2.1 Interface Development.....	104
2.2.2 Characterisation.....	105
2.3 RESULTS AND DISCUSSION.....	106
2.4 FURTHER SOURCE DEVELOPMENT .....	109
2.5 MASS SPECTRA .....	111
2.6 CONCLUSIONS.....	116
REFERENCES.....	117
<b>Chapter 3 The Separation of Cimetidine and Related Impurities by Capillary Zone Electrophoresis / Ultra Violet Detection .....</b>	<b>118</b>
3.1 INTRODUCTION .....	119
3.2 EXPERIMENTAL.....	119
3.2.1 Instrumentation .....	119
3.2.2 Reagents .....	120
3.2.3 Procedures.....	122
i Buffer Preparation.....	122
ii Capillary Conditioning.....	122
iii Analyte Preparation .....	122
iv Injection Technique .....	122
3.3 RESULTS AND DISCUSSION.....	123
3.3.1 Buffer Strength .....	128
3.3.2 Addition of Organic Modifiers .....	129
3.3.2.1 Methanol .....	130
3.3.2.2 Acetonitrile.....	130
3.3.3 Effect of Temperature.....	131
3.4 ELECTROPHEROGRAMS .....	133
3.5 CONCLUSIONS.....	146
REFERENCES.....	148
<b>Chapter 4 Development of CZE/MS Interfaces for a Quattro I with Subsequent Analysis of Cimetidine and Related Impurities .....</b>	<b>149</b>
4.1 INTRODUCTION .....	150
4.2 DEVELOPMENT OF A CO-AXIAL SHEATH FLOW CZE/MS INTERFACE FOR A QUATTRO I MASS SPECTROMETER .....	151
4.2.1 Instrumentation .....	151
4.2.2 Reagents .....	152
4.2.3 Development of a Suitable (Volatile) Buffer System for CZE/MS .....	152
4.2.4 Development of Co-axial Sheath flow Interface.....	153
4.2.5 Optimisation of CZE/MS employing a Co-axial Sheath flow Interface .....	156
4.2.6 Analysis of Cimetidine and Related Impurities by CZE/MS.....	157
4.2.7 Conclusions .....	159

4.3 NANOSPRAY INTERFACE PROCEDURE .....	160
4.3.1 <i>Source Modification</i> .....	160
4.3.2 <i>Modification of Probe for Pressure Flow Nanospray</i> .....	161
4.3.2.1 Production of Drawn, Conductive Coated Spray Tips.....	163
4.3.2 <i>Pressure Flow Nanospray Mass Spectrometry</i> .....	165
4.3.2.1 Conclusions.....	168
4.3.3 <i>Modification of Probe for Nanospray CZE/MS</i> .....	169
4.3.3.1 Instrumentation .....	169
4.3.3.2 Chemicals.....	169
4.3.3.3 Development of CZE / Nanospray /MS .....	170
4.3.3.4 Results / Discussion .....	173
4.3.3.5 Conclusions.....	174
4.4 ELECTROPHEROGRAMS AND MASS SPECTRA .....	176
4.5 OVERALL CONCLUSIONS.....	192
REFERENCES.....	193
<b>Chapter 5 Accurate Mass Determination of Narrow Electrophoretic Peaks using an Orthogonal Acceleration Time-of-Flight Mass Spectrometer .....</b>	<b>194</b>
5.1 INTRODUCTION .....	195
5.2 EXPERIMENTAL.....	196
5.2.1 <i>CZE Separation</i> .....	196
5.2.2 <i>Mass Spectrometry</i> .....	197
5.2.3 <i>Chemicals and Reagents</i> .....	198
5.3 RESULTS / DISCUSSION .....	198
5.3.1 <i>Migration Time Reproducibility</i> .....	199
5.3.2 <i>Peak Efficiency</i> .....	200
5.3.3 <i>Exact Mass Data</i> .....	201
5.3.4 <i>Preliminary Investigation of Quantification</i> .....	202
5.4 MASS ELECTROPHEROGRAMS AND SPECTRA.....	203
5.5 CONCLUSIONS.....	211
REFERENCES.....	212
<b>Chapter 6 The Incorporation of Reactive Species in the Sheath Flow for CZE/MS.....</b>	<b>213</b>
6.1 INTRODUCTION .....	214
6.2 EXPERIMENTAL.....	215
6.2.1 <i>Instrumentation</i> .....	215
6.2.1.1 Loop Injections.....	215
6.2.1.2 Capillary Zone Electrophoresis / Mass Spectrometry .....	216
6.2.2 <i>Chemicals and Reagents</i> .....	216
6.3 RESULTS / DISCUSSION .....	217
6.3.1 <i>Cimetidine and Related Impurities</i> .....	217
6.3.1.1 Loop Injection to Determine the Extent of Exchange .....	217
6.3.1.2 CZE/MS Employing D <sub>2</sub> O Sheath Flow.....	219
6.3.2 <i>Propranolol and Atenolol</i> .....	221
6.3.2.1 Loop Injection to Determine the Extent of Exchange .....	221
6.3.2.1 CZE/MS Employing D <sub>2</sub> O Sheath Flow.....	223
6.3.3 <i>Fully Deuterated CZE/MS</i> .....	224
6.4 MASS ELECTROPHEROGRAMS AND SPECTRA .....	226
6.5 CONCLUSIONS.....	233
REFERENCES.....	234
<b>Chapter 7 Separation of Nicotine Metabolites by CZE/MS.....</b>	<b>235</b>
7.1 INTRODUCTION .....	236
7.2 EXPERIMENTAL.....	238
7.2.1 <i>CZE/UV Separation</i> .....	238
7.2.2 <i>CZE/MS Analysis</i> .....	238
7.2.3 <i>Investigation of Isobaric Species</i> .....	239
a) Cone Voltage .....	239
b) Product Ion Scans .....	239
7.2.4 <i>Analytes and Reagents</i> .....	240
7.2.4.1 Analysis of Biological Fluid.....	240
7.2.5 <i>Buffer Preparation</i> .....	240

---

7.3 RESULTS / DISCUSSION .....	241
7.3.1 <i>Development of CZE/MS Separation</i> .....	241
7.3.2 <i>Transfer of Analysis to CZE/MS Analysis</i> .....	245
7.3.3 <i>Isobaric Species</i> .....	249
7.3.4 <i>Analysis of Biological Samples for Nicotine Metabolites</i> .....	251
7.4 ELECTROPHEROGRAMS AND MASS SPECTRA .....	252
7.5 CONCLUSIONS.....	264
REFERENCES.....	265
<b>Chapter 8 Conclusions.....</b>	<b>266</b>
8.1 CONCLUSIONS.....	267
8.2 OVERALL CONCLUSIONS.....	269
8.3 FUTURE WORK.....	270
REFERENCES.....	271
8.4 MAJOR SYMPOSIA AND MEETINGS ATTENDED .....	272
8.5 PUBLICATIONS .....	272

## **Chapter 1**

### ***Instrumental Theory and Literature Review***

## **Section 1.1**

### ***Capillary Electrophoresis***

### ***1.1.1 Introduction***

Electrophoresis is defined as the movement of electrically charged particles in a conductive liquid medium, usually aqueous, under an applied electric field.

Tiselius<sup>1</sup> in the 1930s used the principle of electrophoresis to effect the separation of proteins in solution. Hjertén<sup>2</sup> initially demonstrated electrophoresis in narrow tubes. At that time only millimetre bore capillaries were available and many problems were encountered with diffusion caused by Joule heating. Mikkers *et al.*<sup>3</sup> later demonstrated electrophoresis in narrow bore (200 µm) Teflon tubes. The smaller diameter tubes reduced convective diffusion. Pioneering experiments by Jorgenson and Lukacs<sup>4</sup> using 75 µm i.d. Pyrex glass capillaries significantly reduced the diffusion problems of wider bore tubes. The greater heat dissipation available with narrow capillaries meant higher separation voltages could be used (up to 30 kV). High voltages reduce separation time and increase efficiency. Efficiencies as high as  $4 \times 10^5$  theoretical plates were obtained. They suggested that fused silica capillaries would be more suitable than glass due to their UV transparency.

The term capillary electrophoresis (CE) can be used to describe a family of techniques, which includes capillary zone electrophoresis (CZE); micellar electrokinetic chromatography (MEKC); capillary electrochromatography (CEC); capillary gel electrophoresis (CGE); capillary isoelectric focusing (CIEF) and capillary isotachopheresis (CITP). CZE, MEKC and CGE are zonal separation techniques, whereas CIEF is considered a focusing technique and CITP a moving boundary or displacement technique. CEC can be classified as a chromatographic technique, with analytes partitioning between stationary and mobile phases.

A major limitation of CZE is the inability to separate neutral species. MEKC employs micelles as a pseudo-stationary phase and can readily separate, along with CEC, neutral species. Therefore CZE, MEKC and CEC can be classed as complementary techniques. CGE is used to separate macromolecules on the basis of size. CIEF separates charged analytes on the basis of their isoelectric point (useful for separating proteins and peptides). In CITP the analyte is introduced between two buffers of differing

conductivity, resulting in the formation of analyte bands, the length of which is a function of concentration.

### 1.1.2 Theory of Migration and Electroosmotic Flow

Separation in capillary zone electrophoresis is based on differential migration of charged species under the influence of an applied electric field. The velocity ( $v$ ) of an ion through the capillary can be given by

$$v = \mu_e E = \frac{\mu_e V}{L} \quad \dots(1.1.1)$$

$\mu_e$  = Electrophoretic mobility;  $E$  = Applied electric field;  $V$  = Applied Voltage;  $L$  = Capillary length.

The electric field strength is constant, therefore separations are achieved on the basis of differences in the analytes' electrophoretic mobility ( $\mu_e$ ), which is constant for a given medium and can be calculated from:

$$\mu_e = \frac{q}{6\pi\eta r} \quad \dots(1.1.2)$$

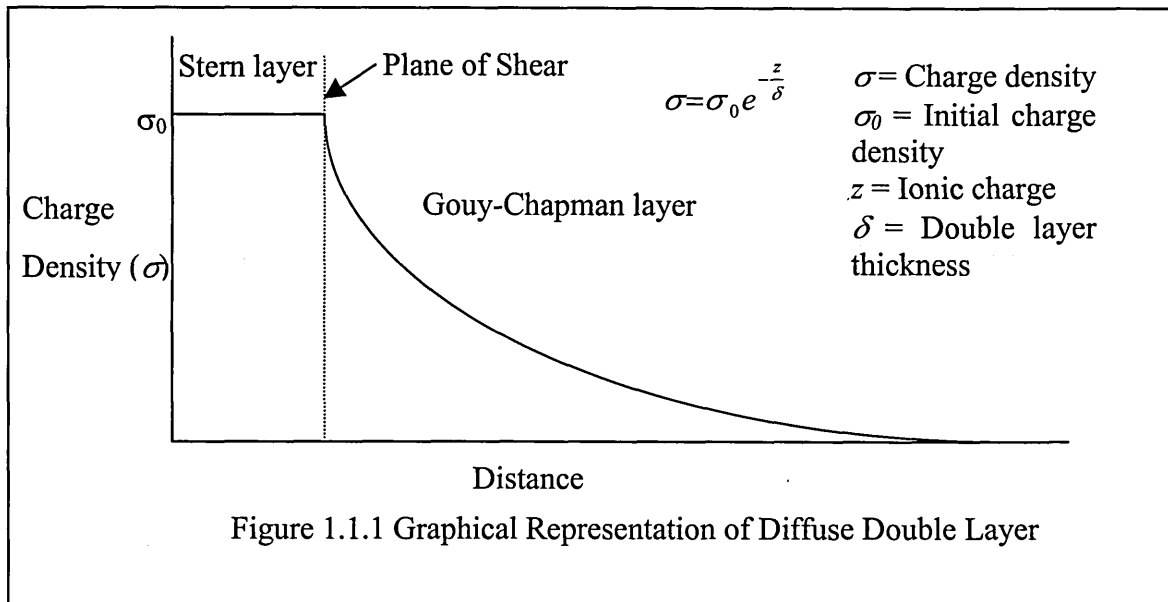
$q$  = Number of charges on an ion;  $\eta$  = Buffer viscosity;  $r$  = Hydrated ion radius

From Equation 1.1.2 it is evident that small, highly charged species will have higher mobilities.

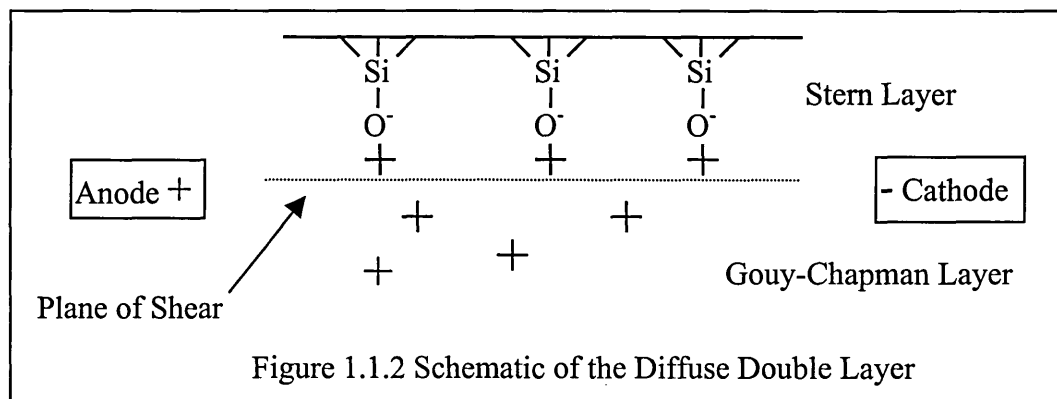
In CZE, in addition to the sample ions, the buffer solution also moves through the capillary under the influence of the electric field. This phenomenon is termed *electroosmotic flow (EOF)*. The flow is usually from the anode to the cathode, *i.e.* from the inlet to outlet vials.

The EOF arises as a result of the inner surface of the buffer filled capillary acquiring a net charge. In the case of fused silica, the surface silanol (Si-OH) groups become increasingly ionised to negatively charged silanoate (Si-O<sup>-</sup>) groups at pH values above three. The anionic silanoate groups attract cations from the buffer, which form a fixed inner layer of cations at the capillary wall (known as the *Stern layer*). These cations are not of a sufficient charge density to neutralise the surface charge, so a second diffuse

layer of cations is formed (known as the *Gouy-Chapman layer*). This is represented graphically in Figure 1.1.1.



The two layers form a *diffuse double layer* of cations. When an electric field is applied, the mobile outer layer is attracted towards the cathode. Since the cations are solvated, they drag the bulk solution with them thus generating an EOF (Figure 1.1.2).



Between the Stern (fixed) and Gouy-Chapman (diffuse) Layers is a *plane of shear*. Application of a voltage generates an electrical imbalance (the potential difference across the layers), which is given the term *zeta potential* ( $\zeta$ ) and can be calculated using Equation 1.1.3.

$$\zeta = \frac{4\pi\delta e}{\epsilon} \quad \dots(1.1.3)$$

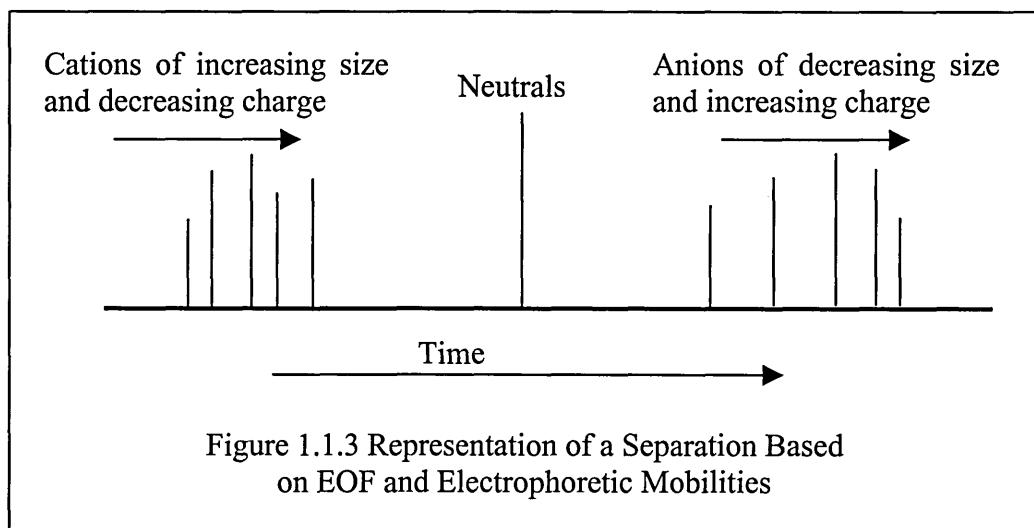
$\delta$  = Thickness of diffuse double layer;  $e$  = Charge per unit surface area;  $\epsilon$  = Dielectric constant of buffer.

The EOF is proportional to the Zeta potential, which is in turn proportional to the thickness of the double layer<sup>5</sup> ( $\delta$ ), the thickness of which can be calculated using Equation 1.1.4 and is inversely proportional to buffer concentration. Typically, a 10 mM buffer would produce a layer approximately 1 nm thick,

$$\delta = \left[ \frac{\epsilon_0 RT}{2cF^2} \right]^{0.5} \quad \dots(1.1.4)$$

$\epsilon_0$  = Permittivity of a vacuum ( $8.854 \times 10^{-12} \text{ F m}^{-1}$ );  $R$  = Gas constant ( $8.314 \text{ J K}^{-1} \text{ mol}^{-1}$ );  $c$  = Electrolyte concentration;  $F$  = Faraday constant ( $96500 \text{ C mol}^{-1}$ ).

Charged analytes separate due to differences in their electrophoretic mobilities (Equation 1.1.2) and will migrate towards the electrode of opposite charge. The EOF is usually greater than the electrophoretic mobility of anions and so they are carried along behind the EOF towards the detector. Neutral analytes are not influenced by the electric field and therefore move through the capillary at the same rate as the EOF and are consequently detected as one peak. This situation is represented in Figure 1.1.3.



From Figure 1.1.3 and Equation 1.1.2 it can be seen that small, highly charged cations would migrate fastest and small, highly charged anions would migrate slowest (due to their migration against the EOF).

The velocity of the EOF ( $v_{EOF}$ ) is given by

$$v_{EOF} = \frac{\varepsilon \zeta E}{4\pi\eta} \quad \dots(1.1.5)$$

The electroosmotic mobility ( $\mu_{EOF}$ ) is given by

$$\mu_{EOF} = \frac{\varepsilon \zeta}{4\pi\eta} \quad \dots(1.1.6)$$

and is dependent solely on buffer characteristics and is independent of the applied electric field.

The addition of a neutral analyte (e.g. thiourea) to the sample can be used to experimentally determine the EOF velocity (Equation 1.1.7) and mobility (Equation 1.1.8)

$$v_{EOF} = \frac{l}{t_m} \quad \dots(1.1.7)$$

$l$  = Length of capillary from inlet to detector;  $t_m$  = Migration time of neutral marker.

$$\mu_{EOF} = \frac{v_{EOF}}{E} \quad \dots(1.1.8)$$

Cations migrate towards the cathode under the influence of electrophoretic mobility and EOF, so therefore move in front of the EOF and are separated through differences in their electrophoretic mobilities. The observed velocity ( $v_{obs}$ ) and observed mobilities ( $\mu_{obs}$ ) are given by Equations 1.1.9 and 1.1.10 respectively.

$$v_{obs} = v_{EOF} + v_e \quad \dots(1.1.9)$$

$$\mu_{obs} = \mu_{EOF} + \mu_e \quad \dots(1.1.10)$$

Therefore actual analyte mobility and velocity ( $\mu_e$  and  $v_e$  respectively) can be calculated from the EOF and observed analyte mobility (or velocity).

### 1.1.2.1 Experimental Factors Controlling EOF

The EOF is usually beneficial; however, it needs to be controlled. At high pH, the EOF may be too rapid and analytes may migrate before separation can occur. At low pH the reduced wall charge can result in decreased EOF velocity leading to lengthy analysis times. Some CE techniques, *i.e.* capillary gel electrophoresis and capillary isotachopheresis, require no EOF.

Control of the EOF can be achieved through manipulation of experimental parameters. These include modification of the capillary wall, separation voltage and buffer conditions (*i.e.* pH, concentration, ionic strength, composition *etc.*).

### 1.1.3 Dispersion

Separation in capillary zone electrophoresis is based on differential migration of charged analytes. The difference required to separate two analytes depends on the analyte zone lengths. Dispersive processes increase zone length and therefore reduce separation efficiencies and consequently should be controlled.

A measure of efficiency and hence dispersion can be obtained using the van Deemter equation (Equation 1.1.11), which is traditionally used in chromatography and gives the height equivalent to a theoretical plate (HETP),  $H$ .

$$H = 2\lambda d_p + \frac{2\gamma D_m}{u} + \frac{1}{30} \left( \frac{k'}{1+k'} \right)^2 \frac{d_p^2 u}{D_{sz}} \quad \dots(1.1.11)$$

$\lambda$  = Tortuosity factor;  $d_p$  = Particle diameter;  $\gamma$  = Obstructive factor for diffusion;  $D_m$  = Diffusion coefficient of solute in free solution;  $u$  = Migration velocity;  $k'$  = Zone capacity ratio;  $D_{sz}$  = Diffusion coefficient in stationary zone.

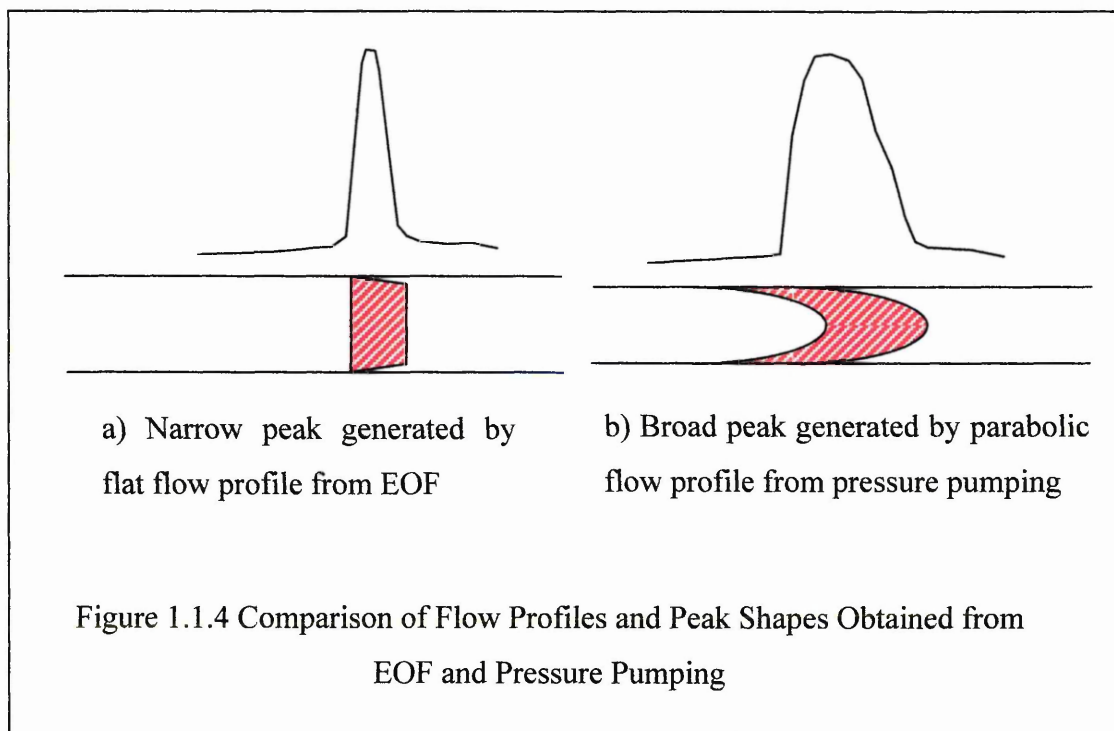
This can be simplified to

$$H = A + \frac{B}{u} + Cu \quad \dots(1.1.12)$$

The A and C-terms represent dispersion factors associated with the chromatographic packing material and can thus be discounted for the purposes of CZE, thus leading to dispersion occurring through longitudinal diffusion only. Hence in ideal conditions (*i.e.* small injection plug length, no analyte / wall interactions) the only contribution to zone broadening in CZE is longitudinal diffusion (otherwise known as axial diffusion).

The EOF has a relatively flat flow profile compared to pumped flow, which has a parabolic flow profile (Figure 1.1.4). Frictional drag causes the EOF to be slower at the capillary wall, but this is negligible when considering the overall flow profile. Thus, all molecules experience the same velocity caused by EOF regardless of cross-sectional location and they elute as a narrow band, resulting in narrow peaks with high

efficiencies. In pumped flow the velocity in the centre of the tube is greater than at the edges, the result of which are relatively broad peaks.



Radial convection is thus insignificant due to the flat-flow profile. Convective broadening is reduced through the non-convective nature of the capillaries. Thus HETP can be calculated using Equation 1.1.13,

$$H = \frac{2D_m}{\mu_e E} = \frac{2D_m}{v_e} \quad \dots(1.1.13)$$

The reason for using high field strengths becomes evident in Equation 1.1.13; analytes spending less time in the capillary have less chance to diffuse. A more convenient measure of efficiency is the number of theoretical plates (N).

$$N = \frac{l}{H} = \frac{(\mu_e + \mu_{EOF})V}{2D_m} \quad \dots(1.1.14)$$

Efficiency is independent of capillary length (Equation 1.1.14). Capillary lengths should be minimised, to obtain fast separations. However, analyte resolution often dictates the length required for adequate separation.

The number of theoretical plates (N) can also be obtained directly from an electropherogram (Equation 1.1.15).

$$N = 5.54 \left( \frac{t}{w_{0.5}} \right)^2 \quad \dots(1.1.15)$$

$w_{0.5}$  = Temporal peak width at half height.

Calculated efficiency (from Equation 1.1.15) is often less than theoretical efficiency (from Equation 1.1.14). This is because other minor dispersive effects occur.

### 1.1.3.1 Minor Dispersive Sources

There are a number of contributions to zone dispersion in addition to longitudinal diffusion. These include temperature gradients (generated by Joule heating), injection plug length, analyte interactions with capillary wall and electrodispersion. If any of these values dominate the diffusion term, theoretical limits cannot be obtained and increasing the voltage has minimal effects.

#### *a) Joule Heating and Temperature Gradients<sup>6</sup>*

An advantage of performing electrophoresis in narrow-bore capillaries is the reduction of heating effects. Heating can cause non-uniform temperature gradients and local changes in viscosity with subsequent zone broadening. It is advantageous to use as high a field strength as possible (E term in Equation 1.1.13) but temperature effects ultimately limit the voltage used, irrespective of capillary dimensions and temperature control methods.

The heat generated by the passage of a current is known as Joule heating and is a function of the power (product of voltage and current) generated and is determined by the capillary dimensions, buffer conductivity and applied voltage.

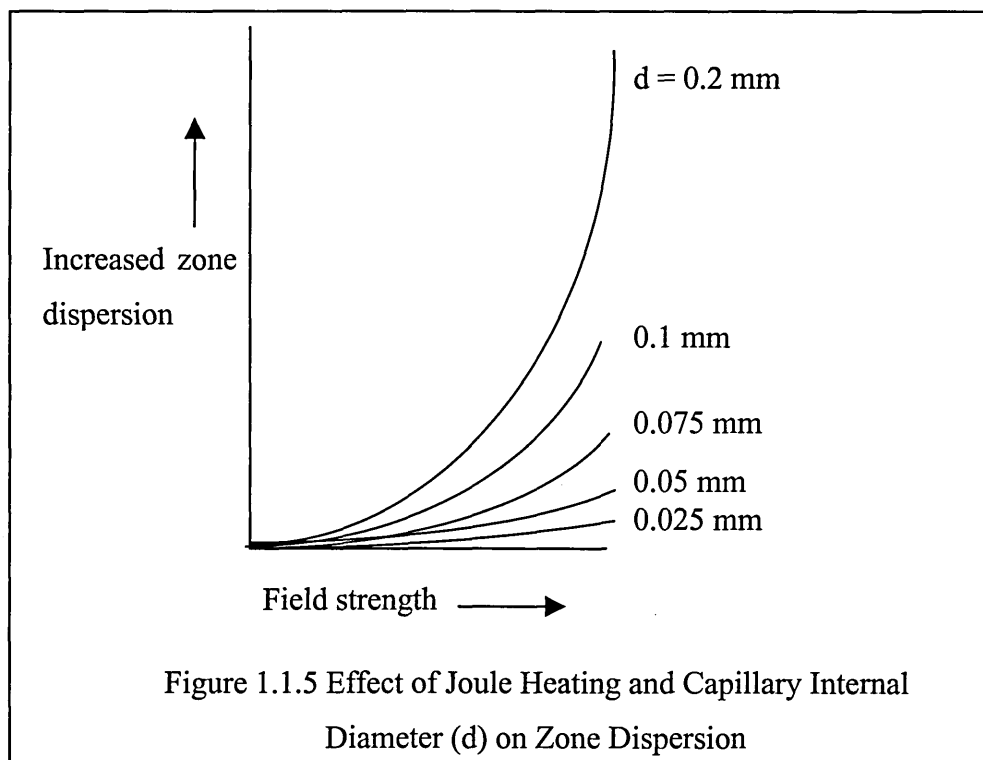
Increases in temperature are not (necessarily) detrimental to the separation, but temperature gradients are. Dissipation of heat through the walls can result in higher temperatures at the capillary centre thus causing viscosity differences in the buffer leading to zone deformations. Figure 1.1.5 indicates the advantage of using narrow capillaries.

Control of temperature gradients is critical since a one-degree change in temperature can result in 2 – 3% change of viscosity (and consequently 2 – 3% changes in mobility).

A variety of methods can be used to limit Joule heating

- Decreased field strength - proportional decrease in heat generated, at the expense of efficiency and resolution.
- Reduce capillary internal diameter – current  $\propto$  (resistance)<sup>2</sup>, therefore drastic decrease in current. Decreased sensitivity, especially with in-column UV absorbance (decreased path length).
- Decrease ionic strength / concentration of buffer or use a low conductivity buffer, such as organic zwitterions Tris (2-amino-2-(hydroxymethyl)-1,3-propanediol) and Caps (3-cyclohexylamino-1-propanesulphonic acid).
- Active temperature controls – thermostatically monitor temperature and remove heat from capillary. This can be achieved in two ways, high-velocity air cooling via a thermostatically controlled fan or liquid cooling around the capillary.

Temperature control is important not only for reducing Joule heating, but also for maintaining a constant temperature from analysis to analysis.



### *b) Injection Plug Length*

It is important that the sample plug length is kept to a minimum. Increasing plug length significantly reduces efficiency. A practical limit of injection length is less than 1 – 2% of the total capillary length (this corresponds to 7 mm for a 70 cm capillary). Modern instrumentation can reproducibly load such small volumes, but detection difficulties may necessitate larger injection volumes (see t-ITP Section 1.1.8.6).

### *c) Analyte-wall Interaction*

Interaction between the analyte and the capillary wall is detrimental to CZE. Depending on the interaction, peak tailing and even total adsorption of the analyte can occur. The main cause of interaction is the adsorption of cationic species to the negatively charged capillary wall. The large area-to-volume ratio (preferable for minimising Joule heating) of the capillary increases the likelihood of adsorption. Proteins and peptides are especially susceptible to adsorption because of the numerous charges present.

Interaction is dependant on adsorption / desorption kinetics and EOF velocity (*i.e.* a fast EOF will not allow an equilibrium to be reached, resulting in the formation of peak tails) and capillary effective length (longer capillary – more interaction). Decreasing the EOF can result in reduced adsorption, this can be achieved by increasing buffer concentration or ionic strength (decreasing zeta potential and hence the EOF), although this can lead to increased Joule heating.

An alternative approach is to perform the analysis at pH extremes. At low pH the silanol groups would be fully protonated and hence cationic species will no longer be able to interact. At high pH the wall and analyte would be deprotonated therefore wall interactions would be limited by charge repulsion, however this method may be limited by sample instability at pH extremes. Capillary coatings can also be used to minimise or eradicate wall interactions.

#### *d) Electrodispersion*

Differences in sample zone and running buffer conductivities can have three effects,

- Skewed peak shape.
- Analyte zone length, either focusing (lower conductivity sample), or defocusing (higher conductivity sample) of analyte zones.
- Temporary isotachophoretic states, due to an excess of a certain ion.

When the analyte zone has a higher mobility than the running buffer its leading edge will be diffuse and the trailing edge sharp. Conversely, when an analyte zone has a lower mobility than the buffer the leading edge will be sharp and trailing edge diffuse. When sample and buffer are of similar conductivity there will be no peak distortions. The causes of these distortions are a mismatch in conductivity and hence field across the zone. When the analyte has a higher mobility (*i.e.* higher conductivity and lower resistance) than the buffer, the front edge of the analyte zone diffusing into the buffer experiences a higher voltage drop and ions are accelerated away from the zone, resulting in peak fronting. Analyte ions at the trailing edge experience a similar voltage drop, but in the direction of migration and are accelerated back into the analyte zone, resulting in a shape trailing edge. Conversely, sharp front edges and diffuse trailing edges are obtained for ions of opposite charge and the reverse situation (low conductivity sample and high conductivity buffer).

These distortions always occur and may be insignificant compared to other dispersion effects; they are most evident in samples containing analytes of widely differing mobilities. Peak shape distortions are usually only detrimental to resolution and can be solved by matching sample matrix and running buffer.

#### ***1.1.4 Resolution***

Resolution (R) of sample components is the purpose of separation techniques, the degree of separation can be defined as

$$R = \frac{2(t_2 - t_1)}{w_1 + w_2} \quad \dots(1.1.16)$$

t = Migration time; w = Temporal baseline peak width.

Separation in CZE is primarily due to efficiency rather than selectivity, because of the sharp analyte zones. Small differences in solute mobility can lead to fully resolved zones.

Resolution can be calculated as a function of efficiency

$$R = \frac{1}{4} \sqrt{N} \left( \frac{\Delta\mu}{\bar{\mu}} \right) \quad \dots(1.1.17)$$

Where  $\Delta\mu = \mu_2 - \mu_1$  and  $\bar{\mu} = \frac{\mu_2 + \mu_1}{2}$

(Velocity or the inverse time function can be used to replace mobility).

The combination of Equations 1.1.14 and 1.1.17 results in a theoretical equation that does not require calculation of efficiency and relates EOF to resolution,

$$R = 0.177 \Delta\mu \sqrt{\frac{V}{D(\bar{\mu} + \mu_{EOF})}} \quad \dots(1.1.18)$$

In contrast with efficiency, the voltage must be quadrupled to double resolution; Joule heating prohibits the benefits that would be gained from this.

Infinite resolution (and efficiency) will be obtained when  $\bar{\mu}$  and  $\mu_{EOF}$  are equal, but opposite, *i.e.* the ion migrates in the opposite direction, at the same rate as the EOF, but analysis time consequently approaches infinity. Capillary length also influences separation. As the length increases, two analytes of differing mobility have more time to separate. However, analysis time also increases, therefore the shortest capillary that gives adequate resolution should be used.

### **1.1.5 Instrumentation**<sup>7,8</sup>

A schematic of a capillary electrophoresis system is shown in Figure 1.1.6, this basic set-up comprises inlet and outlet vials; fused silica capillary; power supply and detector (usually linked to some kind of data handling device, *e.g.* integrator or PC).

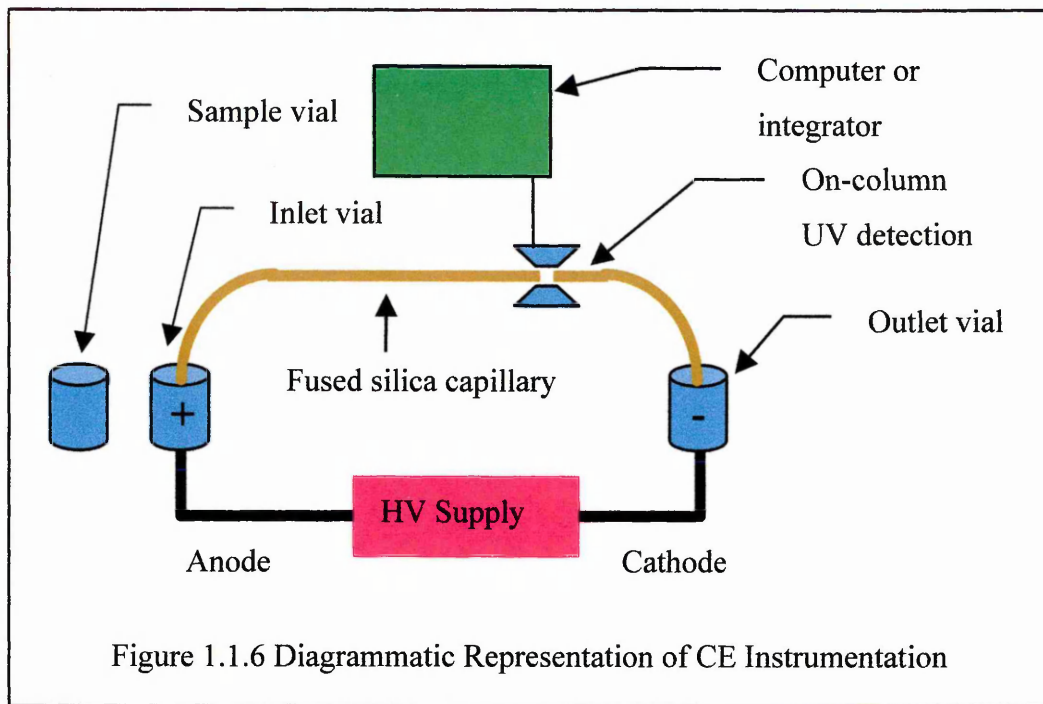


Figure 1.1.6 Diagrammatic Representation of CE Instrumentation

### 1.1.5.1 Inlet / Outlet Vials

The inlet and outlet vials contain an equal level (to prevent siphoning) of buffer solution. Both vials and the capillary contain the same buffer solution. The composition of the buffer is the most critical variable in CE, small changes in concentration or pH can cause significant changes in migration and therefore the overall separation. Electrolytic breakdown of the buffer can occur<sup>9</sup>, releasing hydrogen ions at the anode and hydroxide ions at the cathode, changing the pH of the solution. This leads to irreproducible separations, it is therefore necessary to replenish the buffer vials on a regular basis.

### 1.1.5.2 Fused Silica Capillary

Fused silica capillaries that are 30 – 100 cm long with internal diameters (i.d.) of 10 – 100  $\mu\text{m}$  and outer diameters (o.d.) 150 – 375  $\mu\text{m}$  are typically utilised. UV/vis detection can take place on-column due to the transparency of fused silica to UV/vis light. The cell window is simply fabricated by removal of the polyimide coating. Efficiency is independent of column length; however, adequate analyte resolution usually dictates capillary length.

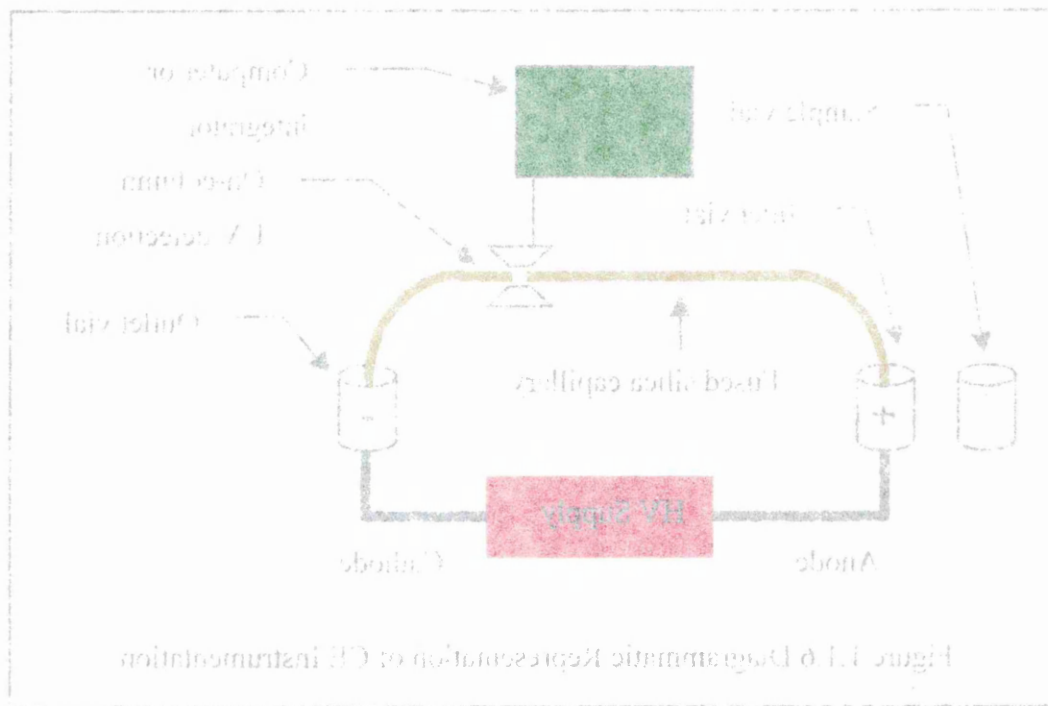


Figure 11.6 Degasimetric Resistorless CE Instrumentation

### 11.2.1.2.1 Inlet/Outlet Vials

The inlet and outlet vials contain an equal level to prevent siphoning of buffer solution. Both vials at the capillary contain the same *only* a solution. The composition of the buffer is not a critical variable in CE; small changes in concentration or pH can cause significant changes in migration and therefore the overall separation. Electrolytic breakdown of the buffer can occur, releasing hydrogen ions at the anode and hydroxyl ions at the cathode, changing the pH of the buffer. The need to replenish the buffer vials on a regular basis.

### 11.2.1.2.2 Fused Silica Capillary

Fused silica capillaries are 50–100 cm long with internal diameters of 0.1–100 μm and outer diameters of 0.5–1.5 mm and typical outlet flow detection can take place over a distance of 10–20 cm. The transparency of fused silica is 99.999% at 200 nm, which is why it is used for UV detection. Efficiency is also improved by removal of the polyimide coating. Efficiency is reduced of certain length however, adequate length results in useful detection capillary length.

Capillaries are often thermostated to help dissipate heat and maintain a constant temperature, thereby minimising diffusion by thermal gradients.

Capillary conditioning is necessary prior to use and between runs to maintain a reproducible surface and hence migration times. Base conditioning to remove adsorbates and refresh the surface by deprotonation of the silanol groups is commonly used. Before the column is first used it is important to thoroughly wash the capillary, usually with 0.1 M NaOH for at least 20 – 50 column volumes, followed by water (10 – 20 column volumes) and finally electrolyte (20 – 50 column volumes). The wash periods can be significantly reduced in-between analyses.

A potential problem with base conditioning when low pH electrolytes are used is a hysteresis of the wall charge, which can result in an irreproducible EOF. It is therefore advisable to flush the capillary with acid (*e.g.* 0.1 M HCl) before use and between analyses.

### 1.1.5.3 Detectors

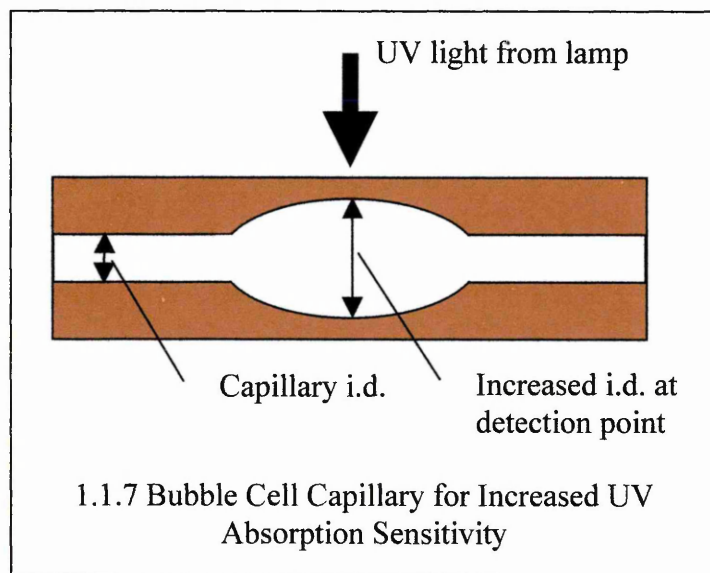
A variety of detectors can be used, the most common are summarised in Table 1.1, along with approximate detection limits. UV/vis absorbance is typically employed, due to its wide applicability.

Table 1.1 Common Detectors and Approximate Detection Limits

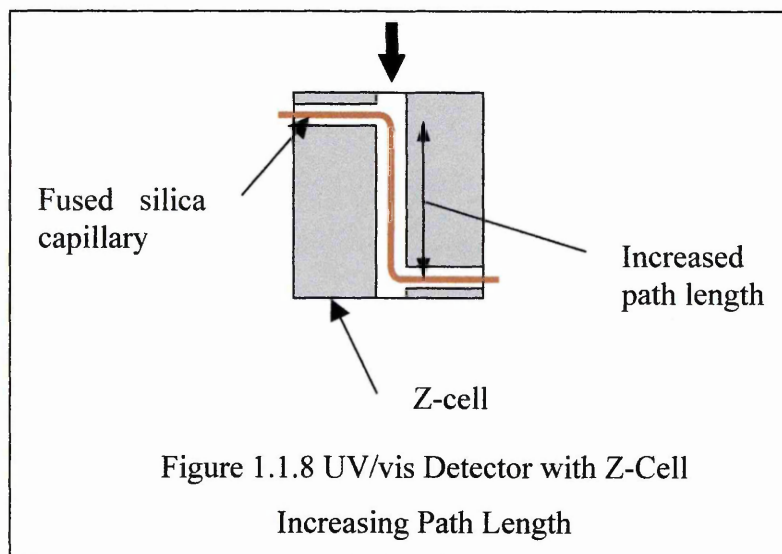
Detector	Mass detection limit (moles)	Concentration detection limit (molar)*
UV/vis absorbance	$10^{-13} - 10^{-16}$	$10^{-5} - 10^{-7}$
Laser-induced fluorescence	$10^{-18} - 10^{-20}$	$10^{-13} - 10^{-16}$
Conductivity	$10^{-15} - 10^{-16}$	$10^{-7} - 10^{-9}$
Mass spectrometry	$10^{-16} - 10^{-17}$	$10^{-8} - 10^{-10}$

\* Depends upon volume of sample injected

In the case of UV/vis absorption, the effective path length of the window (*i.e.* capillary internal diameter) limits detection sensitivity. A number of methods have been suggested to improve sensitivity by increasing the effective path length. This can be achieved using a 'Bubble Cell' in which the i.d. of the capillary is increased at the point of detection (Figure 1.1.7). Bubble cells increase sensitivity, however, they are extremely fragile, difficult to produce and expensive. Heiger<sup>8</sup> demonstrated a 3-fold increase in analyte intensity using a 150  $\mu\text{m}$  bubble cell *cf.* a 50  $\mu\text{m}$  capillary.



An alternative approach is to use a Z-cell, in which the capillary is bent; detection then takes place along the length of the capillary rather than across (Figure 1.1.8). However, the path length cannot be too long as closely migrating species will not be detected separately. Moring *et al.*<sup>10</sup> demonstrated an order of magnitude increase in sensitivity using a 3 mm Z-cell.



In addition, the spherical nature of the fused silica can result in a decrease in sensitivity due to the dispersion of UV/vis light through the capillary wall. This can be alleviated through the use of square or rectangular fused silica or employing a detector that has a lens prior to the capillary, which focuses the light into the inside of the capillary.

Overall sensitivity is reduced compared to HPLC; this is due to a number of factors. These include reduced path length for optical detection, reduced injection volumes and column capacity. However, an advantage over HPLC is a reduction in extra column dispersion (and hence increased efficiency) as detection takes place on-column rather than post-column.

Sample stacking can also be employed to enhance sensitivity. The sample is injected into the capillary in a solvent of lower conductivity than the buffer (*e.g.* deionised water). When the separation voltage is applied, the sample plug experiences a higher electric field than the rest of the capillary. Cations will migrate to the front of the sample plug where they become stacked against the higher conductivity of the running buffer. The converse occurs with anions (*i.e.* they stack between the trailing edge of the sample plug and buffer). Thus, the analyte migrates through the capillary as a zone that is narrower than the sample plug.

#### **1.1.5.4 Power Supply**

The function of the power supply is to provide an electric field across the capillary. Most can function in constant voltage or current modes. Voltages up to 30 kV and currents of 300  $\mu\text{A}$  are usually available (a maximum of 50 kV can be used, beyond which electrical breakdown of air can occur resulting in a corona discharge). Stable regulation of the voltage ( $\pm 0.1\%$ ) is required to maintain high migration time reproducibility.

The power supply generally has the capability to switch polarity. Under normal conditions the EOF is in the direction of the cathode, injection occurring at the anode. In certain circumstances the EOF is reversed and it may be necessary to reverse the polarity of the electrodes, *i.e.* to switch the cathode to the injection end. This is best

achieved using a dual polarity supply, maintaining the outlet electrode as ground and the high voltage electrode driven with a positive or negative voltage.

### ***1.1.6 Sample Injection***

The sample is usually diluted in the buffer (or water to reduce conductivity, for stacking effects, see Section 1.1.8.6) and is loaded into a small sample vial (a few  $\mu\text{L}$  to a few hundred  $\mu\text{L}$ ). Only a small volume is required since usually only a few nanolitres are injected on column.

There are two types of injection, *hydrodynamic* and *electrokinetic injection*.

#### **1.1.6.1 Hydrodynamic injection**

Injections can be performed by application of pressure to the inlet vial, vacuum to the outlet vial or by siphoning (*i.e.* raise inlet vial relative to outlet vial). With hydrodynamic injection, the quantity of analyte loaded is independent of sample matrix and analyte mobility. The volume of sample loaded ( $V$ ) can be calculated using the Hagen-Poiseuille equation (Equation 1.1.19).

$$V = \frac{\Delta P d^4 \pi t}{128 \eta L} \quad \dots(1.1.19)$$

$P$  = Pressure differential across capillary;  $d$  = Capillary i.d.;  $\pi$  = Pi (3.142);  $t$  = Time;  $\eta$  = Viscosity;  $L$  = Total length.

For injection by siphoning, the pressure differential ( $\Delta P$ ) for use in Equation 1.1.19 is given by

$$\Delta P = \rho g \Delta h \quad \dots(1.1.20)$$

$\rho$  = Buffer density;  $g$  = Gravitational constant ( $6.67 \times 10^{-11} \text{ Nm}^2 \text{ kg}^{-2}$ );  $\Delta h$  = Height difference of vials.

#### **1.1.6.2 Electrokinetic injection**

An electric field can be applied to the sample vial causing sample components to

migrate into the capillary. The quantity of sample loaded is dependent on the electrophoretic mobility of the individual analytes. Discrimination occurs for ionic species, since more mobile ions are loaded to a greater extent than less mobile. Thus for multiple injections, ionic analytes will be injected preferentially, therefore selectively depleting these analytes (whereas hydrodynamic injection results in reproducible analyte concentration over multiple injections).

The quantity injected ( $Q$ ) can be calculated by

$$Q = \frac{(\mu_E + \mu_{EOF}) V \pi r^2 C t}{L} \quad \dots(1.1.21)$$

$\mu_E$  = Electrophoretic mobility;  $\mu_{EOF}$  = EOF mobility;  $V$  = Voltage;  $r$  = Capillary radius;  $C$  = Analyte concentration.

### **1.1.7 Operational Parameters**

#### **1.1.7.1 Applied Voltage**

Variation in the applied voltage will directly affect the field strength and hence the EOF velocity. A higher voltage increases the EOF velocity, reducing migration times (consequently leading to shorter analysis times), improving resolution and efficiency. A simple view would be to use as high a voltage as an instrument could provide. However, high voltages lead to higher current and increased Joule heating. In practise a voltage should be used, which does not lead to temperature effects within the capillary.

#### **1.1.7.2 Buffer pH**

Variations in buffer pH have significant effect on the EOF velocity. This is because the pH alters the charge density of the capillary wall. Increasing the pH of a buffer will increase the extent of dissociation of the surface silanols of a fused silica capillary, resulting in an increased surface charge. This surface charge is proportional to the zeta potential of which EOF velocity is a function. Therefore, from Equation 1.1.5 EOF velocity will increase at higher pH.

Manipulation of buffer pH can be useful for separating analytes of differing acidities or basicities. The analytes are in equilibrium (fully ionised  $\leftrightarrow$  neutral), variation of the pH can thus alter the position of the equilibrium and be employed as a tool for separation. Typically for a basic analyte as the buffer pH is reduced, the sample will become increasingly positively charged (*i.e.* protonated) and migrate at a faster rate towards to the cathode (and detector). At elevated pH values the analyte will be neutral (*i.e.* ion suppressed) and migrate under the influence of the EOF. Typically, the buffer pH is manipulated to optimise analyte separation and not EOF velocity.

### 1.1.7.3 Buffer Concentration / Ionic Strength

When a capillary is adequately thermostatted, increasing the buffer concentration will reduce the EOF velocity. This is because the double layer becomes compressed, which in-turn reduces the zeta potential and EOF velocity. However, if thermostating is inadequate Joule heating will increase (due to an increased conductivity) leading to a reduced viscosity and hence faster EOF.

The correct running buffer selection is essential to the success of a CZE separation. The sensitivity of EOF to changes in pH requires that the buffer maintain a constant pH. Effective buffer systems have a range of  $\pm 1$  pH unit at the  $pK_a$ . Multibasic buffers (such as citrate and phosphate) have more than one useful  $pK_a$  and can be used over a range of pH values.

A successful buffer must have

- Good buffering capacity at the chosen pH
- Low absorbance at the chosen wavelength (if direct UV detection is being used)
- Low conductivity (*i.e.* large, minimally charged ions) to minimise current generation (and thus Joule heating)

Common inorganic buffers include sodium tetraborate, disodium hydrogenphosphate and sodium dihydrogenphosphate, and organic buffers include ammonium acetate / formate, Tris (2-amino-2-(hydroxymethyl)-1,3-propanediol) and Caps (3-cyclohexylamino-1-propanesulphonic acid). Typical concentrations are between

1 – 100 mM, the lower limit is determined by buffer stability (*i.e.* maintaining a steady pH), the upper limit is ultimately restricted by Joule heating. Zwitterionic buffers (Tris and Caps) can be used at an elevated concentration without a significant increase in conductivity (thus reducing Joule heating problems).

In addition, it is important to match buffer and sample mobility to prevent peak shape distortions (Section 1.1.3.1 d).

#### 1.1.7.4 Addition of Organic Modifiers

The effect of voltage and pH can be readily predicted, however, the addition of organic modifiers results in a complex situation. It is difficult to predict what the effect of adding an organic modifier to the buffer will be. This is because it can alter a number of variables, including viscosity, dielectric constant and zeta potential; depending upon which modifier and how much is used. For example, the addition of methanol up to 50 % to an aqueous phase will increase viscosity, above 50 % viscosity then decreases. Tsuda *et al.*<sup>5</sup> reported that the EOF velocities obtained using acetonitrile, water and methanol were in fact proportional to the ratio of their dielectric constant to their viscosity ( $\epsilon/\eta$ ).

The addition of organic modifiers can also have effects on analyte solubility and the degree of hydration. Manipulation of the analyte hydration sphere can result in enhanced separation of similar analytes<sup>11</sup> (*e.g.* the separation of iodide and chloride, and azide and perchlorate anions is not possible without the addition of methanol).

##### *a) Non-aqueous Capillary Zone Electrophoresis*<sup>12,13</sup>

In certain circumstances it may prove difficult to investigate a problem employing aqueous conditions, especially when the analytes are hydrophobic and their solubilities are insufficient for adequate detection. This can be overcome by using a non-aqueous buffer system (*i.e.* 100% organic solvent), typically comprising a mixture of methanol / acetonitrile. A buffer may or may not be required, but if used solubility problems may arise with inorganic buffers.

It has been demonstrated<sup>14</sup> that complementary selectivity can be obtained by performing an analysis under aqueous and non-aqueous conditions. Ellis *et al.*<sup>14</sup> developed a separation method for the analysis of cimetidine and related impurities under both aqueous and non-aqueous conditions. Two of the analytes could not be solubilised in the aqueous phase, but could be analysed using a non-aqueous buffer. The selectivity obtained under the two separation conditions was different. Co-migrating species under aqueous conditions were well separated using the non-aqueous buffer. Efficiencies were significantly higher and migration time reproducibilities were also improved for the non-aqueous separation. The increase in efficiency can be rationalised as a reduction in analyte-wall interaction (observed in aqueous separation as peak tailing) through the presence of the organic solvents.

This study demonstrated the complementary nature of these separation techniques. However, before non-aqueous separation conditions are regularly employed, further investigation of the background theory is necessary to provide adequate understanding of the underlying separation mechanisms. For example, little is understood about acid / base theory in organic solvents ( $\text{pH}^*$ ), also how an organic solvent (*e.g.* acetonitrile) alone can support an EOF.

#### **1.1.7.5 Surface Active Agents**

Surfactants (anionic, cationic, ampholytic, zwitterionic and non-ionic) can be used as buffer additives below the critical micelle concentration (concentration at which micelles are formed). The surfactant molecules act as solubilising agents for hydrophobic analytes, as ion-pairing reagents or as wall modifiers.

#### **1.1.7.6 Chiral Selectors<sup>15</sup>**

Chiral analysis is becoming increasingly important in pharmaceutical analysis. Chiral analysis by CZE usually involves the addition of a chiral species to the buffer. Each isomer interacts differently with the additive, effecting separation. Common chiral

additives are cyclodextrins, crown ethers and bile salts. Adjusting the type and concentration of the additive can alter selectivity.

#### **1.1.7.7 Temperature**

Although the main purpose of instrumental ovens is the maintenance of a constant temperature, altering the temperature can be beneficial. Increased temperature will alter (typically reduce) the buffer viscosity, and hence EOF and analysis time. Care must be taken at elevated temperatures, as this may cause zone dispersion, sample decomposition and buffer boiling (especially when high percentages of organic modifier are being used).

#### **1.1.7.8 Capillary wall modifications**

In some cases, it can be important to modify the inner wall of the capillary with some chemical functionality, to either alter the EOF or prevent adsorption of analytes to the wall. The use of pH extremes may render the need for derivatisation unnecessary, although the analysis of proteins outside physiological conditions can irreversibly alter protein structure. Wall modifications fall into two categories, bonded or dynamic coatings.

##### *a) Bonded Phases*

A number of wall coatings have been used and generally involve silylation followed by deactivation with a functional group. Unfortunately the siloxane bond has limited stability (pH 4 – 7) and hydrolysis limits lifetime.

Depending on the type of deactivation, the EOF can be reversed or eliminated. Neutral deactivation eliminates EOF; this is due to the decreased wall charge. Cationic deactivation results in a reversed EOF, *i.e.* from cathode to anode. Ampholytic deactivation results in a reversible EOF, depending on the pH of the buffer.

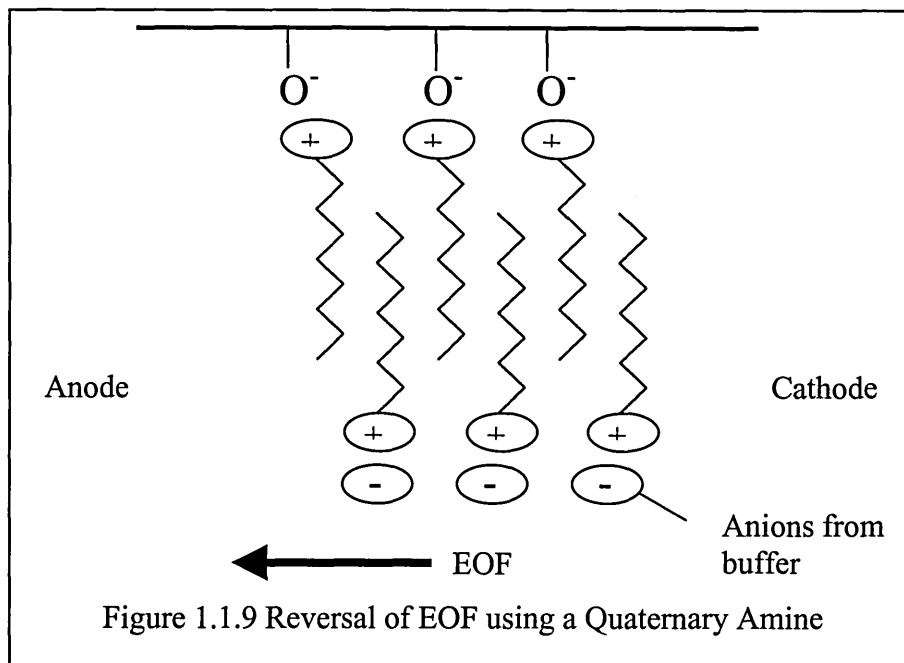
Bonded modifications are intended to be permanent, with little or no maintenance required. The bonding must also be able to withstand washing without detrimental effects to the phase.

*b) Dynamic Deactivation*

The addition of modifiers to the running buffer is an alternative to bonded deactivation. During an analysis the coating is continuously being regenerated, so therefore stability can be improved.

Common additives include hydrophilic polymers (masking wall charge and reduce EOF), surfactants (decrease or reverse EOF, however, may irreversibly denature proteins) and quaternary amines (decrease or reverse EOF, can also act as ion-pairing reagents).

Reversal of the EOF can be achieved by the addition of a quaternary amine (alkyl ammonium salt) to the buffer, this is graphically represented in Figure 1.1.9. The cationic head-groups interact with the silanoate groups on the capillary wall; the hydrophobic alkyl tail thus extends into the capillary. The alkyl chains associate with quaternary amines in solution through hydrophobic interactions. The cationic head group of the associated amine attracts anions from the buffer, which are (upon application of a voltage) attracted to the anode. These anions are solvated and drag the bulk solution towards the anode, resulting in a reversal in direction of the electroosmotic flow. Common quaternary amines include cetyltrimethylammonium bromide or chloride (CTAB and CTAC respectively) and tetradecyltrimethylammonium bromide (TTAB).



Additives interact with the wall and alter charge and / or hydrophobicity as with bonded phases. These modifiers are easy to use and optimise, simply requiring dissolution in the buffer. The addition of a dynamic modifier to the buffer can have unpredictable effects on the sample, especially in biological applications. Also increased wash and equilibration times may be necessary to generate a reproducible surface and constant EOF. The additive may affect post column detection, *e.g.* addition of surfactants to a CZE/MS analysis could result in the ion current being dominated by the surfactant.

### 1.1.8 Modes of Capillary Electrophoresis

#### 1.1.8.1 Capillary Electrochromatography (CEC)

One major drawback of CZE is the inability to separate neutral compounds. CEC combines the efficiency of CZE with the selectivity of HPLC. CEC employs a fused silica capillary packed with an HPLC stationary phase (1.5 – 5  $\mu\text{m}$ ,  $\text{C}_{18}$ , SCX and mixed mode phases have been used). The mobile phase is driven through the column under the influence of an applied electric field, which generates an EOF.

As in HPLC, CEC separations are based on differential partition between a stationary and mobile phase. The separations performed by HPLC and CEC only differ in the method of movement of the analyte (and buffer) through the column. In HPLC the

mobile phase is pumped through the column under pressure, resulting in a parabolic flow profile. In CEC the mobile phase moves through the column by EOF, generating a flat flow profile.

The packing material typically used is silica based and therefore contains silanol groups on its surface. These groups act in a similar way to those on the capillary inner surface and generate an EOF (Figure 1.1.10).

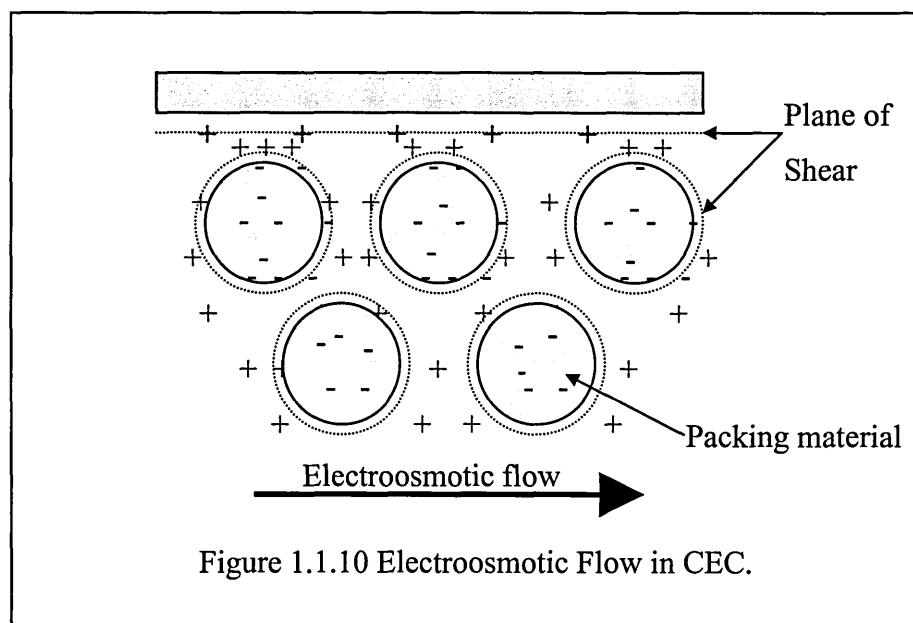


Figure 1.1.10 Electroosmotic Flow in CEC.

Pretorius *et al.*<sup>16</sup> initially demonstrated CEC in 1974, investigating the effect of an applied voltage compared to pressure to draw a compound through a packed column. This work confirmed the theory that band broadening would be reduced, due to the flat flow profile generated by the electroosmotic flow (EOF), which as predicted, reduced some of the diffusion mechanisms found in HPLC.

No further work was reported until 1981 when Jorgenson and Lukacs<sup>17</sup> obtained data using non-aqueous CEC in a 170  $\mu\text{m}$  i.d. column. Although the method was crude it indicated that highly efficient separations were possible. Stevens and Cortes<sup>18</sup> published work that indicated CEC efficiency would not be as high as expected. They concluded that if the packing material went below 50  $\mu\text{m}$  particle diameter ( $d_p$ ) there would be insufficient flow to allow separations to occur. This was thought to be due to double layer overlap, the interaction of mobile layers around the stationary phase particles

being more pronounced when  $d_p$  was reduced, disrupting the EOF. These conclusions were shown to be inaccurate by Knox and Grant<sup>19</sup> in 1987. This report included a purely theoretical look at CEC. The Debye-Hückel equation was used to determine the double layer thickness and the mean channel sizes of the packed column. With this information, it was possible to predict electrolyte concentrations and the  $d_p$  at which double layer overlap would occur. It was concluded that particles with a  $d_p$  less than 1  $\mu\text{m}$  could be used and this was later confirmed experimentally by Knox and Grant<sup>20</sup>.

Interest in CEC began to increase from 1994 with a growing number of papers appearing in the literature. Initially the main focus of research was the successful packing of capillaries and the investigation into the effects of experimental parameters. Initially packing CEC capillaries was problematic, especially in the formation of the frits. The function of the frit within the column is to retain the packing material in the capillary. Frits are generally fabricated by localised heating of the packing material to form a sintered plug. A novel device has been suggested by research groups at Glaxo Wellcome<sup>21-23</sup>, which allows the burning of reproducible and robust frits.

A lack of reproducibility in frit burning and packing problems led to a number of research groups<sup>24-27</sup> developing a novel CEC method, in which the stationary phase was permanently bonded to the capillary walls, producing monolithic beds. Therefore, no retaining frits were required. The monolithic beds were claimed to be faster and simpler to prepare than conventional CEC, with comparable efficiencies.

Ramsey *et al.*<sup>28</sup> developed a novel technique using semiconductor technology. An EOF was generated in an open channel, etched on a microchip, chemically modified with octadecylsilane. Peak efficiencies between 1000 and 14000 were reported for this initial development. Improvements in the channel path and dimensions were suggested to increase efficiency.

A further problem encountered with CEC was the formation of bubbles within the capillary. This has been attributed to 'hot spots' or Joule heating within the packed bed leading to the formation of bubbles, breaking the electrical connectivity and cessation of EOF. Two simple methods can be used to minimise Joule heating; the application of a

supplementary pressure to the inlet and outlet vials preventing the formation of bubbles and the use of low conductivity buffers, reducing the conductivity within the column and hence Joule heating.

Carney *et al.*<sup>29</sup> suggested a novel method to minimise bubble formation, which they demonstrated to be a function of frit length and applied voltage. Short frits and reduced voltage produced fewer bubbles. However, rebonding octadecylsilane (C<sub>18</sub>) to the frit reduced bubble formation, even in long frits exposed to high voltages. Frits are generally formed by a pyrolytic process, altering the structure of the material, leading to velocity changes in the EOF, and consequently formation of bubbles. Rebonding C<sub>18</sub> to the frits generated fewer bubbles, due to the constant EOF velocity through the whole packed section.

Tsuda<sup>30-32</sup> used the principles of CEC to improve separations on narrow bore HPLC. Initially HPLC apparatus was used which led to a pressurised CEC system. Pressurised CEC reduces bubble formation, thus allowing higher concentrations of electrolytes to be used. However, Kraak *et al.*<sup>33</sup> reported successful CEC performed at ambient pressure, claiming that with suitable precautions in column and mobile phase preparation bubble formation can be avoided.

A further development on pressurised CEC was suggested by Behnke and Bayer<sup>34</sup>, in which the inlet vial was connected to a gradient LC system. This meant the system could be pressurised and also allowed the solvent composition to be altered throughout the analysis (in a way similar to gradient LC). Taylor and Teale<sup>35</sup> using gradient-CEC-MS in the study of drug mixtures later confirmed this work. A further variation of the gradient-CEC was suggested by Yan *et al.*<sup>36</sup> using two power supplies to generate a gradient by means of the EOF. The electrokinetic gradient system has the advantage of supplying an instant gradient to the separation capillary, unlike the gradient CEC system demonstrated by Taylor and Teale<sup>35</sup>, which has a twenty minute lag for the gradient to reach the separation capillary.

The majority of published data has been obtained using standard HPLC reversed phase C<sub>18</sub> packing material. Smith and Evans<sup>22</sup> investigated the separation of highly polar pharmaceuticals and concluded that they were difficult to analyse by CEC using

conventional reverse phase packing materials. They suggested the use of a cation exchanger in place of C<sub>18</sub> silica. The SCX material was found to resolve the highly basic compounds with extremely high efficiencies (8 million plates per metre), which was attributed to focusing effects. Other research groups<sup>37-41</sup> using ion exchange materials have confirmed this work. A further advantage of using ion exchange materials is the fast EOF generated over a wide pH range. C<sub>18</sub> packing materials rely on ionised silanoate groups to generate an EOF, this is highly pH dependant (pH 4 – 11). The EOF in SCX materials is generated by ionised sulphonic acid groups, which remain ionised over a much greater pH range (pH 2 – 11). Bartle *et al.*<sup>39</sup> attempted to define the behaviour of cation-exchange materials in CEC, however, no clear conclusions could be drawn, and they suggested that the anomalous results obtained require further investigation. Smith and Evans<sup>40</sup> compared standard C<sub>18</sub>, ion exchange and a mixed mode (SCX / C<sub>6</sub>) phases, they concluded that C<sub>18</sub> and mixed mode phases exhibited similar selectivities. The ion exchange materials exhibited significantly different selectivities, with a complete reversal of elution order.

#### *a) Packing Methods*

An initial problem in the growth of CEC was the fabrication of reliable packed columns. Extensive method development has been cited in the literature.

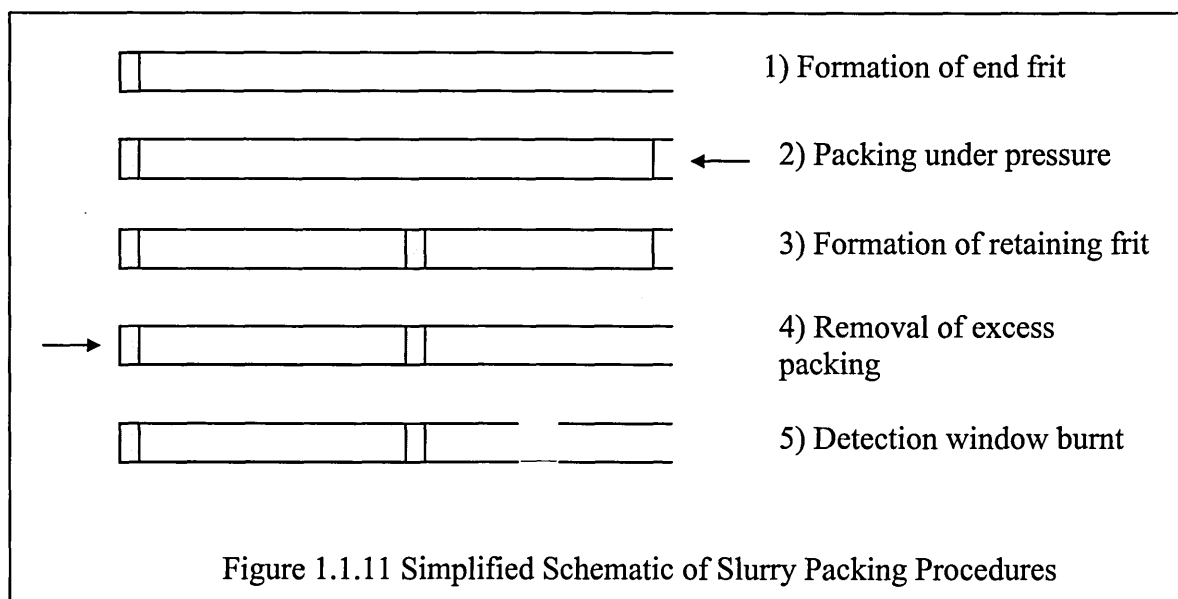
The method of packing can be divided into two main categories, *pressure* and *electrokinetically driven*. Both methods require stationary phase slurries in a solvent (typically acetone).

The initial packing step is the preparation of a retaining frit for the stationary phase to pack against. This frit can be formed by tapping the end of the capillary into silicate solution<sup>20, 21, 42-44</sup> or silica gel solution<sup>34, 45, 46</sup> to a length of ~1 mm, which is then secured by sintering. Once the inlet frit is in place the column can be packed.

*Pressure packing* - there have been several methods devised to slurry pack a column under pressure. These vary in the way the pressure is applied, through using an HPLC pump<sup>43-47</sup> a HPLC column packer<sup>22, 23, 34</sup>, centripetal force<sup>48</sup> or supercritical fluid<sup>49</sup>. The

use of an HPLC pump is most common (as they are widely available), however, they are limited in the pressure that they can supply. The column packer offers a higher packing pressure, which allows for faster, more efficient packing. The highly efficient packing of  $\mu$ -HPLC, GC, and SFC columns inspired the supercritical fluid method.

Figure 1.1.11 shows a simplified schematic of the slurry packing procedure.



*Electrokinetic packing* - was devised by an American group and has resulted in a patent application<sup>50</sup>. The capillary is inserted into a vial containing the stationary phase slurry, to which a voltage is slowly ramped up to 30 kV. This causes the packing material to migrate along with the buffer, resulting in a homogeneously packed column.

Electrokinetically packed columns can produce higher efficiencies than slurry packed because of the ability to pack small particle sizes, *i.e.* less than 1  $\mu\text{m}$   $d_p$ . This can be especially difficult by slurry packing methods.

Once the packed bed has reached a sufficient length (typically 20 cm) a retaining frit is fabricated and the columns are conditioned. The second frit can be burnt at the desired point and the initial frit left in place<sup>34,44,45</sup>, alternatively, the initial frit can be replaced and then a second (outlet) frit burnt. The later method was suggested by research groups at Glaxo Wellcome<sup>21-23</sup>, through the development of a frit burning device.

b) Dispersion in CEC

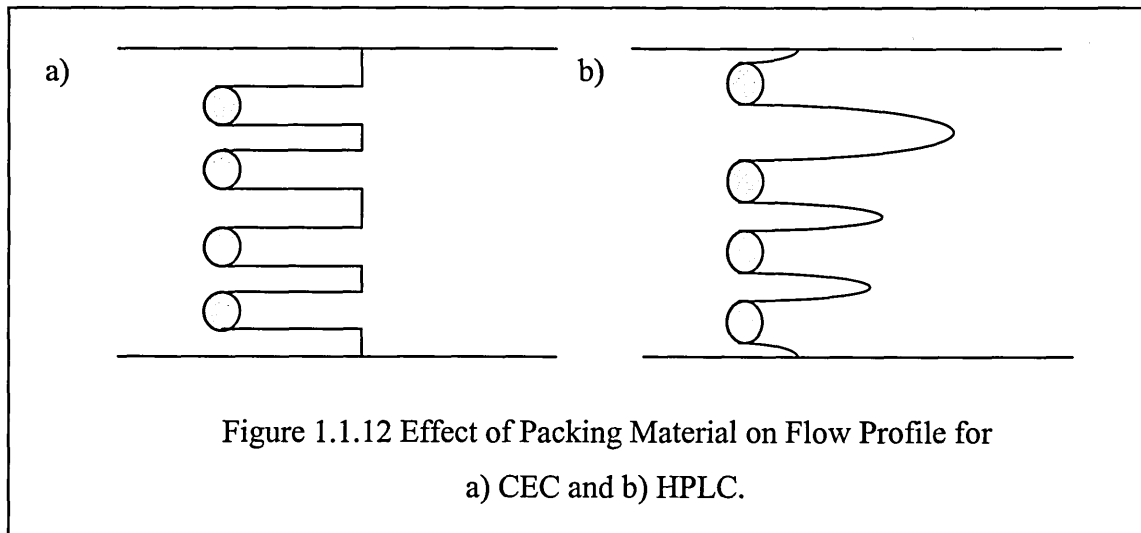
As in pressure driven HPLC, flow dispersion, resistance to mass transfer as well as longitudinal diffusion affects the plate height and hence efficiency. Therefore the complete Van Deemter equation must be used,

$$H = 2\lambda d_p + \frac{2\gamma D_m}{u} + \frac{1}{30} \left( \frac{k'}{1+k'} \right)^2 \frac{d_p^2 u}{D_{sz}} \quad \dots(1.1.11)$$

Which can be greatly simplified to Equation 1.1.12

$$H = A + \frac{B}{u} + Cu \quad \dots(1.1.12)$$

The A-term represents contributions from flow inhomogeneity in the packed bed (stream splitting and velocity variation within and between channels). Figure 1.1.12 shows how the flow rate may be expected to vary within a packed bed under EOF and pressure flow.



Under EOF all velocities will be almost identical since  $\mu_{EOF}$  does not vary with channel diameter ( $d_c$ ), providing  $d_c > 10\delta$ . In the case of pressure flow there will be a parabolic flow distribution over any channel, and the mean flow rate will vary between channels, wider channels providing higher flow rates.

Therefore, only the contribution from the variability in the direction of flow as the liquid negotiates the particles within the column has any significance on diffusion. The A-term in CEC is generally less than that obtained with HPLC for any particle size and can be further decreased on reduction of  $d_p$  (as demonstrated by Knox and Grant<sup>20</sup>). The

C-term arises from non-instantaneous rate of equilibration of analyte between the stationary and mobile phases.

Reduction of particle diameter will reduce diffusion ( $H \propto d_p^2$ ), and the use of sub-micron particles will result in the A- and C- terms becoming insignificant compared with longitudinal diffusion (B-term).

So as with CZE, the B-term of the van Deemter equation is dominant and efficiencies are significantly increased compared with HPLC.

Overall, CEC appears to be an extremely useful, complementary technique to CZE and HPLC, exhibiting the advantages of both techniques. However, further development is necessary to minimise bubble formation and to allow the routine production of packed columns. The use of ion exchange materials also requires further investigation, to define the focusing effects that are observed. The recent examination of packing materials through the use of molecular modelling software<sup>51</sup> will hopefully assist in defining the separation mechanisms involved in CEC separations using C<sub>18</sub> and ion exchange materials.

However CEC still primarily remains a research tool, requiring significant investigation into the underlying theory, and will remain so until these areas are further defined. Until then CEC will remain (an extremely useful) complementary separation technique to both CZE and HPLC.

#### **1.1.8.2 Micellar Electrokinetic Chromatography (MEKC)**

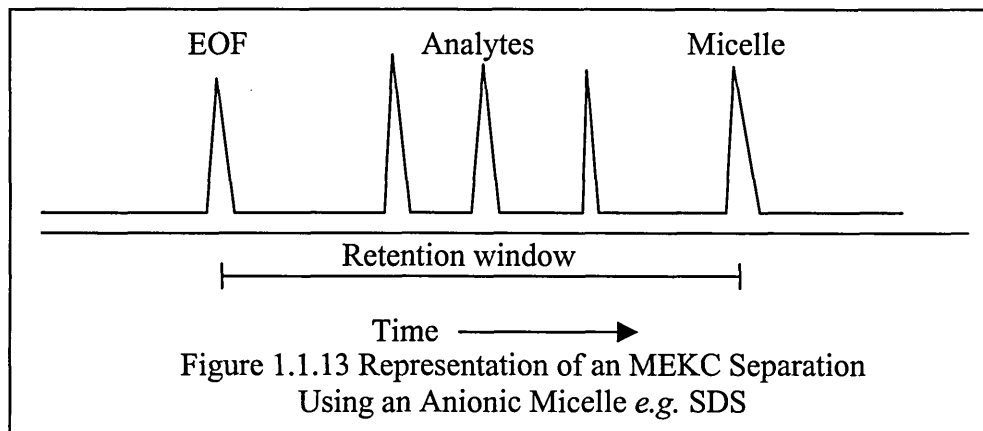
MEKC is a combination of electrophoresis and chromatography introduced by Terabe *et al.*<sup>52</sup> in 1984. MEKC is a useful complementary technique to CZE as it allows the simultaneous separation of neutral and ionic species and thus also provides an alternative to CEC.

Separation of neutral species is achieved by the use of a pseudo-stationary phase in the buffer, which is usually a surfactant above its critical micelle concentration (*e.g.* 8 – 9

mM for sodium dodecylsulphate, SDS). The micelles formed are generally spherical, with the hydrophobic tails pointing inwards and the charged heads orientated towards the buffer. The micelles are usually charged and migrate either with or against the EOF. However, the electrophoretic mobilities of the micelles are low, therefore flow is usually in the direction of the EOF.

Neutral species are separated due to partitioning between the micelles (through hydrophobic and electrostatic interactions) and the buffer. The greater the interaction, the longer the migration time, when not interacting with the micelle the analyte is carried along with the EOF.

Hydrophilic analytes do not interact with the micelles and migrate with the EOF, followed by increasingly hydrophobic (or associated) analytes, finally the micelles along with those analytes totally retained are detected (Figure 1.1.13).



The region in which the neutral analytes migrate is termed the 'retention window'. Resolution between analytes can be improved by increasing the time-scale of the retention window. This can be achieved by increasing the concentration or changing the surfactant. However, high concentrations can be problematic due to Joule heating experienced on increasing the ionic (surfactant) concentration.

Selectivity can be manipulated in MEKC by simply changing the surfactant (differing size, charge, geometry *etc.*). A limitation of MEKC is a lack of suitable surfactants for all types of analytes. Further selectivity can be obtained through the addition of modifiers (*i.e.* pH, buffer concentration, organic modifier *etc.*) to the buffer. These may affect the charge on the micelle or the analyte-micelle interaction; also the use of a

secondary pseudo-stationary phase (*e.g.* cyclodextrins) can improve separations of very hydrophobic analytes.

Chiral separations can be effected by MEKC through the use of a chiral pseudo-stationary phase providing selectivity between isomers. Terabe *et al.*<sup>53</sup> obtained a chiral separation through the use of bile salt micelles.

### **1.1.8.3 Capillary Gel Electrophoresis (CGE)**

CGE is directly comparable with traditional slab electrophoresis, with a number of advantages. These include significantly higher field strengths that can be employed without Joule heating effects (due to the non-convective nature of fused-silica capillaries), on column detection and simple automation.

CGE has generally been employed in the biological sciences for the separation of macromolecules (*i.e.* proteins and nucleotides) and was introduced by Cohen and Karger<sup>54</sup>. Separations are based on size and not charge-to-size ratio as in CZE. The addition of sub-units to macromolecules (*e.g.* amino acids to proteins and nucleotides to DNA fragments) results in a uniform increase in both size and charge, thus maintaining a constant charge-to-size ratio. The analytes migrate through a polymer network, which acts as a 'molecular sieve'. As charged analytes migrate through the polymer, they become hindered, with smaller analytes migrating first. Separations can be highly efficient with over  $10^7$  plates /m being generated for oligonucleotides.

### **1.1.8.4 Capillary Isoelectric Focusing (CIEF)**

CIEF is a focusing type of electrophoresis, in which amphoteric analytes (usually proteins) are separated by differences in their isoelectric points (pI). Amphoteric compounds can exist as either anions or cations, depending on the pH of the solution; the pH at which the analyte is neutral is termed the isoelectric point (pI).

The separation capillary is filled with a solution of ampholytes and the sample. An electric field is applied, creating a pH gradient across the capillary. The analytes form

narrow zones within the capillary at a position corresponding to their isoelectric points. If an analyte diffuses out of the zone, it encounters a different pH, acquires a charge and migrates back into the zone. Once a steady state has been achieved the focused zones are mobilised past the detector, which can be achieved by hydrodynamic flow (*i.e.* by pressure) or electrophoretic mobilisation.

#### **1.1.8.5 Capillary Isotachopheresis (CITP)**

CITP is a 'moving boundary' electrophoretic technique. A combination of two buffer systems is used, one of a higher mobility (leading electrolyte) and the other a lower mobility (trailing electrolyte) relative to the analytes. The capillary is filled with the leading electrolyte, the sample is then injected, and the capillary is then placed in a vial containing trailing electrolyte, an electric field is then applied in the *constant current* mode.

The analytes arrange in zones of increasing mobility, with subsequent differing electric fields, the zone of highest mobility experiences the lowest field. Therefore all zones migrate at the same velocity, resulting in sharp boundaries between analytes. If diffusion occurs into another zone the ion experiences a different electric field and diffuses back into the correct zone. The zones migrate through the capillary and are subsequently detected.

A unique feature of CITP is the data output, which features steps instead of the more familiar peaks. This is because the zones elute with very little separation, so no baseline is observed. The length of the steps or zones is proportional to the concentration of the analyte, as there are no peak heights measured (and no response differences); quantification using CITP is straightforward. Requiring that only a concentration *vs.* zone length calibration be performed for one analyte, all other analytes of similar molecular weight and ionic charge can be quantified without individual calibration.

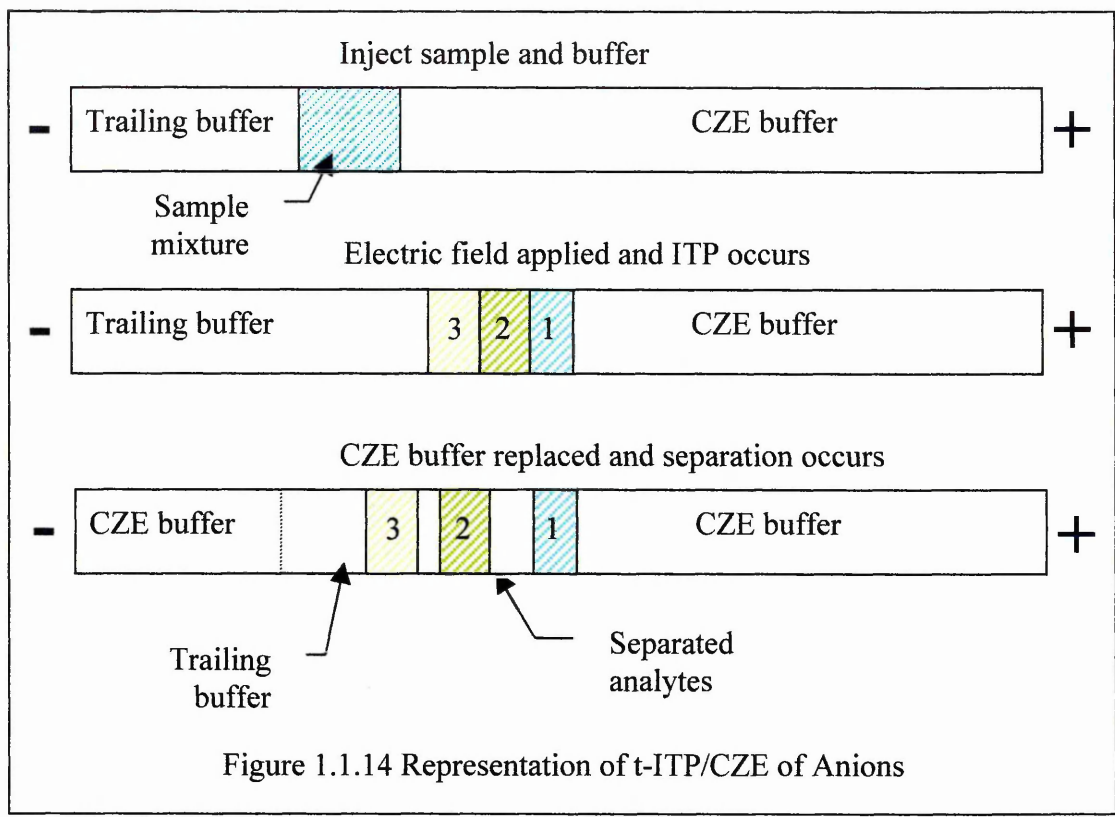
### 1.1.8.6 On-column Transient Isotachophoresis Preconcentration (t-ITP)

Capillary isotachophoresis can be used to concentrate diffuse analyte zones; it can also be used as a preconcentration stage prior to separation by CZE. Used as a preconcentration method it is termed t-ITP (the term transient is used as the analyte migration changes between ITP and CZE mode) and was initially developed by Karger *et al.*<sup>55,56</sup>.

In t-ITP the sample is injected between two buffers of differing conductivity, focusing then occurs on application of an electric field. The composition of the buffer is then changed such that ITP can no longer occur and the analytes are separated by CZE in the same capillary.

There are two basic modes of t-ITP, if the CZE buffer has a higher conductivity (mobility) than the sample (as in Figure 1.1.14) it can be used as the leading buffer. The sample is injected followed by a (lower conductivity) trailing buffer, ITP occurs. The trailing buffer is replaced with the CZE buffer and separation occurs. Alternatively, if the CZE buffer is of a lower mobility (conductivity) the sample is injected (into a capillary already filled with the CZE buffer) along with a salt that acts as a leading buffer, ITP occurs. After stacking occurs the analytes are separated by CZE.

A further benefit of t-ITP is the ability to inject larger volumes of dilute samples, t-ITP allows these samples to be focused and separated by CZE. Karger *et al.*<sup>56</sup> demonstrated t-ITP/CZE/MS for the analysis of proteins. The detection limits using t-ITP were increased by a factor of 100 to  $\sim 10^{-7}$  M, with injection volumes up to 750 nL in  $\sim 2.2$   $\mu$ L column ( $\sim 35\%$  column volume).



## References

---

- (1) Tiselius A. *Transactions of the Faraday Society* **33** (1937) 524
- (2) Hjerten S. *Chromatography Reviews* **9** (1967) 122
- (3) Mikkers FEP; Everaerts FM; Verheggen Th.PEM. *Journal of Chromatography* **169** (1979) 11
- (4) Jorgenson JW; Lukacs KD. *Journal of Chromatography* **218** (1981) 209
- (5) Tsuda T; Nomera K; Nakagawa G. *Journal of Chromatography* **248** (1982) 241
- (6) Knox JH. *Chromatographia* **26** (1988) 329
- (7) Baker DR. *Capillary Electrophoresis*. 1st Ed.; Wiley-Interscience: New York; 1995
- (8) Heiger DN. *High Performance Capillary Electrophoresis, An Introduction*. 1st Ed.; Hewlett Packard: France; 1992
- (9) Macka M; Andersson P; Haddad PR. *Analytical Chemistry* **70** (1998) 743
- (10) Moring SE; Reel RT; van Soest REJ. *Analytical Chemistry* **65** (1993) 3454
- (11) Harrold MP; Wajtusik MJ; Riviello J; Henson P. *Journal of Chromatography* **640** (1993) 463
- (12) Desbene-Monvernay A; Mofaddel N. *Annalysis* **27** (1999) 144
- (13) Tjornelund J; Hansen SH. *Journal of Biochemical and Biophysical Methods* **38** (1999) 139
- (14) Ellis DR; Palmer ME; Tetler LW; Eckers C. *Journal of Chromatography A* **808** (1998) 269
- (15) Wren SAC. *Journal of Chromatography* **636** (1993) 57
- (16) Pretorius V; Hopkins BJ; Schieke JD. *Journal of Chromatography* **99** (1974) 23
- (17) Jorgenson JW; Lukacs KD. *Journal of Chromatography* **218** (1981) 209
- (18) Stevens TS; Cortes HJ. *Analytical Chemistry* **55** (1983) 1365
- (19) Knox JH; Grant IH. *Chromatographia*. **24** (1987) 135
- (20) Knox JH; Grant IH. *Chromatographia*. **32** (1991) 317
- (21) Smith NW; Evans MB. *Chromatographia* **38** (1994) 649
- (22) Smith NW; Evans MB. *Chromatographia* **41** (1995) 197
- (23) Boughtflower RJ; Underwood T; Paterson CJ. *Chromatographia* **40** (1995) 329
- (24) Fujimoto C; Fujise Y; Matsuzawa E. *Analytical Chemistry* **68** (1996) 2753
- (25) Liao JL; Chen W; Ericson C; Hjerten S. *Analytical Chemistry* **68** (1996) 3468
- (26) Peters EC; Petro M; Svec F; Fréchet JM. *Analytical Chemistry* **69** (1997) 3646
- (27) Palm A; Novotny MV. *Analytical Chemistry* **69** (1997) 4499
- (28) Jacobson SC; Hergenröder R; Koutny LB; Ramsey JM. *Analytical Chemistry* **66** (1994) 2369
- (29) Carney RA; Robson MM; Bartle KD; Myers P. *Journal of High Resolution Chromatography* **22** (1999) 29
- (30) Tsuda T. *Analytical Chemistry* **59** (1987) 521
- (31) Tsuda T. *Analytical Chemistry* **60** (1988) 1677
- (32) Tsuda T. *LC-GC International* **5** (1992) 26
- (33) van den Bosch SE; Heemstra S; Kraak JC; Poppe H. *Journal of Chromatography A* **755** (1996) 165
- (34) Behnke B; Bayer E. *Journal of Chromatography A* **680** (1994) 93
- (35) Taylor MR; Teale P. *Journal of Chromatography A* **768** (1997) 89
- (36) Yan C; Dadoo R; Zare RN; Rakestraw DJ; Anex DS. *Analytical Chemistry* **68** (1996) 2726
- (37) Kitagawa S; Tsuji A; Watanabe H; Nakashima M; Tsuda T. *Journal of Microcolumn Separations* **9** (1997) 347

- 
- (38) Wei W; Luo G; Yan C. *American Laboratory* January (1998) 20C
- (39) Cikalo MG; Bartle KD; Myers P. *Analytical Chemistry* **71** (1999) 1820
- (40) Smith N; Evans MB. *Journal of Chromatography A* **832** (1999) 41
- (41) Cikalo MG; Bartle KD; Myers P. *Journal of Chromatography A* **836** (1999) 25
- (42) Rebscher H; Pyell U. *Chromatographia* **38** (1994) 737
- (43) Yamamoto H; Bauman J; Erni F. *Journal of Chromatography* **593** (1992) 313
- (44) Whitaker KW; Sepaniak MJ. *Electrophoresis* **15** (1994) 1341
- (45) Li S; Lloyd DK. *Analytical Chemistry* **65** (1993) 3684
- (46) Rebscher H; Pyell U. *Chromatographia* **42** (1996) 171
- (47) Gordon DB; Lord GA; Jones DS. *Rapid Communications in Mass Spectrometry* **8** (1994) 544
- (48) Fermier AM; Colón LA. *Journal of Microcolumn Separations* **10** (1998) 439
- (49) Robson MM; Raulin S; Sheriff Sm; Raynor MW; Bartle KD; Clifford AA; Myers P; Euerby MR; Johnson CM. *Chromatographia*. **43** (1996) 313
- (50) Yan C. *Electrokinetic Packing Of Capillary Columns*. **US Patent Application 08 142, 917** (Oct 29 1993)
- (51) Myers P. Oral Presentation at 24th Annual BMSS Meeting, University of Reading, 13 – 15th September, 1999
- (52) Terabe S; Otsuka K; Ichikawa K; tsuchiya A; Ando T. *Analytical Chemistry* **56** (1984) 111
- (53) Terabe S; Shibata M; Miyashita Y. *Journal of Chromatography* **480** (1989) 403
- (54) Cohen AS; Karger BL. *Journal of Chromatography* **397** (1987) 409
- (55) Foret F; Szoko E; Karger BL. *Journal of Chromatography* **608** (1992) 3
- (56) Thompson TJ; Foret F; Vouros P; Karger BL. *Analytical Chemistry* **65** (1993) 900

## **Section 1.2**

### ***Mass Spectrometry***

### ***1.2.1 Introduction***

A mass spectrometer must, in the most basic form be able to achieve the following functions:

- Produce gas phase ions from sample molecules.
- Separate the ions produced according to their mass-to-charge-ratio ( $m/z$ ), and subsequently detect and record them.

Mass spectrometers require an elaborate vacuum system to maintain low pressures ( $10^{-4}$  -  $10^{-9}$  mbar), in order that the ion beam is not attenuated by collisions with air particles.

Mass spectrometry evolved around the beginning of the century from the studies of ions in electrostatic and magnetic fields. During the following decades the instrumentation was refined and provided useful information on the isotopic abundance of various elements. By the 1940s reliable mass spectrometers were commercially available. These instruments were designed for use as quantitative tools specifically for the petroleum industry. By the middle of the 1950s commercial mass spectrometers were available for both quantitative and qualitative determinations based upon mass-to-charge ratio ( $m/z$ ). Beginning in 1960, there was a major trend towards using mass spectrometers for structural elucidation by studying fragmentation patterns. Recently, mass spectrometry has advanced greatly in many areas including the characterisation of biological compounds.

### ***1.2.2 Instrumentation<sup>1</sup>***

The main components of a mass spectrometer are as follows:

- Inlet systems
- Ionisation sources
- Mass analysers / filters
- Detectors

### 1.2.2.1 Inlet Systems

The purpose of the inlet system is to transfer the sample from atmospheric pressure to the high vacuum of the instrument. There are three types of the inlet commonly found, which accommodate various types of sample.

- Batch Inlet - The simplest inlet, in which the sample is volatilised externally and allowed to leak into an ionisation region.
- Direct Probe Inlet - Solids and non-volatile liquids can be introduced into the ionisation region by means of a probe, inserted through a vacuum lock.
- Chromatographic Inlet - Mass spectrometers are often coupled with chromatographic systems to permit on-line detection of separated mixtures. Specialised inlet systems / ion sources are required to be able to cope with the large volume of solvent from liquid chromatographic techniques expanding into the high vacuum region. Gas chromatography, however, can be interfaced directly with ion sources such as electron ionisation, but GC/MS is outside the context of this study. Liquid chromatographic interfacing will be dealt with in more detail in Section 1.2.2.2.

### 1.2.2.2 Ionisation Sources

The ion source, traditionally, consists of a small chamber, which is held under vacuum, into which the sample is introduced and ionised. Ions formed are ejected from the source into the mass analyser by a potential difference held between an exit slit and a repeller plate (or a potential gradient across a number of sampling orifices).

The classical mass spectrometry ionisation source is electron ionisation (EI). Sample vapour is introduced into a chamber, which is then ionised by a beam of electrons produced by a heated tungsten filament. The ions are then ejected out of the source by a repeller electrode.

This is summarised (1.2.i):



Thus a radical cation is formed (this is called a molecular ion). The ionising electron is accelerated by a voltage to 70 eV. This high energy interaction in conjunction with the

high vacuum of the instrument ( $10^{-6}$  mbar) can leave some molecules with excess internal energy, which causes bonds to break leading to ion fragmentation (Scheme 1.2.ii):



Intact molecular ions are sometimes not detected; therefore, a technique called chemical ionisation (CI) was developed, in which a reagent gas (such as methane) is introduced into the ion source. Interaction of an ion and a molecule can lead to a reaction generating a new charged species, this process is termed an *ion / molecule reaction*.

For example, the reaction between a methane ion and methane results in the formation of a carbocation ( $CH_5^{+}$ ) (Scheme 1.2.iii):



For ion / molecule reactions of this type to occur much higher source pressures ( $10^{-3}$  mbar) are required *cf.* EI sources. Many collisions will occur within the source at these high pressures resulting in an equilibration of internal energies.

If an analyte (M) is present in the source this can collide with the carbocation (called reactant gas ion) to form a protonated molecule,  $[M+H]^{+}$ . This is summarised:



There are numerous reagent gases (for example, hydrogen, ammonia, butane, methanol *etc.*), different gases result in various degrees of fragmentation, which can be related to the proton affinity (PA) of the reactant gas. The lower the PA the more exothermic the reaction between reactant gas and analyte. For highly exothermic reactions fragmentation can occur. For example, the use of methane (PA  $551 \text{ kJ mol}^{-1}$ ) as a reactant gas frequently results in fragmentation, whereas isobutane (PA  $824 \text{ kJ mol}^{-1}$ ) results primarily in the formation of a protonated molecule ( $[M+H]^{+}$ ).

An inlet system has been developed which allows liquid chromatography to be interfaced to an EI source; this was termed particle beam. The eluent from the LC passes through a nebuliser, forming droplets, which then pass into a desolvation

chamber where solvent evaporates. Further solvent is removed when the droplets pass through a skimmer into an evacuated chamber. Any solvent still associated with the analyte is removed when the droplets pass through a second skimmer and heated wire grid into the ion source (either EI or CI).

Unfortunately, a prerequisite of both EI and CI (and consequently particle beam) is that the analyte needs to be volatile. Most biological molecules are polar and therefore involatile. Fast atom bombardment (FAB) was developed to enable mass spectrometry to be used in the study of involatile polar compounds. An atom or ion gun is used to project heavy fast atoms (argon or xenon) or ions (caesium,  $\text{Cs}^+$ ) onto the surface of a target solution (matrix). The matrix consists of the analyte dissolved in a high boiling point solvent (such as glycerol, 3-nitrobenzyl alcohol), which does not evaporate quickly in the ion source. The impact of the atoms or ions on the surface of the solution results in the desorption of 'secondaries' (positive and negative ions and neutrals) into the region above the matrix surface. A set of lenses held at a potential will accelerate the ions (either positive or negative) into the mass analyser. FAB usually results in protonated ions, with little or no internal energy, thus fragmentation occurs to a lesser extent than in EI. A development of FAB, continuous-flow FAB, allows chromatographic systems to be directly interfaced to FAB (see Section 1.2.2.2 b).

For capillary electrophoresis to be successfully interfaced to mass spectrometry the analyte emerging from the column needs to be transferred into the vacuum system (and ionised). The ionisation interfaces used to accomplish this are electrospray (ESI, a form of atmospheric pressure ionisation) and continuous-flow fast atom bombardment (flow-FAB), which are discussed in the following sections.

#### *a) Atmospheric Pressure Ionisation (API)*

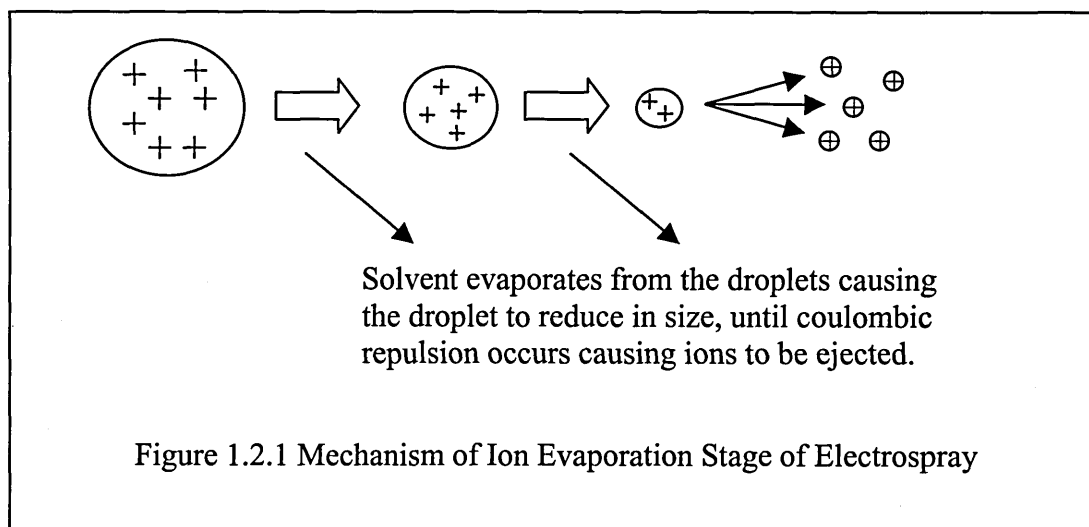
A stream of solvent containing the analyte of interest (often liquid chromatographic eluent) undergoes nebulisation to form a spray of fine droplets at atmospheric pressure. The droplets carry an excessive positive or negative charge. The droplets are transported through a heater, in which solvent evaporates, as the droplets decrease in

size, electrostatic repulsion occurs causing charged particles to be expelled. These particles can then be sampled into the mass spectrometer.

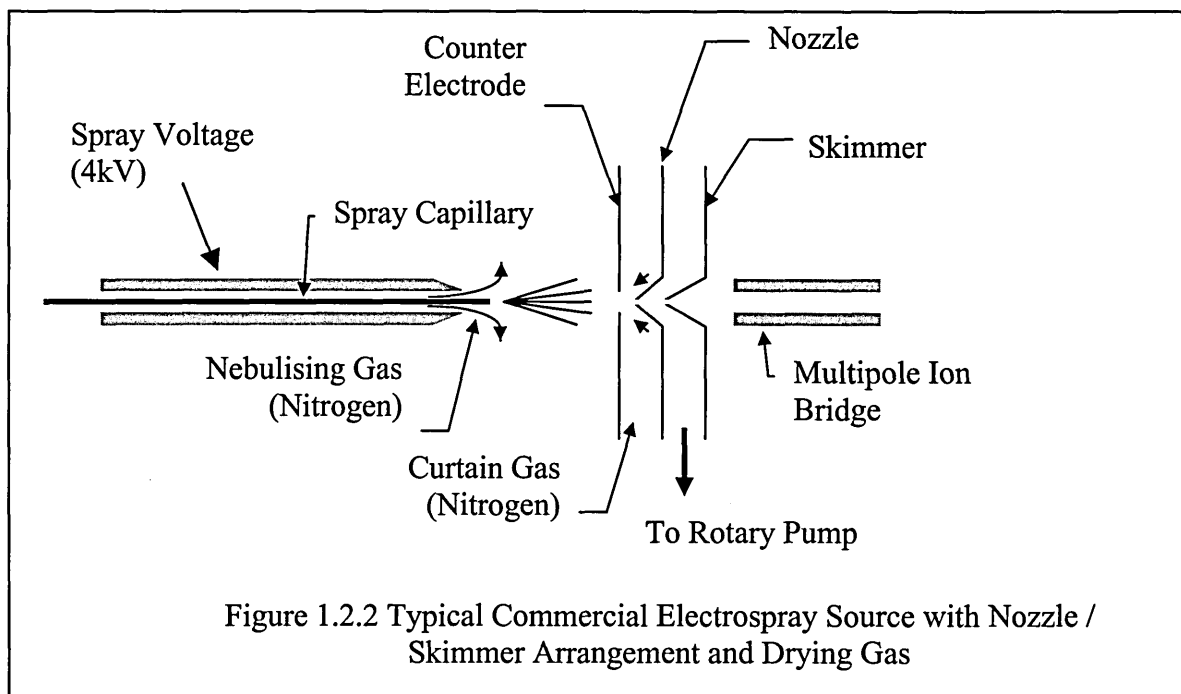
Sensitivity is increased if a secondary ionisation step occurs. This can be in the form of a high electric field (electrospray, see below), high temperature (thermospray) or the combination of high temperature and plasma discharge (plasmaspray or atmospheric pressure chemical ionisation (APCI)). These ionisation techniques (along with FAB) are termed 'soft' ionisation methods, which result in little or no fragmentation and the generation of protonated molecules.

*i) Electrospray Ionisation (ESI)*

ESI is an atmospheric pressure ionisation (API) technique, that is ionisation takes place at atmospheric pressure and ions are then transferred into the vacuum system of the mass spectrometer. Ionisation is achieved during the electrostatic nebulisation of a solution of analyte ions by a high electrical field gradient ( $> 3 \text{ kVcm}^{-1}$ ) between a spray needle and counter electrode. Highly charged droplets are formed in a dry bath gas of nitrogen. These charged droplets shrink as neutral solvent evaporates until the charge density exceeds the Rayleigh limit and coulombic repulsion causes the droplet to divide (Figure 1.2.1). The Iribane and Thomson<sup>2,3</sup> model suggests that the smaller droplets continue to evaporate and the process repeats until evaporation of charged solutes occurs.



The evaporation of solvent is aided through the use of nebulising and bath gas (typically nitrogen). The nozzle / skimmer inlet arrangement allow the ions to be sampled from atmospheric pressure into the high vacuum of the instrument by passing through differentially (rotary) pumped chambers. A typical commercial electrospray source is represented in Figure 1.2.2.



ESI was originally described by Dole *et al.*<sup>4,5</sup>, studying the intact ions of synthetic polymers in excess of 100 kDa, with detection by Faraday-cage. No data was published for the following fourteen years until Fenn *et al.*<sup>6,7</sup> used ESI with a quadrupole mass analyser. Demonstrating fundamental aspects of ESI, the analysis of modest molecular weight biomolecules and its ability as an interface for combining liquid chromatography and mass spectrometry was achieved<sup>8</sup>. A Russian group<sup>9</sup>, working independently, using a magnetic sector instrument, almost simultaneously reported similar results.

An advantage of electrospray ionisation is the formation of multiply charged ions, *i.e.*  $[M+zH]^{z+}$  where  $z > 1$ . Large molecules can contain many basic sites, which can all become protonated. A mass spectrometer analyses ions by differences in mass-to-charge ratios ( $m/z$ ), when singly charged ions ( $z = 1$ ) are detected,  $m/z = m$ . Increasing the number of charges on a molecule reduces the observed  $m/z$ , thus  $m/z < m$ , thus allowing large molecules to be analysed on instruments having limited upper-mass

range.

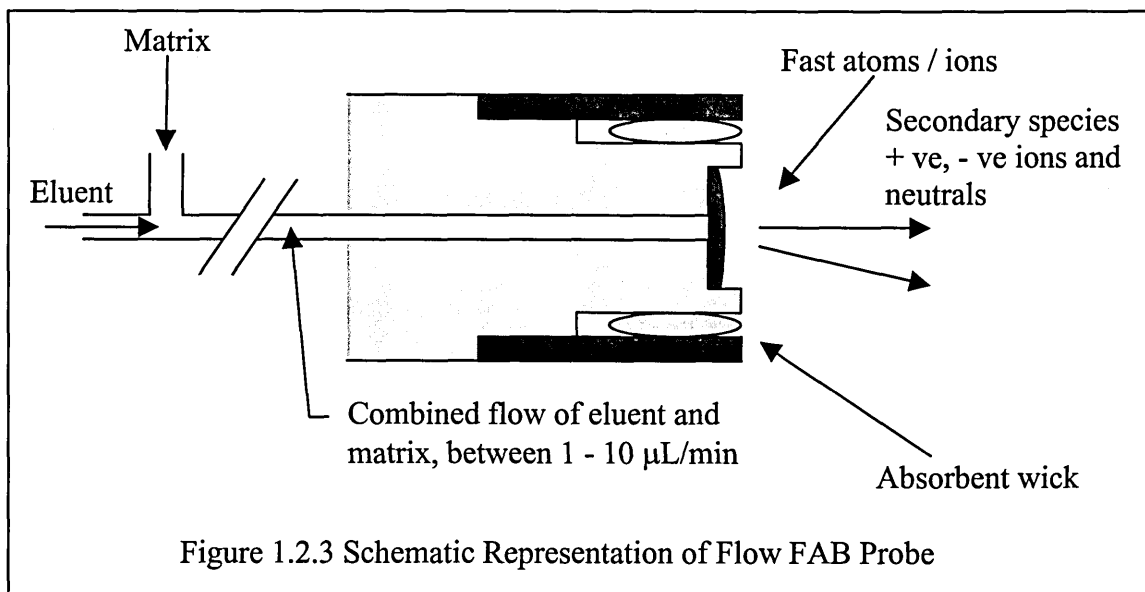
The use of multiply charged ions was initially demonstrated by Fenn *et al.*<sup>10</sup>. Polyethylene glycol oligomers with a nominal molecular mass of 17.5 kDa were observed bearing a net charge of +23. The reduction in the mass-to-charge ratio allowed these ions to be detected on an instrument of low upper-mass limit. The multiple protonation of basic sites of peptides and proteins extended the mass range of analysis up to 40 kDa using a quadrupole mass spectrometer of  $m/z$  limit 1600<sup>11</sup>. Other laboratories rapidly confirmed this work<sup>12</sup>. The utility of multiple charging has allowed the analysis of molecules with RMM greater than ~2.5 MDa<sup>13</sup> using conventional mass spectrometers.

#### *ii) Atmospheric Pressure Chemical Ionisation (APCI)*

APCI is performed on similar instrumentation to ESI. Nebulisation is achieved by a thermal process rather than using the high potential associated with ESI. The fine mist of sample and solvent is carried by a flow of nitrogen past a corona discharge needle where ionisation occurs. The plasma generated at the corona discharge strips electrons from neutral solvent (or nitrogen) molecules, which then react with the analyte in similar ways to CI.

#### *b) Continuous Flow Fast-atom-bombardment (cf-FAB)*

Continuous-flow FAB (otherwise known as dynamic FAB) employs a constant flow of matrix onto the target area. The liquid flow is normally comprised of the eluent from a chromatographic separation mixed with the matrix. The flow FAB probe (Figure 1.2.3) employs a heated metallic frit at the target area, which aids the evaporation of solvent and matrix from the probe tip and prevents freezing as the liquid evaporates in the vacuum. This results in flow rates of 1 - 10  $\mu\text{L}/\text{min}$  being readily dealt with. To obtain such flow rates from standard (4.6, 2.1 mm) analytical columns a substantial split is required, thus reducing sensitivity, therefore microbore (<1 mm) HPLC and CE techniques (which produce these flow rates) are ideally suited to flow FAB. Flow FAB has been demonstrated<sup>14-18</sup> to be readily combined directly with CE.



### 1.2.2.3 Mass Analysers

A mass analyser is used to separate ions due to differences in their mass-to-charge ratio ( $m/z$ ). The classical mass analyser is the magnetic sector analyser. There are two main types of magnetic sector, single and double focusing mass analysers. In single focusing instruments ion separation is achieved using a magnet. The magnetic field is swept to focus ions of similar mass-to-charge ratio sequentially onto the detector. Therefore a single focusing instrument has directional focusing capabilities. Double focusing instruments employ a magnet and an electrostatic analyser (ESA, usually referred to as an electric sector). The ESA functions to focus any energy spread at the detector, with momentum separation achieved by the magnet, resulting in a higher resolution spectrum. Double focusing instruments can have two orientations, an instrument with the ESA before the magnet is known as *forward geometry* and if the ESA is placed after the magnet *reverse geometry*.

Magnetic sector instruments generally scan too slowly for routine use with capillary electrophoresis, as the peak widths are of the order of a few seconds. Therefore fast scanning analysers are frequently used for this type of work. The most widely used are quadrupole mass filters (Section 1.2.2.3 a), and increasingly, time-of-flight analysers (ToF MS, Section 1.2.2.3 b). Ion traps (IT MS) and Fourier-transform ion-cyclotron-

resonance (FT-ICR MS) mass spectrometers have also been used.

Ion traps consist of a ring (similar in shape to a doughnut) with two end cap electrodes. Application of radio frequency potentials to the electrodes can result in ions being stored within the cell and then selectively removed and detected.

FT-ICR consists of an ion cell contained within the solenoid of a superconducting magnet, under an extremely high vacuum ( $10^{-9}$  mbar). An ion contained within the cell is constrained to move in a circular direction, perpendicular to the magnetic field. The frequency of circulation depends on the magnetic field strength and ion mass-to-charge ratio, the ions are prevented from escaping by application of a d.c. voltage across trapping plates within the cell. Ions are excited to a greater orbit by the application of a radio frequency (r.f.) pulse. The increased ion motion causes image currents to be detected on receiver plates of the cell. The decay of these images is monitored as the coherent motion of the ions is destroyed by collisions. This electrical signal is transformed from the 'time-domain' to 'frequency-domain' by the mathematical process of Fourier-transformation, resulting in the generation of a mass spectrum.

Frequencies can be detected with a high degree of accuracy, therefore ultra high resolutions can be obtained ( $3 \times 10^8$  for the  $O^+$  ion). However, resolution decreases rapidly with increasing mass-to-charge ratio.

#### *a) Quadrupole Mass Filters<sup>19</sup>*

The quadrupole mass filter consists of four short, parallel, rod-like electrodes with a hyperbolic, elliptical or circular cross-section (Figure 1.2.4). The diagonally opposed electrodes are at the same potential and are separated by the distance  $2r_0$ . One pair of rods is attached to the positive terminal of a d.c. source and the other pair to the negative terminal. A variable radio frequency a.c. potential is applied to each pair of rods, with one pair being  $180^\circ$  out of phase with the other.

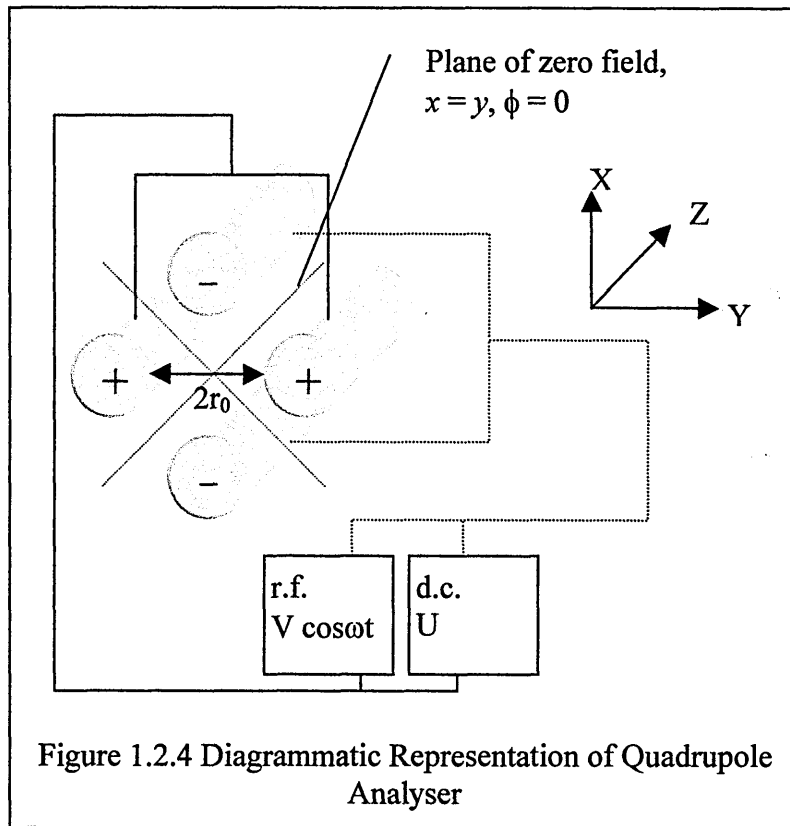


Figure 1.2.4 Diagrammatic Representation of Quadrupole Analyser

The potential ( $\phi$ ) applied to the electrodes is of the form

$$\phi_0 = U + V \cos \omega t \quad \dots(1.2.1)$$

$U =$  d.c. voltage;  $V \cos \omega t =$  r.f. potential

The potential at any point ( $x, y$ ) in the quadrupole field is then:

$$\phi = \frac{\phi_0(x^2 - y^2)}{r_0^2} \quad \dots(1.2.2)$$

Thus for  $x = y, \phi = 0$ , this gives rise to planes of zero field strength (represented as red lines in Figure 1.2.4). At all other positions within the rods, the oscillating electric field causes the ions to be alternatively attracted and repelled. The electric field has no effect on the ion in the  $z$ -axis, and requires an accelerating potential between the ion source and the assembly in order for ions to be transmitted through the rods.

The oscillatory nature of the electric field results in two different trajectories between the rods (dependant on the parameters  $U, V, \omega, m/z$  and  $r_0$ ). The first is for a stable trajectory, in which the ion oscillates along the  $z$ -axis, with amplitude of less than  $r_0$ . The second is for an unstable trajectory, in which the amplitude of the oscillations

increases exponentially and the ion eventually collides with or passes between the rods and is lost. So therefore for a particular  $m/z$  value there are specific d.c. voltage (U), r.f. amplitude (V) and frequency ( $\omega$ ) values, which allow stable trajectory ( $r_0$  is fixed) and hence for the ion to be transmitted. A mathematical solution for the stable transmission of ions through the field results in two important parameters,  $a$  and  $q$ ,

$$a = \frac{8zU}{m\omega^2 r_0^2} \quad ; \quad q = \frac{4zV}{m\omega^2 r_0^2} \quad ; \quad \frac{a}{q} = \frac{2U}{V} \quad \dots(1.2.3)$$

The conditions for stability can be represented on a stability diagram (Figure 1.2.5). The zone of stable combinations of  $a$  and  $q$  lies between the two curves representing the limits of stability in the  $x$  and  $y$  directions.

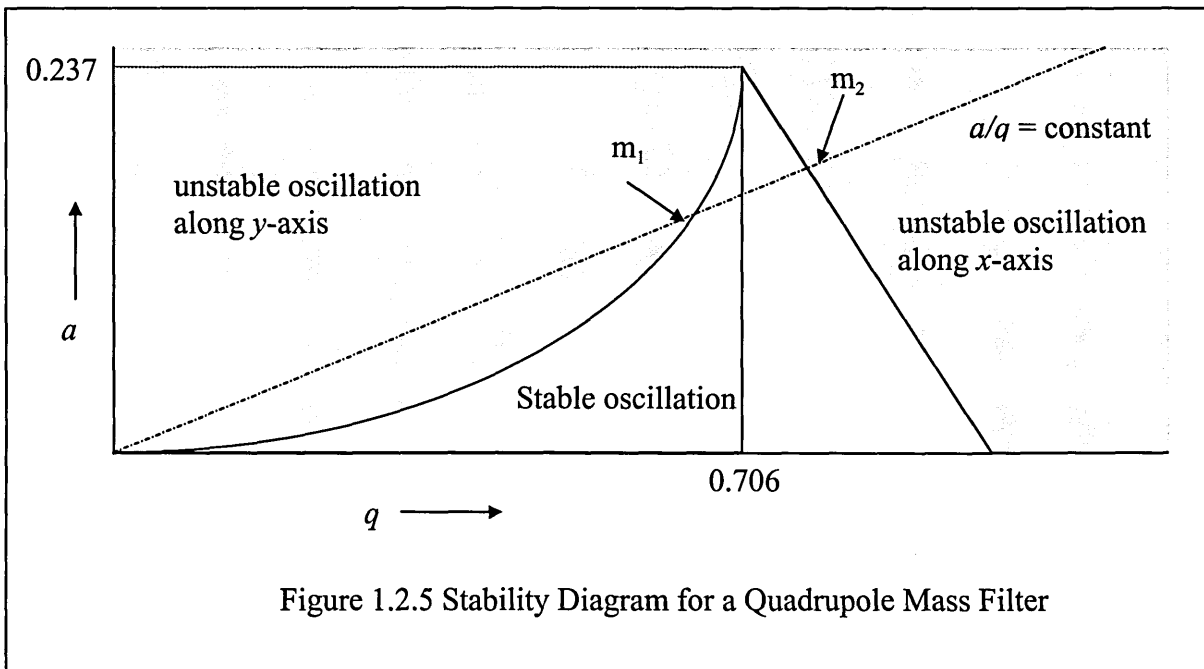


Figure 1.2.5 Stability Diagram for a Quadrupole Mass Filter

Therefore for the values of  $a/q = \text{constant}$  all ions between  $m_1/z$  and  $m_2/z$  will pass through the rods. For maximum resolution a value of  $a/q = \text{constant}$  must be chosen that intersects the curve as close to the apex as possible, therefore transmitting only a small range of  $m/z$  at a time. 'Scanning' of  $a/q = \text{constant}$  (*i.e.* changing the parameters U, V and  $\omega$ ) will result in consecutive  $m/z$  values to be transmitted.

It is easier to change voltages (U and V) than frequency ( $\omega$ ). Therefore to transmit ions of differing  $m/z$  value, the frequency is maintained constant and the voltages are varied in such a way that U/V (or  $a/q$ ) remains constant. Therefore by continuously increasing or decreasing U and V (whilst keeping the ratio constant) ions of increasing or

decreasing  $m/z$  successively traverse the quadrupole assembly resulting in a mass spectrum.

In a triple quadrupole instrument, there are three sets of quadrupole rods placed in series (generally termed Q1, Q2 and Q3). The middle quadrupole (Q2, which can also be a hexa- or octapole) is used in the 'r.f. only' mode, which means it simply acts as a focusing lens, it can also act as a collision cell for tandem mass spectrometry experiments, allowing collision induced dissociation (CID) to occur. Triple quadrupoles have a significant advantage over a single quadrupole for structural elucidation using tandem mass spectrometry (MS/MS) scanning methods.

#### *Tandem Mass Spectrometry (MS/MS) Scanning Techniques*

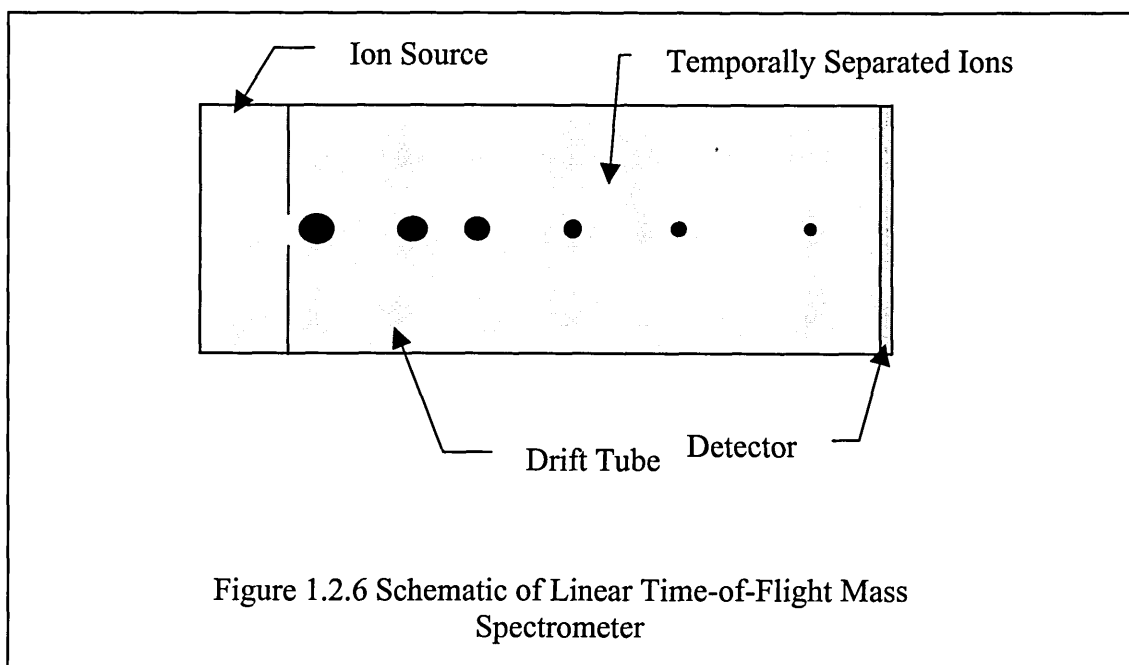
There are four types of MS/MS scanning techniques that can aid in structural elucidation:

1. *Product Ion Scan*: Q1 is set to transmit one ion of interest, CID occurs in Q2, Q3 is scanned and the fragment ions detected. Useful for determining / confirming structure.
2. *Precursor Ion Scan*: Q1 is set scanning, CID occurs in Q2, Q3 is set to transmit one ion of interest. The mass spectrum obtained indicates all the precursor ions to a chosen product. Confirmatory / complementary information to product ion scans, screening mixtures for a *constant neutral loss* (see below).
3. *Multiple Reaction Monitoring (MRM)*: This is the MS/MS version of single ion monitoring (SIM), in which Q1 is static on the ion of interest, CID occurs in Q2 and Q3 is static on the product ion of interest. An increase in sensitivity ( $\sim \times 100$ ) is obtained over scanning MS/MS because of the increased dwell time on each analyte. Useful for rapid screening of 'dirty' samples for known analytes.
4. *Constant Neutral Loss*: The scans of Q1 and Q3 are synchronised with an offset characteristic to the elimination of a neutral species, *i.e.* loss of 44 from carboxylic acids. Useful for screening mixtures for particular classes of compound.

## b) Time-of-flight Analysers<sup>20</sup>

In recent years the technique of time-of-flight mass spectrometry (ToF MS) has re-established itself as a mainstream technique (mainly due to the development of pulsed ionisation techniques, such as a matrix assisted laser desorption / ionisation (MALDI)). ToF MS has distinct advantages<sup>21</sup> over scanning instruments, these include high duty factors (percentage of ions formed that are detected), fast acquisition rates, sensitivity and wide mass range. Recent advances in API sources (electrospray) along with the development of high-speed electronics and computers, the introduction of the ion mirror (reflectron)<sup>22</sup> and orthogonal acceleration<sup>23</sup> (oa-ToF) have further increased the development of ToF MS.

The ToF MS in its simplest form is the linear analyser. Ions are accelerated out of the ion source at a high potential (up to 20 kV) into a field-free 'drift tube' to a detector (schematically represented in Figure 1.2.6).



The length of time taken for an ion to traverse the drift tube depends on velocity, which in turn depends on its mass and charge via energy gained in acceleration. For singly charged ions the length of time taken to travel from the source to the detector is proportional to a function of mass. The lower the mass the faster the flight time (kinetic energy and mass are fixed, therefore velocity varies). The simple nature of the analyser results in increased sensitivity (due to enhanced transmission and the non-

discriminatory mass analysis) for ToF MS compared with that of quadrupole or magnetic sector instruments.

Ions are produced and a short pulse is used to extract them from the ion source (a pulse is used because the start time must be the same for all ions). The ions are then accelerated through an electric field ( $E$  volts). The velocity ( $v$ ) attained by the ions is given by Equation 1.2.4,

$$\frac{mv^2}{2} = zeE \quad \dots(1.2.4)$$

where  $m$  = mass,  $z$  = number of charges on ion,  $e$  = charge on an electron.

Rearrangement gives Equation 1.2.5:

$$v = \sqrt{\frac{2zeE}{m}} \quad \dots(1.2.5)$$

If the distance from the source to the detector is  $d$ , then the time taken for an ion to traverse this distance is given by Equation 1.2.6:

$$t = \frac{d}{v} = \frac{d}{\sqrt{2zeE/m}} = d \left[ \frac{\sqrt{m/z}}{\sqrt{2eE}} \right] \quad \dots(1.2.6)$$

$d$  is fixed,  $E$  is constant and  $e$  is a universal constant. The flight time of an ion,  $t$  is directly proportional to the square root of its  $m/z$  (Equation 1.2.7).

$$t = \sqrt{(m/z)} \times C \quad \dots(1.2.7)$$

where  $C$  = a constant.

### *i) Resolution*

The resolution of a linear ToF MS is limited, particularly at higher mass. This is due to an inherent problem with the technique and a practical problem. Flight times are proportional to the square root of  $m/z$ , the difference between two masses ( $t_m$  and  $t_{m+1}$ ) separated by one mass unit is given by Equation 1.2.8:

$$t_m - t_{m+1} = \Delta t = \left[ \left( \sqrt{m/z} \right) - \left( \sqrt{(m+1)/z} \right) \right] \times C \quad \dots(1.2.8)$$

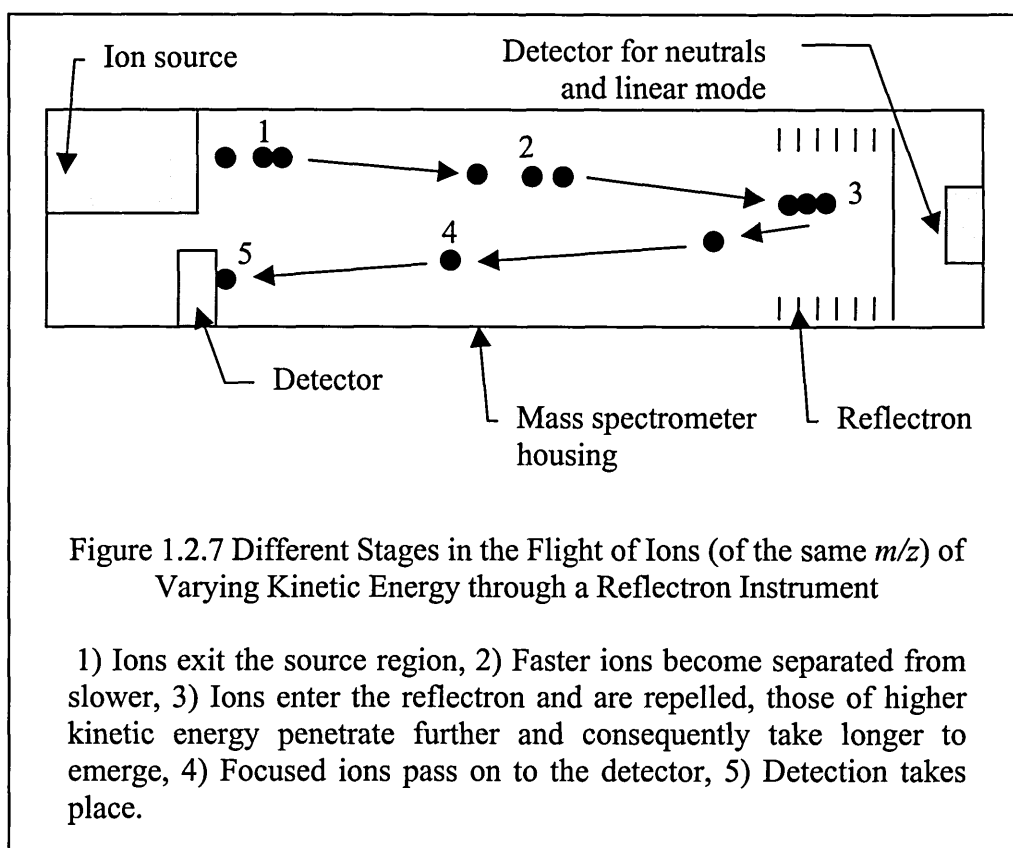
As  $m$  increases,  $\Delta t$  becomes smaller, making the arrival time of ions at the detector smaller and more difficult to differentiate. An (impossible) solution would be to make the flight tube of infinite length.

The practical disadvantage is that not all ions are created at the same time or location in the source thus discrepancies in kinetic energy and flight time arise. This effects (decreases) instrument resolution, but the problem can be reduced by the incorporation of a reflectron into the instrument. Metastable decomposition of ions can also occur within the (field-free) flight tube. If an energy loss is associated with the decomposition, flight time will increase. This results in an increase in the spatial spread of ions and thus decreases resolution. The effects of metastable decomposition can also be reduced through the use of a reflectron.

### *ii) The Reflectron<sup>22</sup>*

A homogeneous electric field is placed at the end of the flight path of the ions, which is the same polarity as the ions (*i.e.* a retarding force). The ions decelerate, and are repelled out of the field, the ions are thus 'reflected' (Figure 1.2.7).

The reflectron corrects positional and velocity discrepancies in the acceleration region of the ToF MS and removes neutral species which may have resulted from in-flight decay. Faster ions (having greater kinetic energy) will penetrate the electrostatic field further than slower ions, thus spending marginally more time in the reflectron, causing the ions to exit the reflectron together, in the same time frame. This results in a decrease in the spatial spread of the ions, leading to an increase in resolution. Resolutions in excess of 5000 (FWHM) are now readily available. However, a decrease in sensitivity (especially at higher mass), is observed when using a reflectron. This is caused by ion loss due to collisions and dispersion from the main beam. ToF analysers frequently contain two detectors (Figure 1.2.7). One which operates in 'linear' mode (no field applied to the reflectron, ions pass straight through and are consequently detected) or 'reflectron' mode where the ions are reflected as described above and consequently detected (the first detector can also be used to detect neutrals).

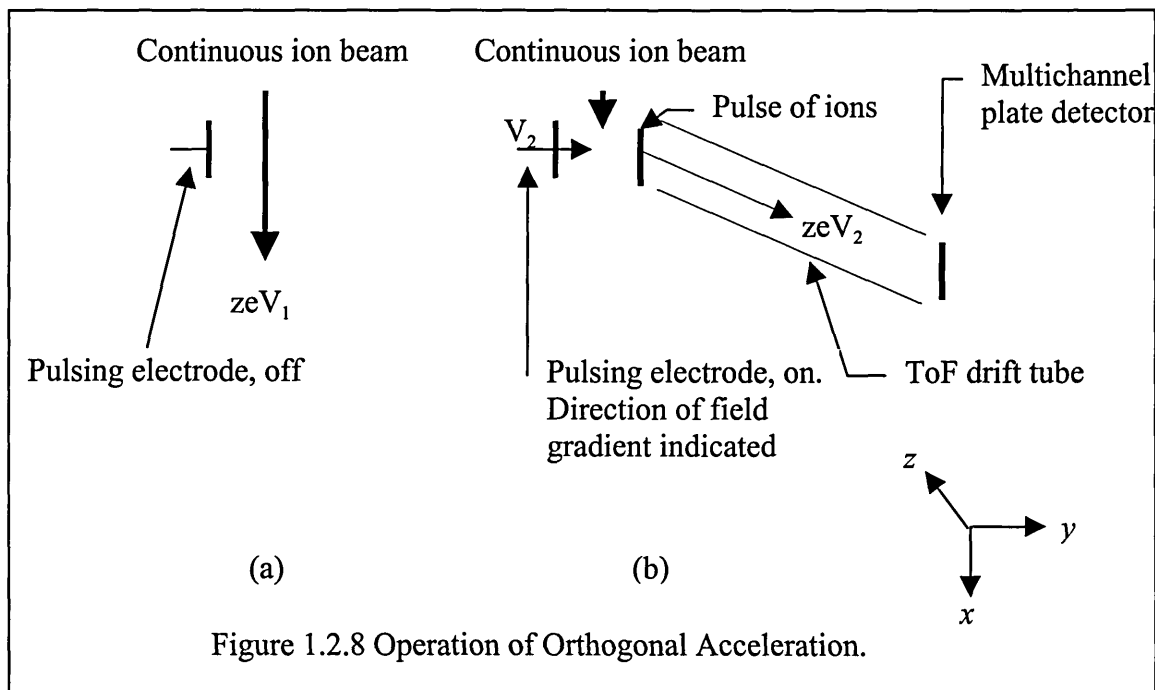


### iii) Orthogonal Acceleration<sup>23</sup>

The development of orthogonal acceleration allows continuous ion sources (*i.e.* electrospray<sup>4</sup>) to be coupled to ToF MS. Orthogonal acceleration is represented graphically in Figure 1.2.8.

Generally an oa-ToF MS will receive ions for mass analysis from a continuous ion source, *i.e.* EI, ESP, APCI *etc.*. The beam leaves the ion source and passes through a series of focusing lenses (quad-, hexa- or octapoles acting in 'r.f. only' mode) to achieve collisional cooling, in which the divergent beam becomes collimated and passes into the orthogonal accelerator (oa). The oa alternates between fill-up mode and pulse mode. In the former state the pulsing electrode and exit slit (usually a grid) are both grounded and the ion beam simply traverses the extraction region (*i.e.* continue in the  $x$ -axis). Sufficient time must be allowed for the ions of  $m/z$  equal to the upper mass limit of the spectrum to reach and fill the extraction region before the extraction pulse is applied. The pulsing electrode is then driven to the potential required to push a packet of ions out of the extraction region towards the exit slit *i.e.* the ions are extracted in the

y-axis. The pulse applied is typically of the order of 100 V, to enable short rise-time and low amplitude. When the last of the ions in the sample have passed through the exit slit, the pulsing electrode returns to ground, and the oa returns to the fill-up mode. Any ions that enter during extraction mode or any of the transition periods are unlikely to acquire any of the characteristics required for successful transmission to the detector.

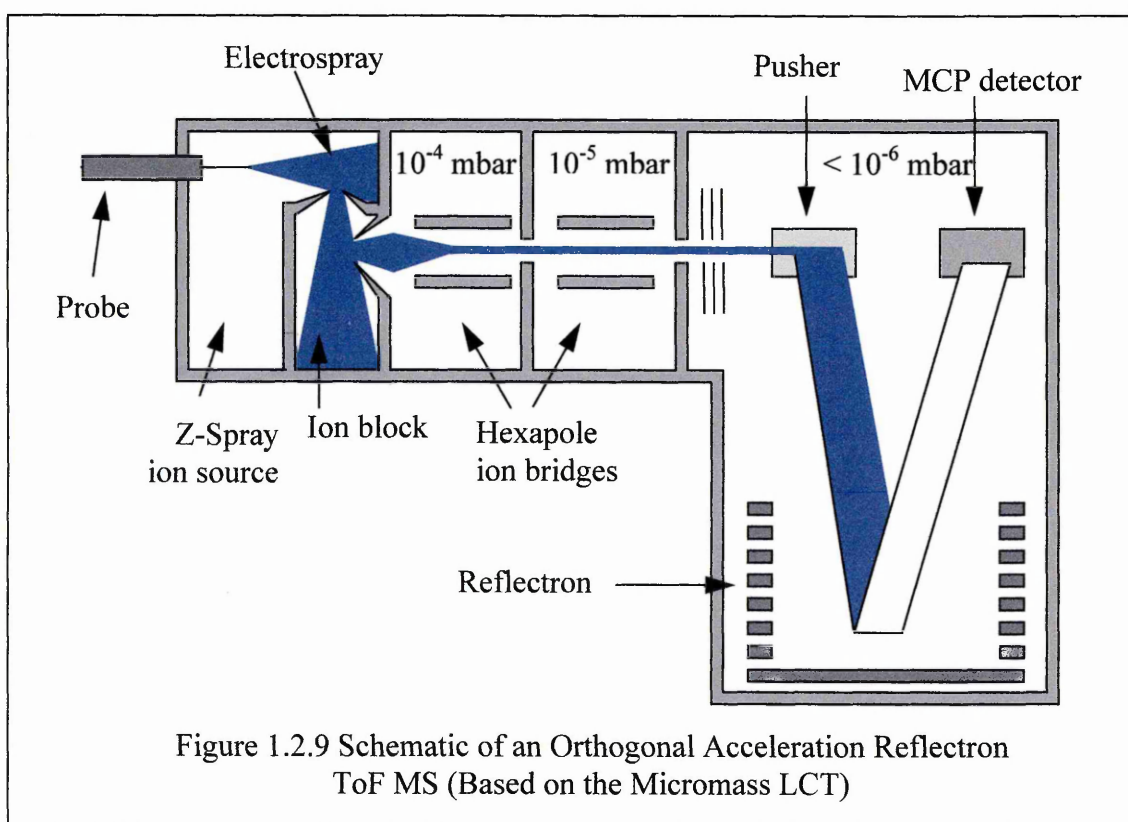


To avoid overlap of consecutive spectra, an extraction pulse cannot be applied until the slowest ion (highest mass) has reached the detector. The duty cycle (time taken for an ion packet to be extracted, traverse the drift tube and be detected) is proportional to  $(m/z)^{1/2}$ , and there is systematic discrimination against low- $m/z$  ions<sup>24</sup>. This discrimination is predictable and in most cases signals are stronger at low- $m/z$  than high- $m/z$ , therefore for practical purposes can be ignored. In most ESI oa-ToF instruments the duty cycle is 5-50% (*i.e.* percentage of ions generated, which are detected) depending on the  $m/z$  of the ion and instrumental parameters (*i.e.* flight tube dimensions).

The pulsing electrode may be operated at repetition rates of up to 20 kHz (resulting in a full spectrum being recorded by the detector every 50 microseconds). The ions are transferred into the drift tube via focusing lenses towards a reflectron, which reflects ions back to the detector (reducing spatial spread due to distributions in kinetic energy).

As ions travel from the pusher to the detector they are separated in mass according to their flight times, with ions of higher mass-to-charge ratio ( $m/z$ ) arriving later at the detector. Each individual spectrum is summed in a histogram memory of a time to digital converter (TDC) until a summed spectrum is transferred to the data station, which typically consists of at least 5000 individual ion packets.

An example of a commercial orthogonal-acceleration reflectron time-of-flight mass spectrometer is schematically reproduced in Figure 1.2.9, which based on the Micromass LCT.



#### 1.2.2.4 Ion Detectors

An ion detector produces an electric current that is proportional to the abundance of an ion impinging on it. Detection frequently takes place off-axis (that is out of line-of-sight), this is to reduce the effect of neutral species contributing to the ion current. Deflection of the ion beam onto the off-axis detector can be achieved using a

conversion-dynode, which is held at a high voltage of the same polarity as the ion beam. The ions are thus redirected onto the detector.

#### *a) Electron Multiplier*

Electron multipliers are by far the most common detectors in mass spectrometry. Ions from the analyser are accelerated by a potential difference of about 2 to 5 keV. The ions collide with the first plate (or dynode) of the multiplier, which causes a number of secondary electrons to be ejected. These electrons are accelerated by a positive potential to a second dynode, where electron amplification occurs once more and so on. Commercial electron multipliers have 10 to 12 dynodes, which provides a current amplification of approximately  $10^6$ , resulting in an electric current, which can be electronically amplified.

#### *b) Photomultiplier*

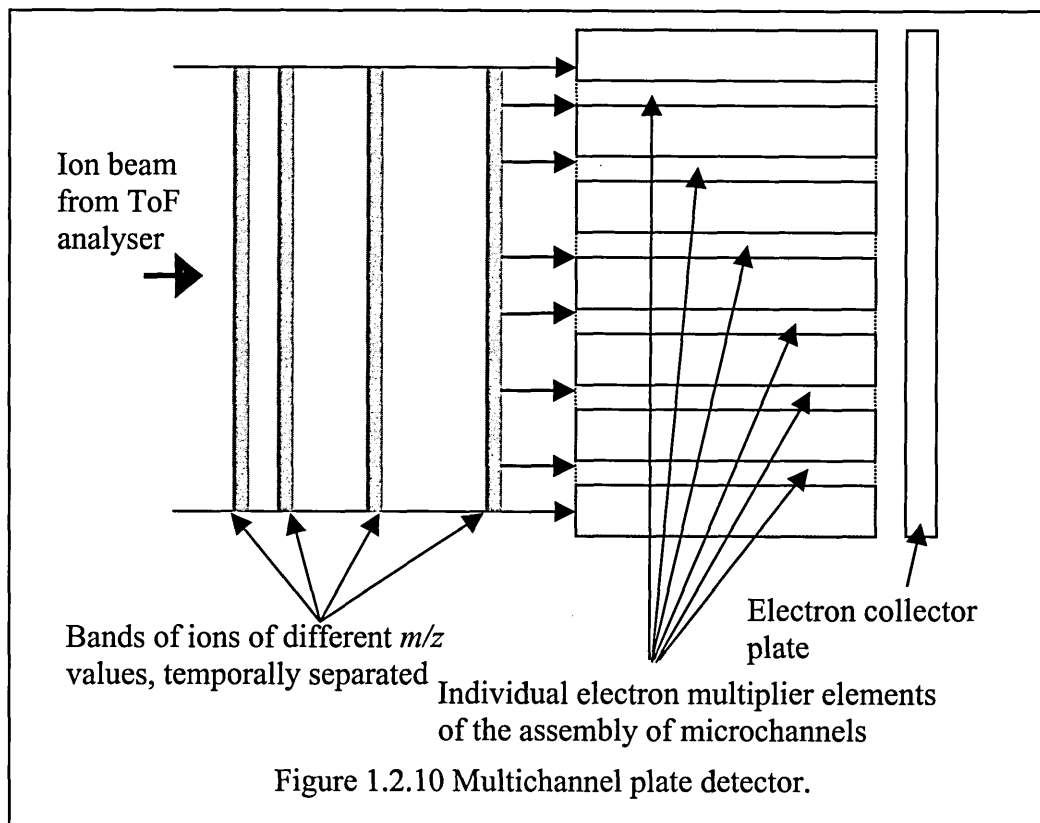
Photomultiplier tubes (PMT) are used in mass spectrometry along with a phosphor, which emits photons when struck by a particle (in this case an ion). The photon then hits a cathode within the PMT, which is coated with a photoemissive material. Upon irradiation electrons are emitted from the cathode, which are accelerated by a potential to an electrode, which consequently emits electrons on to another electrode *etc.* resulting in an electron cascade, as in an electron multiplier.

#### *c) Multichannel Plate Detectors*

A multichannel plate (MCP) detector is an assembly (array) of single point collectors (such as electron multipliers (see above)), packed closely together in a plane (Figure 1.2.10).

MCP detectors are used in ToF instruments, where ions of differing  $m/z$  are separated temporally, resulting in all ions of a specific  $m/z$  ratio being detected at the same time. No ions are lost through scanning and the MCP forms a very sensitive detector. Since the MCP detector records the arrival times of all ions the instrument resolution depends

on the analyser and MCP response time. MCP detectors with a pore size of 10  $\mu\text{m}$  have a response time of  $< 2$  ns, ions of adjacent  $m/z$  are usually separated by 20-30 ns, the MCP therefore does not usually have any appreciable effect on instrument resolution.



## References

---

- (1) a) *Methods in Enzymology, Mass Spectrometry*. McCloskey JA, Eds. Academic Press: London. 1990; Vol. 193
- b) *Practical Organic Mass Spectrometry*. Chapman JR. Wiley: Chichester. 1995; 2nd Edition
- c) *Mass Spectrometry for Chemists and Biochemists*. Johnstone RAW; Rose ME. Cambridge University Press: Cambridge. 1996; 2nd Edition
- (2) Iribane JV; Thomson BA. *Journal of Chemical Physics* **64** (1976) 2287
- (3) Thomson BA; Iribane JV. *Journal of Chemical Physics* **71** (1979) 4451
- (4) Dole M; Mack LL; Hines RL; Mobley RC; Ferguson LD; Alice MB. *Journal of Chemical Physics* **49** (1968) 2240
- (5) Mack LL; Kralik P; Rheude A; Dole M. *Journal of Chemical Physics* **52** (1970) 4977
- (6) Yamashita M; Fenn JB. *Journal of Chemical Physics* **88** (1984) 4451
- (7) Yamashita M; Fenn JB. *Journal of Chemical Physics* **88** (1984) 4671
- (8) Whitehouse C; Dreyer RN; Yamashita M; Fenn JB. *Analytical Chemistry* **57** (1985) 675
- (9) Aleksandrov ML; Gall LN; Krasnov NV; Nikolaev VI; Shkvrov VA. *Journal of Analytical Chemistry of the USSR* **40** (1985) 1227
- (10) Wong SF; Meng CK; Fenn JB. *Journal of Chemical Physics* **92** (1988) 546
- (11) Meng CK; Mann M; Fenn JB. *Zeitschrift fuer Physik D - Atoms Molecules Clusters* **10** (1988) 361
- (12) Covey TR; Bonner RF; Shushan BI; Henion J. *Rapid Communications in Mass Spectrometry* **2** (1988) 249
- (13) Tito M; Robinson C. Oral Presentation at 24th Annual BMSS Meeting, University of Reading, 12 –15th September 1999
- (14) Moseley MA; Deterding LJ; Tomer KB; Jorgenson JW. *Analytical Chemistry* **63** (1991) 109
- (15) Verheij ER; Tjaden UR; Niessen WMA; van der Greef J. *Journal of Chromatography* **554** (1991) 339
- (16) Nichols W; Zweigenbaum J; Garcia F; Johansson M; Henion J. *LC.GC International* **6** (1993) 30
- (17) Gordon DB; Lord GA; Jones DS. *Rapid Communications in Mass Spectrometry* **8** (1994) 544
- (18) Tetler LW; Cooper P. *Analytical Proceedings* **30** (1993) 397
- (19) March RE; Hughes RJ. *Quadrupole Storage Mass Spectrometry*. Chap. 2.iv, pp. 41-52. Wineforder JD; Kolthoff IM Eds. Wiley Interscience: London. 1989 Vol. 102
- (20) Cotter RJ. *Time-of-Flight Mass Spectrometry*. ACS Symposium Series. American Chemical Society: Washington. 1994 Vol. 549
- (21) Guilhaus M; Mlynski V; Selby D. *Rapid Communications in Mass Spectrometry* **11** (1997) 951
- (22) Mamyrin BA; Schmikk DV. *Soviet Physics –Zhurnal Eksperimental'noi I Teoreticheskoi Fiziki* (English Translation) **49** (1979) 762
- (23) Dawson JHJ; Guilhaus M. *Rapid Communications in Mass Spectrometry* **3** (1989) 155
- (24) Chernushevich IV; Ens W; Standing KG. *Analytical Chemistry* **71** (1999) 452A

## **Section 1.3**

# ***Methods of Interfacing Capillary Electrophoresis to Mass Spectrometry***

### 1.3.1 Introduction to CE/MS Interfaces

For a CE/MS interface to be successful, the analyte must be transferred from the separation capillary into the interface system, ionised and extracted into the mass spectrometer. In the case of electrospray the ions must also be transferred from atmospheric pressure into the high vacuum of the mass spectrometer.

The liquid inlet / ionisation methods that have been used in the development of CE/MS are electrospray ionisation (ESI) and continuous-flow fast atom bombardment (cf-FAB) (for a discussion of mass spectral instrumentation *etc.* see Section 1.2).

Capillary electrophoresis is generally performed with both ends of the separation capillary immersed in buffer filled vials. To permit mass spectral detection the outlet end (cathode) of the capillary is connected to the mass spectrometer. Thus, the interface must provide electrical connectivity for the CE separation voltage. If electrospray ionisation is employed the spray voltage is also required to be applied at the interface, resulting in a reduced field strength across the capillary (in the case of positive ion, negative ion would increase the field strength). For example, a 60 cm column with a separation voltage of 30 kV would normally experience a field strength of  $500 \text{ Vcm}^{-1}$ . However, if a spray voltage of 4 kV is applied to the capillary outlet, this would result in a field strength of  $433 \text{ Vcm}^{-1}$ , resulting in increased migration time. Whereas, using cf-FAB the CE voltage must be earthed prior to ionisation, this can be simply achieved using a grounded liquid junction.

A further difficulty in the interfacing of capillary electrophoresis and mass spectrometry is the mismatch in flow rates. The electroosmotic flow (EOF) generated in CZE is typically  $\ll 1 \mu\text{L}/\text{min}$ , whereas traditional ESI requires  $5 - 10 \mu\text{L}/\text{min}$  and cf-FAB  $2 - 10 \mu\text{L}/\text{min}$ .

Therefore, the interface must be able to supplement the low flow rate of the EOF to a suitable rate for ionisation by either ESI or cf-FAB. This can be achieved in two ways,

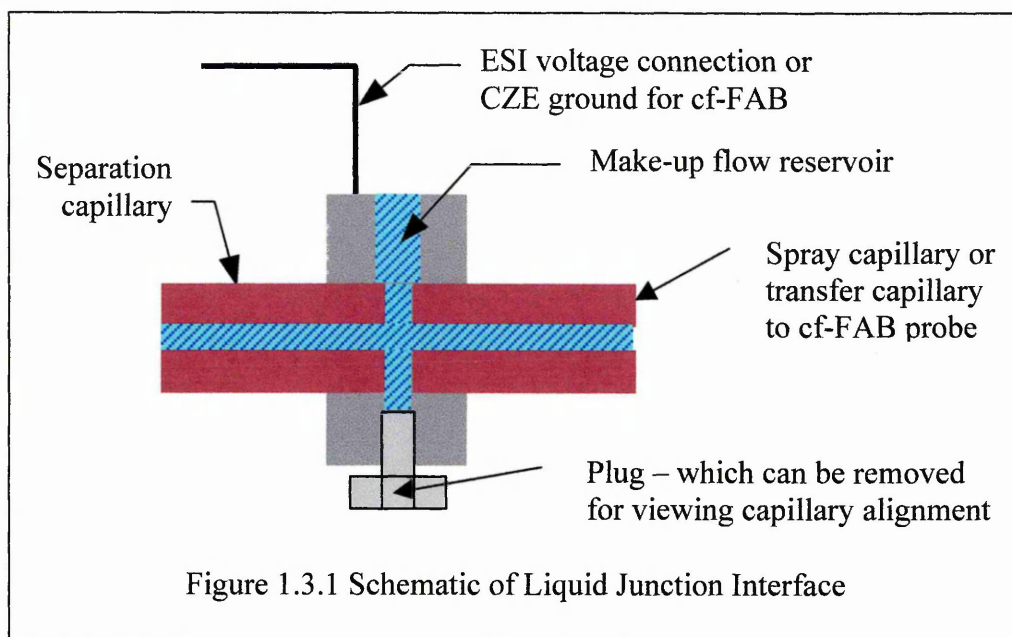
1. Liquid junction
2. Co-axial sheath flow

Liquid junction and co-axial sheath flow interfaces have been demonstrated employing both continuous flow-FAB and electrospray ion sources. The interfaces differ on the method of supplying the make-up flow to the separation capillary.

An alternative approach is to use a low-flow electrospray interface (nanospray, microspray *etc.*, the term nanospray will be used throughout this thesis to avoid confusion) without any make-up flow, as the flow rates are compatible. Nanospray interfaces spray directly at the flow rate of the EOF, and thus are more sensitive as there are no dilution effects of the make-up flow. The voltage required to generate an electrospray is significantly less using nanospray compared to the traditional method. This has a smaller effect on the CE field strength (and migration times). However, only certain (volatile) buffers can be used and in order to achieve a stable spray, a (relatively) high (*i.e.* > 20%) content of organic modifier is required. This can have a significant effect on the separation (Section 1.1.7.4). Whereas organic modifier can be added through the make-up flow with both co-axial sheath flow and liquid junction interfaces. In addition, the narrow i.d. of the nanospray tip (frequently < 25  $\mu\text{m}$ ) can be easily blocked, therefore rigorous filtering of buffer and sample is required, this is less of a problem with co-axial sheath flow or liquid junction interfaces.

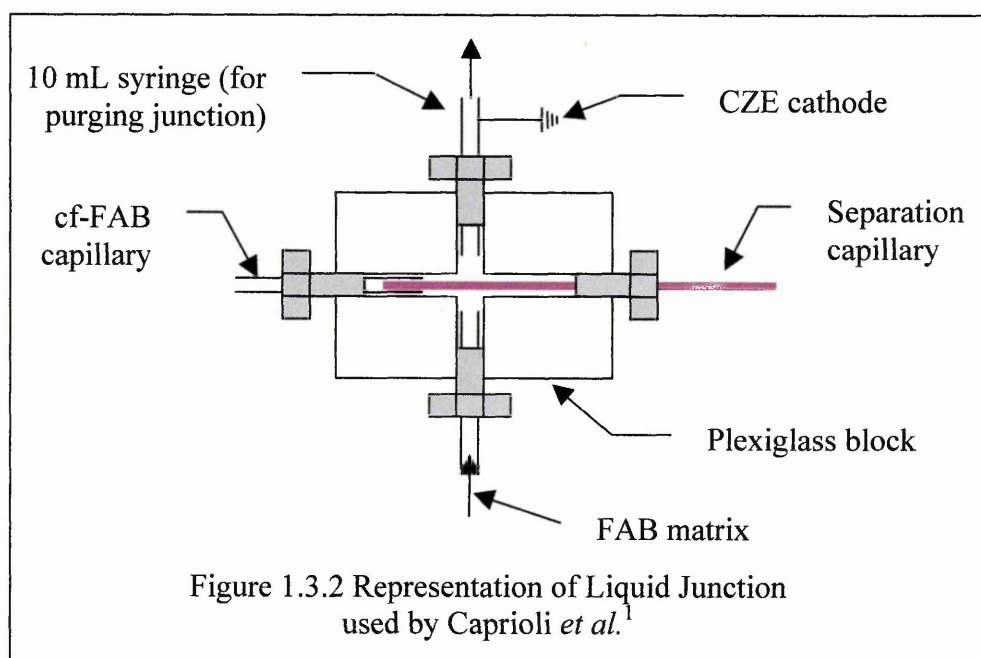
### ***1.3.2 Liquid Junction Interfaces***

The liquid junction interface consists of two separate capillaries, one to perform the separation (normal CE capillary) and one to carry the eluent into the mass spectrometer (either cf-FAB capillary or ESI spray tip). The capillaries are separated by approximately 20  $\mu\text{m}$ ; this gap is filled with a make-up flow either fed by a reservoir or pumped at a suitable flow rate. Liquid junctions have been successfully applied to both ESI and cf-FAB. The major limitation of the liquid junction interface is the difficulty in construction and alignment of the capillaries. A simplified schematic of the interface is shown in Figure 1.3.1.

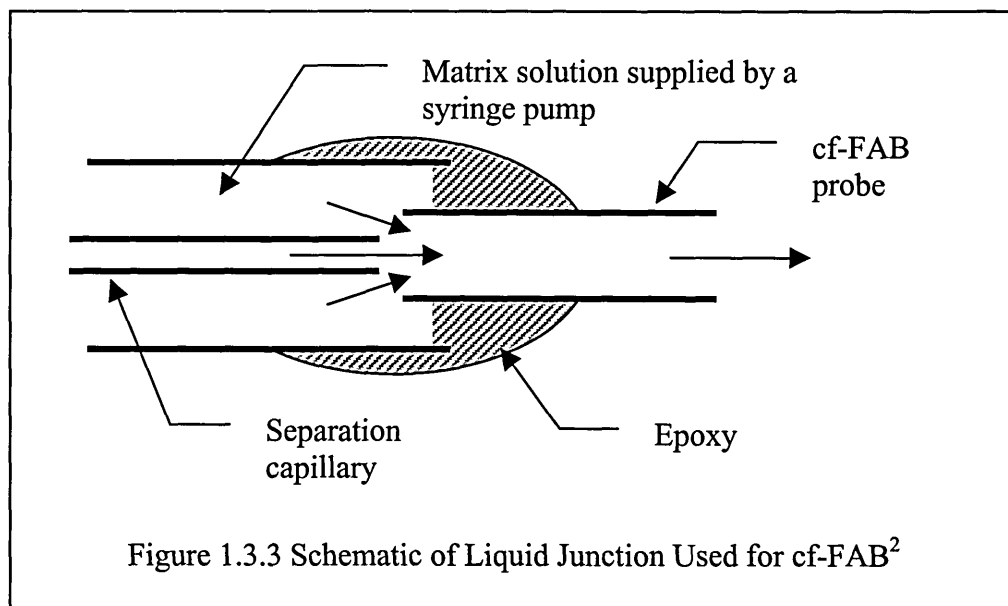


### 1.3.2.1 CZE / Liquid Junction / cf-FAB

The first example of cf-FAB CZE/MS was demonstrated by Caprioli *et al.*<sup>1</sup> using a liquid junction interface. The liquid junction was constructed using a Plexiglas block with two intersecting pathways, as shown in Figure 1.3.2. They cited a limit of detection of 75 fmol of angiotensin II, and indicated that the separation integrity was maintained between CZE-UV and CZE-MS for a peptide mixture from a tryptic digest of  $\beta$ -lactoglobulin A.



Tjaden *et al.*<sup>2</sup> employed pseudo-electrochromatography (p-CEC), which is a variation of CEC, to compare co-axial sheath flow and liquid junction interfaces for cf-FAB ionisation. The co-axial sheath flow interface was achieved using two concentric capillaries (separation capillary 50  $\mu\text{m}$  i.d. 200  $\mu\text{m}$  o.d. inserted into 220  $\mu\text{m}$  i.d. sheath capillary) inserted into the cf-FAB probe. A different liquid junction interface was developed to that of Caprioli *et al.*<sup>1</sup>, and is shown schematically in Figure 1.3.3.



The performance of the system was assessed by analysis of nucleotides, alkaloids and an antiviral drug. They reported full scan detection was possible for nucleotides in 10-50 picomole quantities. The liquid junction interface was reported to be more robust, owing to the difficulties encountered in assembling the co-axial sheath flow probe. The major problem was inserting the 200  $\mu\text{m}$  o.d. separation capillary into the 220  $\mu\text{m}$  i.d. sheath capillary to a length of 75 cm. They state that the post-column addition of the FAB matrix did not have any detrimental effects on either the separation or the ion current.

Gordon *et al.*<sup>3</sup> demonstrated CEC/MS using cf-FAB, using a test mix of steroids. The matrix solution was added to the column flow via a T-piece, in which mixing occurred and a suitable flow-rate was introduced into the mass spectrometer. They concluded that CEC/MS was a suitable alternative to capillary LC/MS and that CEC was a viable substitute to MEKC for interfacing to mass spectrometry.

Henion *et al.*<sup>4</sup> compared the performance of electrospray and cf-FAB for CZE/MS. Both interfaces were coupled to the separation capillary using a liquid junction; enabling comparison of the two different ionisation methods. The electrospray set-up gave molecular weight information only, whereas the cf-FAB gave molecular weight and limited fragmentation information. Sensitivity was comparable for both methods. Increased extracolumn band broadening was observed with cf-FAB; this was reasoned to be due to the increased length of transfer capillary required for the cf-FAB probe compared to the electrospray system. The ruggedness of the two techniques was compared, in both cases the alignment of the liquid junction was critical, with cf-FAB being further hampered by matrix collection on the probe tip. In conclusion, they state that the electrospray interface was the more routine of the two techniques.

#### **1.3.1.2 CZE / Liquid Junction / ESI**

A liquid junction interface was developed by Henion *et al.*<sup>5</sup> for the coupling of capillary electrophoresis to pneumatically assisted electrospray (ionspray, ISP). The interface was constructed from a modified stainless steel T-piece. The T-piece was drilled to accommodate a syringe barrel (to act as the solvent reservoir). The cathode end of the CZE capillary and the ISP needle were positioned centrally in the T-piece, approximately 10 - 25  $\mu\text{m}$  apart by viewing under a microscope (the gap could be further adjusted by loosening and tightening of the fittings). The final port was blocked off with a plug. The make-up flow was gravity fed, and therefore was drawn at a rate suitable for electrospray. The electrospray voltage was applied to the T-piece. The interface was able to compensate for the differences in flow rate obtained in CZE and that required for stable spray in ESI / ISP.

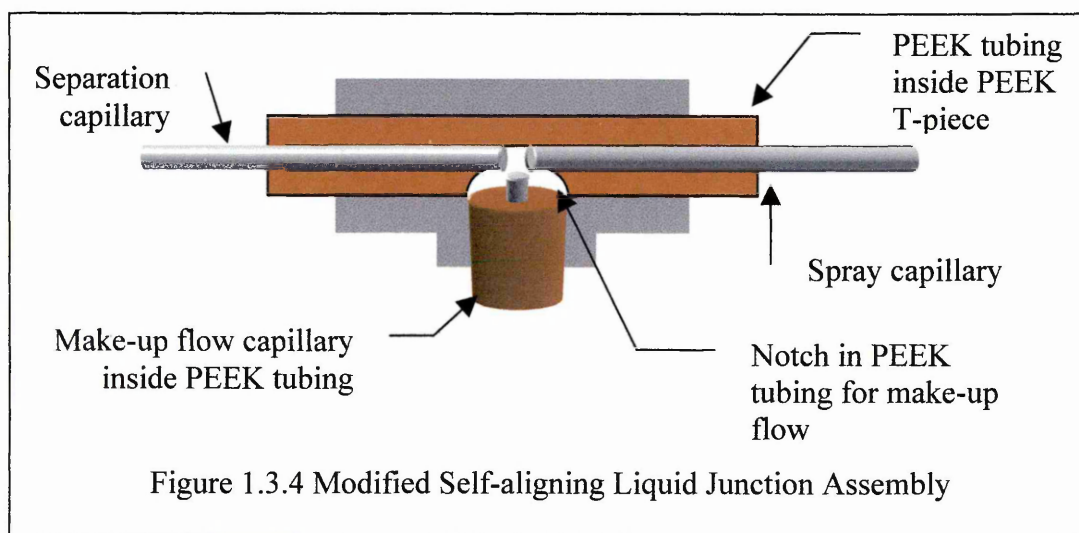
Pleasant *et al.*<sup>6</sup> compared liquid junction and co-axial sheath flow interfaces analysing marine antibiotics and toxins by CZE/MS. They conclude that both interface types are suitable for CZE/MS analysis, but the co-axial arrangement is more robust and reliable. They suggested that a major advantage of the co-axial arrangement is that the composition of make-up flow is independent of the separation buffer, thus allowing a greater range of CZE buffers to be utilised. Using a co-axial sheath flow interface both

CZE/MS and CZE/MS/MS of shellfish toxins yielding structural information was obtained.

They concluded that the disadvantages of a liquid junction *cf.* co-axial sheath flow were

- 1) Contamination of the make-up liquid during capillary conditioning / flushing,
- 2) Contributions to zone dispersion,
- 3) An increase in background signal due to instabilities in the make-up liquid flow rate,
- 4) Non-compatibility with flow injection analysis (FIA).

To redress this Henion *et al.*<sup>7</sup> suggested a self-aligning liquid junction (Figure 1.3.4, reproduced from Reference<sup>7</sup>).



The self-aligning system employs a PEEK T-piece, through which a piece of PEEK tubing passes, the i.d. of which closely matches the o.d. of the fused silica. A notch was cut out of the PEEK tubing which aligns with the tee, allowing positioning of the make-up flow capillary. Instead of a gravity fed make-up flow, the flow was provided by an infusion pump (at  $\sim 2 \mu\text{L}/\text{min}$ ). The self-aligning assembly proved to be more robust and reproducible than the previous design of liquid junction, in addition, the process of aligning the capillaries was much easier.

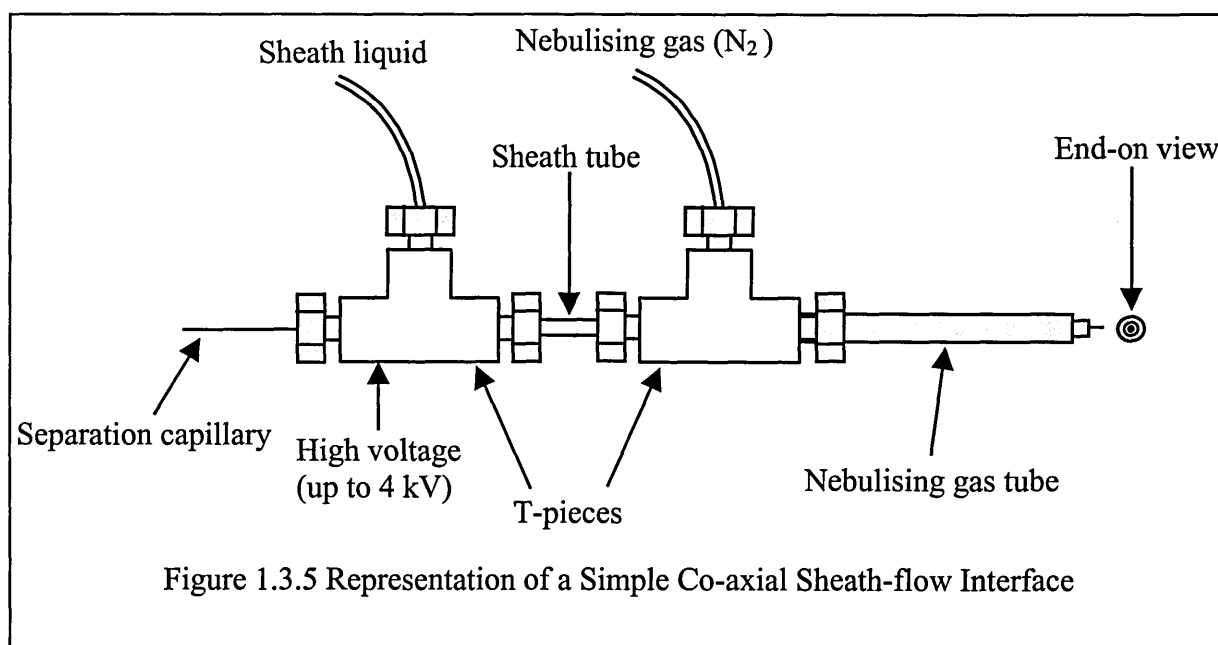
Hirabayashi *et al.*<sup>8</sup> developed an ionisation method analogous to electrospray called sonic spray (SSI), in which ionisation occurs through the introduction of a high-speed

(~2 L/min) nitrogen flow co-axial to the sample tube. The charge density of the droplets was increased by the application of voltage to the interface (~1.2 kV), which would be insufficient to generate electrospray on its own. To prevent an induced laminar flow through the action of the nitrogen, a liquid junction buffer reservoir was situated between the separation and spray capillaries. In addition, the liquid junction could be used to alter the composition of the electrophoretic buffer to aid the desolvation process, *i.e.* inclusion of methanol (MeOH) or acetic acid. The interface was successfully used to analyse neurotransmitters (dopamine and GABA) and gramicidin-S by CZE/MS employing a 15 mM phosphate buffer without any significant interference.

Applications using the liquid-junction interface include pesticides<sup>5</sup>, sulphonated azo dyes<sup>5</sup>, tryptic digest of proteins<sup>5,9</sup>, pharmaceutical compounds<sup>10,11</sup>, herbicidal sulphonylureas<sup>12</sup>, aromatic sulphonates, anionic surfactants, dansylated amino acids and poly(acrylic acid)<sup>13</sup> and marine antibiotics and toxins<sup>6</sup>.

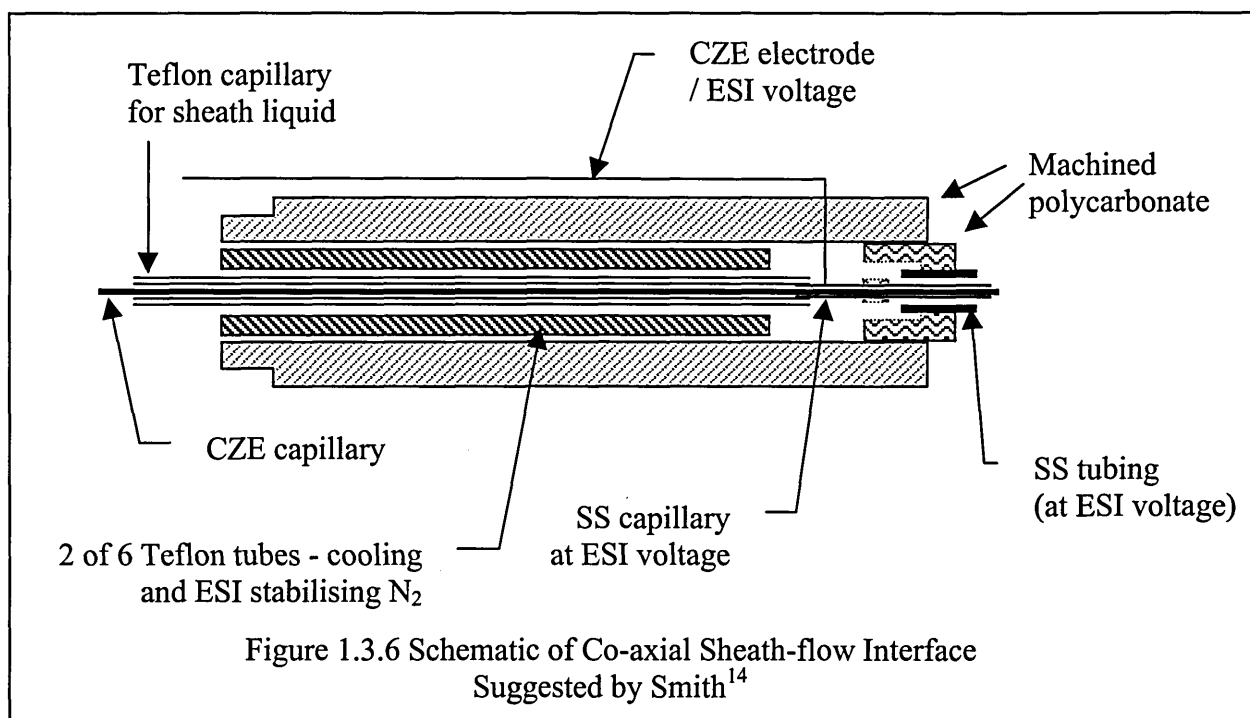
### 1.3.3 CZE / Co-axial Sheath flow / ESI

In a co-axial sheath flow interface, the separation capillary passes through two concentric tubes. The outer tube supplies nebulising gas (to aid in desolvation), between the inner tube and the separation capillary is pumped the sheath liquid, this is shown schematically in Figure 1.3.5.



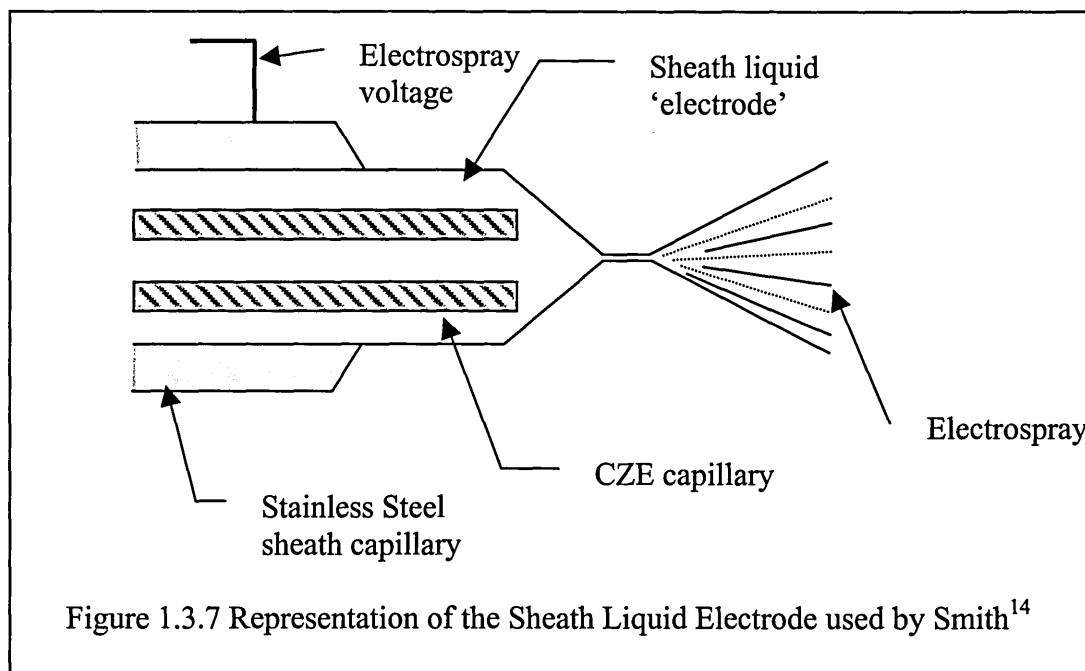
Typical make-up flow rates are 2 – 10  $\mu\text{L}/\text{min}$ , the composition of which is usually 1:1 aqueous / organic solvent (acetonitrile, methanol, 2-propanol) with 0.1%  $\text{v}/\text{v}$  organic acid (acetic / formic acid). As the CZE capillary passes through the sheath tube there are no contributions to zone dispersion by the interface, maintaining separation resolution / efficiency.

The first example of a co-axial sheath flow CZE-MS interface was reported by Smith *et al.*<sup>14</sup> (Figure 1.3.6). This was an improvement to their previous attempts at sheathless CZE/MS<sup>15,16</sup>, owing to certain restrictions imposed by the interface. These limitations included poor tolerance to involatile inorganic buffers (especially at concentrations above  $10^{-2}$  M); organic modifiers were necessary to aid the electrospray process, which could have deleterious effects on the separation. In addition, a metal coating was required at the capillary terminus (to apply electrospray voltage and terminate the CZE voltage), which was both time consuming to produce and unstable.



It was suggested that the use of a co-axial sheath flow would solve these problems. The addition of a make-up flow would increase the CZE flow rate to suitable levels. Involatile buffers of a high concentration could also be used, due to the dilution effect of the sheath-liquid. The electrospray voltage was applied through the sheath liquid

completing the CZE circuit and generating an electro spray (schematically represented in Figure 1.3.7); a metal coating was thus unnecessary.



Smith *et al.* suggested that the co-axial sheath flow interface was more robust and reliable compared to their previous attempts at sheathless interfaces and that this method of interface would allow much broader investigation of analytes by CZE/MS. As a development of this work Smith *et al.*<sup>17</sup> investigated the multiple charging effects observed with various organic sheath-liquids. For a predominately aqueous solvent, a higher charge state was observed, which decreased for methanol and acetonitrile and was the least for isopropanol. 'Tailing' at the high mass side of the peaks was also observed for IPA, this was suggested to be due to incomplete desolvation, yielding solvent / molecule complexes. The shift in charge distribution was attributed to the solvents having a lower surface tension, which causes the molecular species to be formed with a lower degree of association with solvent. However, a much higher degree of solvation was observed with IPA (lowest surface tension of solvents used). This was attributed to instabilities in the spray, which could cause 'microdroplets' to be produced, the size of which would be related to analyte and solvent properties, but less dependant on interactions between solvent and analyte.

The following year (1989) Smith *et al.*<sup>18</sup> demonstrated the rapid separation of a peptide mixture using the above co-axial sheath flow interface. The first mixture consisted of

bradykinin, angiotensin I, porcine insulin and glucagon in a phosphate buffer at pH 11. The analysis of peptides in alkaline buffers reduces the association of the peptide with the capillary wall and thus reduces peak tailing. The sheath flow comprised methanol / water and 10% (v/v) glacial acetic acid, to produce an overall acidic sheath liquid flow, aiding the electrospray process. The second mixture contained proteins (bovine insulin, sperm whale and horse myoglobin), which were separated employing a Tris/HCl buffer at pH 8.4 (to avoid protein denaturation), with an acidic sheath flow.

Smith *et al.*<sup>19</sup> described the modification of a commercially available capillary electrophoresis instrument (Beckman P/ACE 2000) to be used for CZE/MS, with subsequent analysis of peptide mixtures.

Tomer *et al.*<sup>20</sup> compared the use of nano-HPLC and CZE interfaced via co-axial sheath flow to a mass spectrometer for the analysis of macrolide antibiotics. CZE separations were performed at both high and low pH (at low pH, 3-aminopropyltrimethoxysilane (APS) derivatised columns with -30 kV were used to minimise analyte-wall interactions, for more details see Section 1.1.7.8). Unfortunately, the low sensitivity of the mass spectrometer in full scan mode required increased injection volumes, which led to column overloading (resulting in increased zone dispersion). Therefore, only SIM analysis was possible for CZE/MS. Baseline separations were not achieved, this was likely due to the structural similarity (and thus charge-to-size ratio) of the analytes. Overall, they conclude that either CZE or nano-HPLC could be used to separate macrolide antibiotics, but the increased loadability of nano-HPLC columns proves advantageous where sensitivities are low. CZE/MS resulted in higher peak efficiencies, shorter analysis time, but nano-HPLC/MS gave improved detection limits and chromatographic separation.

The effect of different sheath liquids and acidic and basic buffers on the CZE separation of peptides with MS and tandem MS detection has been investigated<sup>21</sup>. The analysis of peptides with acidic buffers can be problematic due to the interaction of analytes with the capillary wall when bare fused silica is used. The use of chemically modified capillary walls can reduce the interaction and thus increase efficiency. In this case an APS coating was used to provide a surface of aminopropyl groups with a net positive charge. In conclusion, they suggest that the use of a 10 mM acetic acid pH 3.4 buffer

gave the best sensitivity when used with an APS coated column. Peak efficiencies of up to 250 000 theoretical plates were achieved from 160 fmol of a peptide (Lys-bradykinin). CZE/MS/MS was also demonstrated on less than 1 pmol of peptide yielding sufficient structural information to confirm the peptide sequence.

In 1994 Naylor *et al.*<sup>22</sup> reported the analysis of the hydrophobic drug mifentidine, using a non-aqueous separation medium consisting of ammonium acetate (5 mmol/L) in methanol containing acetic acid (100 mmol/L). The sheath liquid comprised 60:40 2-propanol : water 1% acetic acid (v/v). Reported detection limits were 80 fmol for the standards analysed.

In an in-depth investigation of the effects of the sheath liquid on separations, Karger *et al.*<sup>23</sup> concluded that moving ionic boundaries might be formed in the capillary as liquid sheath counterions migrate down the separation capillary. This may be particularly problematic if low electroosmotic flow systems are being used. Analyte migration order may change or be delayed, when compared with CZE/UV systems. To minimise the effects they recommended:

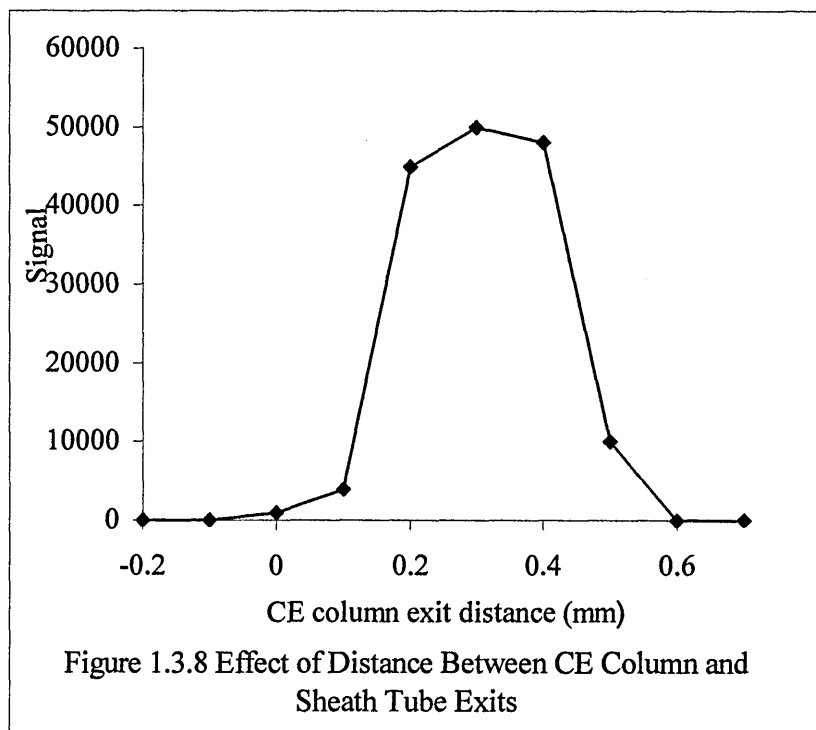
- Use of a common counterion in CZE buffer and sheath liquid (e.g. ammonium acetate and acetic acid)
- Use of a sheath liquid counterion with a  $pK_a$  and electrophoretic mobility similar to the CZE buffer
- Use of pressure (~10 mbar) applied to the capillary inlet vial to introduce laminar flow through the column to overcome the migration of the ionic boundary through the capillary
- Use of a capillary that generates sufficient EOF
- Use of a sheathless interface

The first two recommendations could readily be achieved employing volatile buffer systems (frequently required for stable electrospray) and corresponding organic acids (*i.e.* ammonium acetate / acetic acid, ammonium formate / formic acid *etc.*). The third point could be achieved providing commercial instrumentation is used; home built systems frequently do not have pressure control (especially <50 mbar). The use of a buffer at high pH with an uncoated capillary or a low pH buffer with an amine coated capillary would both generate a high EOF (due to the fully ionised surface of the

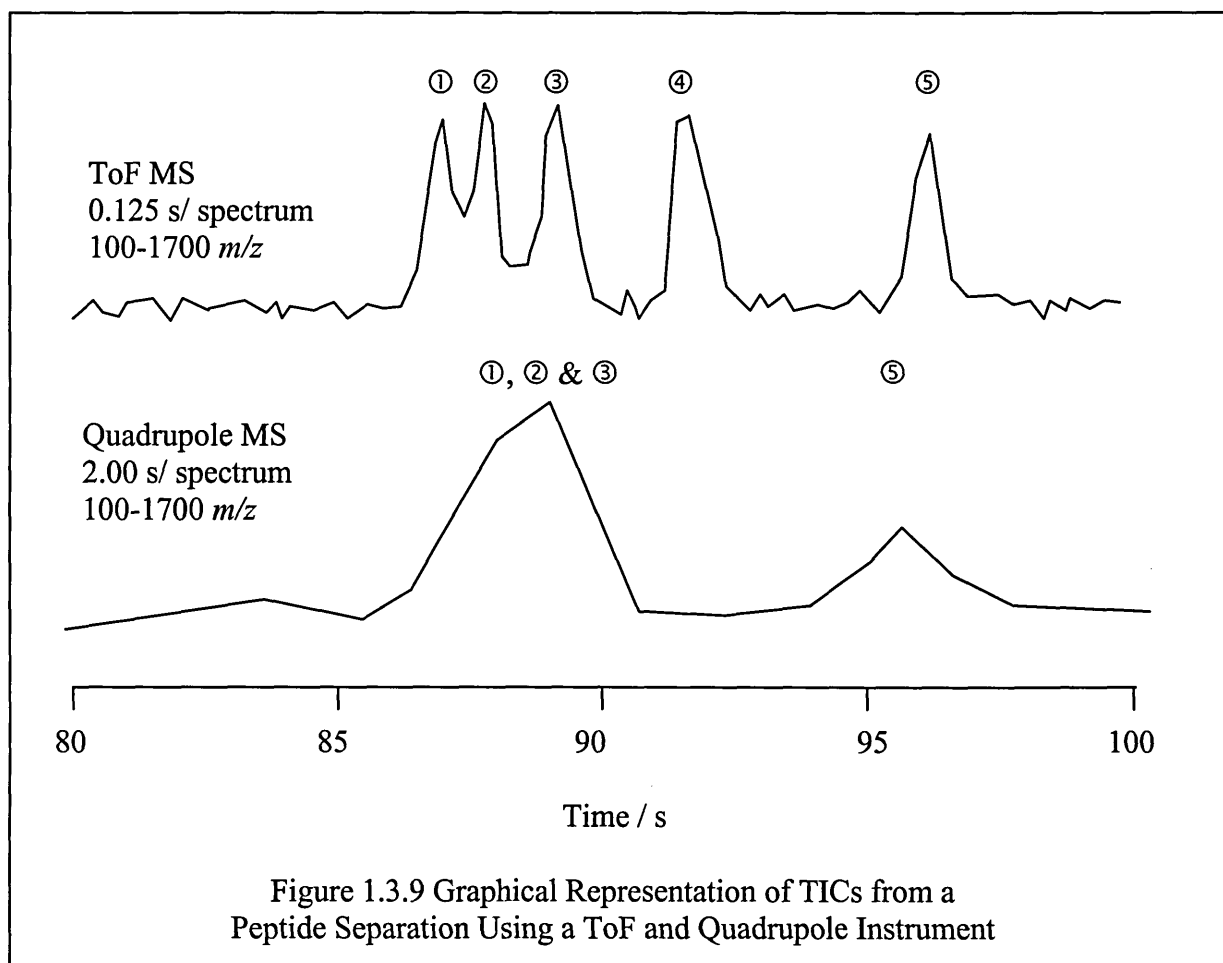
capillary). Although surface modification can increase the EOF, the velocity of the moving boundary may still be faster than the EOF. Finally the use of a sheathless interface solves this problem, but there are many associated problems with sheathless interfaces, *i.e.* connectivity problems, limited buffer use *etc.*

Tetler *et al.*<sup>24</sup> investigated the influence of capillary dimensions on the performance of a co-axial sheath flow interface for CZE/MS, in particular the i.d., o.d. and wall thickness. In conclusion decreasing all of the sheath capillary dimensions and the o.d. of the separation capillary enhances sensitivity. However, the use of narrow wall tubing can result in increased breakage after prolonged use due to the brittle nature of the tubing.

Banks<sup>25</sup> performed a comprehensive study of the optimisation of a peptide separation, which employed a liquid sheath probe. The probe was constructed so as to enable the manipulation of column outlet relative to the sheath and the nebulising gas tubes. The results are reproduced in Figure 1.3.8. The signal optimises with the CZE column protruding 0.3 mm from the sheath tube, this was consistent with the range 0.2 – 1.0 mm, which had previously been suggested<sup>14,21</sup>.



distortion that was observed with the quadrupole instrument was quite severe, the first three peaks appeared to co-migrate and the fourth peak was not detected, without prior knowledge of the separation or sample, interpretation would be impossible. This data demonstrated the advantage of ToF analysers over quadrupoles for high-resolution, fast separations.

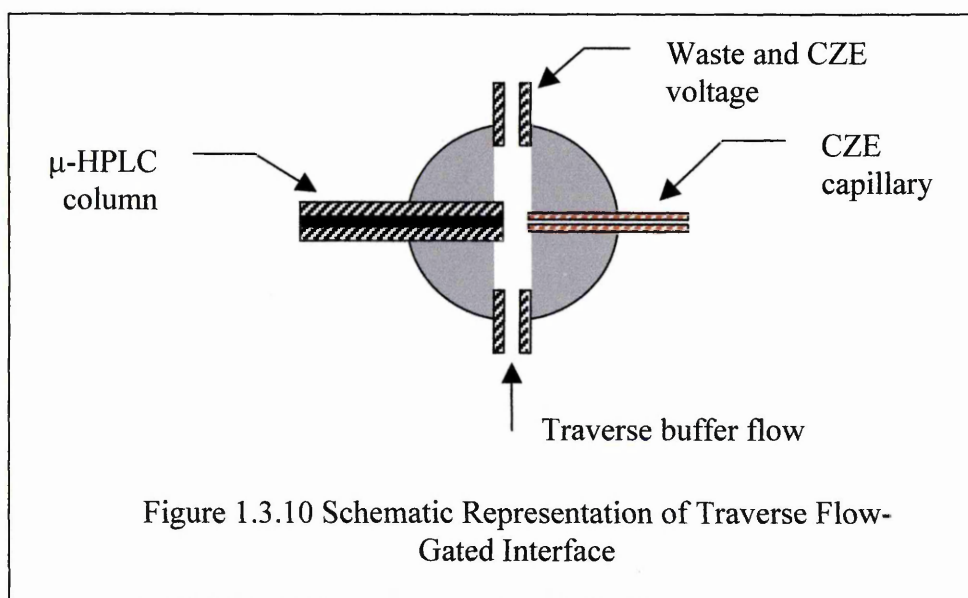


Belder and Stöckigt<sup>29</sup> used a magnetic sector instrument for the analysis of basic pharmaceutical compounds, they suggested that the use of polyethylene glycol or polyvinyl alcohol coated columns would increase separation performance and efficiency. The use of a sector MS instead of a quadrupole gave more reliable mass accuracies and higher resolution. However, the scanning speed of sectors is poor compared with quadrupoles and ToF mass analysers and can result in poor temporal resolution of closely migrating species.

Cole *et al.*<sup>30</sup> have demonstrated a non-aqueous (methanolic) separation of the anti-cancer drug Tamoxifen using CZE/MS with the inclusion of surfactant (sodium dodecyl

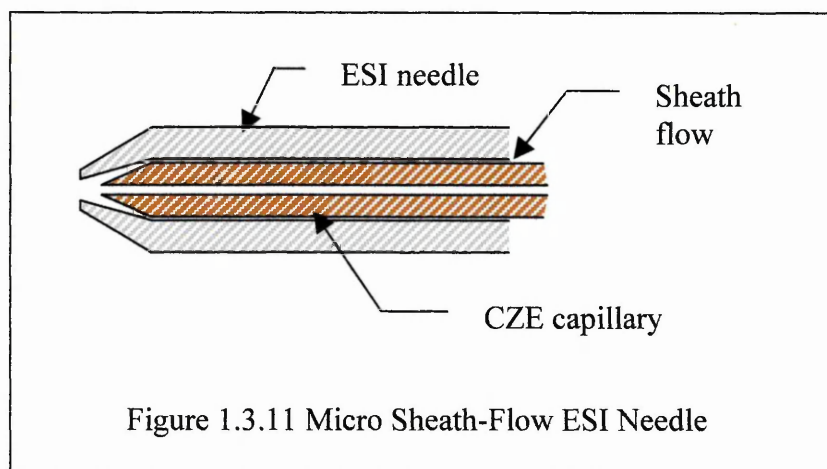
sulphate, SDS). The inclusion of SDS improved the separation at the expense of electrospray sensitivity of the analytes (N-desmethyltamoxifen signal reduced by a factor of  $\sim 3$ ). The inclusion of the SDS resulted in a reduced EOF, which can lead to improved resolution (*i.e.* reduce the  $\mu_{\text{EOF}}$  contribution to  $\mu_{\text{OBS}}$  of analytes). In addition, the increased solubility of Tamoxifen in organic solvent will decrease the tendency for hydrophobic analytes to aggregate and adhere to the capillary wall.

Jorgenson *et al.*<sup>31</sup> demonstrated a novel two-dimensional chromatographic system, which employs separation by partition ( $\mu$ -HPLC column) and differential migration (CZE column). The sample was injected onto a  $\mu$ -HPLC, which was in turn connected to a CZE capillary with subsequent mass spectral detection. The coupling of the  $\mu$ -HPLC column and CZE capillary was accomplished using a traverse flow-gating interface (Figure 1.3.10).



In normal operation the eluent from the  $\mu$ -HPLC was flushed out to waste by the traverse buffer flow, with the CZE voltage applied. To perform an injection, the voltage and buffer flow was switched off, the analyte then allowed to diffuse across the gap, and the CZE voltage applied (to perform an electrokinetic injection). After the injection, the voltage was switched off and the buffer flow switched on to purge the interface. The CZE voltage was then switched on and separation performed. A co-axial sheath flow interface was constructed out of a nanospray tip modified to take a make-up flow of approximately 50 nL/min. The capillary tip was ground to a point in a micro-lathe and

inserted into an electrospray needle (Figure 1.3.11). The micro sheath flow needle resulted in a stable electrospray at a flow rate of ~500 nL/min. The resulting system yielded separations that were a combination of both chromatographic techniques, which allowed a protein digest to be mapped in less than fifteen minutes.



Tanaka *et al.*<sup>32</sup> developed a simultaneous separation of cationic, neutral and anionic analytes by CZE/MS. The use of an alkaline buffer and sheath flow resulted in a fast EOF (allowing the anions to be rapidly detected). The cationic and neutral analytes were ionised using positive ion electrospray. Once the cationic and neutral species were detected, the ionisation polarity was reversed and the anions were then analysed by negative ion electrospray, this process was performed automatically. Electrokinetic chromatography / mass spectrometry (EKC/MS) was also performed with a range of pseudo-stationary phases (sodium dodecyl sulphate (SDS), sulphobutyl ether  $\beta$ -cyclodextrin ( $\beta$ -CD-SBE(IV)) and 4-sulphonated calix[6]arene (Cx-SO<sub>3</sub>)). SDS was detected as an ammonium adduct in positive ion, but did not deteriorate the detection sensitivity of analytes, the pseudo-stationary phases  $\beta$ -CD-SBE(IV) and Cx-SO<sub>3</sub> gave no background signal in the mass spectrometer, and were useful alternatives for selectivity to SDS.

Her *et al.*<sup>33</sup> developed a reversed EOF separation of triazines with mass spectral detection. All analytes were baseline resolved using a dynamically modified capillary (using cetyltrimethylammonium bromide, CTAB), whereas normal EOF was unable to resolve the analytes. The composition of the sheath flow was highly critical using reversed EOF. Initially a highly acidic (trifluoroacetic acid) sheath flow was used,

which significantly degraded the CZE resolution, which was consistent with the 'moving boundary' theory suggested by Karger *et al.*<sup>23</sup>. An increase in sheath liquid pH (ammonium acetate) resulted in an increase in resolution and sensitivity. The authors did not report any problem with CTAB dominating the ion current, thus indicating dynamic coated capillaries can be readily used for CZE/MS analysis.

Lausecker *et al.*<sup>34</sup> compared CZE/MS and  $\mu$ -HPLC/MS for the analysis of pharmaceutical compounds. The separation efficiency and detection limits were found to be superior for CZE, for both standards and biological samples. Sample pre-treatment was necessary, to achieve suitable sensitivities, liquid-liquid extraction being preferable to solid phase extraction.

A non-aqueous separation with on-line mass spectral detection of tricyclic antidepressants and amitriptyline and its related metabolites has been demonstrated by Dovichi *et al.*<sup>35</sup>. An acetonitrile / methanol solvent system which contained ammonium acetate was used to separate the analytes, with a pure methanol sheath liquid. The flow rate of the nebulising gas was found to affect the baseline stability, separation efficiency and migration times, a flow rate of 0.4 L/min gave the best conditions. The effect of nebulising gas flow rate on the CZE separation was suggested to be due to pressure differentials across the capillary inducing a laminar flow; once optimised detection limits of 3 pg (injected on column) were obtained.

Ingendoh *et al.*<sup>36</sup> have developed an orthogonal co-axial sheath flow interface, which was held at ground potential, application of 4 kV to the inlet to the mass spectrometer generated the electrospray. CZE/MS becomes simplified in this configuration, as the column outlet can be grounded allowing higher separation voltages to be used, also the electrospray voltage can be altered during an analysis without affecting the separation. The orthogonal sampling of the electrospray allowed the use of a phosphate buffer without detrimental effects to the analyte sensitivity.

Takada *et al.*<sup>37</sup> modified a commercial APCI source for use with CZE/MS. A co-axial sheath flow electrospray probe was used to deliver the analyte into the source, which incorporated a heated vaporiser and discharge electrode. The APCI interface was

demonstrated to be able to generate analyte ions without significant background ions from a sodium phosphate buffer.

A novel ionisation technique based on electrospray has been developed by Bayer *et al.*<sup>38</sup>, which they have termed 'Co-ordination-ionspray' (CIS). The interface has been based on a co-axial sheath flow electrospray probe. The sheath flow is comprised of an aqueous solution of metal ions (lithium, palladium or silver), pneumatic nebulisation occurs at the probe tip and complexation occurs between the analyte and metal ion. In some cases a voltage (~1.5 kV) is required to enhance the nebulisation of the analyte. CIS/MS is especially useful for analytes that do not ionise well by electrospray, *i.e.* terpenes, sugars, alcohols, PAHs *etc.* CIS/MS was demonstrated to be a suitable interface for CZE/MS and p-CEC/MS employing silver complexes of unsaturated fatty acids.

The effect of electrospray needle voltage on EOF has been investigated<sup>39</sup> experimentally by CZE/UV. The EOF was determined employing a normal CZE configuration. The cathodic end of the capillary was then inserted into a ~7.5 cm SS capillary, which was in turn was inserted into the outlet buffer vial. The outlet electrode (cathode) was electrically disconnected from the instrument (*i.e.* no longer grounded).

When a positive voltage was applied to the SS capillary the EOF was noted to increase, when a negative voltage applied, the EOF decreased. Using a 25 mM ammonium acetate (pH 4.2) buffer, with  $\pm 5$  kV applied, the variation in EOF was quite significant ( $\pm 17\%$ ) and increased further when the pH was reduced (using ammonium citrate pH 3,  $\pm 31\%$ ). Above pH 8 the effect became negligible.

The variation in the EOF was attributed to the degree of ionisation of the silanol groups on the inner surface of the capillary. The charge density increased (*i.e.* more free silanoate groups) as a radial positive field was applied to the capillary. An increase in charge density resulted in an increase in the zeta potential ( $\zeta$ ), which will consequently increase the EOF.

When a negative radial field was applied, the surface charge density was decreased,  $\zeta$  decreases, as does the EOF. The authors stated that migration times and efficiencies might be further disturbed when the composition of the sheath-liquid was different to the separation buffer (*i.e.* the moving boundary theory<sup>23</sup>).

#### ***1.3.4 Nanospray CZE Interfaces***

Nanospray (or nanoelectrospray, microelectrospray) was initially demonstrated by Wilm and Mann<sup>40</sup>. It differs from conventional electrospray by having a narrow spraying tip (achieved by drawing fused silica or glass capillary) and thus a low flow rate ( $\sim$  nL/min) generating small droplet sizes and consequently requires a reduced voltage for the onset of electrospray. Other groups later confirmed the work<sup>41,42</sup>.

Nanospray offers an ideal interface for CZE/MS as the flow rates supplied and required are compatible, therefore no dilution effects of make-up flows are observed, making nanospray a more sensitive interface. The first demonstration of CZE/MS employed a nanospray interface in which the cathodic end of the capillary terminated in a metal capillary, which was held at the electrospray voltage<sup>43-45</sup>.

A number of alternative methods have been suggested for nanospray CZE/MS. These include tapering the separation capillary tip, which is then metal-coated (Figure 1.3.12a). A metal wire can be inserted into the capillary (Figure 1.3.12b), or a microdialysis junction (Figure 1.3.12c) can be employed, alternatively the polymer coating can be removed and a voltage contact made via silver conductive paint (Figure 1.3.12d).

Nanospray can be achieved by either manufacturing the end of the separation capillary into a sprayer tip or butting the separation capillary to a spray tip (typically a drawn, gold plated fused silica capillary). The butt connection is crucial to the success of the interface, to maintain electrical connectivity (and hence EOF) and minimise zone dispersion. Examples of butted capillaries include the use of Teflon sleeves and stainless steel zero-dead-volume unions.

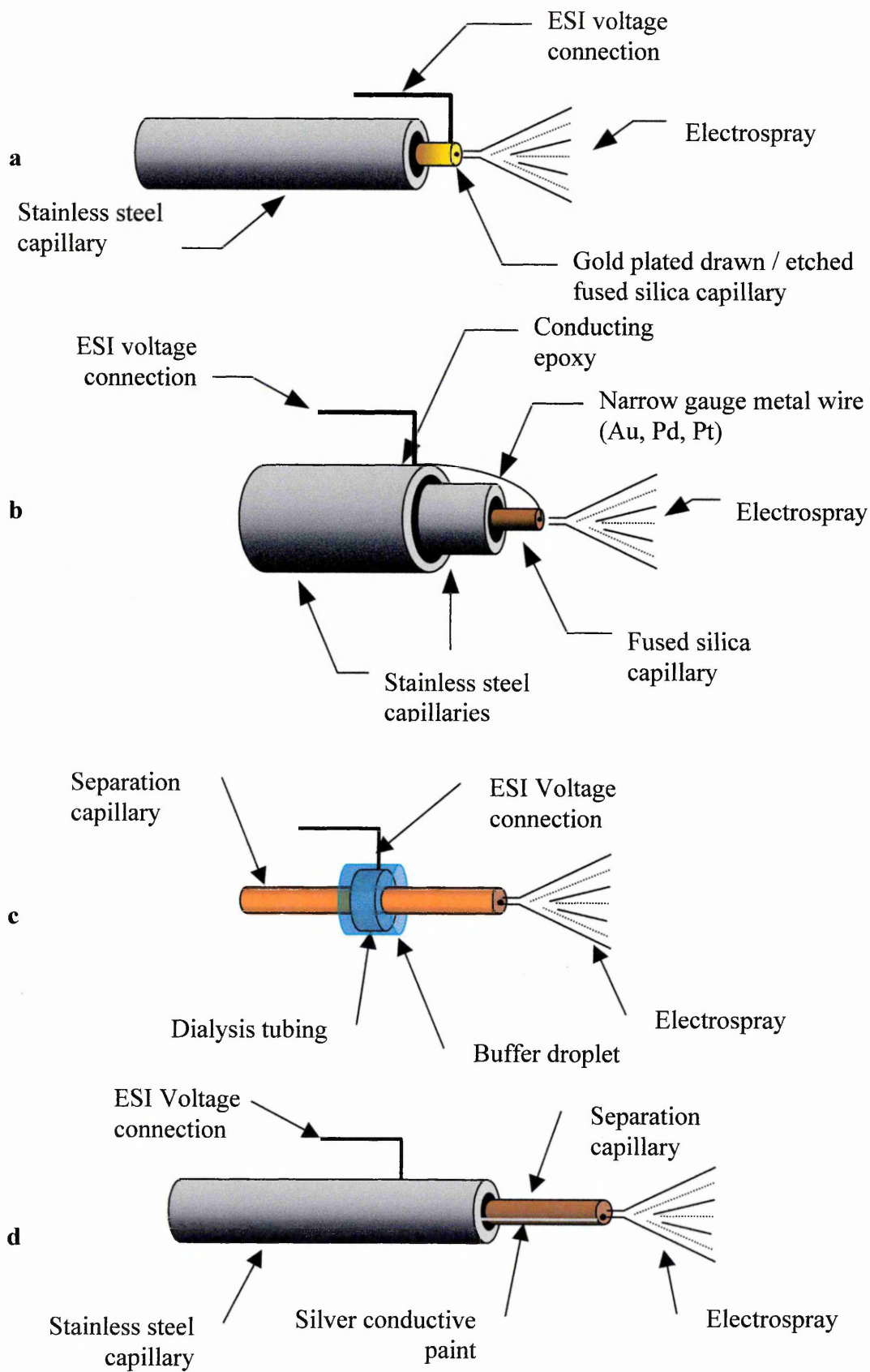


Figure 1.3.12 Various Forms of Nanospray Interface, a) Gold Plated Drawn / Etched Separation Capillary, b) In-capillary Electrode, c) Microdialysis Junction, d) Conducting Silver Paint Interface

The gold plated tips are commercially available<sup>46</sup>, and are readily manufactured<sup>47-71</sup>, unfortunately specialist equipment is required (for vapour deposition of the metal coating). The tips can be either drawn, to produce a narrow wall (usually by heat), or mechanically shaped (with a microlathe), then etched using 48 % HF (a flow of water (up to 6  $\mu$ l/min) through the capillary is required to prevent etching of the inner surface of the capillary). The tips are then dried and coated with a thin layer of gold or silver by vapour deposition. This conductive coating allows transmission of the electrospray voltage to the emerging liquid. Several groups<sup>72,73</sup> have suggested methods of derivatising the spray tip to improve the life time and stability of the coating. Kriger *et al.*<sup>72</sup> developed a method that required rigorous cleaning of the surface and then reaction with (3-mecaptopropyl)-trimethoxysilane, which acts as a molecular adhesive for the gold coating. The stability was tested by immersion in various solvents, only aqua regia and a 1:4 mix of 30% hydrogen peroxide / concentrated sulphuric acid (a strong oxidant) were found to damage the coating. Mechanical durability was tested with adhesive tape, no deterioration of the surface was observed. It was also noted that the coating withstood electrical discharges, the most common form of tip deterioration.

Valaskovic and McLafferty<sup>73</sup> suggest an alternative method by coating the gold with a protective layer of SiO<sub>x</sub> (a coating of SiO by thermal evaporation was produced, exposure of which to the atmosphere rapidly forms a SiO/SiO<sub>2</sub> insulating layer). Long term stability was improved, as was mechanical strength (to discharges *etc.*).

Volaskovic and McLafferty<sup>51</sup> also identified two possible sources of error for electrokinetic injection volume and migration times whilst using nanospray tips. Evaporation of solvent from the tip during injection can lead to an induced flow within the capillary, leading to an underestimation of injection volume, a critical factor for quantitative analysis. Immersion of the tip in buffer solution or application of a droplet of buffer will prevent the induced flow. If the solvent is electrosprayed at a greater rate than the EOF, laminar flow can be induced during analyses reducing migration times, the use of modified capillaries or buffers with a fast EOF would render this effect negligible.

Smith *et al.*<sup>47</sup> once more led the development of tapered conductive tips for CZE/MS. The first article to be published on the subject appeared in 1994, since then great interest has been shown in the development and application of the technique. Smith demonstrated the analysis of tryptic digests, on a 10  $\mu\text{m}$  i.d. capillary employing silver-coated tips; sample injections were of the order of 30 fmol. However, silver adducts of the peptides were observed. Smith suggested that these could be used in the determination of the charge state of a mass spectral peak, however in the case of a complex or incomplete separation these extra peaks could cause confusion and make spectral interpretation problematic.

In a continuation of this work<sup>48</sup>, Wahl and Smith compared sheath flow and sheathless interfaces at various buffer concentrations employing 100 and 10  $\mu\text{m}$  i.d. capillaries. The analyte sensitivity decreased with increasing buffer strength. Reduction of the capillary i.d. did not affect sensitivity, especially when a sheathless interface was employed. However, it was noted that it was necessary to filter the buffer whilst employing small i.d. capillaries, to prevent blockage.

In a novel development Smith *et al.*<sup>49</sup> demonstrated a method for the direct sampling of human erythrocytes into an APS modified CZE capillary, with the subsequent detection of the  $\alpha$  and  $\beta$  haemoglobin chains employing high resolution FT-ICR MS. The capillary inlet was etched with HF and attached to a micromanipulator, allowing electrokinetic injection of 5 – 20 cells (viewed under a 256x microscope) to be performed. Cell rupture occurred on mixing with the running buffer (ammonium acetate) owing to osmotic shock, after which separation occurred. It was suggested that the use of t-ITP techniques would allow smaller cell populations to be studied.

McLafferty *et al.*<sup>52</sup> demonstrated high resolution CZE/MS using FT-ICR MS via sheathless ESI. Mass spectral data was acquired at a resolution of  $\sim 60\,000$  FWHM from amol ( $0.7 - 3 \times 10^{-18}$  mole) injections of 8 – 29 kDa proteins. Tandem mass spectrometry of carbonic anhydrase gave 9 sequence specific fragment ions on an injection of  $9 \times 10^{-18}$  moles. This demonstrated the low sample quantities required for CZE separations and the high resolution and sensitivity that could be obtained from FT-ICR MS.

Volmer *et al.*<sup>60</sup> reported the first example of low-mass trace analysis by sheathless CZE/MS, in the analysis of isomeric sulphonamides in the low ppb (ng/mL) range from milk extracts. Conventional MS/MS could not differentiate between the isomers, so therefore a quasi-MS/MS/MS method was developed. In-source collision-induced dissociation (CID) was used as the first collision stage, then conventional MS/MS produced specific isomeric ions, with detection in the low fmol range.

Thibault *et al.*<sup>61</sup> investigated the effects of various sheathless interface arrangements. A one-piece column was compared with butted columns, using one of three connectors, i) double-tapered ferrule butt connector, ii) fused silica connector and iii) Teflon connector. The butted arrangement was the most desirable, as it allowed disposal of damaged tips without the loss of the separation capillary. The Teflon connector was the easiest to use, but gave a high background signal and increased analysis time compared to the one-piece column. The fused silica connector also gave an extended analysis time, whereas the ferrule connector gave a separation similar to that of the one-piece column. The increase in analysis time was attributed to dead-volume present in the connection, this was avoided using the double tapered ferrule, which was drilled to the exact required size, and allowed exact alignment of the capillaries. The ferrule connector was used for subsequent analyses of peptide mixtures. The effect of various capillary coatings was also examined. An APS derivatised single-piece column gave a fast separation, but with poor analyte resolution. A dynamic polybrene coating gave an improved separation compared to the APS column, but unfortunately the column surface had to be re-generated between runs, which resulted in tip blockages from the multiple wash stages. Covalent coatings were also examined on a one-piece capillary, MAPTAC and BCQ ([3-(methacryloylamino)propyl]trimethyl ammonium chloride, and [(Acryloylamino)propyl]-trimethylammonium chloride respectively), which differ by a single methyl group, gave results similar to those obtained with the polybrene coating. The covalent coating is preferential to the dynamic coating due to the lack of rinsing required between analyses. The BCQ/MAPTAC columns gave the best overall peak efficiencies ( $1.5 - 5 \times 10^5$  plates). Overall, amol sensitivities were obtained for peptides on both one-piece and butted capillaries with sheathless MS detection.

Figeys and Aebersold<sup>62</sup> employed a liquid junction to connect a spray tip and separation capillary. On-line SPE was facilitated through an immobilised C<sub>18</sub> plug at the inlet of the capillary. Two different mass spectrometers were compared to determine their suitability, an ion trap (IT) and a triple quadrupole (TQ). The peptides were hydrodynamically injected in to the capillary and the SPE material, after equilibration with an ESI compatible buffer the sample was eluted and separated, with subsequent MS detection. The IT was used in data dependant scan mode, *i.e.* when an ion passes a threshold level automatic product ion scanning is performed. The data obtained were compared to those previously obtained (without the SPE stage) on a TQ<sup>53</sup>. The LOD obtained for both systems were comparable, however the LOD for the MS/MS data was improved by a factor of ten for the IT. The TQ produced more low-mass information than the IT, but the higher sensitivity and mass resolution compensated for this. Sequence specific ions were readily produced, resulting in the identification of unknown proteins from sequence database searches in a single analysis.

Lee *et al.*<sup>68</sup> demonstrated the advantage of using a fast duty cycle time-of-flight MS, with acquisition rates up to 4 kHz (*i.e.* 80 spectra / s). The fast acquisition rate allowed in excess of 150 data points to be taken over narrow electrophoretic peaks of 2 – 4 s width. Consequently even higher separation efficiencies could be dealt with, sufficient data points would be obtained on a peak 100 – 120 ms base width to accurately describe the peak shape. The authors, in agreement with Banks and Dresch<sup>28</sup>, conclude that ToF mass spectrometers are ideally suited as detectors for fast separation techniques, such as CZE.

A novel technique was suggested by Fang *et al.*<sup>74</sup> in which a narrow gold wire was inserted into the terminus of the fused silica capillary (Figure 1.3.12b), to which the electrospray voltage was applied. The interface was attached to a home built ToF MS and on-line mass spectrometric analysis of peptides was obtained at a level of 40-80 fmol (injected).

As part of a review, Herring and Qin<sup>75</sup> compared different types of nanospray interface including a direct electrode technique, using a palladium wire, rather than a gold wire. Palladium was used as it adsorbs hydrogen, which is thought to be generated at metal interfaces forming bubbles causing a break in the EOF and hence the separation. They

suggested that this technique gave the best overall stability and appeared to last indefinitely. However, a number of limitations were discovered. A small decrease in resolution was obtained due to turbulence at the tip caused by the wire. Multiple oxidation of peptides (especially those containing Methionine) was also observed, however a precise mechanism of this oxidation could not be provided.

A variation of the direct electrode technique was suggested by Cao and Moini<sup>76,77</sup>, in which a small hole was cut in the capillary using an abrasive disk. A platinum wire was then inserted through the hole and fixed with epoxy resin. The electrospray voltage (and thus CZE ground) could then be applied through the wire. They reported a stable electrospray and separation current were obtained for an extended period of time.

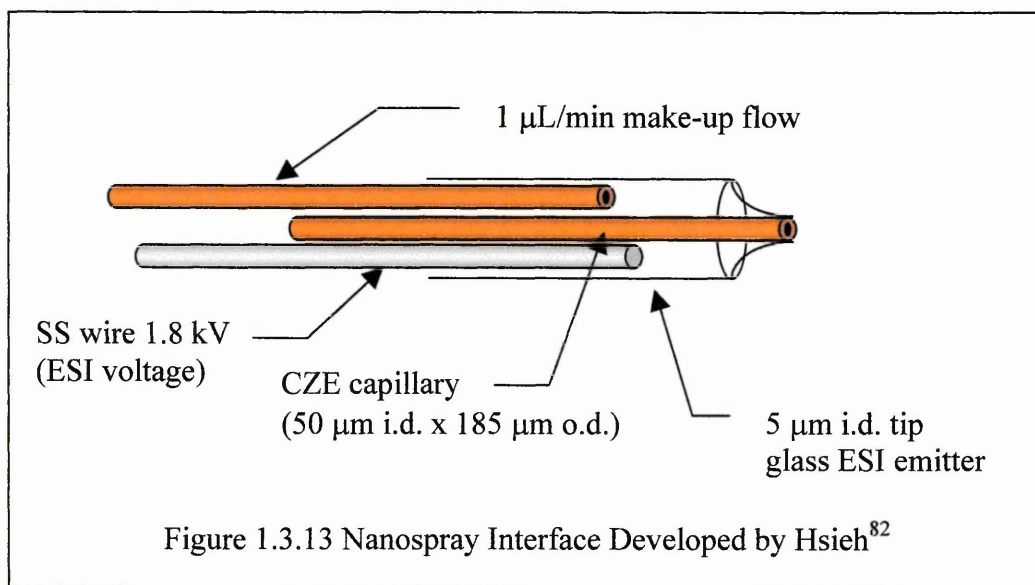
Recently Moini *et al.*<sup>78</sup> suggested the inclusion of hydroquinone as a buffer additive to prevent the formation of bubbles when using a direct electrode system. However, bubble suppression was only achieved when using a platinum electrode. This they suggested was due the inert surface of the electrode compared with stainless steel.

A microdialysis junction has been suggested by Severs *et al.*<sup>79,80</sup>, which employs an electrospray emitter, butted to the separation capillary with microdialysis tubing. The capillary is then positioned within a pipette tip filled with the background electrolyte, to which the electrospray voltage is applied. The use of the membrane allows electrolytic transfer to occur thus completing the circuit. They suggest this type of interface could be readily constructed, reducing preparation time compared to metallised tips.

Mazereeuw *et al.*<sup>81</sup> suggested a novel interface that uses no electrospray or cathode voltage for the separation or generation of electrospray. The capillary outlet (drawn from 75  $\mu\text{m}$  to 10  $\mu\text{m}$  i.d.) was located approximately 1 mm from the mass spectrometer inlet. The voltage drop of the CZE high voltage supply was sufficient to generate an electrospray, which could then be sampled directly into the mass spectrometer. Detection limits of up to one-order of magnitude lower than conventional nanospray interfaces were reported.

Hsieh *et al.*<sup>82</sup> developed a nanospray interface, which employs a makeup flow swept across the outlet of the capillary (Figure 1.3.13).

The separation capillary was inserted into a glass ESI emitter (with a 5  $\mu\text{m}$  i.d. tip). The emitter was flushed with a make-up liquid comprising 1:1 MeOH : H<sub>2</sub>O, 0.2% Acetic acid at 1  $\mu\text{L}/\text{min}$ , to which the ESI voltage was applied. The make-up solvent flowed towards the 5  $\mu\text{m}$  tip; any excess liquid passed out the non-spray end.



The function of the make-up solvent was to:

- Remove any existing air bubbles arising due to electrohydrolysis, therefore providing a stable current
- Eliminate any excess analyte from the tip
- Improve the electrospray process (without affecting separation) through the inclusion of MeOH and acetic acid

It was claimed that the 1  $\mu\text{L}/\text{min}$  did not affect the nanospray flow rate, which was determined by the emitter tip and spray voltage (approximated to be 50 nL/min). The nanospray interface was used to analyse standard peptide mixtures on an orthogonal-acceleration time-of-flight mass spectrometer.

### *1.3.5 Alternative Electroseparation Techniques / MS*

#### **1.3.5.1 Capillary Electrochromatography and Pseudo-electrochromatography**

Capillary electrochromatography (CEC) combines the efficiency of CZE with the selectivity of HPLC. CEC employs a fused silica capillary packed with an HPLC stationary phase. The mobile phase is driven through the column under the influence of an applied electric field, which generates an EOF. Pseudo-electrochromatography (p-CEC) is similar to CEC, except that the mobile phase is driven through the column by pressure as well as EOF. Further details of CEC are given in Section 1.1.8.1.

Tjaden *et al.*<sup>2</sup> successfully interfaced pseudo-electrochromatography to cf-FAB. In a follow up article Niessen *et al.*<sup>83</sup> interfaced p-CEC to co-axial sheath flow negative-ion electrospray, analysing aromatic glucuronides and food colourings. They reported that the p-CEC voltage was useful for ‘tuning’ the separation for specific analytes and that interfacing to electrospray mass spectrometry was straightforward, the data obtained being similar to  $\mu$ -LC. The only complication being encountered was the necessity to ground the p-CEC voltage prior to the spray, which resulted in increased stability.

Further instrumental developments of pseudo-electrochromatography electrospray mass spectrometry (p-CEC/MS) were suggested by Tjaden *et al.*<sup>84</sup> over their previous attempts using cf-FAB<sup>2</sup> and ESI<sup>83</sup>. The separation voltage was applied across the capillary via two liquid junctions, rather than direct application through unions. The use of a decoupled electrical contact was demonstrated to prevent bubble formation resulting in a more robust system. As a further refinement the electrospray voltage could be employed as an electrode for p-CEC, reducing zone dispersion.

Gordon *et al.*<sup>85</sup> demonstrated the use of capillary electrochromatography (CEC) interfaced to mass spectrometry via electrospray for the analyses of non-ionic disperse textile dyes. Once more CEC was demonstrated to be a useful alternative to micellar electrokinetic chromatography (MEKC) for analysing neutral compounds, especially when interfaced to a mass spectrometer. Increased sensitivity can be obtained with CEC over CZE as a result of the increased sample loadability (due to the packing material)

and higher efficiency over conventional HPLC. This first example of 'true' CEC/MS utilising ESI showed a promising development in the analysis of neutral compounds.

CEC/MS of pharmaceutical compounds was performed by Lane *et al.*<sup>86</sup>, but significantly lower efficiencies were obtained compared to CEC/UV. They attributed this to increased zone dispersion in the unpacked section of the capillary (25 cm packed bed at inlet, 90 cm total length). This was confirmed using a totally packed capillary of 92 cm, the separation obtained was similar to that achieved by CEC/UV, therefore confirming increased dispersion occurs in the unpacked section. Finally they inverted the original column, so that the unpacked section was at the inlet and the packed bed at the outlet, unfortunately no data could be obtained with this orientation. A further development<sup>87</sup> was to utilise a modified co-axial sheath flow probe; enabling short packed columns and high field strengths to be used. A standard Micromass CE/MS tri-axial interface was modified to shorten the section of probe inserted into the mass spectrometer. The normal probe housing was removed and replaced with a plastic box, which was interlocked to a 30 kV power supply. Within the box was mounted a vial holder containing sample and running buffer vials, electrokinetic injection was possible by using a spring loaded clamp, moving the capillary and HT electrode from one vial to the other. Connections for sheath liquid and nebulising gas were also made to the box. The resulting interface/instrument allowed column lengths of 43 cm with field strengths of  $617 \text{ Vcm}^{-1}$ , which is representative of the conditions regularly employed for CEC (or CZE)/UV.

Lord *et al.*<sup>88</sup> reported the use of tapers and restrictors as alternatives to silica frits in CEC (/MS). The tapers resulted in the suppression of bubbles during analyses. The use of a taper at the capillary outlet resulted in higher sensitivity compared to standard sheath flow interfaces. In addition, it was suggested that a taper at the inlet would facilitate the sampling of micro-environments, such as cell contents.

Taylor and Teale<sup>89</sup> developed a reproducible mobile phase gradient system for CEC/UV and CEC/MS, allowing short column lengths and low ionic strength buffers. The gradient was achieved using a T-piece, with a HPLC pump, CEC column and waste outlet attached. As the gradient supplied by the HPLC pump changed the buffer at the CEC inlet constantly changed therefore a gradient would be sampled into the CEC

column. Unfortunately there was a delay of 17 minutes between the gradient change at the pump and reaching the detector. The use of a gradient would allow stacking of dilute samples at the column head, increasing sensitivity.

Ding and Vouros<sup>90</sup> have demonstrated an application of CEC/MS for the analyses of DNA adduct mixtures, with the potential of *in vitro* screening of PAH-DNA adducts mixtures for risk assessments.

Paterson *et al.*<sup>91</sup> demonstrated CEC/MS to be a viable analytical technique for the analysis and quantification of potential drug candidates.

An on-line automated CEC/MS/MS system has been developed by Lane *et al.*<sup>92</sup> for the analyses of combinatorial libraries. The capillaries were packed with C<sub>18</sub>, C<sub>6</sub>, SCX and mixed mode C<sub>6</sub> / SCX (reversed phase / ion-exchange material) phases. Column efficiencies of 3.6 – 4 x10<sup>5</sup> theoretical plates were reported.

### 1.3.5.2 Transient Isotachopheresis (t-ITP) / CZE / MS

t-ITP can be used as a preconcentration method prior to CZE analyses. Further details of t-ITP are given in Section 1.1.8.6. Increased detection limits of proteins have been demonstrated by Karger *et al.*<sup>93</sup> by using on-column transient isotachopheretic sample preconcentration CZE/MS (t-ITP/CZE/MS) employing a co-axial sheath flow interface. To determine the increase in sensitivity the analyses were performed initially by CZE/MS and then by t-ITP/CZE/MS. A major limitation of CZE is the reduced injection volumes (maximum of 2% column volume <50 nL), t-ITP allows the injection of significantly higher volumes >100 nL. With CZE/MS proteins were detectable at the fmol (on-column) level (50 nL injection of  $\mu$ mol samples). Using t-ITP/CZE/MS (leading electrolyte ammonium acetate, and trailing electrolyte 6-aminohexanoate) proteins were still detected at fmol levels, but from a 750 nL injection of a nmol sample, thus demonstrating the increase in detection limits using on-line t-ITP.

Locke and Thibault<sup>94</sup> demonstrated an improvement in detection limits of at least two-orders of magnitude for marine toxins over that previously obtained<sup>6</sup>. Detection limits

of low nmol quantities were obtained employing on-line capillary isotachopheresis prior to CZE/MS. They also reported the use of CITP/CZE/MS/MS for unambiguous identification of individual toxins.

Hunt *et al.*<sup>95</sup> has described membrane preconcentration transient isotachopheresis capillary electrophoresis (mPC-tITP-CZE) coupled to ion trap MS via a porous glass-joint sheathless interface for the analysis of tumour peptides. The combination of mPC-tITP-CZE/MS has resulted in detection limits (< 50 amol) comparable with immunological samples and was able to resolve peptides not differentiated after multiple stages of HPLC. Membrane preconcentration (employing a polystyrene divinyl benzene (PSDVB) membrane) was performed on-line. This was achieved by placing the membrane between two pieces of fused silica held in place by a Teflon union. t-ITP allows significantly higher injection volumes (90 % vs. 10 %) to be analysed without severe zone dispersion occurring. Nanospray was achieved through HF etching of the separation capillary tip. The high voltage necessary for the electrospray process and to terminate the CZE voltage was applied through a porous glass joint. The joint was fabricated by etching the capillary wall to a thickness of < 20  $\mu\text{m}$ , which was then centred in a notched Teflon sleeve. The joint was then immersed in a 1 % acetic acid solution to which the ESI voltage was applied. Sequence specific MS/MS data was obtained from a 5  $\mu\text{L}$  injection of a 1:1 diluted HPLC fraction from  $10^{10}$  tumour cells, representing 250 amol of peptide with a  $S/N$  ratio of >10.

### ***1.3.6 Summary***

The initial development of CZE/MS led to the introduction of two distinct techniques, co-axial sheath flow and liquid junction. Both served to increase the flow emerging from the CZE capillary to suitable rates for ionisation by cf-FAB or ESI. As ESI became more widespread, its generality and ease of use led to the decline of research employing cf-FAB as an ionisation method for CZE.

The performance of the two interface techniques seems to be comparable, however the co-axial sheath flow is readily set-up and used. The sheath flow interface, theoretically, should also provide improved data (especially separation integrity) over a liquid

junction, owing to the reduced dead volume within the interface decreasing the extent of zone dispersion. This theoretical improvement and ease of use has perhaps been reflected in the relative increase of research performed using the co-axial sheath flow interface.

During 1996 Wilm and Mann<sup>40</sup> suggested a novel low-flow ionisation method termed nanospray. The introduction of an ionisation / interface that operated at similar flow rates to CZE generated great interest in developing CZE/MS employing nanospray. A number of methods have been developed, including metallised-sharpened tips, in-capillary electrode, microdialysis junction and conductive painted tips. Each method has its advantages and drawbacks. Metallised tips appear to be the most appropriate, especially as they are commercially available, however lengthy preparation time and instability of the metal coating (which can be improved by derivatisation prior to coating) has led to researchers questioning their suitability.

Of the interface techniques available, the most suitable for routine use appears to be the co-axial sheath flow systems, owing to the reported ease of optimisation and general use. In addition, sheath flow interfaces are commercially available from instrument manufacturers. Liquid junctions are limited in their widespread use; this can be attributed to the expertise required in aligning the capillaries and the associated contribution to zone dispersion. The nanospray interfaces demonstrated to date offer improved sensitivity over make-up flow designs, however at the cost of increased complexity (*cf.* co-axial designs) especially in the method employed to provide the ESI voltage / CZE current connection. Improvements in the metal coating stability and robustness are required before nanospray interfaces are adopted as a routine method for CZE/MS. In addition, nanospray requires a proportion of organic solvent in the buffer (to aid in the desolvation process), which can have significant effects on the separation integrity and migration order *cf.* CZE/UV. Therefore, care is required when a separation is transferred from UV/vis to MS detection when a sheathless interface is employed.

This author believes that with the current technology and methodology that is cited in the literature the interface of choice for CZE/MS is the co-axial sheath flow system. Owing to its ease of use and set-up would allow rapid CZE/MS method development from existing CZE/UV procedures.

The overall increase in CZE/MS applications suggests that CZE/MS is a viable analytical method, especially useful in sample limited situations. However, CZE/MS is still not a routine technique *cf.* LC/MS. Difficulty remains with the generation of stable separation current / ion current, employing the current interface designs. As demonstrated by Karger *et al.*<sup>23</sup>, Her *et al.*<sup>33</sup> and Lazar and Lee<sup>39</sup> method transfer from CZE/UV to CZE/MS is not always straightforward. Apart from the need for low conductivity, volatile buffers (that do not dominate the ion current); a mismatched buffer and make-up flow can have significant effect on the separation. This has been associated with the migration of make-up flow counter-ions through the capillary, affecting the EOF and hence separation.

The development and use of sheathless interfaces has improved sensitivity compared to the make-up flow designs, owing to the lack of dilution of analytes emerging from the column. This was especially observed when coupled to transient-isotachopheresis / capillary zone electrophoresis (t-ITP/CZE), detection limits of < 50 amol of peptides have been reported<sup>95</sup>. CZE/MS in combination with these sample preconcentration techniques has resulted in sensitivities that can rival other analytical techniques.

At present, another major limitation of CZE/MS is the CZE instrumentation itself. Typically the instruments are designed with optical (*i.e.* UV/vis, fluorescence) detection in mind, which can lead to problems when interfacing to a mass spectrometer, the main problem being the necessity to increase the column length (up to 1 m) due to spatial constraint between the instruments and hence elevated migration times. Certain instruments (Beckman P/ACE CE systems) contain a current monitoring circuit between the two electrodes, which has to be overridden when the outlet electrode is not used. Smith *et al.*<sup>19</sup> have described a method of modifying the P/ACE for CZE/MS use. Also instrumentation may require physical modification, *i.e.* holes drilled, through which the capillary can pass. Various research groups have overcome these problems by designing and fabricating their own CE instrumentation<sup>87</sup>. However, these frequently lack some of the facilities provided by commercial instruments, *i.e.* accurate and precise control of injections (both hydrodynamic and electrokinetic), which are essential for quantification purposes. Hewlett Packard are the only manufacturer who produce both CE and MS instrumentation<sup>96</sup>, and therefore have developed an interface / instrumentation which resolves these problems.

With these limitations, CE/MS at present primarily remains a research tool, yet this author believes that as instrumentation is improved and simplified (such as the development of specialised, dedicated instrumentation), widespread use should increase as a complementary technique to LC/MS.

## References

---

- (1) Caprioli RM; Moore WT; Martin M; DaGue BB; Wilson K; Moring S. *Journal of Chromatography* **480** (1989) 247
- (2) Verheij ER; Tjaden UR; Niessen WMA; van der Greef J. *Journal of Chromatography* **554** (1991) 339
- (3) Gordon DB; Lord GA; Jones DS. *Rapid Communications in Mass Spectrometry* **8** (1994) 544
- (4) Nichols W; Zweigenbaum J; Garcia F; Johansson M; Henion J. *LC·GC International* **6** (1993) 30
- (5) Lee ED; Mück W; Henion JD; Covey TR. *Biomedical and Environmental Mass Spectrometry*. **18** (1989) 844
- (6) Pleasance S; Thibault P; Kelly J. *Journal of Chromatography* **591** (1992) 325
- (7) Wachs T; Sheppard RL; Henion J. *Journal of Chromatography B* **685** (1996) 335
- (8) Hirabayashi Y; Hirabayashi A; Koizumi H. *Rapid Communications in Mass Spectrometry* **13** (1999) 712
- (9) Johansson IM; Huang EC; Henion JD; Zweigenbaum J. *Journal of Chromatography* **554** (1991) 311
- (10) Johansson IM; Pavelka R; Henion JD. *Journal of Chromatography* **559** (1991) 515
- (11) Wachs T; Sheppard RL; Henion J. *Journal of Chromatography B* **685** (1996) 335
- (12) Garcia F; Henion J. *Journal of Chromatography* **606** (1992) 237
- (13) Garcia F; Henion JD. *Analytical Chemistry* **64** (1992) 985
- (14) Smith RD; BarinagaCJ; Udseth HR. *Analytical Chemistry* **60** (1988) 1948
- (15) Olivares JA; Nguyen NT; Yonker CR; Smith RD. *Analytical Chemistry* **59** (1987) 1231
- (16) Smith RD; Olivares JA; Nguyen NT; Udseth HR. *Analytical Chemistry* **60** (1988) 436
- (17) Loo JA; Udseth HR; Smith RD. *Biomedical and Environmental Mass Spectrometry* **17** (1988) 411
- (18) Loo JA; Udseth HR; Smith RD. *Analytical Biochemistry* **179** (1989) 404
- (19) Smith RD; Udseth HR; Barinaga CJ; Edmonds CG. *Journal of Chromatography* **559** (1991) 197
- (20) Parker CE; Perkins JR; Tomer KB; Shida Y; O'Hara K; Kono M. *Journal of the American Society of Mass Spectrometry* **3** (1992) 563
- (21) Moseley MA; Jorgenson JW; Shabanowitz J; Hunt DF; Tomer KB. *Journal of the American Society of Mass Spectrometry* **3** (1992) 289
- (22) Tomlinson AJ; Benson LM; Gorrod JW; Naylor S. *Journal of Chromatography B* **657** (1994) 373
- (23) Foret F; Thompson TJ; Vouros P; Karger BL; Gebauer P; Bocek P. *Analytical Chemistry* **66** (1994) 4450
- (24) Tetler LW; Cooper PA; Powell B. *Journal of Chromatography A* **700** (1995) 21
- (25) Banks JF. *Journal of Chromatography A* **712** (1995) 245
- (26) Ashcraft AE; Major HJ; Lowes S; Wilson ID. *Analytical Proceedings Including Analytical Communications* **32** (1995) 459
- (27) Foret F; Kirby DP; Vouros P; Karger BL. *Electrophoresis* **17** (1996) 1829
- (28) Banks JF; Dresch T. *Analytical Chemistry* **68** (1996) 1480
- (29) Belder D; Stöckigt D. *Journal of Chromatography A* **752** (1996) 271
- (30) Lu W; Poon GC; Carmichael PL; Cole RB. *Analytical Chemistry* **68** (1996) 668
- (31) Lewis KC; Opiteck GJ; Jorgenson JW; Sheeley DM. *Journal of the American Society of Mass Spectrometry* **8** (1997) 495

- 
- (32) Tanaka Y; Kishimoto Y; Otsuka K; Terabe S. *Journal of Chromatography A* **817** (1998) 49
- (33) Tsai C; Chen Y; Her G. *Journal of Chromatography A* **813** (1998) 379
- (34) Lausecker B; Hopfgartner G; Hesse M. *Journal of Chromatography B* **718** (1998) 1
- (35) Liu C; Li X; Pinto D; Hansen EB; Cerniglia CE; Dovichi NJ. *Electrophoresis* **19** (1998) 3183
- (36) Ingendoh A; Kiehne A; Greiner M. *Chromatographia* **49** (1999) S-87
- (37) Takada Y; Sakairi M; Koizumi H. *Analytical Chemistry* **67** (1995) 1474
- (38) Bayer E; Gfrörer P; Rental C. *Angewandte Chemie International Edition* **38** (1999) 992
- (39) Lazar IM; Lee ML. *Journal of the American Society of Mass Spectrometry* **10** (1999) 261
- (40) Wilm M; Mann M. *Analytical Chemistry* **68** (1996) 1
- (41) Emmett MR; Caprioli RM. *Journal of the American Society of Mass Spectrometry* **5** (1994) 605
- (42) Andren PE; Emmett MR; Caprioli R. *Journal of the American Society of Mass Spectrometry* **5** (1994) 867
- (43) Olivares JA; Nguyen NT; Yonker CR; Smith RD. *Analytical Chemistry* **59** (1987) 1231
- (44) Smith RD; Olivares JA; Nguyen NT; Udseth HR. *Analytical Chemistry* **60** (1988) 436
- (45) Schmeer K; Behnke B; Bayer B. *Analytical Chemistry* **67** (1995) 3656
- (46) New Objective Inc., Cambridge, MA USA based on the method in Valaskovic GA; Kelleher NL; Little DP; Aaserud DJ; McLafferty FW. *Analytical Chemistry* **67** (1995) 3802 and Valaskovic GA; McLafferty FW. *Journal of the American Society of Mass Spectrometry* **7** (1996) 1270
- (47) Wahl JH; Gale DC; Smith RD. *Journal of Chromatography A* **659** (1994) 217
- (48) Wahl JH; Smith RD. *Journal of Capillary Electrophoresis* **1** (1994) 62
- (49) Hofstadler SA; Swanek FD; Gale DC; Ewing AG; Smith RD. *Analytical Chemistry* **67** (1995) 1477
- (50) Muddiman DC; Rockwood AL; Gao Q; Severs JC; Udseth HR; Smith RD; Proctor A. *Analytical Chemistry* **67** (1995) 4371
- (51) Volaskovic GA; McLafferty FW. *Rapid Communications in Mass Spectrometry* **10** (1996) 825
- (52) Volaskovic GA; Kelleher NL; McLafferty FW. *Science* **273** (1996) 1199
- (53) Figeys D; van Oostveen I; Ducret A; Aebersold R. *Analytical Chemistry* **68** (1996) 1822
- (54) Wu J; Qian MG; Li MX; Liu L; Lubman. *Analytical Chemistry* **68** (1996) 3388
- (55) Hofstadler SA; Severs JC; Smith RD; Swanek FD; Ewing AG. *Journal of High Resolution Chromatography* **19** (1996) 617
- (56) Kelly JF; Ramaley L; Thibault P. *Analytical Chemistry* **69** (1997) 51
- (57) Wu JT; Huang P; Li MX; Lubman DM. *Analytical Chemistry* **69** (1997) 2908
- (58) Lazar IM; Xin B; Lee ML; Lee ED; Rockwood AL; Fabbi JL; Lee HG. *Analytical Chemistry* **69** (1997) 3205
- (59) Lazar IM; Lee ED; Rockwood AL; Lee ML. *Journal of Chromatography A* **791** (1997) 269
- (60) Bateman KP; Locke SJ; Vomer DA. *Journal of Mass Spectrometry* **32** (1997) 297

- 
- (61) Bateman KP; White RL; Thibault P. *Rapid Communications in Mass Spectrometry* **11** (1997) 307
- (62) Figeys D; Aebersold R. *Electrophoresis* **18** (1997) 360
- (63) Huang P; Wu JT; Lubman DM. *Analytical Chemistry* **70** (1998) 3003
- (64) Bateman KP; White RL; Yaguchi M; Thibault P. *Journal of Chromatography B* **794** (1998) 327
- (65) McComb ME; Krutchinsky AN; Ens W; Standing KG; Perreault H. *Journal of Chromatography A* **800** (1998) 1
- (66) Lazar IM; Lee ED; Rockwood AL; Lee ML. *Journal of Chromatography A* **829** (1998) 279
- (67) Lazar IM; Lee ML. *Journal of Microcolumn Separations* **11** (1999) 117
- (68) Lazar IM; Rockwood AL; Lee ED; Sin JCH; Lee ML. *Analytical Chemistry* **71** (1999) 2578
- (69) Guo X; Chan HM; Guevremont R; Siu KWM. *Rapid Communications in Mass Spectrometry* **13** (1999) 500
- (70) Gucek M; Vreeken RJ; Verheij ER. *Rapid Communications in Mass Spectrometry* **13** (1999) 612
- (71) Barnidge DR; Nilsson S; Markides KE; Rapp H; Hjort K. *Rapid Communications in Mass Spectrometry* **13** (1999) 994
- (72) Kriger MS; Cook KD; Ramsey RS. *Analytical Chemistry* **67** (1995) 385
- (73) Valaskovic GA; McLafferty FW. *Journal of the American Society of Mass Spectrometry* **7** (1996) 1270
- (74) Fang L; Zhang R; Willaims ER; Zare RN. *Analytical Chemistry* **66** (1994) 3696
- (75) Herring CJ; Qin J. *Rapid Communications in Mass Spectrometry* **13** (1999) 1
- (76) Cao P; Moini M. *Journal of the American Society of Mass Spectrometry* **8** (1997) 561
- (77) Cao P; Moini M. *Rapid Communications in Mass Spectrometry* **12** (1998) 864
- (78) Moini M; Cao P; Bard AJ. *Analytical Chemistry* **71** (1999) 1658
- (79) Severs JC; Harms AC; Smith RD. *Rapid Communications in Mass Spectrometry* **10** (1996) 1175
- (80) Severs JC; Smith RD. *Analytical Chemistry* **69** (1997) 2154
- (81) Mazereeuw M; Hofte AJP; Tjaden UR; van der Greef J. *Rapid Communications in Mass Spectrometry* **11** (1997) 981
- (82) Hsieh F; Baronas E; Muir C; Martin SA. *Rapid Communications in Mass Spectrometry* **13** (1999) 67
- (83) Hugener M; Tinke AP; Niessen WMA; Tjaden UR; van der Greef J. *Journal of Chromatography* **647** (1993) 375
- (84) Dekkers SEG; Tjaden UR; van der Greef J. *Journal of Chromatography A* **712** (1995) 201
- (85) Lord GA; Gordon DB; Tetler LW; Carr CM. *Journal of Chromatography A* **700** (1995) 27
- (86) Lane SJ; Boughtflower R; Paterson C; Underwood T. *Rapid Communications in Mass Spectrometry* **9** (1995) 1283
- (87) Lane SJ; Boughtflower R; Paterson C; Morris M. *Rapid Communications in Mass Spectrometry* **10** (1996) 733
- (88) Lord GA; Gordon DB; Myers P; King BW. *Journal of Chromatography A* **768** (1997) 9
- (89) Taylor MR; Teale P. *Journal of Chromatography A* **768** (1997) 89
- (90) Ding J; Vouros P. *Analytical Chemistry* **69** (1997) 379

- 
- (91) Paterson CJ; Boughtflower RJ; Higton D; Palmer E. *Chromatographia* **46** (1997) 599
- (92) Spikmans V; Lane SJ; Tjaden UR; van der Greef J. *Rapid Communications in Mass Spectrometry* **13** (1999) 141
- (93) Thompson TJ; Foret F; Vouros P; Karger BL. *Analytical Chemistry* **65** (1993) 900
- (94) Locke SJ; Thibault P. *Analytical Chemistry* **66** (1994) 3436
- (95) Settlage RE; Russo PS; Shabanowitz J; Hunt DF. *Journal of Microcolumn Separations* **10** (1998) 281
- (96) HP <sup>3D</sup>CE and HP 1100 Mass Spectrometer, Hewlett Packard, Paolo Alto, CA USA

## **Chapter 2**

*Adaptation of A VG MassLab Trio3 Thermospray  
Interface for Operation as an Electrospray Ionisation  
Interface*

## 2.1 Introduction

Dole *et al.*<sup>1</sup> first demonstrated Electrospray ionisation (ESI) in 1968. Using a high electric field to effect electrostatic nebulisation, they showed that the technique was capable of producing gas phase ions from high molecular weight polymers in solution. Little further development was reported until the early 1980s when Fenn *et al.*<sup>2-5</sup> used the technique to produce multiply charged ions with subsequent mass spectral detection. ESI was shown to be a soft ionisation technique producing ions that would result in the detection of large (>100 kDa), intact polar molecules. This has generated tremendous interest in the analysis of biomolecules by mass spectrometry. Liquid chromatographic techniques (*i.e.* HPLC, CZE *etc.*) can be readily interfaced to mass spectrometry using ESI, resulting in on-line detection of complex mixtures. Another ionisation technique that generates ions as a result of a spray is thermospray<sup>6</sup> (TSP), in which ions are formed by vaporisation of an analyte dissolved in a volatile buffer. TSP is also a soft ionisation technique, applicable to polar and ionic compounds, typically, of low to moderate molecular weight (<1000 Da).

ESI has many advantages over TSP; most importantly, it can generate multiply charged ions from high molecular weight compounds, permitting the analysis of these analytes on conventional mass spectrometers. The hardware involved in TSP is similar to that required by ESI. Both techniques require similar levels of source vacuum and focusing lenses. So therefore, conversion of a commercial TSP source to ESI can be achieved without any major instrumental modification.

In ESI analyte ions are formed by electrostatic nebulisation of a liquid containing analyte and solvent at atmospheric pressure. The solvated ions pass from atmosphere into the high vacuum of the source, during which desolvation of the ions occurs. Desolvation can be achieved with the use of a counter-flow of heated bath gas<sup>7</sup>, a heated transfer capillary<sup>8</sup> or a heated spray chamber<sup>9</sup>; all methods are further aided by collisional activation in the reduced pressure region of the source. The production of ions by ESI is therefore dependent on the stability of the spray and successful desolvation. Most commercial ESI sources use counter-flow bath gas, but this would be difficult to implement in a TSP source without major modification, whereas the use of a

heated capillary would be straightforward and could also resolve the additional problem of transporting the ions into the vacuum system.

To date two research groups have independently converted commercial TSP sources for use in ESI mode. Jackett and Moini<sup>10</sup> developed an ESI interface for a Finnigan-MAT TSQ-70 (triple quadrupole) mass spectrometer. The interface was based on a heated capillary for desolvation, which was followed by the existing skimmer and lenses of the standard TSP source to transport the ions into the analyser region of the mass spectrometer. The source was in-line with the mass analyser and utilised the TSP pumping system. They reported picomole sensitivities of Cytochrome C and Gramicidin S, which were comparable to previously reported spectra<sup>7,8</sup>.

Tjaden *et al.*<sup>11</sup> demonstrated orthogonal ESI also employing a TSQ-70 TSP source. Desolvation was also accomplished using a heated transfer capillary. The orthogonal ESI source design was significantly easier to construct than that suggested by Jackett<sup>10</sup>. In addition, it had the additional benefit of neutral species not being sampled into the mass analyser. The TSP probe was replaced by a heated transfer capillary, which fitted directly into the ion source. Increased pumping capacity (28 m<sup>3</sup> / hour compared to 16 m<sup>3</sup> / hour) was necessary to maintain an adequate vacuum pressure within the TSP source region. Optimum sensitivity was obtained using a conical shaped repeller electrode, which resulted in a modified field within the expanding jet of analyte. Picomole sensitivity of infused lysozyme was demonstrated. In addition, applications of  $\mu$ -LC/MS (Acyl-coenzyme A compounds, detection limits of 50 – 100 pmol) and CZE/MS (employing a co-axial sheath flow interface for the analysis of inositol phosphates by negative ion, 9 pmol of each injected) were reported.

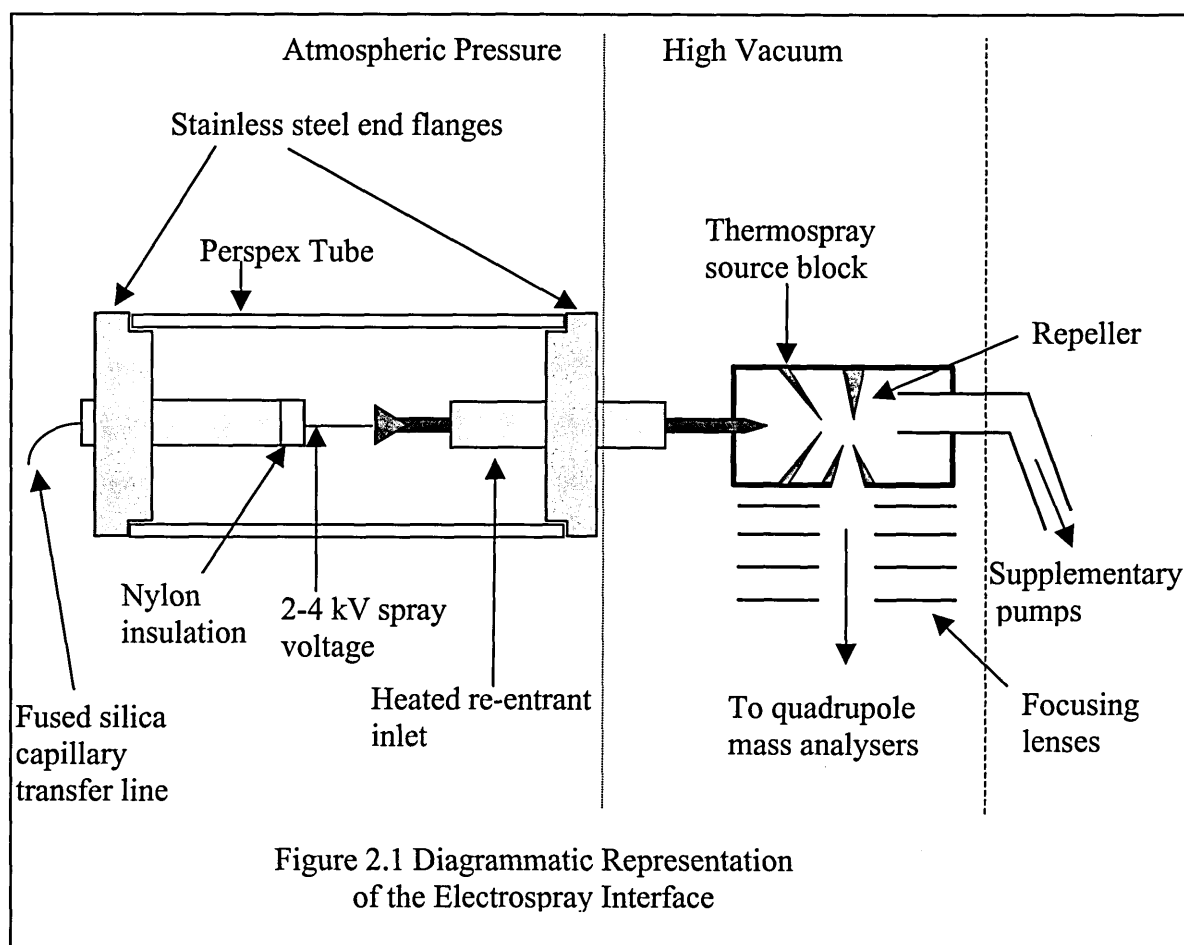
Van der Hoeven *et al.*<sup>12</sup> demonstrated an adaptation of the ESI modified TSP source to perform APCI. This was achieved by employing the existing ESI source (modified to include a focusing tube lens) with either pneumatic or thermospray nebulisation and a discharge electrode to facilitate ionisation by APCI. They report that signal intensities were improved at an increased source pressure (*i.e.* poorer vacuum), and detection limits of 2 ng/mL of reserpine (a common characterisation compound for APCI).

The two reported home-built ESI interfaces employed either an in-line or an orthogonal entry system. Both methods were developed on the same instrumentation producing similar sensitivities. However, the system adopted by Tjaden *et al.*<sup>11</sup> required little instrumental modification and was therefore simple and cheap to implement. Therefore, the reported ease of conversion of a thermospray source to perform as an electrospray interface prompted us to investigate this modification on our instrumentation.

## 2.2 Experimental

### 2.2.1 Interface Development

All experiments were performed on a VG MassLab Trio3 triple quadrupole mass spectrometer (now Micromass, Manchester, UK). The ESI interface adaptation is shown in Figure 2.1.



Fused silica capillary was used to connect a stainless steel syringe needle (400  $\mu\text{m}$  i.d. x 700  $\mu\text{m}$  o.d. x 20 mm) via a zero-dead-volume union to the solvent delivery system. The solution was electrosprayed directly from the needle using an applied voltage of approximately + 3.0 kV (Wallis R103/3/26R 10 kV power supply, Worthing, UK). The needle was situated approximately 3 mm from the transfer capillary and was housed inside a Perspex tube to prevent electric shock / discharge during use. The tube was attached to the mass spectrometer housing via a machined stainless steel disk, the other end flange held the electrospray probe in-line with the transfer capillary, both disks were on a common earth to the instrument.

A stainless steel capillary of 700  $\mu\text{m}$  i.d. x 1.6 mm o.d. and a length of 235 mm (SS HPLC tubing) was used to transport the analytes from atmospheric pressure into the high vacuum of the mass spectrometer. A 10 mm diameter cone was fitted to the atmospheric side of the capillary to enhance ion sampling. The capillary was fixed in a direct re-entrant inlet, which was heated to 50  $^{\circ}\text{C}$ , in addition the TSP source block was heated to 200  $^{\circ}\text{C}$ , both the transfer capillary and source block were maintained at ground potential.

The TSP source was unmodified, with the exception of the installation of a T-piece into the supplementary vacuum line, allowing increased pumping from two Balzers UNO 016B pumps (16  $\text{m}^3$  / hour each, Pfeiffer, Milton Keynes, UK).

The mobile phase was delivered at 350  $\mu\text{L}/\text{min}$  and split (Acurate Split AC-70, LC Packings, Presearch, Letchworth Garden City, UK) to yield a final flow of 5  $\mu\text{L}/\text{min}$  to the needle. Samples were injected employing a 20  $\mu\text{L}$  loop. The mobile phase comprised 1:1 MeOH : H<sub>2</sub>O (Milli-Q purifier, Millipore, Fisons Loughborough, UK) + 1 % acetic acid (all HPLC grade, Aldrich, Poole, UK) and was degassed daily by ultrasonication.

### 2.2.2 Characterisation

Initial tuning and development was performed using an infusion of Gramicidin S (1 – 3  $\mu\text{g}/\text{mL}$ ), monitoring the  $[\text{M}+2\text{H}]^{2+}$  ion at  $m/z$  571. Further characterisation of the

interface involved the analysis of a range of compounds, of both high and low molecular masses. The high-mass analytes were cytochrome c,  $\alpha$  and  $\beta$  chain haemoglobin mixture (both from Sigma, Poole, UK), bovine serum albumin (Biomedical Sciences department, SHU), and nonyl phenylethoxylate surfactant (NP14, Wilton Research Centre, ICI, Wilton, UK). The low-mass analyte was the pharmaceutical drug substance cimetidine (SmithKline Beecham Pharmaceuticals, Harlow, UK). All chemicals were used without purification and were dissolved in the mobile phase.

Mass spectra were obtained for 0.1 mg/mL haemoglobin mixture, cytochrome c, saturated BSA solution, undiluted NP14, and 0.1 mg/mL cimetidine in full scan mode. Further mass spectra of cimetidine were obtained in a dilution series of 1000 – 1  $\mu$ g/mL in order to determine the limit of detection.

### ***2.3 Results and Discussion***

The aim of this work was to develop an electrospray interface that was stable and effective with both high and low  $M_r$  compounds.

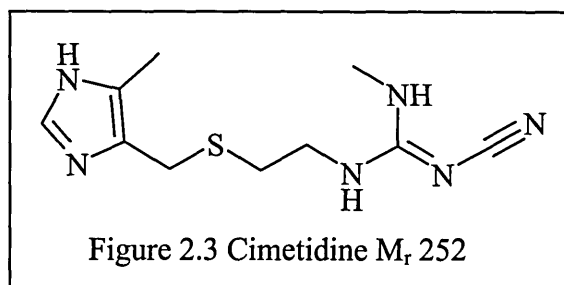
The resulting ESI interface with the modified TSP pumping system developed a source pressure of approximately  $5 \times 10^{-4}$  mbar, which is typical of atmospheric pressure ionisation (API) techniques.

The ESI probe consisted of a needle without a co-axial gas flow. Therefore liquid flow rates were limited to ‘traditional’ electrospray (1 – 10  $\mu$ L/min), and not the higher flow rates associated with ionspray (>100  $\mu$ L/min) owing to inefficient desolvation at these elevated flow rates.

A continuous infusion of 3  $\mu$ g/mL Gramicidin S (at 5  $\mu$ L/min), a cyclic decapeptide antibiotic ( $M_r$  1141), was used to optimise the instrument and assess the ability of the interface to analyse moderate mass compounds. Figure 2.2 (Section 2.5 Mass Spectra) shows the doubly charged ion,  $[M+2H]^{2+}$ , at  $m/z$  571, which was acquired in MCA mode. This corresponds to 160 pmol Gramicidin S being consumed. The critical

parameter for optimum sensitivity was the repeller voltage, high mass ions optimised around 220 V and low mass 140 V.

The analysis of pharmaceutical compounds by ESI/MS is important, due to their polar nature prohibiting their analysis by classical MS methods (*i.e.* EI). In addition, ESI is simple to interface to liquid chromatography, thus allowing the on-line determination of an analyte in complex mixtures. Cimetidine is an H<sub>2</sub>-antagonist used in the treatment of gastric ulcers, which was marketed under the name Tagamet by SmithKline Beecham Pharmaceuticals, its structure is shown in Figure 2.3.



The polar and basic nature of the compound makes it an ideal model compound for pharmaceutical analysis. Figure 2.4 shows the mass spectrum of a 20 μL injection of 1 mg/mL cimetidine featuring an ion at  $m/z$  253, corresponding to the protonated molecule,  $[M+H]^+$ . 100 μg/mL cimetidine resulted in a signal-to-noise (S/N) ratio of 6:1 (Figure 2.5). To determine the limit of detection of the mass spectrometer employing the ESI interface a serial dilution of cimetidine was performed. This resulted in a detection limit of 10 μg/mL (LOD defined as a signal to noise ratio of 3:1).

An envelope of peaks was observed for the mass spectrum of the synthetic polymer nonyl phenylethoxylate surfactant (NP14) (Figure 2.6, the corresponding mass assignments are given in Table 2.1). The main ion series corresponds to  $[M+H]^+$  and  $[M+Na]^+$  ions. The envelope extends across the  $m/z$  range 500 – 1000 Da (7 > sub-units < 18) separated by 44 Da, *i.e.* -OCH<sub>2</sub>CH<sub>2</sub>- ethoxymer sub-units. The envelope is a result of the number of ethoxymer sub-units within the polymer *i.e.* discrete compounds. The appearance of the spectrum should not be confused with that obtained for multiply charged peptides and proteins, where each peak in the spectrum corresponds to a multiply charged ion.

Table 2.1 Mass Assignments of Nonyl Phenylethoxylate Peak Envelope (Figure 2.6)

Number of ethoxymers	$[M+H]^+$	$[M+Na]^+$
7	528	551
8	572	595
9	616	639
10	660	683
11	704	727
12	748	771
13	792	815
14	836	859
15	880	903
16	924	947
17	968	991
18	1012	1035

For the high-mass determination of the interface, various proteins were analysed. Cytochrome C is an important electron transfer compound in aerobic respiration of animals. The multiply charged spectrum obtained from an 8 pmol/ $\mu$ L solution of Cytochrome C (horse heart, 12326 Da) at a flow rate of 5  $\mu$ L/min is shown in Figure 2.7. The data was acquired over the mass range 800 – 1400 / 30s (MCA mode) for 11 minutes, corresponding to approximately 450 pmol of analyte being consumed. The spectrum contains the multiply charged species in the range  $[M+9H]^{9+}$  to  $[M+15H]^{15+}$  allowing the detection of a >10000 Da peptide on an instrument of upper mass limit 4000 Da. Reconvolution of the data (employing MassLynx v2.1 software, Micromass) resulted in a spectrum (Figure 2.8) of the  $[M+H]^+$  ion, which corresponded to  $12329 \pm 3$ , this agrees favourably with the chemical average mass of 12327.

Haemoglobin is the oxygen carrying species present in mammalian blood, it is composed of two peptides ( $\alpha$  and  $\beta$  chains) comprising 141 and 146 amino acids. The peptide chains are associated with a porphyrin ring system (containing iron), to which the oxygen binds. The mass spectrum of the  $\alpha$  and  $\beta$  haemoglobin chains (Figure 2.9) contains two multiply charged envelopes (for  $[M+12H]^{12+}$  to  $[M+18H]^{18+}$ ), one for each chain. Reconvolution of this spectrum (Figure 2.10) results in the generation of the

$[M+H]^+$ , corresponding to 15086 and 15823, the  $\alpha$  and  $\beta$  chains respectively. These correspond with the theoretically calculated masses of 15126 and 15867 Da (these data were obtained with the instrument uncalibrated, hence the mass discrepancy).

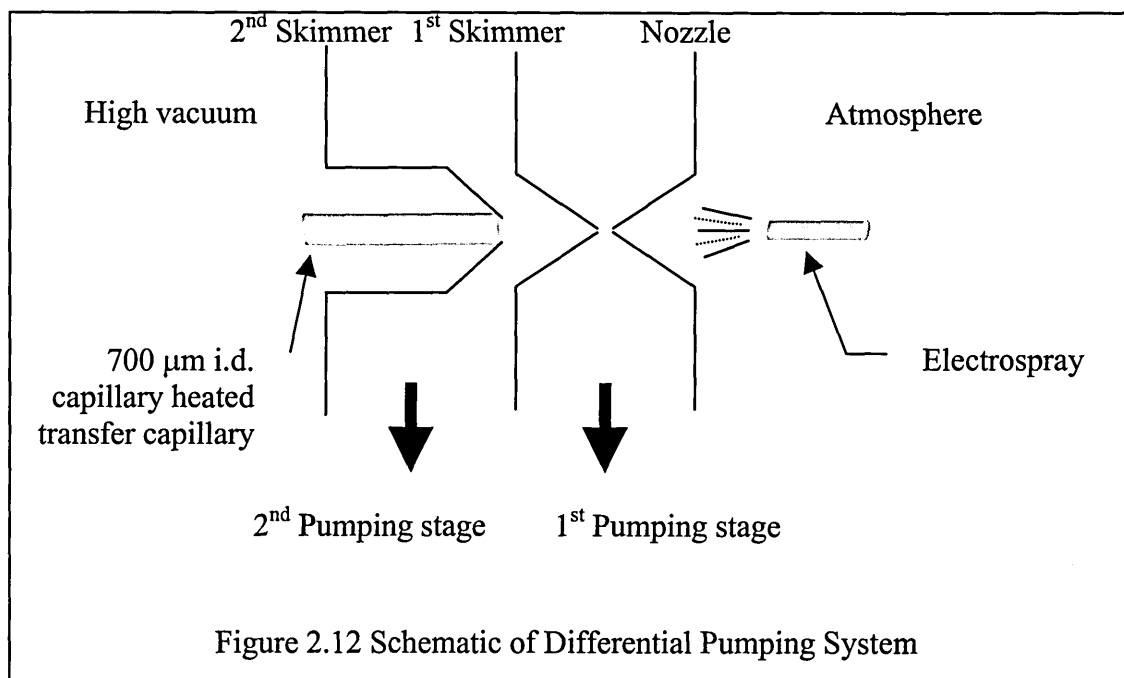
Finally bovine serum albumin (BSA) a protein of 66267 Da, was analysed. The mass spectrum of BSA (Figure 2.11) contains a number of peaks corresponding to multiply charged species. Reconvolution of the spectrum yields a  $M_r$  of 66.4 kDa.

#### ***2.4 Further Source Development***

After the above data were obtained, the heated transfer capillary became blocked whilst utilising an involatile phosphate buffer. After failed attempts to clear the blockage, the capillary was replaced with an identical new piece of tubing. However, a vacuum could not be maintained with the new 700  $\mu\text{m}$  i.d. capillary. This was attributed to the original capillary being slightly occluded, the internal diameter being sufficiently narrow to maintain an adequate vacuum. The heated transfer capillary was then replaced with 500  $\mu\text{m}$  i.d. stainless steel HPLC tubing. The narrower capillary provided a sufficient vacuum, however, analyte transmission was poor, and the generated ion current was insufficient to be detected with any sensitivity.

Using the 700  $\mu\text{m}$  i.d. capillary a differential pumping system (from a particle beam source) was developed (Figure 2.12).

The orifice diameters were nozzle 500  $\mu\text{m}$ , 1<sup>st</sup> skimmer 500  $\mu\text{m}$  and 2<sup>nd</sup> skimmer 700  $\mu\text{m}$  (transfer capillary). Two Balzers UNO 016B pumps were used as previous on the source outlet, and a single UNO 016B on the two stages of the differential pumping.



However, no ions were observed, the ion source ion gauge gave a reading of  $5 \times 10^{-6}$  mbar, a significantly lower pressure than obtained with the original design ( $5 \times 10^{-4}$  mbar). When the roughing pumps were backed off, the source pressure increased to between  $1 - 0.5 \times 10^{-5}$  mbar, and ions were observed. This was likely to be due to poor transmission through the skimmers at the reduced source pressure. In addition, the differential pumping system was taken from a particle beam interface, in which ions are formed after desolvation (therefore the assembly is held at ground potential), whereas in ESI ions are formed prior to desolvation and thus require focusing voltages to pass through skimmer lenses. The application of a voltage to individual lenses was not possible without major modification of the interface. This would also affect signal intensity. Overall beam stability was poor and slight vacuum changes resulted in a loss of signal.

A new mass spectrometer was obtained (Micromass Quattro I, triple quadrupole mass spectrometer), which has a commercially developed electrospray source, therefore this interface development was not pursued any further.

## 2.5 Mass Spectra

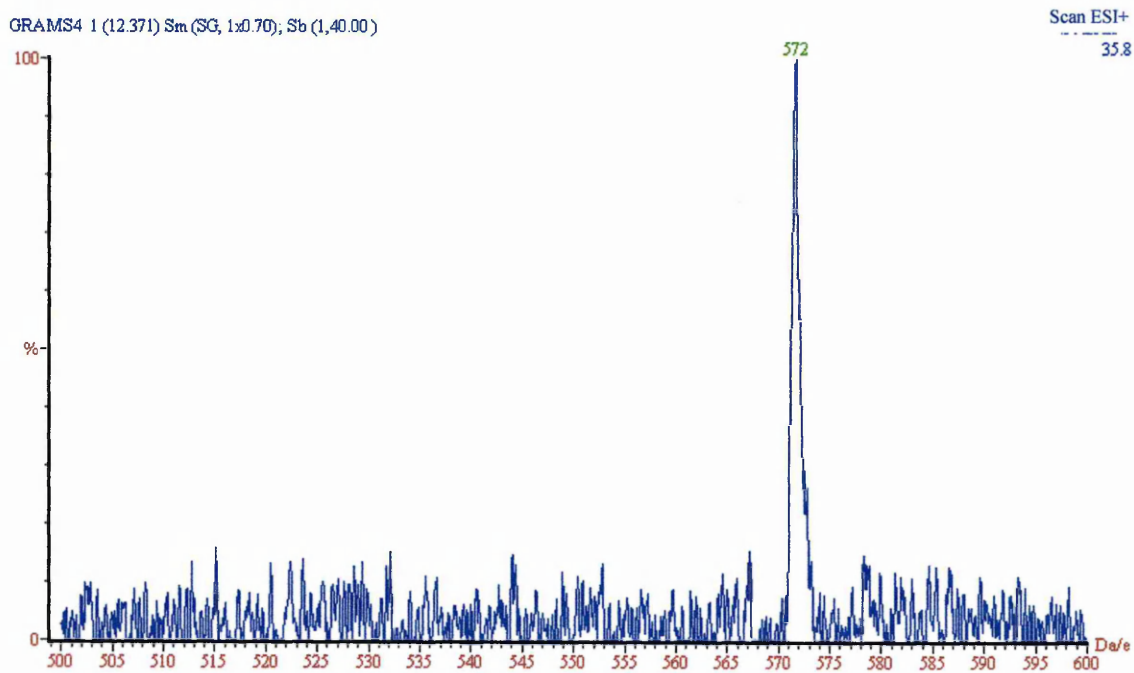


Figure 2.2 Continuous Infusion of Gramicidin S  
(160 pmol Consumed)

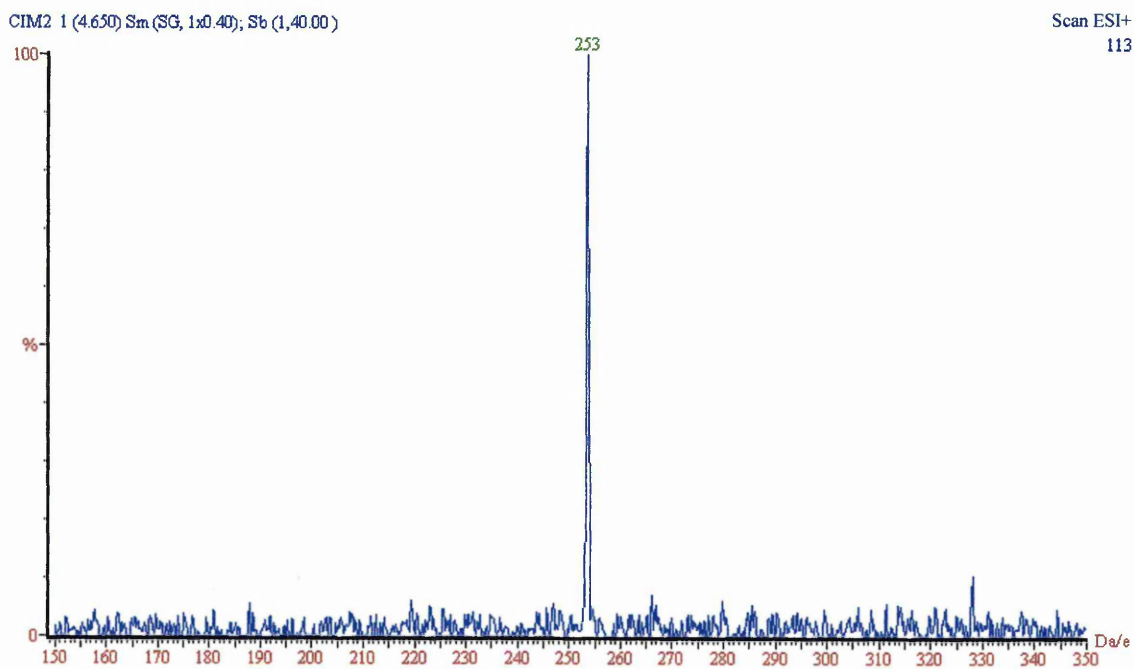


Figure 2.4 20  $\mu$ L Injection of 1 mg/mL  
Cimetidine,  $M_r$  252

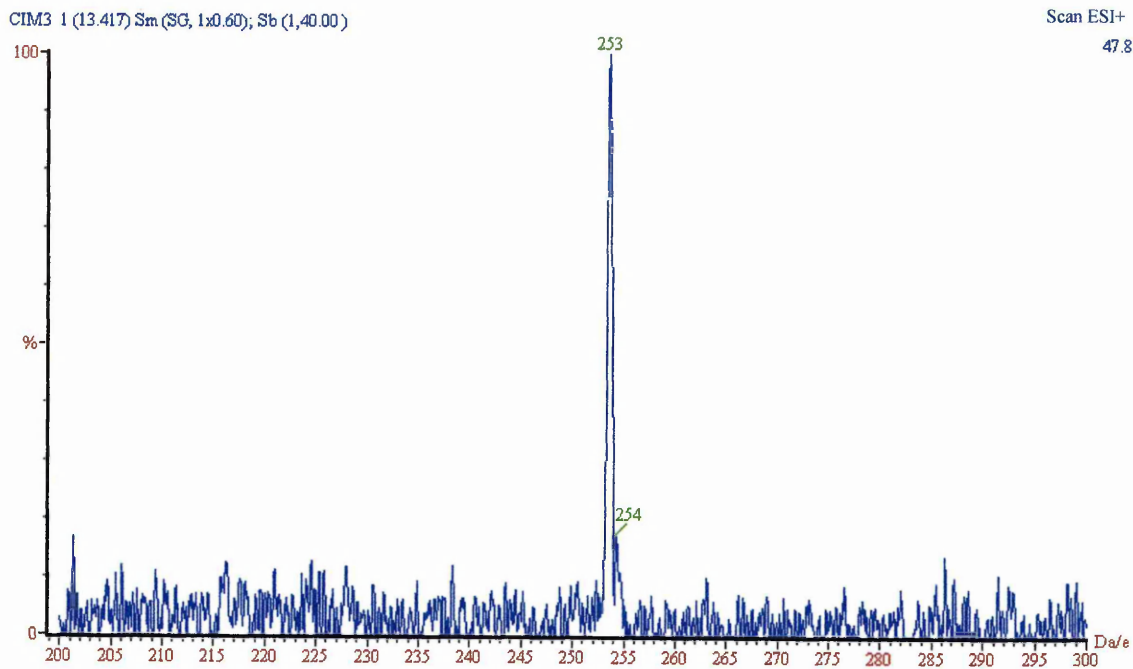


Figure 2.5 100 µg/mL Cimetidine at a S/N Ratio of 6:1

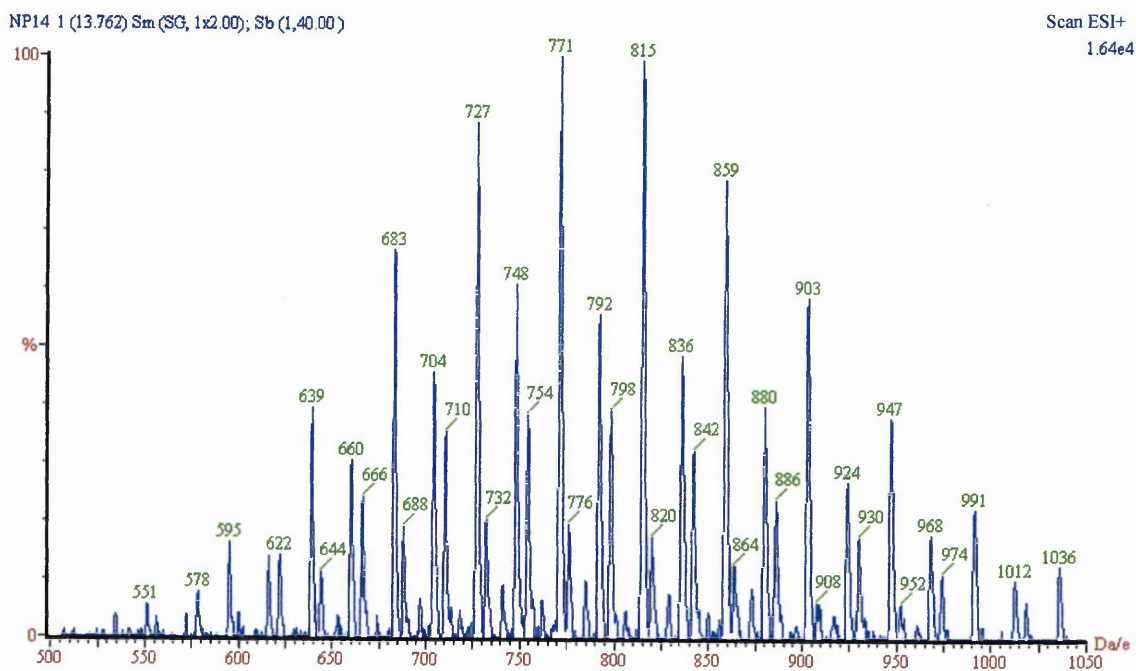


Figure 2.6 Mass Spectrum of Synthetic Polymer  
Nonyl Phenylethoxylate  
(Mass Assignment Table 2.1)

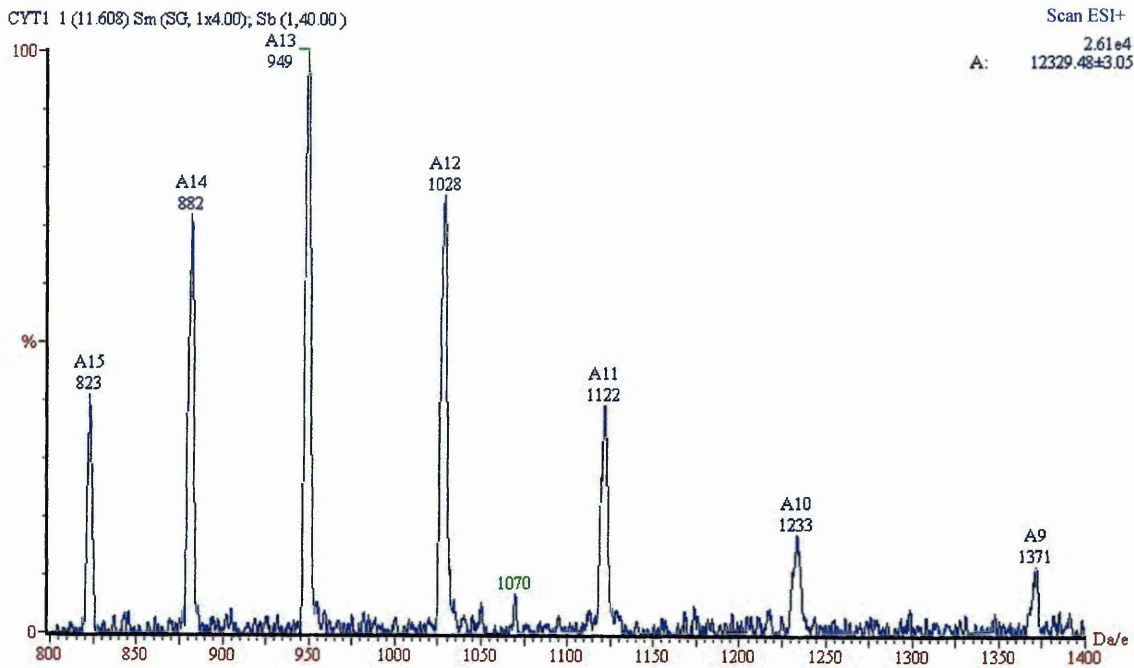


Figure 2.7 Mass Spectrum of 450 pmol Cytochrome C  
Displaying Multiple Charging from  $[M+9H]^{9+}$  to  $[M+15H]^{15+}$

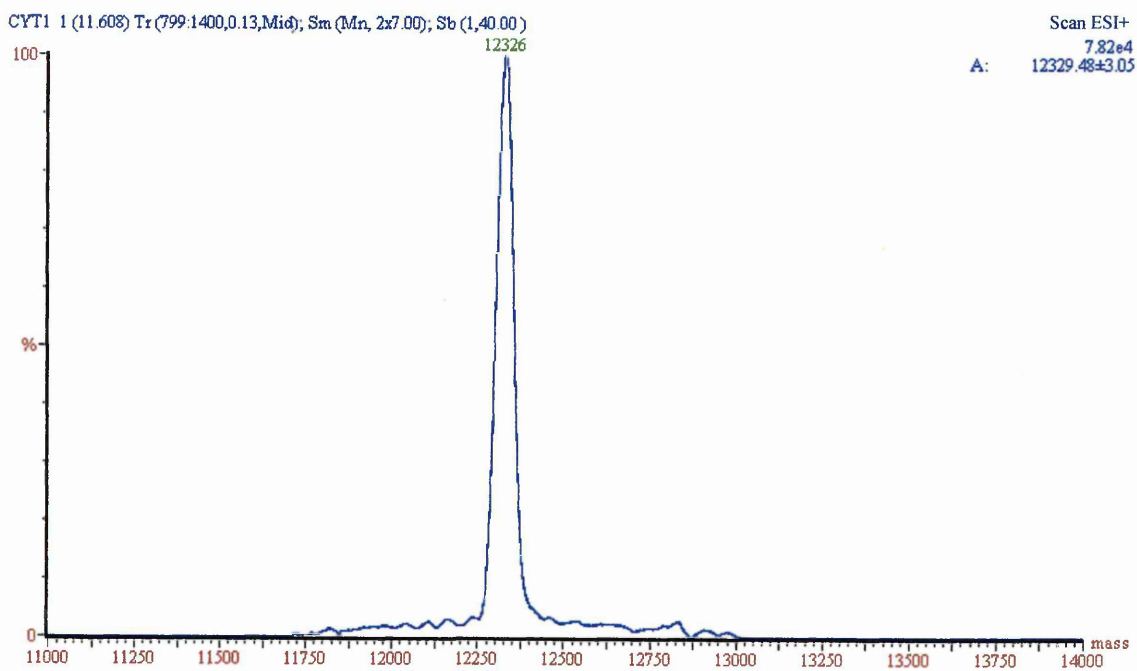


Figure 2.8 Reconvoluted Mass Spectrum of Cytochrome C,  
Experimental Mass  $12329 \pm 3$ , Calculated Mass 12327

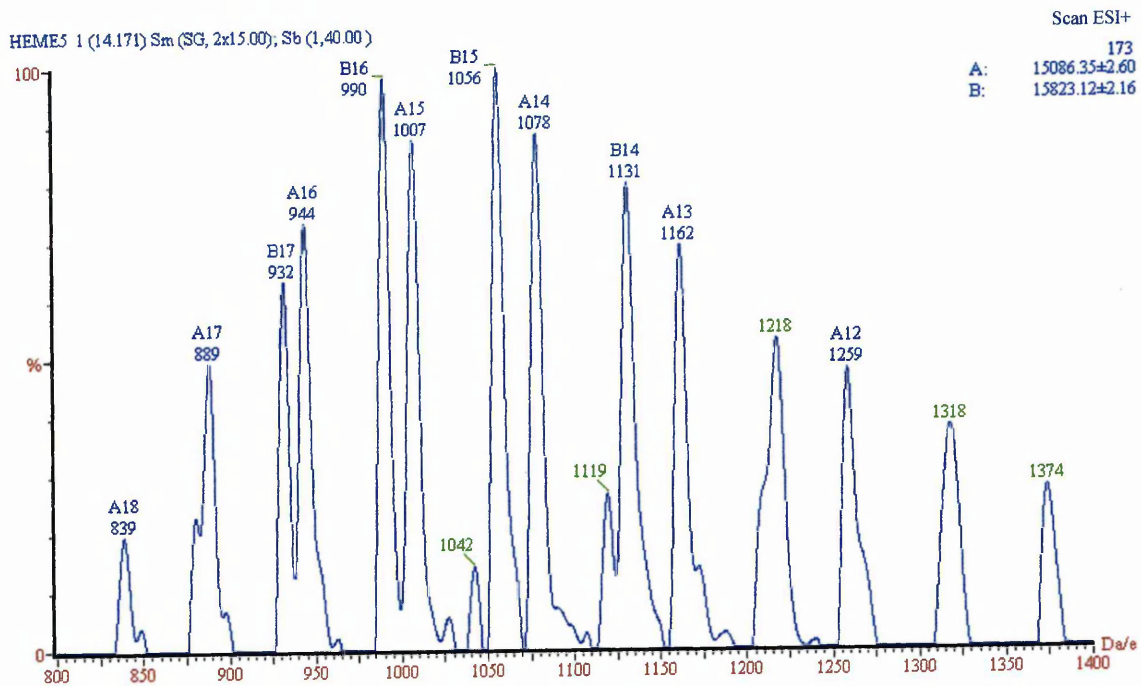


Figure 2.9 Mass Spectrum of Multiply Charged  $\alpha$  and  $\beta$  Haemoglobin Chains

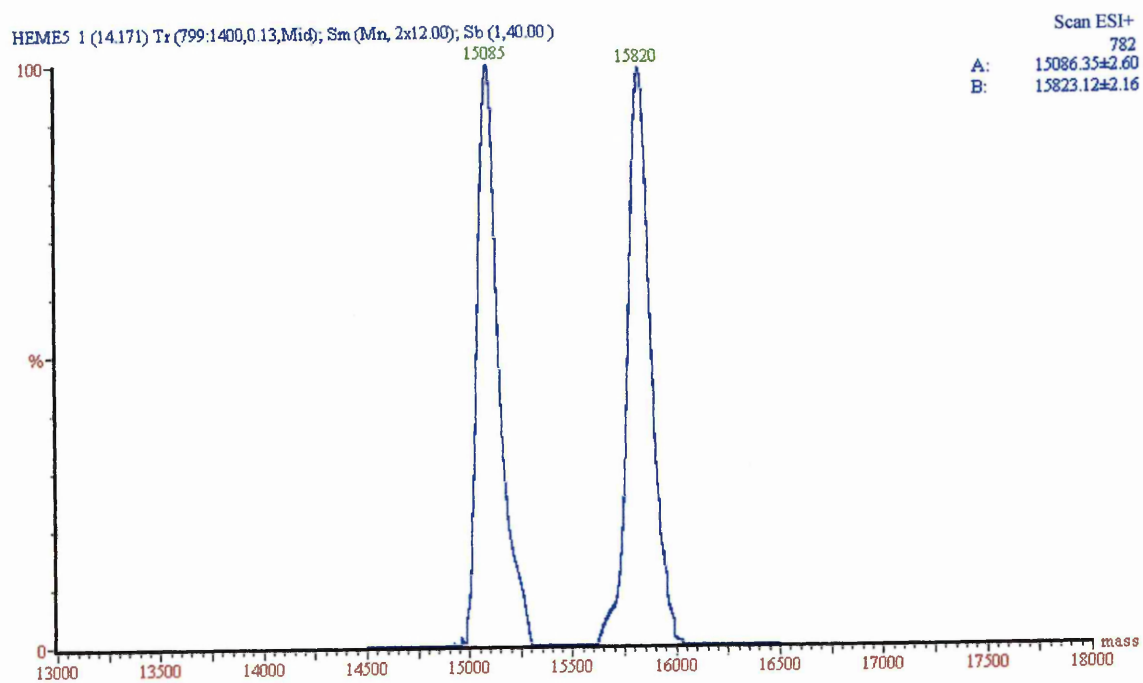


Figure 2.10 Reconvoluted Mass Spectrum of  $\alpha$  and  $\beta$  Haemoglobin Chains

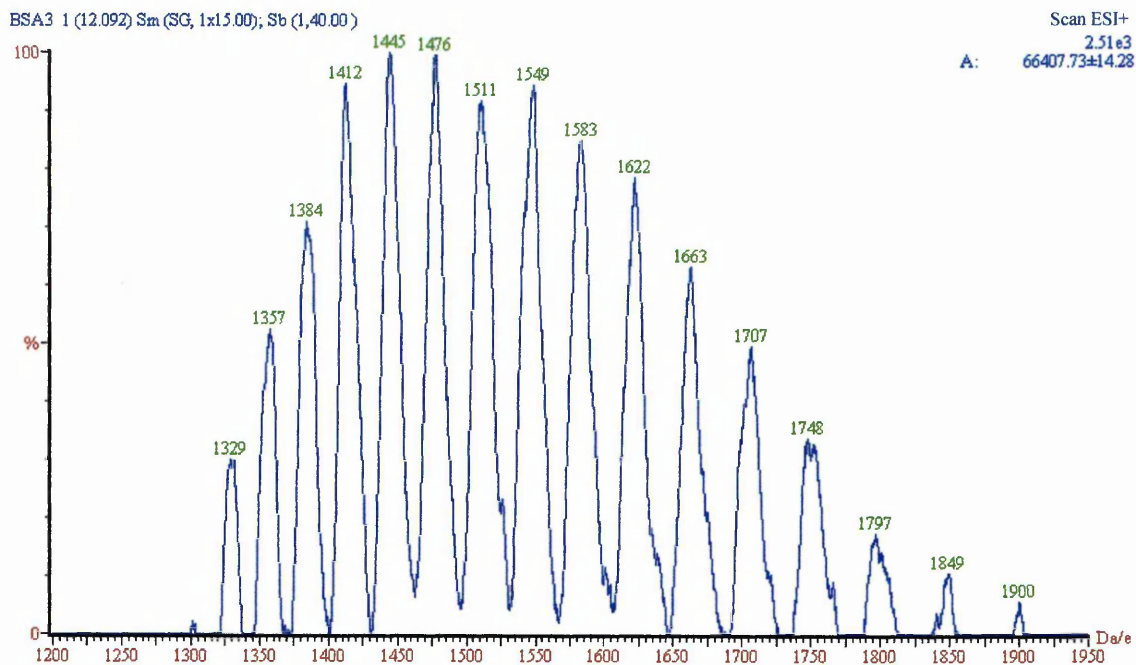


Figure 2.11 Mass Spectrum of Bovine Serum Albumin Displaying Multiply Charged Species

## 2.6 Conclusions

The home built ESI interface in conjunction with the TSP source, offered the advantages of commercial ESI interfaces, but at a fraction of the cost. The ESI interface worked well with large biomolecules and was accurate in its molecular mass measurement. The ESI source compared favourably with other examples<sup>10,11</sup> of in-house interfaces and with earlier approaches. The LOD achieved compared well with those obtained with other in-house manufactured ESI, but was still unable to achieve the sensitivity of commercially developed sources.

The 700  $\mu\text{m}$  heated transfer capillary became permanently blocked when a sample containing phosphate was analysed. Replacement capillaries were not suitable; an adequate vacuum could not be maintained employing the new 700  $\mu\text{m}$  i.d. tubes, whereas insufficient analyte transmission was obtained with 500  $\mu\text{m}$  i.d. capillaries. Therefore a differential pumping system was developed, which employed two stages of pumping prior to the heated transfer capillary. However, the pumping speed of the rotary pump was too high and the ion transmission was poor. The use of a lower backing pressure pump could have solved this problem (unfortunately this was not available).

A further modification to aid ion transmission would be to apply focusing voltages to the skimmers within the differential pumping system. However, this would require major modification, such that the skimmers would need to be electrically isolated from each other and the housing, whilst still maintaining a vacuum.

A new instrument has been obtained, which has a commercially developed electrospray source, therefore this development was not pursued any further.

## References

---

- (1) Dole M; Mack LL; Hines RL; Mobley RC; Ferguson LD; Alice MB. *Journal of Chemical Physics* **49** (1968) 2240
- (2) Yamashita M; Fenn JB. *Journal of Physical Chemistry* **88** (1984) 4451
- (3) Yamashita M; Fenn JB. *Journal of Physical Chemistry* **88** (1984) 4671
- (4) Whitehouse CM; Dreyer RN; Yamashita M; Fenn JB. *Analytical Chemistry* **57** (1985) 675
- (5) Wong SF; Meng CK; Fenn JB. *Journal of Physical Chemistry* **92** (1988) 546
- (6) Blakley CR; Vestal ML. *Analytical Chemistry* **55** (1983) 750
- (7) Fenn JB; Mann M; Meng MK; Wong SF; Whitehouse CM. *Mass Spectrometry Reviews* **9** (1990) 37
- (8) Chowdhury SK; Katta V; Chait BT. *Rapid Communications in Mass Spectrometry* **4** (1990) 81
- (9) Allen MH; Vestal ML. *Journal of the American Society of Mass Spectrometry* **3** (1992) 18
- (10) Jackett S; Moini M. *Reviews of Scientific Instruments* **65** (1994) 591
- (11) van der Hoeven RAM; Buscher BAP; Tjaden UR; van der Greef J. *Journal of Chromatography A* **712** (1995) 211
- (12) van der Hoeven RAM; Tjaden UR; van der Greef J. *Rapid Communications in Mass Spectrometry* **10** (1996) 1539

## **Chapter 3**

*The Separation of Cimetidine and Related Impurities by  
Capillary Zone Electrophoresis / Ultra Violet Detection*

### **3.1 Introduction**

Cimetidine (N-cyano-N-methyl-N'-[2(5-methyl-1H-imadazolyl-4-yl)methylthio-ethyl]guanidine) is the active component of the pharmaceutical drug substance Tagamet developed by SmithKline Beecham. Cimetidine is an H<sub>2</sub>-receptor antagonist and is used to heal gastric and duodenal ulcers by reducing gastric acid output. It can also be used for relief of peptic oesophagitis (over-production of stomach acid leading to inflammation of the oesophagus) and Zollinger-Ellison syndrome<sup>1</sup> (a condition where a gastric acid-secreting tumour develops).

Regulation of the contents of commercially available medication is stringent. Consequently, it is necessary to develop analytical methods that can characterise by-products and impurities of active components. This is generally accomplished using HPLC. Methods have been developed that are specific for the presence of cimetidine-related impurities employing HPLC/UV<sup>2</sup> and HPLC/MS<sup>3,4</sup>. A CZE<sup>5</sup> method has also been developed to quantify the cimetidine present in pharmaceutical preparations. Numerous alternative HPLC<sup>6,7</sup> and capillary electrophoretic (employing CZE<sup>8</sup> or MEKC<sup>9</sup>) methods of determining cimetidine and its major metabolite (cimetidine sulphoxide, SK&F 92452) in biological fluids have been reported. However, there has been no development of a CZE method to specifically identify cimetidine and its impurities. Therefore, the objective of this investigation was to develop such an analysis.

### **3.2 Experimental**

#### **3.2.1 Instrumentation**

Initial separations were performed using a PrinCE Model 310 (PrinCE Technologies, Emmen, The Netherlands). On-column UV detection was performed at a wavelength of 230 nm using a Phillips PU 4225 detector. Electropherograms were recorded by a Hewlett Packard 3395 integrator. Un-coated fused silica capillaries of 50 µm i.d. x 375 µm o.d. were purchased from Composite Metal Services Ltd (Hallow, UK). Capillary lengths were 60 cm, with an effective length of 44 cm (*i.e.* distance from inlet

to detector). On-column detection was facilitated by the removal of the polyimide outer coating to form a window using a capillary burner (EK 1.2, Capital HPLC, Edinburgh UK)

Subsequent separations were performed on a PrinCE Model 560 instrument, with on-column detection using a Bischoff Lambda 1010 UV detector ( $\lambda$  230 nm, time constant 0.2 s, range 0.1 Au), both operated under PC control using WinPrinCE embedded in DAX data acquisition software (Version 6.0, PrinCE Technologies). Un-coated fused silica capillaries of 75  $\mu\text{m}$  i.d. x 375  $\mu\text{m}$  o.d. (Composite Metal Services Ltd, Hallow, UK), 85 cm in length, with an effective length of 53 cm (*i.e.* distance from inlet to detector) were used. Separations were achieved with a field strength of  $\sim 350 \text{ Vcm}^{-1}$  (30 kV), unless otherwise indicated.

The column oven and sample tray were maintained at a constant temperature of 20  $^{\circ}\text{C}$  (by Peltier cooling) unless otherwise indicated.

All samples and separation buffers were degassed prior to analysis using a Branson 1210 ultrasonic bath and filtered through a 0.2  $\mu\text{m}$  syringe filter. pH measurements were made using a Hanna Instruments Checker (Fisher, Loughborough, UK), which was calibrated using solutions of known pH.

### 3.2.2 Reagents

Cimetidine and related compounds were obtained from SmithKline Beecham (Harlow, UK) their structures are shown in Table 3.1. Acetonitrile (MeCN) and methanol were of HPLC grade, water was distilled and deionised by a Milli-Q purification system (Millipore, Fisons, Loughborough, UK) sodium tetraborate, sodium dihydrogen phosphate and disodium hydrogen phosphate were of reagent grade and were purchased from Aldrich (Poole, UK). All other materials were of reagent grade or better.

Table 3.1 Analyte Structures

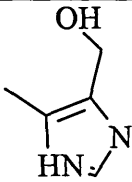
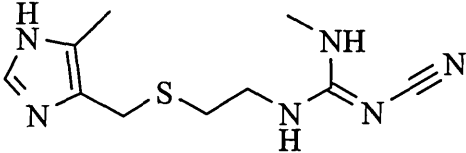
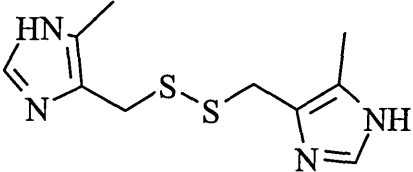
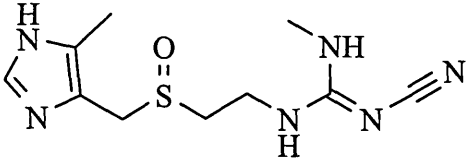
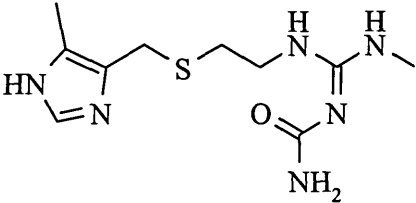
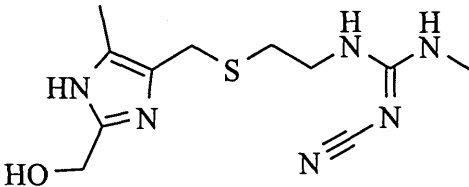
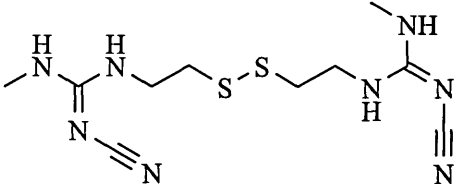
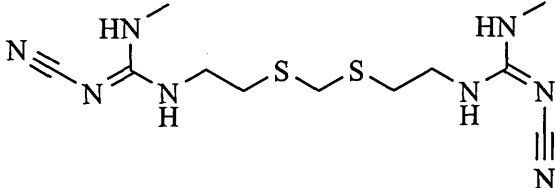
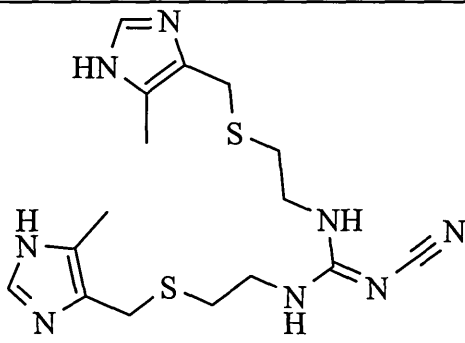
Structure	Name	$M_r$
	Cet-OH	112
	Cimetidine	252
	SK&F 91207	254
	SK&F 92452	268
	SK&F 92422	270
	SK&F 88958	282
	SK&F 82964	314
	SK&F 105779	328

Table 3.1 Continued

Structure	Name	$M_r$
	SK&F 92506	392

### 3.2.3 Procedures

#### *i Buffer Preparation*

Separation buffers were prepared by dissolution of suitable quantities of electrolyte in water. The pH was altered to the desired value using 0.1 M NaOH (when an increase in pH was required) or 0.1 M HCl (for a decrease in pH). Fresh buffers were prepared on a daily basis to improve reproducibility.

#### *ii Capillary Conditioning*

The capillary was conditioned prior to use and between separations with NaOH (0.1 M, 2 bar, 2 min), followed by water (2 bar, 0.8 min) and finally the relevant buffer (2 bar, 3 min).

#### *iii Analyte Preparation*

Individual stock solutions of each analyte (1000  $\mu\text{g/mL}$ ) were prepared in water and diluted to a working concentration of 100  $\mu\text{g/mL}$  (Philips detector) or 10  $\mu\text{g/mL}$  (Bischoff detector) using water. SK&F 82964 and 105779 were found to be insoluble in water and took no further part in this investigation using an aqueous solvent<sup>10</sup>.

#### *iv Injection Technique*

Injections were performed hydrodynamically, at a pressure of 25 mbar for 0.2 min. (Model 310) or 10 mbar for 0.07 min. (Model 560).

The volume ( $V$ ) injected into the CZE capillary can be calculated using Equation 3.1,

$$V = \frac{\Delta P d^4 \pi t}{2.132 \times 10^5 \eta L} \quad \dots(3.1)$$

$P$  = Pressure differential across capillary – 25 and 10 mbar

$d$  = Capillary i.d. – 50 and 75  $\mu\text{m}$

$t$  = Time – 0.2 and 0.07 min.

$\eta$  = Viscosity  $\sim$  1 cP

$L$  = Total length – 60 and 85 cm.

These correspond to injections of

- Prince 310, 50  $\mu\text{m}$  x 60 cm, 25 mbar / 0.2 min  
7.7 nL or 770 pg of each analyte in column (0.6 % of capillary volume)
- Prince 560, 75  $\mu\text{m}$  x 85 cm, 10 mbar / 0.07 min  
3.8 nL or 38 pg of each analyte in column (0.1 % of capillary volume)

Injections were substantially less than 2 % of the capillary volume and therefore would not have a significant contribution to zone dispersion. The increased injection volume (and hence reduced sensitivity) of the Prince 310 was likely due to the reduced detection path length (50  $\mu\text{m}$  vs. 75  $\mu\text{m}$ ). In addition, the UV lamp in the Bischoff detector (PrinCE 560) was newer than in the Philips detector, light energy (and hence detection efficiency) decreases with age, thus limiting detection.

### ***3.3 Results and Discussion***

Previous CZE analyses<sup>5,8</sup> reported on cimetidine, have employed different values of buffer pH (pH 7 and 2) to achieve separation. Initial development work<sup>10</sup>, employing the PrinCE 310 instrument, to separate Cimetidine, SK&F 92422 and 92506, was conducted over a range of pH values. A complete separation was achieved when a buffer of pH 3.1 was used. It was noted that the migration times decreased during replicate injections, this was attributed to electrolytic depletion and changes in pH of the buffer vials. Therefore, the inlet and outlet vials were replenished with fresh buffer every five analyses.

The whole procedure was repeated after a new instrument, a PrinCE 560 and Bischoff 1010 UV detector, became available. Computer-controlled data acquisition, rather than

the use of a chart recorder, offered data of superior appearance and quality. In addition, the reproducibility was improved owing to the dual lift system of the PrinCE 560 allowing a waste vial to be employed during capillary conditioning.

Migration times were longer for the PrinCE 560 compared to the PrinCE 310 due to the increased column length (and hence reduced applied field). Significant peak tailing (especially for cimetidine and SK&F 88958) was observed in the initial data<sup>10</sup> compared to that obtained using the PrinCE 560. The reason for this is not known, but in both analyses, the appearance of the data was reproducible.

The data obtained employing the PrinCE 560 will be discussed in further detail. When a 10 mM sodium tetraborate buffer adjusted to pH 9.1 under a potential of 30 kV was employed (Figure 3.1, see Section 3.4 Electropherograms) all 7 seven analytes co-migrated, with a migration time equal to that of thiourea (neutral marker). This confirmed that they are uncharged at high pH and migrate at a rate equal to the electroosmotic flow (*i.e.*  $\mu_{\text{EOF}} = \mu_{\text{E}}$ ). Reducing the pH to 8.1 (10 mM sodium tetraborate) resulted in a shoulder forming at the front of the main peak (Figure 3.2), indicating that one of the analytes was developing a charge and migrating under the influence of the EOF and its own mobility. Reducing the separation voltage to 20 kV resulted in an increased separation of the shoulder, but all other analytes migrated with the EOF. Changing the buffer to 10 mM disodium hydrogenphosphate ( $\text{Na}_2 \text{HPO}_4$ ) at pH 7.1 (30 kV) increased the separation (Figure 3.3), resulting in four separated peaks and a leading shoulder on the EOF peak. Reducing the separation voltage to 20 kV further increased the resolution of the leading shoulder from the EOF. A reduction of buffer pH to 3.1 (10 mM sodium dihydrogenphosphate,  $\text{Na H}_2\text{PO}_4$ ) resulted in almost complete resolution of six analytes in less than 8 minutes under an applied voltage of 30 kV (Figure 3.4). Migration times are shown in Table 3.2. At this pH the EOF was significantly reduced, migrating at  $\sim 17$  minutes. Therefore

$$\mu_{\text{EOF}} < \mu_{\text{E}}$$

$\mu_{\text{EOF}}$  = EOF mobility and  $\mu_{\text{E}}$  = analyte electrophoretic mobility

The migration order was determined to be

SK&F 91207, 92422, 92506 (which co-migrates with Cet-alcohol), cimetidine, 92452 and finally 88958.

(No further attempt was made to separate SK&F 92506 and Cet-alcohol. Therefore, only SK&F 92506 was included in further analyses)

Table 3.2 Analyte Migration Times (n=5)

Analyte	Migration time / minutes	% RSD
SK&F 91207	4.585	0.347
SK&F 92422	4.859	0.370
SK&F 92506	5.454	0.397
Cimetidine	7.083	0.472
SK&F 92452	7.330	0.503
SK&F 88958	7.453	0.517
Thiourea (neutral marker)	17.012	0.493

All peaks are fully resolved except for SK&F 92452 and 88958 (that is, using the standard definition of  $R > 1.5$ , rather than baseline resolution), where  $R = 0.7$ . A further decrease in pH to 2.1 (employing a 10 mM sodium dihydrogenphosphate buffer system, Figure 3.5) increased the resolution to  $R = 1.4$ , and further reduced migration times, the EOF was not detected within 30 minutes, thus under these conditions:

$$\mu_{\text{EOF}} \ll \mu_{\text{E}}$$

Overall, the most suitable pH for this analysis was pH 3.1. The peaks were baseline resolved, with reproducible migration times and a reasonable EOF flow rate (migrates < 20 min., corresponding to a flow rate of  $0.83 \text{ mm s}^{-1}$ ).

Caustic capillary washing was performed between analyses. It has been suggested<sup>11</sup> that a hysteresis-effect of wall charge can occur when employing a caustic wash and acidic buffer conditions, leading to shifts (and hence poor reproducibility) in migration time. To evaluate the extent of this effect, washings were performed using 0.1 M HCl rather than 0.1 M NaOH (Figure 3.6). The analyte migration time reproducibilities were improved (Table 3.3) and the EOF reduced to approximately 21 minutes. Lambert and Middleton<sup>11</sup> also demonstrated that conditioning of the capillary at high or low pH can lead to differences in EOF mobility at the same buffer pH, which is consistent with the reduced EOF observed using acidic pH *cf.* alkaline pH.

The resolution of SK&F 92452 and 88958 was improved (from 0.7 to 0.9). This could be attributed to the reduction of the EOF velocity and hysteresis of the capillary surface charge due to pH extremes during the washing procedure.

Table 3.3 Reproducibilities Using Caustic and Acidic Washes Between Analyses (n = 5)

	NaOH Wash		HCl Wash	
	Mean / min.	% RSD	Mean / min.	% RSD
91207	4.585	0.347	4.894	0.246
92422	4.859	0.370	5.208	0.231
92506	5.454	0.397	5.887	0.195
Cimetidine	7.083	0.472	7.829	0.139
92452	7.330	0.503	8.128	0.172
88958	7.453	0.517	8.275	0.152
Thiourea	17.012	0.493	21.731	1.461

Therefore, acid washes were used between all further analyses.

The analyte mobilities and efficiencies employing an acid wash analysis are shown in Table 3.4.

The high efficiencies achieved by electrophoretic separations arise through the flat flow profile of the electroosmotic flow reducing contributions to zone dispersion.

Table 3.4 Analyte Effective Mobilities and Efficiencies

	Effective Mobilities* / $10^{-9} \text{ m}^2 (\text{Vs})^{-1}$	Efficiencies† / m
SK&F 91207	45.1	210 000
SK&F 92422	41.6	190 000
SK&F 92506	35.3	160 000
Cimetidine	23.3	140 000
SK&F 92452	21.9	130 000
SK&F 88958	21.3	110 000
Thiourea	13.1	45 000

Quantification analyses are important in the pharmaceutical industry. Regulatory authorities set a maximum limit (usually 0.1 %) that impurities can be present in drug substances. Peak heights or areas (which are directly proportional to concentration) are frequently used for quantification purposes. To improve reproducibility corrected peak areas are used, *i.e.* the analyte area is divided by the area of an internal standard (which is required to be structurally similar to the analytes, so for convenience the active component of the drug can be used). The use of an internal standard corrects for irreproducibilities arising through variation of injection volume and detector response. The corrected areas for the separation of cimetidine and related compounds are given in Table 3.5, using cimetidine as the internal standard.

---

\* Calculated using  $\mu_E = \left[ \left( l / t_m \right) - \left( l / t_{nm} \right) \right] L / V$   $l$  = Effective length  $t_m / t_{nm}$  = Migration time of analyte and neutral marker respectively  $L$  = Total length  $V$  = Voltage

† Calculated using  $N = 5.54 \left( t / w_{0.5} \right)^2$   $t$  = Migration time,  $w_{0.5}$  = Temporal peak width at half height

Table 3.5 Corrected Peak Areas (Cimetidine used as Internal Standard)

	Corrected area	% RSD
SK&F 91207	0.312	3.696
SK&F 92422	0.173	3.266
SK&F 92506	0.228	7.751
Cimetidine	-	-
SK&F 92452	1.108	0.666
SK&F 88958	1.357	2.394

To attempt to fully resolve the final peaks, various electrolyte and instrumental parameters were altered, namely

- Increasing buffer strength
- Addition of organic solvent
  - Methanol
  - Acetonitrile
- Instrumental temperature

### 3.3.1 Buffer Strength

Initial development of the separation conditions employed a 10 mM buffer, variation of the buffer strength can have considerable effect on the EOF. Increasing the buffer concentration, decreases the double layer thickness ( $\delta$ ) at the capillary wall, which reduces the zeta potential ( $\zeta$ ) and hence the EOF mobility, *i.e.*

$$\mu_{EOF} \propto \zeta \propto \frac{1}{\delta} \quad \dots(3.2)$$

Reduction of the EOF mobility (towards zero) decreases the contribution to an analytes apparent mobility (the sum of EOF and electrophoretic mobilities) thus leading to analytes individual electrophoretic mobilities having an increasing effect on the separation, potentially increasing resolution.

The electropherogram obtained for 15 mM sodium dihydrogenphosphate is shown in Figure 3.7, as with the separation performed at pH 2.1, the EOF was not detected within

30 minutes and SK&F 92452 and 88958 were still not fully resolved (on the basis of  $R > 1.5$ ). The resolution of SK&F 92452 and 88958 was not further improved on increasing the buffer concentration to 20 and 50 mM (sodium dihydrogenphosphate at pH 3.1). However, the peak efficiencies did improve (Table 3.6) even though the current increased (for 30 kV separations 10 mM ~18  $\mu$ A, 15 mM ~24  $\mu$ A, 20 mM ~32  $\mu$ A and 50 mM ~103  $\mu$ A), which would increase the Joule heating contribution to zone dispersion. The increase in efficiency can be attributed to the enhanced focusing of the analyte zones by the higher concentration buffers. The sample was injected into the capillary dissolved in water, so therefore was of low conductivity, as the buffer conductivity ( $\approx$  strength) increases, the analyte zone experiences a higher field strength across the band, resulting in focusing and higher efficiencies (*i.e.* a form of transient-isotachophoresis occurs, See 1.1.8.6).

Table 3.6 Effect of Increasing Buffer Concentration on Analyte Efficiencies

	Number of Theoretical Plates (/ m) at Various Buffer Strengths			
	10 mM	15 mM	20 mM	50 mM
SK&F 91207	210 000	300 000	300 000	330 000
SK&F 92422	190 000	260 000	300 000	355 000
SK&F 92506	160 000	215 000	265 000	340 000
Cimetidine	140 000	175 000	205 000	240 000
SK&F 92452	130 000	170 000	190 000	240 000
SK&F 88958	110 000	155 000	185 000	230 000

Unfortunately increasing the buffer strength did not enhance the resolution even though efficiencies were improved. This is because resolution is proportional to the square root of efficiency. Therefore efficiency needs to be improved significantly to affect resolution (*i.e.* in order for resolution to be doubled, efficiency needs to be quadrupled).

### 3.3.2 Addition of Organic Modifiers

The addition of an organic modifier to the buffer can have unpredictable effects on the separation, which are best determined experimentally. The solvent can alter the viscosity, dielectric constant, zeta potential ( $\zeta$ ) and analyte solubility. Tsuda *et al.*<sup>12</sup>

suggested that in the case of methanol, acetonitrile and 2-propanol the EOF velocity obtained was proportional to the ratio of their dielectric constant to viscosity ( $\epsilon/\eta$ , Table 3.7).

Table 3.7 Dielectric Constant and Viscosity of Various Solvents used in CZE

	Dielectric Constant ( $\epsilon$ )	Viscosity ( $\eta$ ) \ cp	$\epsilon / \eta$
Acetonitrile	36.64	0.37	99.03
Water	87.74	1.00	87.74
Methanol	33.0	0.544	60.66
2-Propanol	20.18	2.038	9.90

Therefore on the basis of  $\epsilon/\eta$  alone, the EOF velocity is highest in acetonitrile, then water, methanol and will be lowest in 2-propanol.

#### 3.3.2.1 Methanol

Theoretically the effect of adding methanol (on the basis of  $\epsilon/\eta$ ) to the buffer would be a decrease in the EOF velocity with respect to that of the buffer in water. This is in-fact the case, Figure 3.8 shows the electropherogram of cimetidine and impurities separated using a buffer comprising 10 mM disodium hydrogen phosphate pH 3.1, 5 % methanol. The migration time of SK&F 92422 increased from 5.208 minutes to 5.835 minutes, and increased further to 7.520 minutes when the proportion of methanol is increased to 15 % (Figure 3.9). With a reduced EOF, individual mobilities should have a greater effect, therefore increasing resolution. The addition of 15 % methanol to the buffer increased the resolution of SK&F 92452 and 88958 from 0.9 to 1.3; however, the peaks are still not fully resolved ( $R > 1.5$ ).

#### 3.3.2.2 Acetonitrile

The EOF velocity should increase upon the addition of acetonitrile to the buffer, if  $\epsilon/\eta$  is the only contribution, therefore reducing the migration times. However, the addition of 5 % acetonitrile (Figure 3.10) increases the migration times of the analytes (*e.g.* SK&F 92422 increased to 5.792, the EOF was not observed within 30 minutes), the migration times increased further when 15 % acetonitrile is present (Figure 3.11). The

result is improved resolution of SK&F 92452 and 88958 (from 0.9) to 1.3 (5 % MeCN) and 1.4 (15 % MeCN).

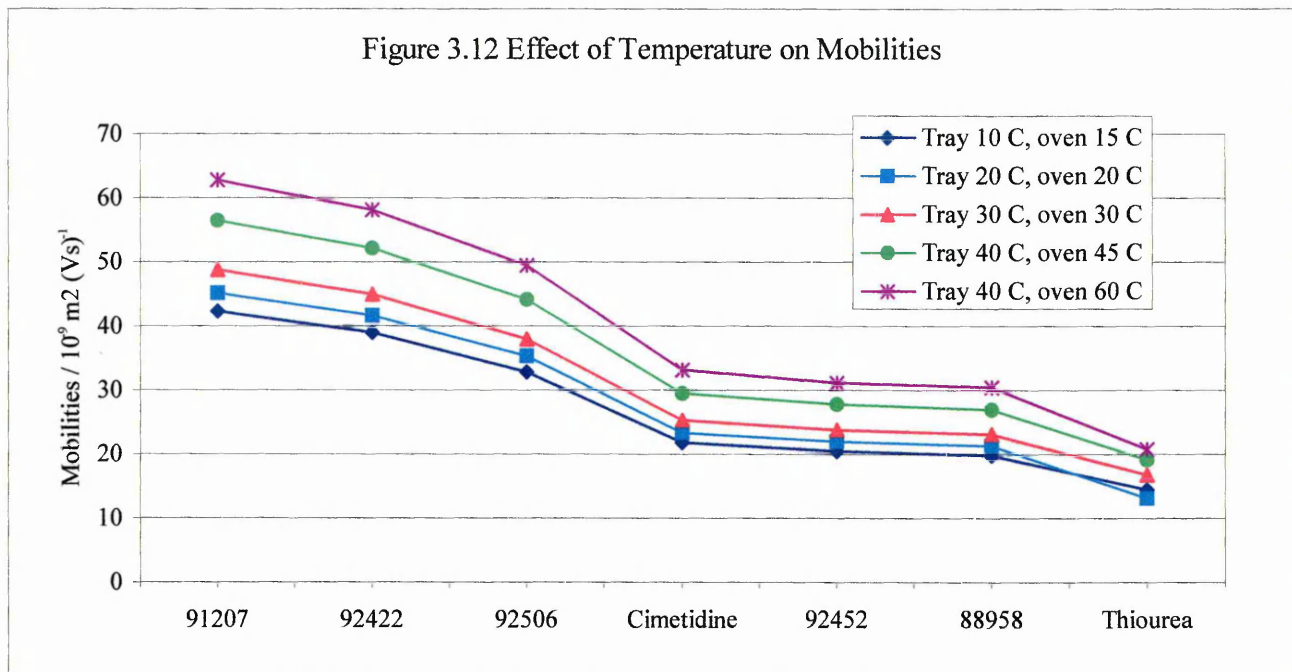
### 3.3.3 Effect of Temperature

Variations in temperature can have a dramatic effect on analyte (and EOF) mobility. A one-degree change in temperature can result in 2 – 3% change of viscosity. Decreasing the temperature increases viscosity, reducing the EOF, conversely, increasing temperature decreases viscosity, reducing migration times (and also increases the EOF). The variation of temperature is summarised in Figure 3.12.

The standard conditions used throughout this study were 20 °C for the sample tray and column oven (—□— on chart). When the tray was cooled to the instrumental limit of 10 °C and the oven to 15 °C (—◆— on chart, electropherogram Figure 3.13), the viscosity increased sufficiently to decrease the mobility of the analytes. Thus, the migration times were increased (*e.g.* the mobility of cimetidine was reduced from  $23.3 \times 10^{-9}$  to  $21.8 \times 10^{-9} \text{ m}^2 (\text{Vs})^{-1}$ ). However, the increase in viscosity was insufficient to effect separation of the SK&F 92452 and 88958 ( $R = 0.9$ ).

Heating the oven and tray to the instrumental maximum (oven 60 °C, tray 40 °C), resulted in increased mobility (—\*— on chart, electropherogram Figure 3.14), *e.g.* cimetidine  $33.2 \times 10^{-9} \text{ m}^2 (\text{Vs})^{-1}$ , but at the expense of the resolution of SK&F 92452 and 88958 ( $R = 0.6$ ).

Figure 3.12 Effect of Temperature on Mobilities



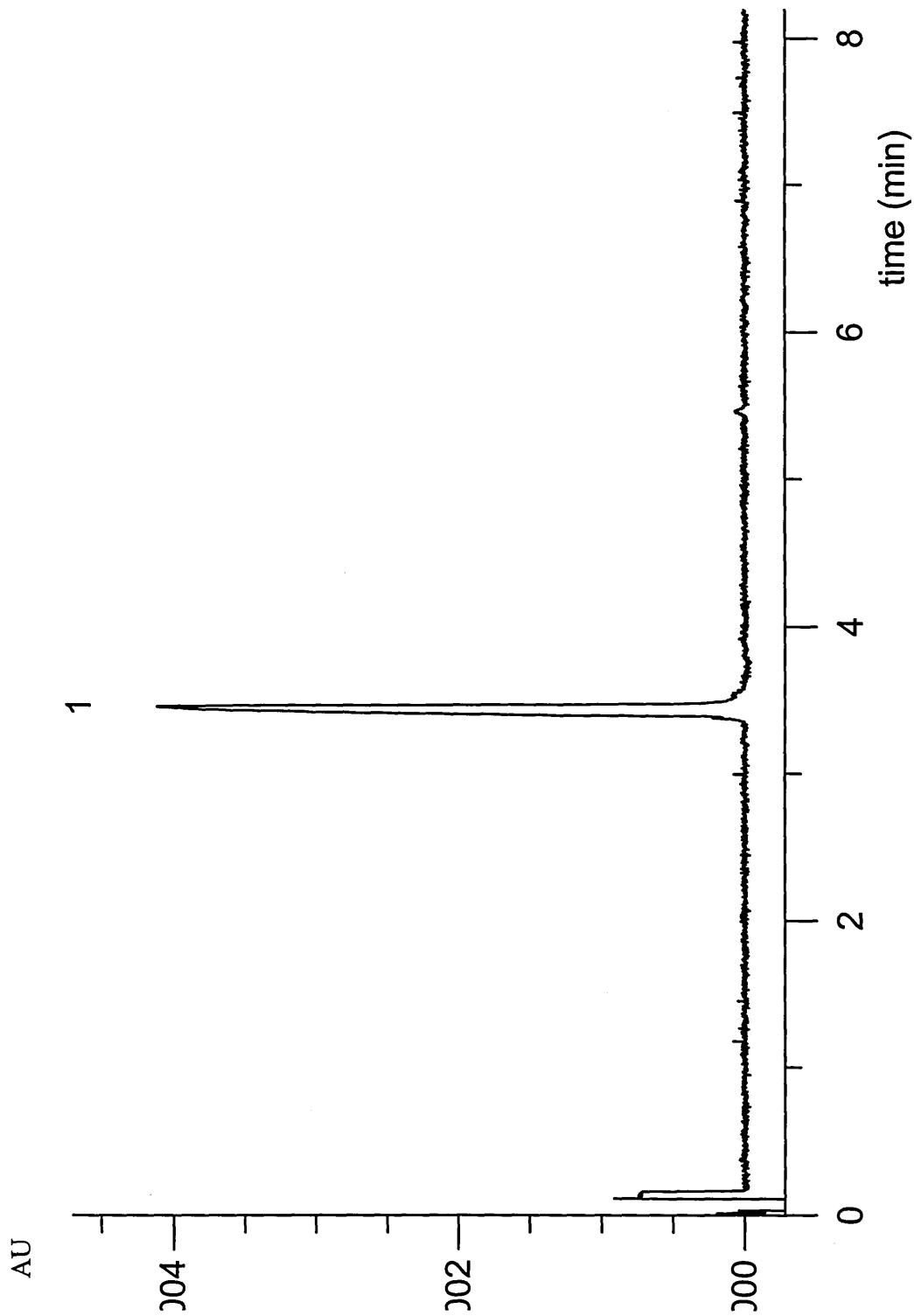


Figure 3.1 10 mM Sodium Tetraborate pH 9.1, 30 kV,  $\lambda_{\text{max}} = 230 \text{ nm}$   
10 mbar / 0.07 min Injection of 10  $\mu\text{g/mL}$  Cimetidine and Related Impurities

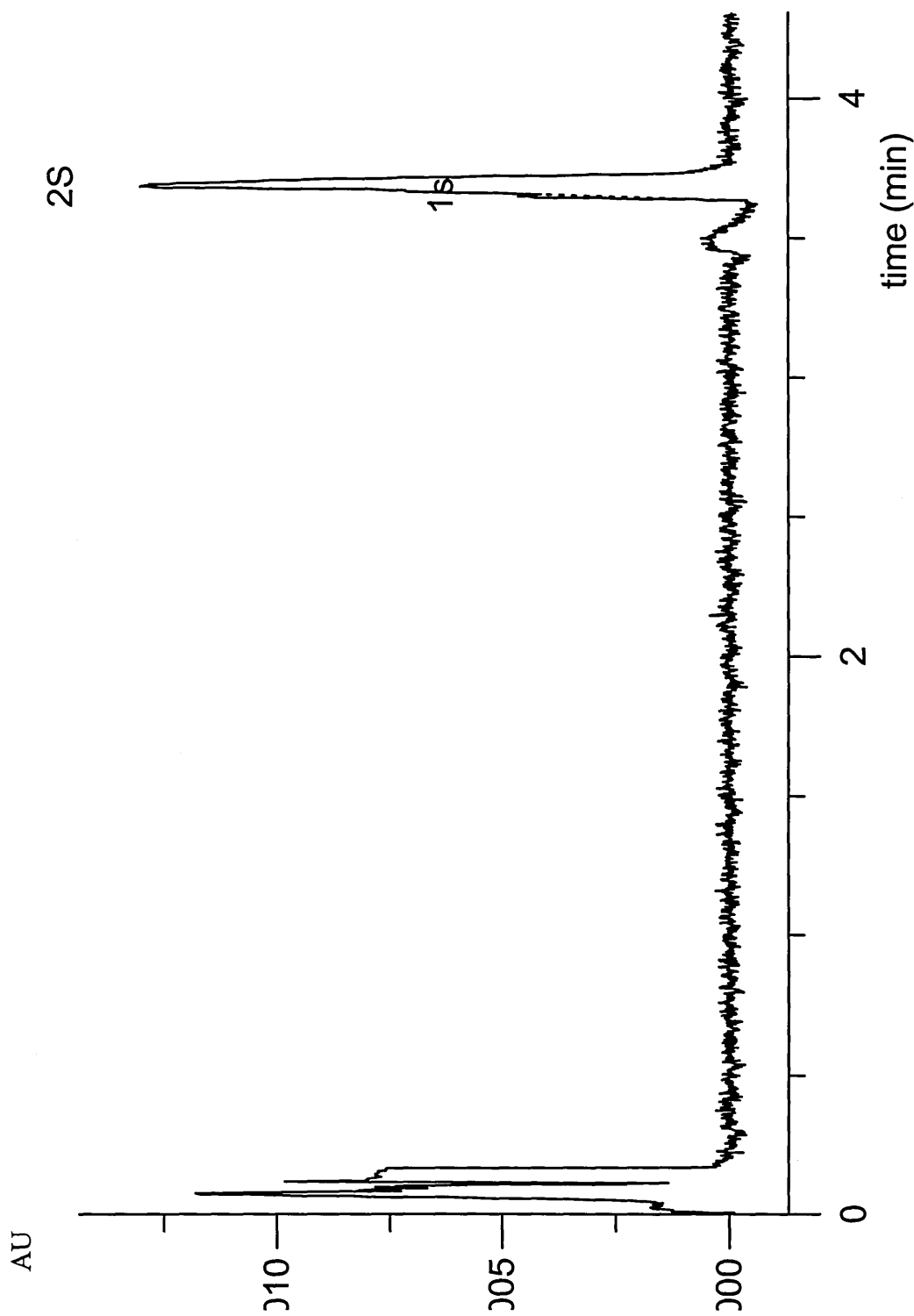


Figure 3.2 10 mM Sodium Tetraborate pH 8.1, 30 kV,  $\lambda_{\text{max}} = 230 \text{ nm}$ , 10 mbar / 0.07 min  
Injection of 10  $\mu\text{g/mL}$  Cimetidine and Related Impurities

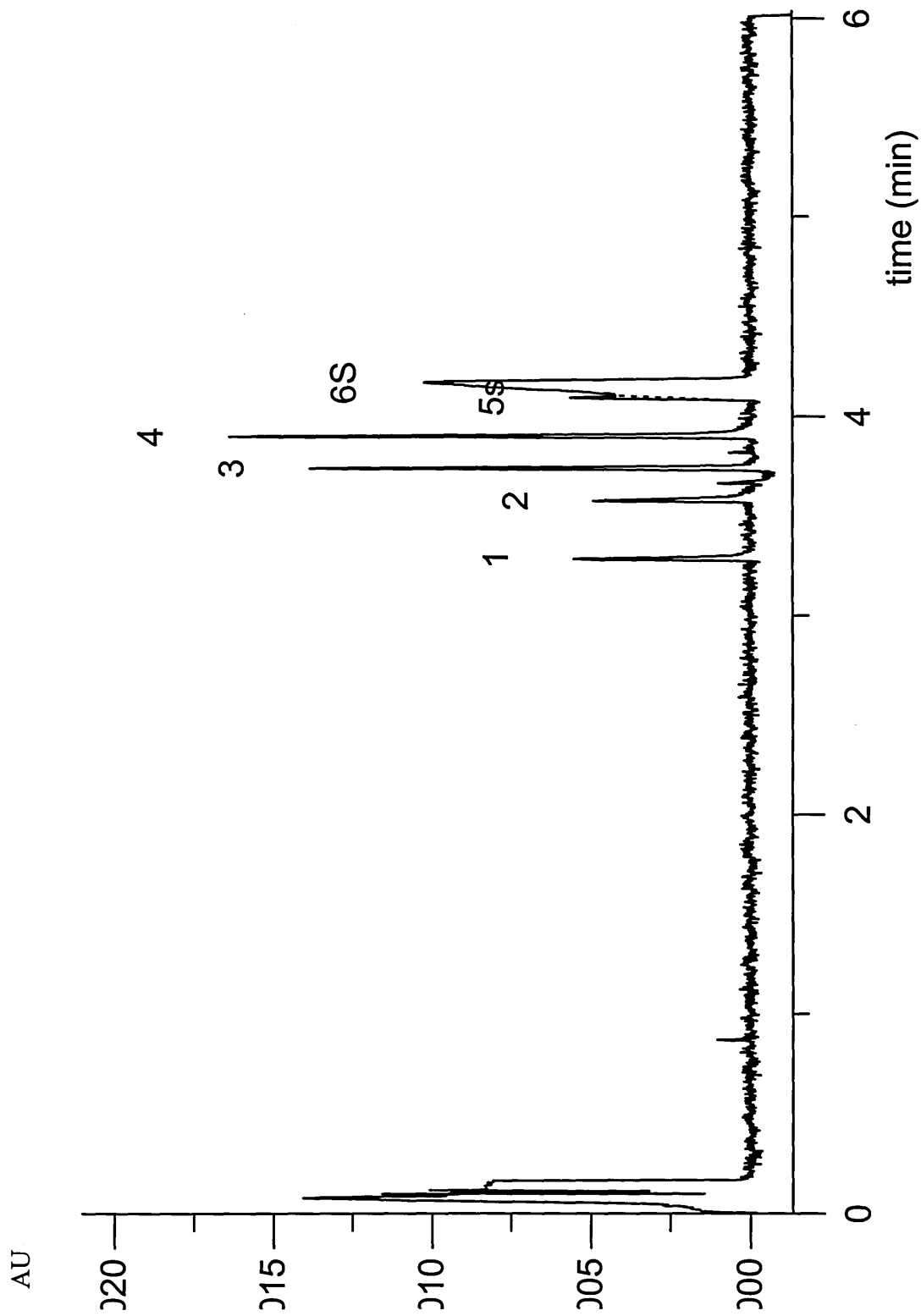


Figure 3.3 10 mM Disodium Hydrogenphosphate pH 7.1, 30 kV,  $\lambda_{\text{max}} = 230 \text{ nm}$ , 10 mbar / 0.07 min  
Injection of 10  $\mu\text{g/mL}$  Cimetidine and Related Impurities

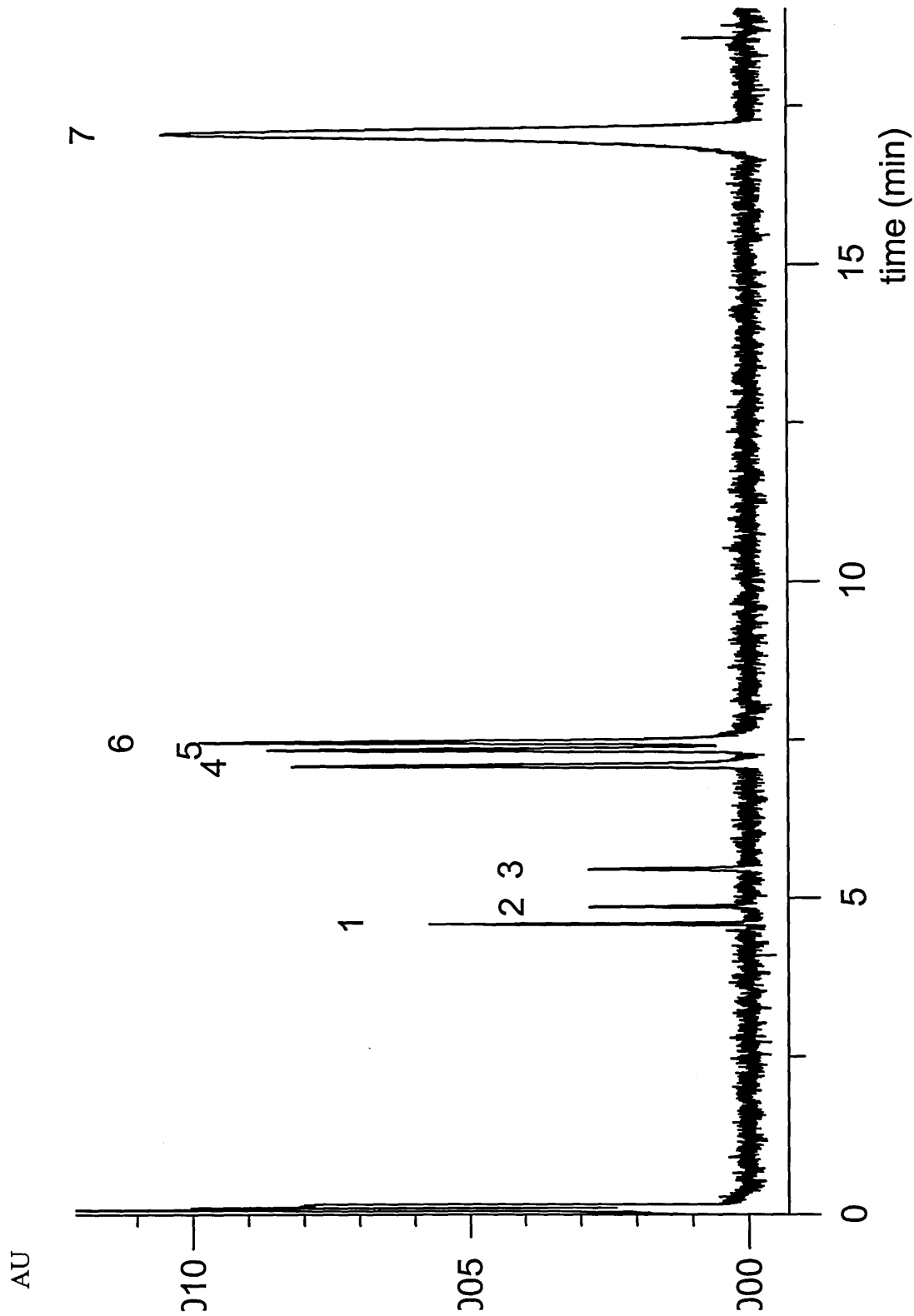


Figure 3.4 10 mM Sodium Dihydrogenphosphate pH 3.1, 30 kV,  $\lambda_{max} = 230$  nm, 10 mbar / 0.07 min  
Injection of 10  $\mu\text{g}/\text{mL}$  Cimetidine and Related Impurities  
1) SK&F 91207; 2) SK&F 92422; 3) SK&F 92506; 4) Cimetidine; 5) SK&F 92452; 6) SK&F 88958 and 7) Thiourea

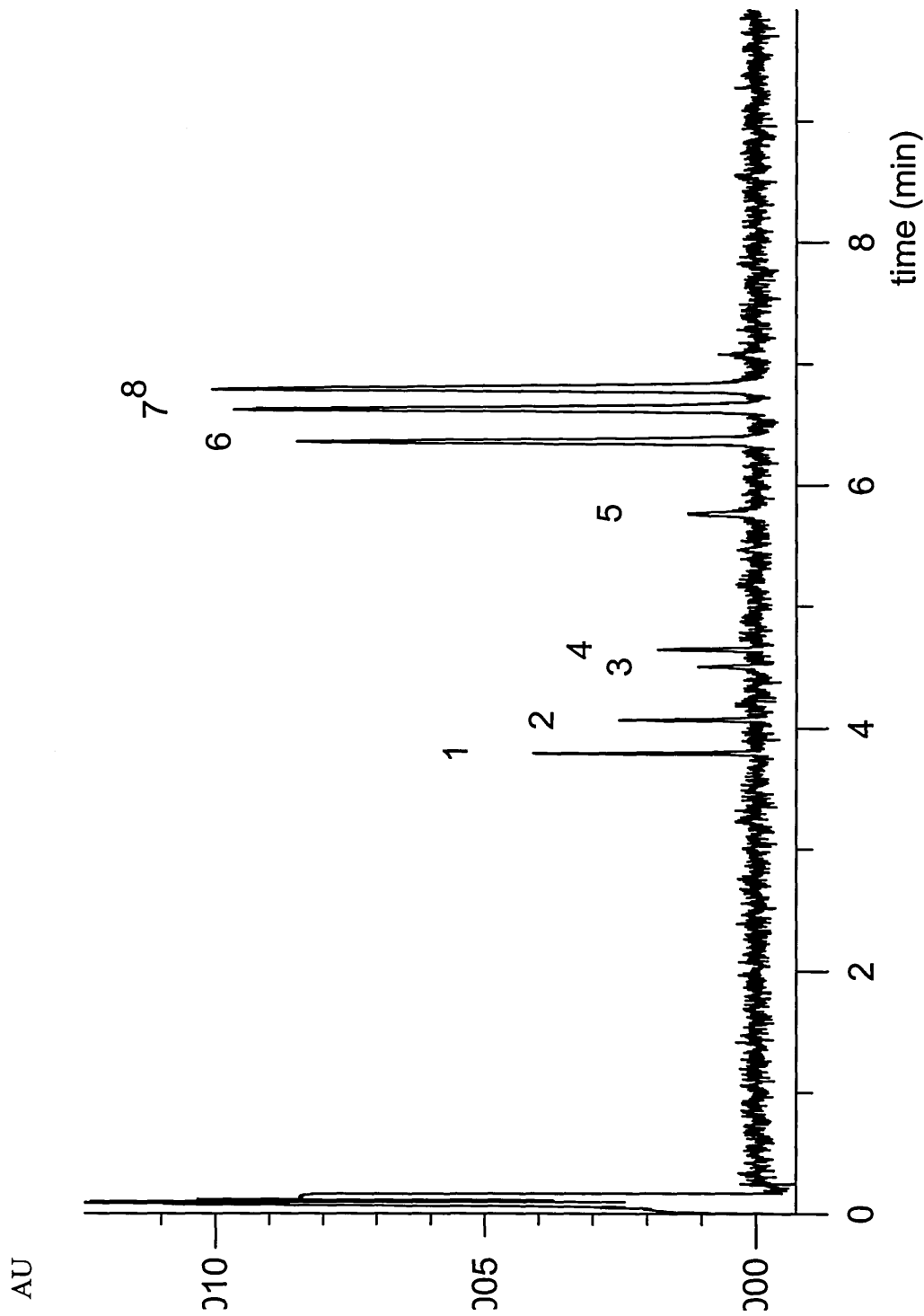


Figure 3.5 10 mM Sodium Dihydrogenphosphate pH 2.1, 30 kV,  $\lambda_{\text{max}} = 230 \text{ nm}$ , 10 mbar / 0.07 min  
Injection of 10  $\mu\text{g}/\text{mL}$  Cimetidine and Related Impurities  
1) SK&F 91207; 2) SK&F 92422; 4) SK&F 92506; 6) Cimetidine; 7) SK&F 92452 and 8) SK&F 88958

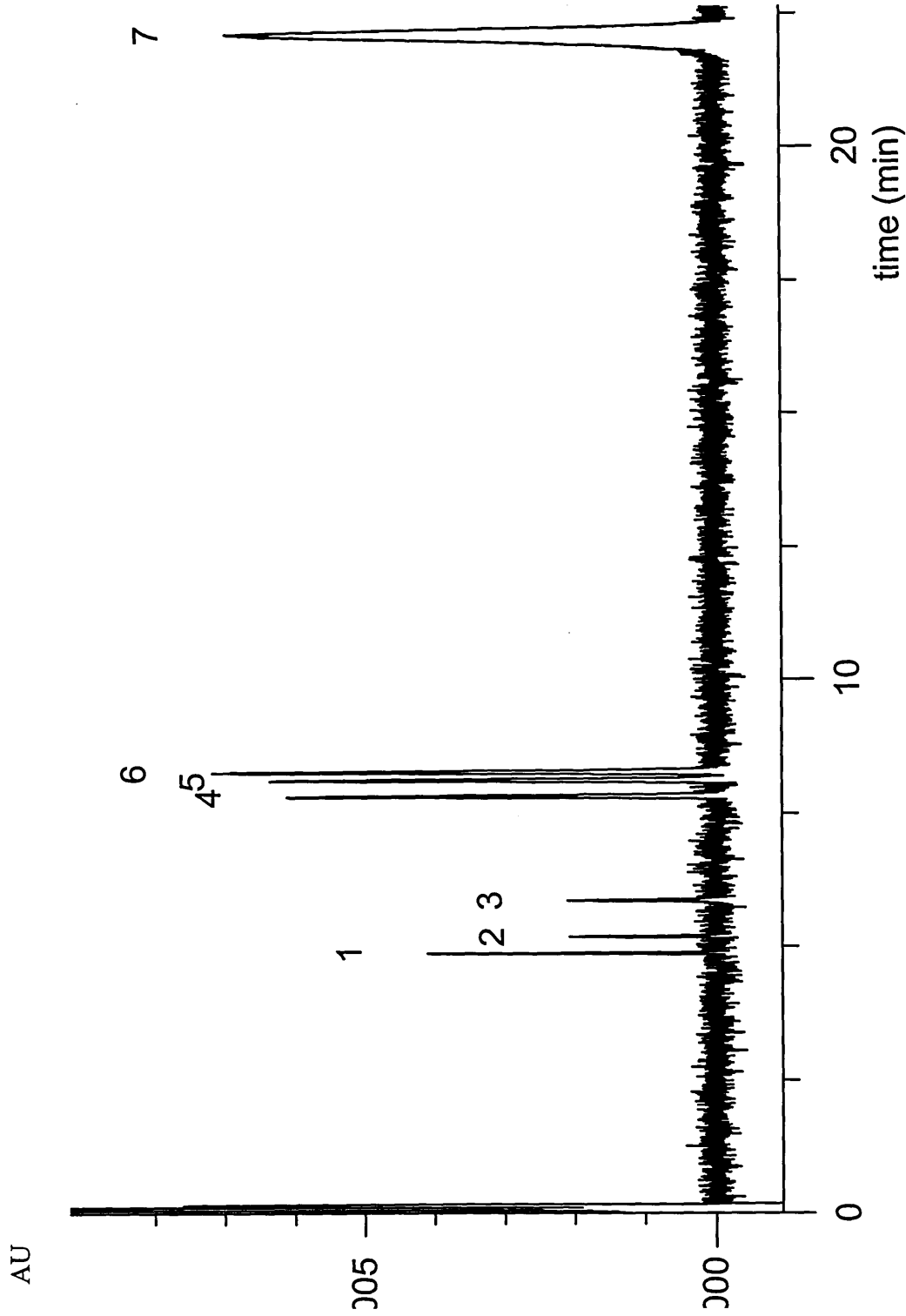


Figure 3.6 10 mM Sodium Dihydrogenphosphate pH 3.1, 30 kV,  $\lambda_{\text{max}} = 230 \text{ nm}$ , 10 mbar / 0.07 min  
Injection of 10  $\mu\text{g/mL}$  Cimetidine and Related Impurities Employing HCl Column Wash  
1) SK&F 91207; 2) SK&F 92422; 3) SK&F 92506; 4) Cimetidine; 5) SK&F 92452; 6) SK&F 88958 and 7) Thiourea

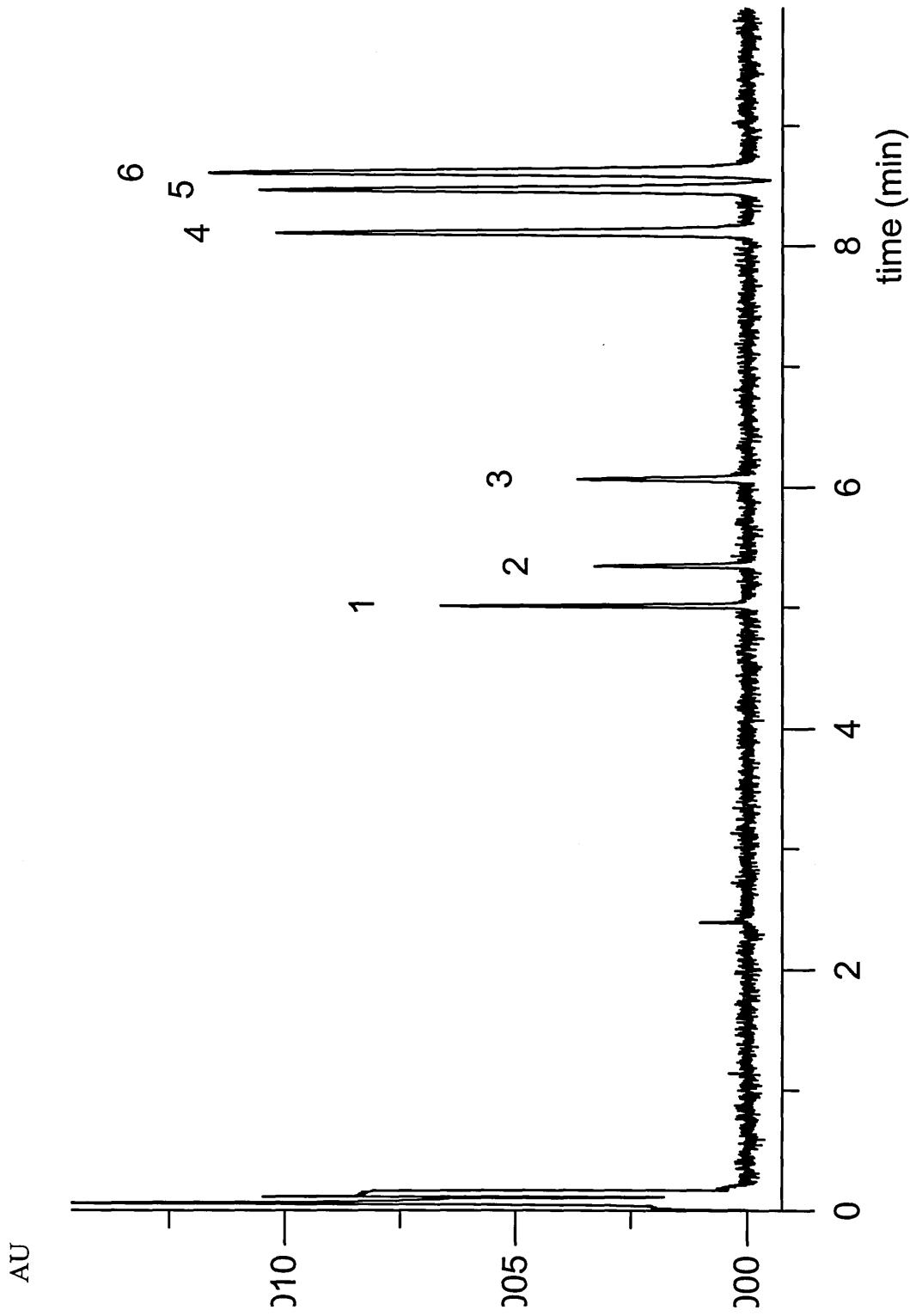


Figure 3.7 15 mM Sodium Dihydrogenphosphate pH 3.1, 30 kV,  $\lambda_{max} = 230$  nm, 10 mbar / 0.07 min  
Injection of 10  $\mu\text{g/mL}$  Cimetidine and Related Impurities  
1) SK&F 91207; 2) SK&F 92422; 3) SK&F 92506; 4) Cimetidine; 5) SK&F 92452 and 6) SK&F 88958

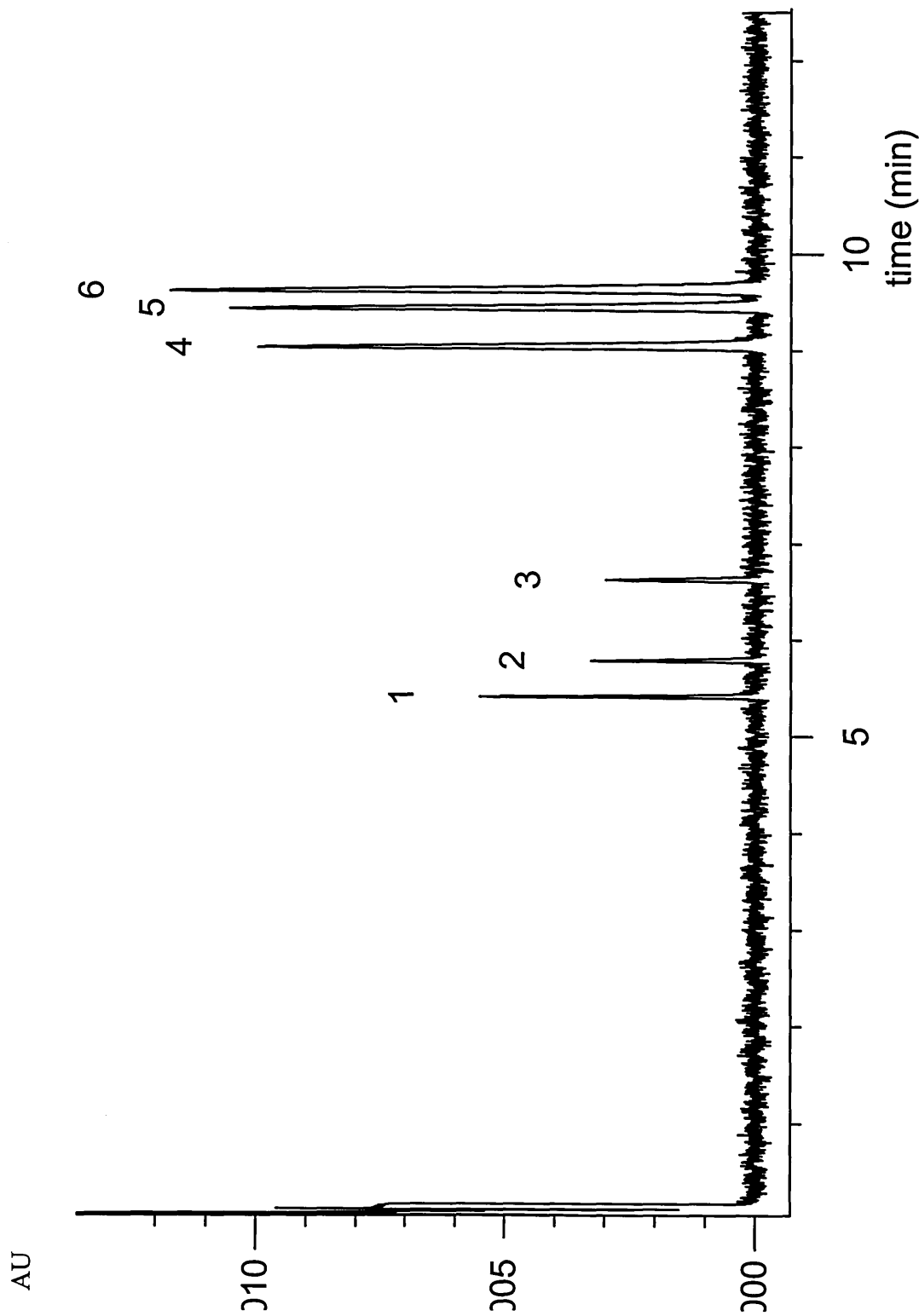


Figure 3.8 10 mM Sodium Dihydrogenphosphate pH 3.1 5 % MeOH, 30 kV,  $\lambda_{max} = 230$  nm, 10 mbar / 0.07 min  
Injection of 10  $\mu$ g/mL Cimetidine and Related Impurities  
1) SK&F 91207; 2) SK&F 92422; 3) SK&F 92506; 4) Cimetidine; 5) SK&F 92452 and 6) SK&F 88958

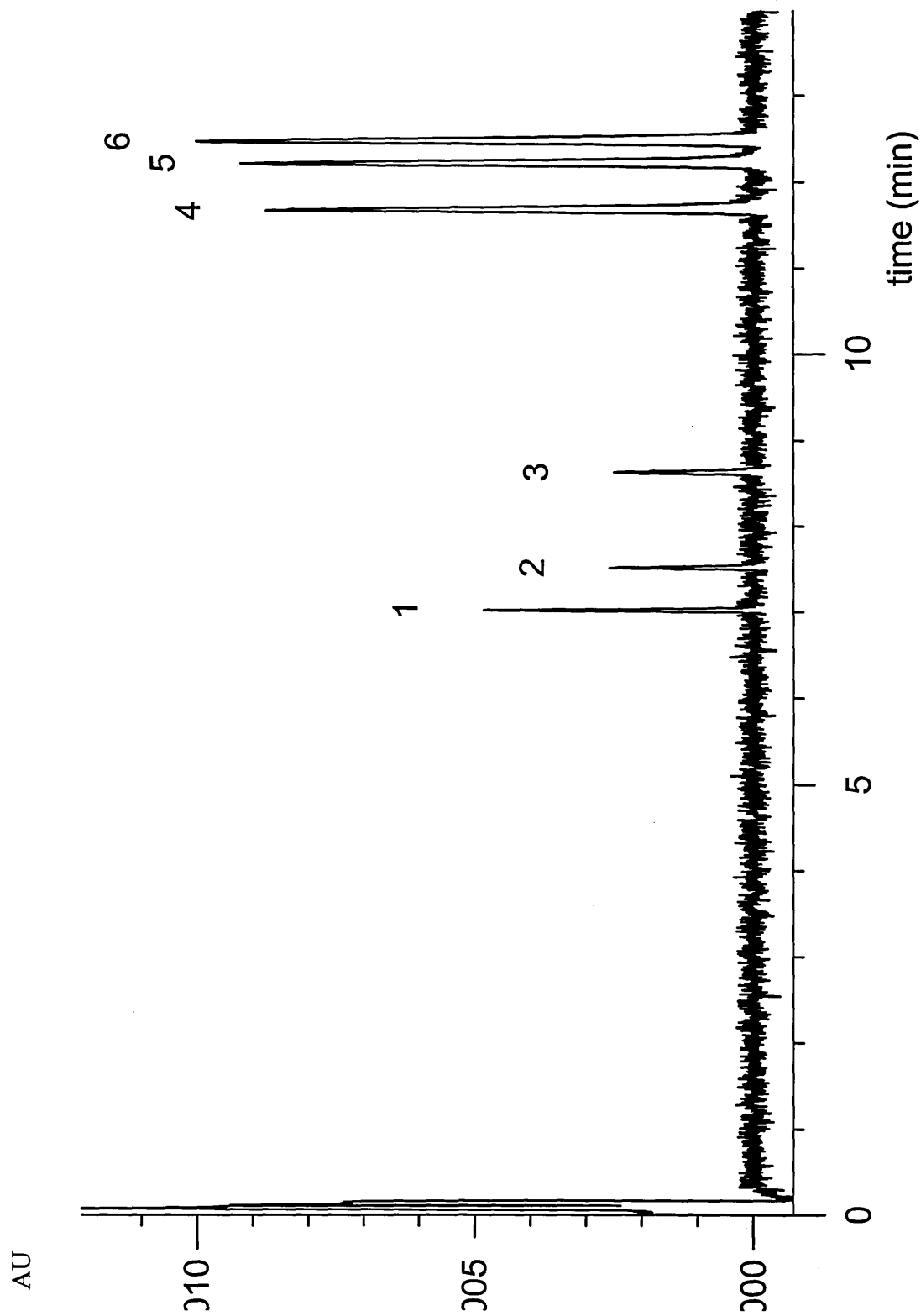


Figure 3.9 10 mM Sodium Dihydrogenphosphate pH 3.1 15 % MeOH, 30 kV,  $\lambda_{max} = 230$  nm, 10 mbar / 0.07 min  
Injection of 10  $\mu\text{g/mL}$  Cimetidine and Related Impurities

- 1) SK&F 91207; 2) SK&F 92422; 3) SK&F 92506; 4) Cimetidine; 5) SK&F 92452 and 6) SK&F 88958

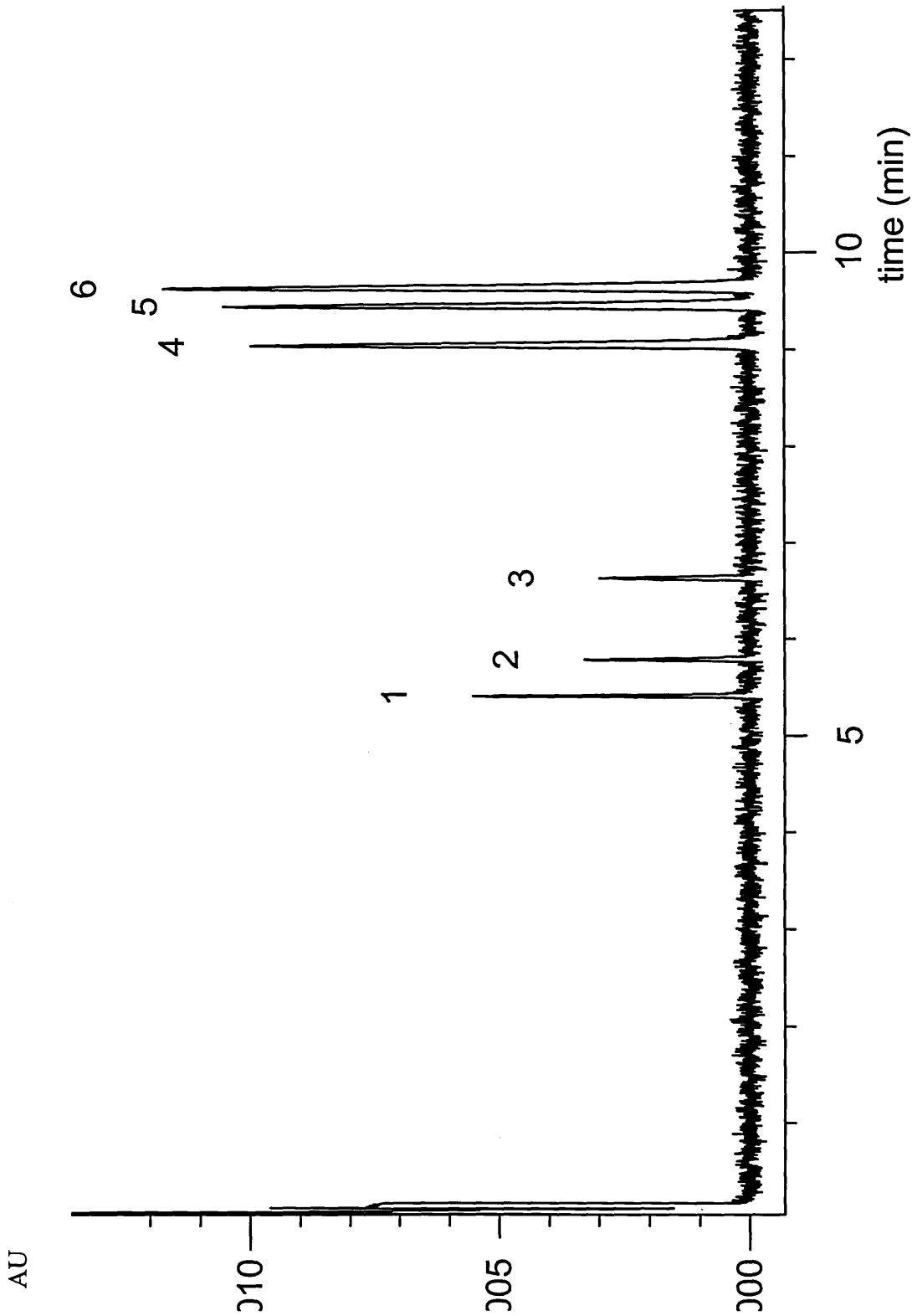


Figure 3.10 10 mM Sodium Dihydrogenphosphate pH 3.1 5 % MeCN, 30 kV,  $\lambda_{max} = 230$  nm, 10 mbar / 0.07 min Injection of 10  $\mu\text{g}/\text{mL}$  Cimetidine and Related Impurities  
1) SK&F 91207; 2) SK&F 92422; 3) SK&F 92506; 4) Cimetidine; 5) SK&F 92452 and 6) SK&F 88958

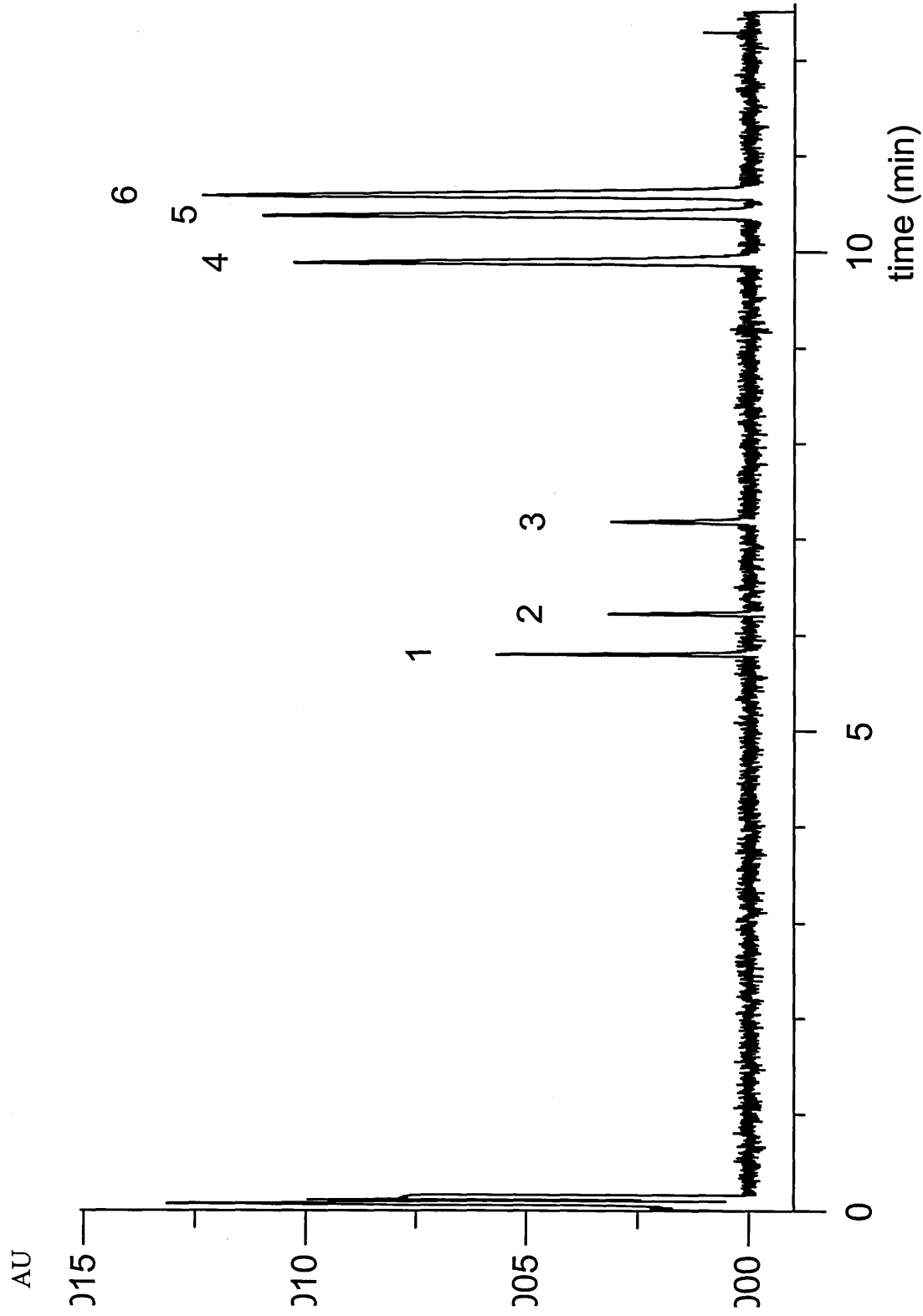


Figure 3.11 10 mM Sodium Dihydrogenphosphate pH 3.1 15 % MeCN, 30 kV,  $\lambda_{max} = 230$  nm, 10 mbar / 0.07 min  
Injection of 10  $\mu\text{g}/\text{mL}$  Cimetidine and Related Impurities  
1) SK&F 91207; 2) SK&F 92422; 3) SK&F 92506; 4) Cimetidine; 5) SK&F 92452 and 6) SK&F 88958

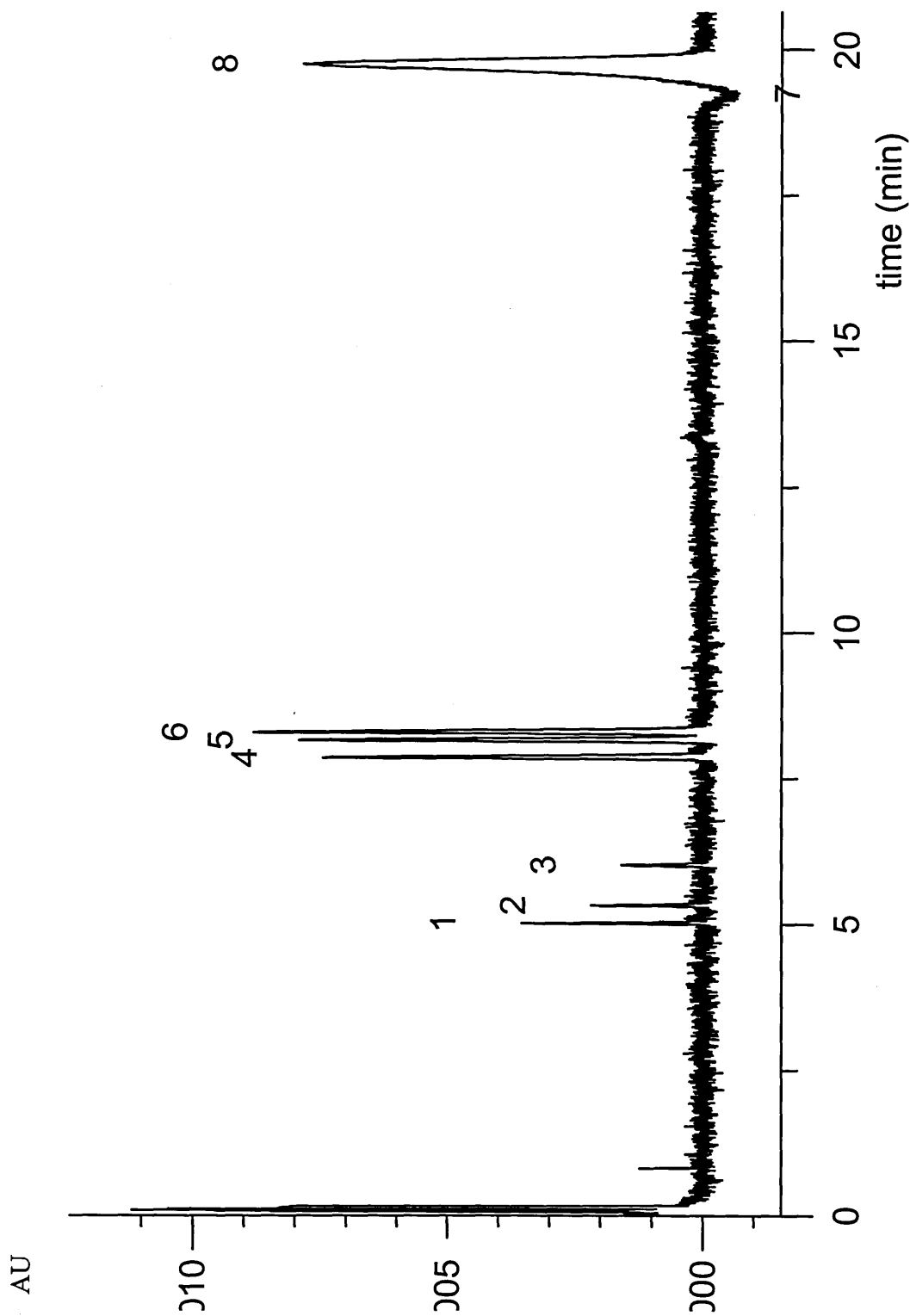


Figure 3.13 10 mM Sodium Dihydrogenphosphate pH 3.1, 30 kV, Tray 10 °C, Column Oven 15 °C,  $\lambda_{max} = 230$  nm, 10 mbar / 0.07 min Injection of 10  $\mu\text{g}/\text{mL}$  Cimetidine and Related Impurities  
1) SK&F 91207; 2) SK&F 92422; 3) SK&F 92506; 4) Cimetidine; 5) SK&F 92452; 6) SK&F 88958 and 7) Thiourea

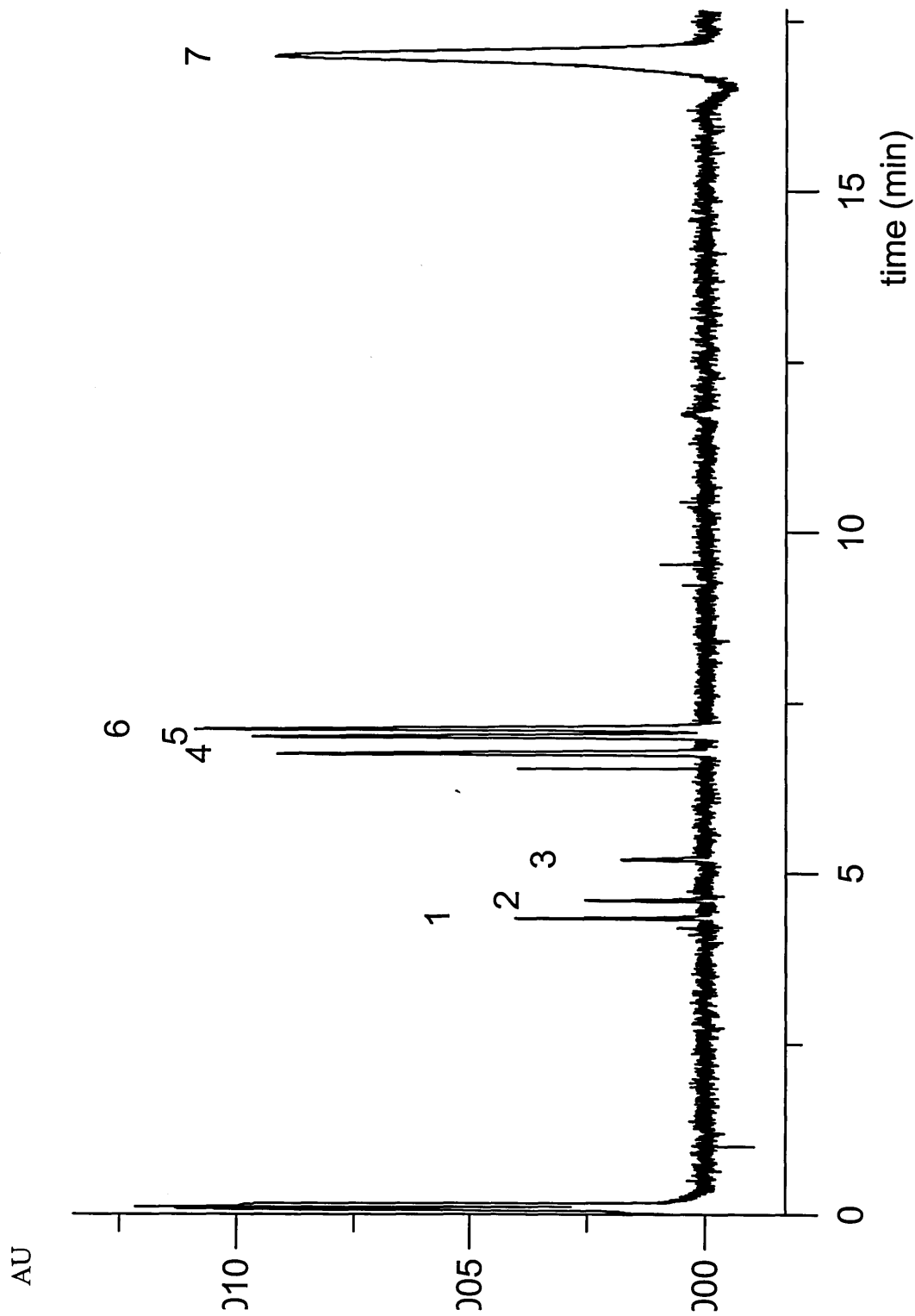


Figure 3.14 10 mM Sodium Dihydrogenphosphate pH 3.1, 30 kV, Tray 40 °C, Column Oven 60 °C,  
 $\lambda_{\text{max}} = 230 \text{ nm}$ , 10 mbar / 0.07 min Injection of 10  $\mu\text{g/mL}$  Cimetidine and Related Impurities  
1) SK&F 91207; 2) SK&F 92422; 3) SK&F 92506; 4) Cimetidine; 5) SK&F 92452; 6) SK&F 88958 and 7) Thiourea

### 3.5 Conclusions

A rapid and efficient separation of a pharmaceutical product and related impurities has been developed and optimised. The effects of pH, buffer strength, organic modifier and temperature have been investigated.

Reduction of pH from high to low (pH 9.1 – 3.1) resulted in the separation of six analytes (two co-migrate and could not be further separated). Four of the analytes were fully resolved (using the standard definition of  $R > 1.5$ ), the remaining two were of baseline resolution. The resolution of these analytes could be improved by a further reduction of pH (2.1); however, the EOF was not detected within 30 minutes.

The resolution could be improved through the addition of acetonitrile (15 %  $R = 1.4$ ) or methanol (15 %  $R = 1.3$ ) to the buffer. Separations can be significantly altered through the addition of an organic modifier, the effect of which cannot be easily predicted. Addition of acetonitrile should increase the EOF velocity (with respect to water) by a factor of  $\epsilon/\eta$ . In both cases the EOF was reduced (thiourea was not observed within 30 minutes) thus indicating that organic modifiers have a more complex role in the nature of the EOF generated.

Efficiencies of  $1 - 2 \times 10^5$  theoretical plates per metre were obtained, which improved on increasing buffer concentration, owing to enhanced sample stacking in the high conductivity buffer. However, the increase in efficiency was insufficient to resolve SK&F 92452 and 88958. This is because resolution is proportional to the square root of efficiency. Thus, a significant increase in efficiency is required to effect resolution.

Modification of the capillary temperature leads to variation in the viscosity of the buffer, and hence EOF and migration times. Decreasing the temperature resulted in an increase in viscosity, this lead to an increase in analysis time (resolution was not affected,  $R = 0.9$ ). Increasing the temperature decreased viscosity and hence both migration time and resolution were reduced ( $R = 0.6$ ).

The addition of organic modifier or reduction of pH (and to a lesser extent buffer strength or temperature) increased the resolution between SK&F 92422 and 88958,

however the analytes were still not completely resolved (*i.e.*  $R < 1.5$ ). The most significant effect of these parameters was the on the EOF mobility, in all cases thiourea was not detected within 30 minutes. Therefore, to reduce analysis time and obtain EOF measurements the chosen separation conditions were 10 mM sodium dihydrogenphosphate at pH 3.1 (adjusted using 0.1 M HCl), which provides adequate (baseline) resolution of all analytes.

The reproducibility of the migration times was improved by flushing the capillary with HCl rather than NaOH between analyses. This was due to a reduction in the variation of capillary wall surface-charge, which led to an irreproducible EOF.

The potential of this method for quantification of cimetidine has been investigated. Corrected peak area reproducibilities were less than 4 % in all cases, except for SK&F 92452 (8 %) indicating that this analysis could be used as a method of quantification.

As a general comparison of the data that was obtained previously<sup>10</sup>, the separation has been improved using the newer computer controlled instrumentation. The extensive peak tailing in the original method was not observed within the repeated work, unfortunately an adequate explanation of this cannot be given. However, it does indicate that methods can be swapped between different instrumentation with little further development.

## References

---

- (1) Brodgen RN; Heel RC; Speight TM; Avery GS. *Drugs* **15** (1978) 93
- (2) Lovering EG; Curran NM. *Journal of Chromatography* **319** (1985) 235
- (3) Haskins NJ; Eckers C; Organ AJ; Dunk MF; Winger BE. *Rapid Communications in Mass Spectrometry* **9** (1995) 1027
- (4) Eckers C; Haskins N; Langridge J. *Rapid Communications in Mass Spectrometry* **11** (1997) 1916
- (5) Arrowood S; Hoyt AM. *Journal of Chromatography* **586** (1991) 177
- (6) Lee RM; Osborne PM. *Journal of Chromatography* **146** (1978) 354
- (7) Bartlett JM; Segelman AB. *Journal of Chromatography* **255** (1983) 239
- (8) Lúkša J; Josic Dj. *Journal of Chromatography B* **667** (1995) 321
- (9) Soini H; Tsuda T; Novotny MV. *Journal of Chromatography* **559** (1991) 547
- (10) Ellis DR; Palmer ME; Tetler LW; Eckers C. *Journal of Chromatography A* **808** (1998) 269
- (11) Lambert WJ; Middleton DL. *Analytical Chemistry* **62** (1990) 1585
- (12) Tsuda T; Nomera K; Nakagawa G. *Journal of Chromatography* **248** (1982) 241

## **Chapter 4**

### ***Development of CZE/MS Interfaces for a Quattro I with Subsequent Analysis of Cimetidine and Related Impurities***

## 4.1 Introduction

The first example of CZE/MS was demonstrated by Smith *et al.*<sup>1,2</sup> in 1987-8 employing a sheathless interface, in which electrospray was effected directly from the capillary outlet. They reported limitations of spraying directly from the capillary; amongst which were buffer incompatibilities and unstable spray at extremely low (electroosmotic) flow rates. Later they demonstrated a co-axial sheath flow interface<sup>3,4</sup> which appeared to remedy these problems. The separation capillary passed through a series of concentric tubes, through which flows a make-up liquid. The sheath liquid, is typically comprised of 50 % organic solvent with 0.1 % acetic acid added and compensates for low flow rates to provide a net flow of  $\sim 1 - 10 \mu\text{L}/\text{min}$ . These flow rates would allow routine operation of electrospray. In addition, high concentrations of buffers could be employed, as the dilution effect of the sheath liquid would reduce the background signal from these ions. However, dilution of the sample would also occur, thus decreasing sensitivity with respect to a sheathless interface.

The alternative approach is to use the low-flow electrospray (nanospray) variant; described in Section 1.3.4. The majority of nanospray CZE/MS that has been reported employs a drawn, conductive-coated fused silica spray needle. The electrospray voltage and CZE voltage termination are applied to the conductive coating on the capillary tip. Various methods for the production of drawn, conductive-coated tips have been reported in the literature. Methods of sharpening the tip include a SFC capillary drawer<sup>5</sup>, weights<sup>6</sup>, etching by HF acid<sup>7</sup> and micro-machining techniques<sup>8</sup>. The capillaries are then gold coated by sputter coating. To improve the lifetime and robustness of the gold coating a number of methods of derivatisation have been suggested. Valaskovic and McLafferty<sup>9</sup> demonstrated that a gold coated tip further coated with a SiO/SiO<sub>2</sub> insulating layer, increased lifetimes and stability over un-coated tips. Kriger *et al.*<sup>10</sup> suggested an improved method based on that devised by Majda *et al.*<sup>11</sup>, in which the fused silica surface is derivatised with a 'molecular adhesive' prior to coating. The coating stability was significantly improved, with lifetimes up to 100 hours and the ability to withstand electrical discharges and solvent effects.

Another method of interfacing CZE/MS has been suggested by Henion *et al.*<sup>12</sup>, which employs a liquid junction interface, however, due to geometrical constraints, this interface was not suitable for use on our instrumentation.

In this chapter, the development of interfaces for CZE/MS employing both co-axial sheath flow and nanospray approach is reported. The co-axial sheath flow interface was based on that initially demonstrated by Smith *et al.*<sup>3</sup> owing to the simplicity of construction. The sheathless interface was developed from the work reported by Gaskell *et al.*<sup>13</sup> in which they converted a Micromass electrospray source for use as a nanoflow inlet for infusion. In addition, a further development of this nanoflow interface for CZE/MS is reported.

## ***4.2 Development of a Co-axial Sheath flow CZE/MS Interface for a Quattro I Mass Spectrometer***

### **4.2.1 Instrumentation**

A Quattro I mass spectrometer (Micromass, Manchester, UK), with an electrospray (ESI) source was used throughout. All unions, ferrules and fittings were obtained from Supelco (Poole, UK). Un-coated fused silica of 50  $\mu\text{m}$  i.d. x 375  $\mu\text{m}$  o.d. was obtained from Composite Metal Services Ltd. (Harrow, UK). The sheath flow tube was purchased from Micromass (P/N SAJ473D, Manchester, UK) and was 600  $\mu\text{m}$  i.d. x 295 mm, and the replacement probe tip was manufactured by Ash Instruments (Macclesfield, UK).

All separations were performed on a PrinCE 560 (Prince Technologies, Emmen, The Netherlands) at a potential of + 30 kV (supplied to the inlet electrode). Injections were performed hydrodynamically.

Volatile buffers were used throughout, to prevent the possibility of source contamination.

The sheath liquid was delivered by a Harvard Apparatus Model 11 (Edenbridge, UK) syringe pump, using Hamilton Gastight syringes between 50 – 500  $\mu\text{L}$  (Supelco, Poole UK).

#### 4.2.2 Reagents

Cimetidine and related compounds were obtained from SmithKline Beecham (Harlow, UK), the structures of which are shown in Table 3.1 (Chapter 3). Stock solutions were diluted to 50  $\mu\text{g}/\text{mL}$  (SIR analyses) or 100  $\mu\text{g}/\text{mL}$  (full scan analyses) with water. Acetonitrile and methanol were of HPLC grade. Water was distilled and deionised by a Milli-Q RG purification system (Millipore, Fisons, Loughborough, UK). Ammonium acetate and acetic acid were of HPLC grade or better and were purchased from Aldrich (Poole, UK). All other materials were of reagent grade or better.

#### 4.2.3 Development of a Suitable (Volatile) Buffer System for CZE/MS

It is widely accepted that inorganic buffers (phosphate, borate *etc.*) are not suitable for mass spectrometry. They frequently dominate the ion current and rapidly contaminate the ion source, which consequently requires regular cleaning. In addition, when concentrated involatile buffers are used, skimmer and nozzles orifices can become blocked leading to a decrease in sensitivity. However, in recent years mass spectrometry manufacturers have developed ESI (and APCI) ion sources that can cope with concentrated involatile buffers even at flow rates above 1 mL/min, without regular cleaning. This is achieved using orthogonal entry and novel source designs (*e.g.* Micromass Z-Spray, see Chapter 5). Older instrumentation can be more susceptible to source contamination, so therefore it is advantageous to use volatile buffers (*i.e.* ammonium acetate, formate, *etc.*).

There are only a limited number of volatile buffers that are amenable to CZE/MS. Most are weak conjugate bases and therefore have low  $\text{pK}_a$ s (*e.g.* ammonium acetate  $\text{pK}_a$  4.7, ammonium formate  $\text{pK}_a$  3.7). Consequently, analyses are required to be performed under acidic conditions. Fortunately the pharmaceutical compounds investigated were basic and thus could be separated under these conditions (*i.e.* at pH 3.1). Ammonium

acetate at pH 3.7 (adjusted with acetic acid) was chosen to replace disodium hydrogenphosphate as the buffer for the cimetidine separation. The separation obtained utilising UV detection (at 230 nm) and 10 mM ammonium acetate pH 3.7 at 30 kV is shown in Figure 4.1 (Section 4.4 Electropherograms and Mass Spectra), Table 4.1 summarises the separation data.

Table 4.1 Separation Data for Ammonium Acetate Analysis (n = 4)

	Migration time ( $t_m$ ) / min	$t_m$ % RSD	Theoretical Plates /m	Mobilities / $10^{-9} \text{ m}^2 (\text{Vs})^{-1}$
SK&F 91207	4.800	0.59	260 000	39.003
SK&F 92422	5.105	0.55	255 000	36.065
SK&F 92506	5.830	0.56	227 000	30.313
Cimetidine	7.835	0.58	166 000	19.945
SK&F 92452	8.172	0.57	154 000	18.705
SK&F 88958	8.304	0.59	129 000	18.248
Thiourea	23.174	1.14	53 000	10.190

The migration times and reproducibility are not significantly increased compared to the phosphate separation. In addition, the efficiency has increased. Thus the improved separation obtained using ammonium acetate is suitable for separating cimetidine and related impurities by capillary zone electrophoresis / mass spectrometry. The resolution of SK&F 92452 and 88958 is comparable to the phosphate separation (0.9). Temporal resolution is not as important with mass spectrometric detection compared to UV detection, as analytes can be differentiated by mass (except isobaric species).

#### 4.2.4 Development of Co-axial Sheath flow Interface

The original Micromass electrospray probe was disassembled, leaving the main body, probe shaft and nebulising gas T-piece. The sheath tube was inserted through the nebulising gas T-piece and secured with a graphite ferrule. A second T-piece was then connected to the end of the sheath tube. The latter T-piece was attached to the syringe pump via a length of fused silica (a minimum of 50 cm was used to prevent current leakage to the pump). A 1 cm length of polyimide was removed from the tip of the separation capillary (50  $\mu\text{m}$  i.d. x 375  $\mu\text{m}$  o.d. and 1 m in length) to improve

conductivity and wetting of the capillary tip. The capillary was then inserted into the sheath tube and was fixed by a 400  $\mu\text{m}$  i.d. graphitised vespel ferrule so that it protruded approximately 0.1 – 1.0 mm from the sheath tube. The original electrospray probe tip was replaced by one of larger internal diameter (to accommodate the wider sheath tube). The assembly is shown in Figure 4.2.

Nebulising and bath gases (nitrogen) were used to aid the desolvation process at flow rates of 30 – 45 L/hr and 125 – 225 L/hr, respectively (optimised for each separation). The source temperature was typically set at 65 °C. The sheath flow was supplied at rates of 1 – 5  $\mu\text{L}/\text{min}$  and comprised 1:1 MeCN : H<sub>2</sub>O + 0.1 % acetic acid and was thoroughly degassed daily by ultrasonication.

Electrospray was generated through the application of 3.25 – 3.75 kV to the probe (which also completed the electrophoretic circuit, thus generating a field strength of  $\sim 265 \text{ Vcm}^{-1}$  in the capillary). The interface position and instrument tuning were optimised by electrophoretic infusion of an analyte (typically cimetidine) in mobile phase (*i.e.* using  $\mu_E$  and EOF to deliver sample to the probe tip) when required.

Mass spectral data were acquired in either full scan mode across the  $m/z$  range of 250 – 425 Da in 0.6s, or by selected ion recording (SIR) with a 1 Da window across each mass with a 0.08s dwell time.

Care was taken to supply a common earth to all instrumentation.

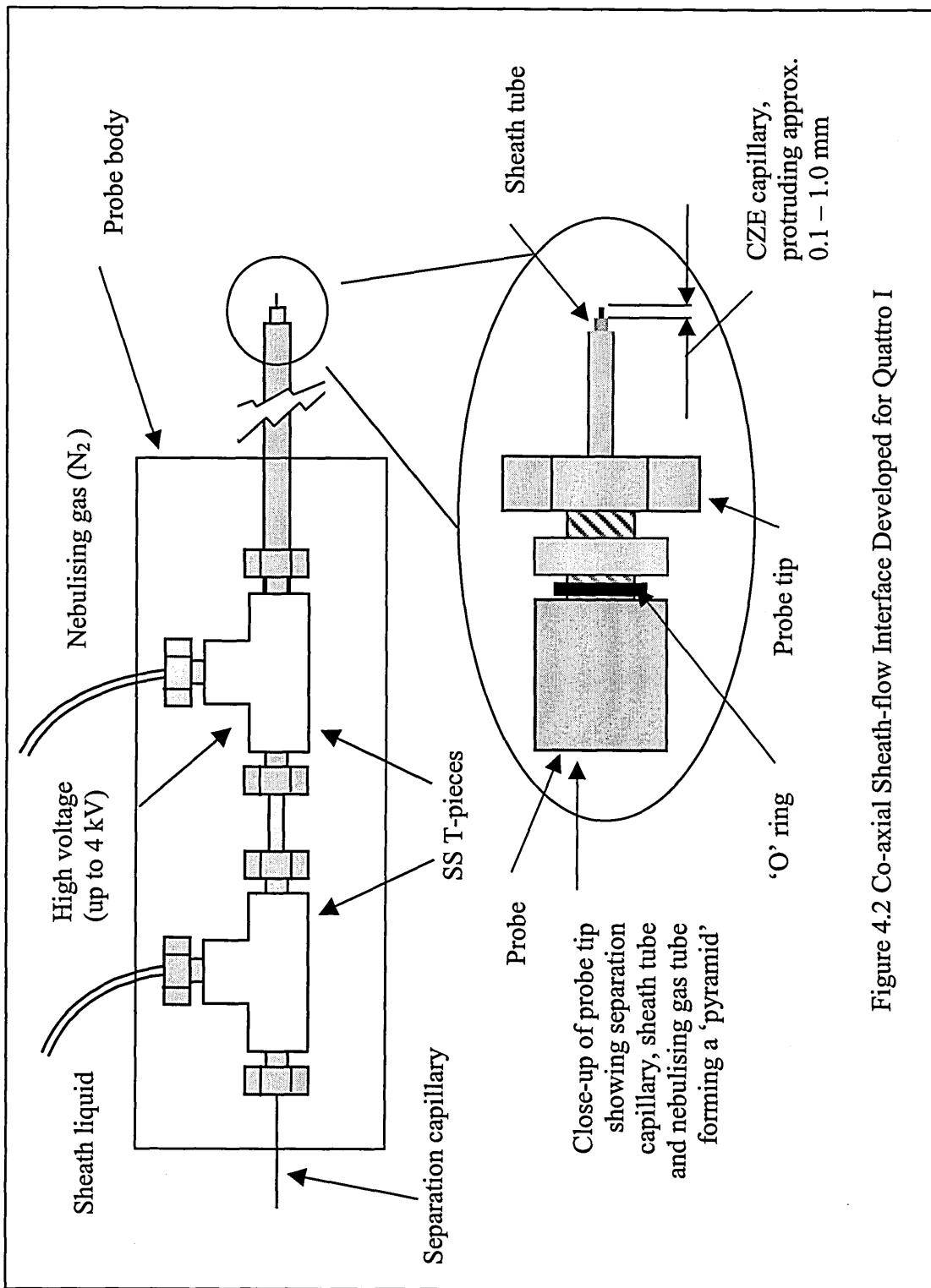


Figure 4.2 Co-axial Sheath-flow Interface Developed for Quattro I

#### 4.2.5 Optimisation of CZE/MS employing a Co-axial Sheath flow Interface

The interface was optimised by electrokinetic infusion of cimetidine and SK&F 88958 at a concentration of 25 µg/mL (*i.e.* sample in 10 mM ammonium acetate pH 3.7). This was achieved by adjusting source lens voltages, gas flow rates, probe location and capillary to sheath tube position.

The most critical parameters were nebulising gas flow rate and capillary position, if these values were not optimised sensitivity was significantly reduced.

The nebulising gas flow rate was higher than that required for normal electrospray operation (gas flow rates of ~ 10 L/hr for liquid flow rates < 10 µL/min). Typically, for CZE/MS the analyte intensity optimised at 40 L/hr. Increasing the flow rate further resulted in a reduction of the analyte intensity with a significant increase in the solvent ion intensity. This was potentially caused by inefficient mixing of the sheath liquid and analyte, therefore reducing the amount of analyte sampled into the mass spectrometer. Bath gas flow rates were reduced (compared to normal electrospray) to approximately 150 – 200 L/hr.

The capillary position has been demonstrated in the literature<sup>3,14,15</sup> to be the most critical parameter for sensitive CZE/MS. The optimum determined in our laboratory was between 0.1 – 1.0 mm; this compares well with cited values<sup>3,14,15</sup>.

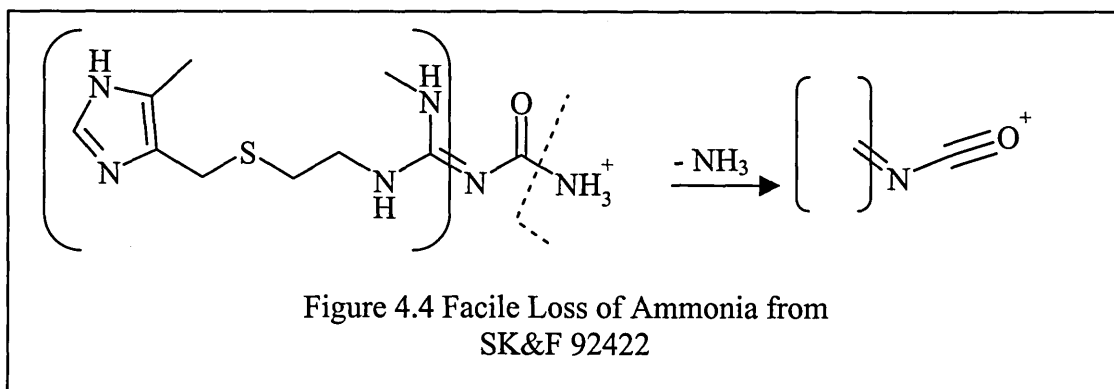
The effect of the sheath flow rate was also investigated; analyte sensitivity was optimised at 3 µL/min, at higher flow the signal decreased (due to dilution effects). At lower rates the spray became unstable and intermittent (as demonstrated by Smith *et al.*<sup>3</sup>).

It was necessary to switch off the sheath-liquid, nebulising gas and electrospray voltage during the wash / injection process. This was due to the sheath-liquid and nebulising gas inducing laminar flow within the capillary and the electrospray voltage inducing an EOF. This resulted in an under-estimation of the injection volume and caused the introduction of bubbles into the capillary during the exchanging of vials (*i.e.* between

buffer and sample vials). Therefore at the end of an analysis the turn off procedure was to stop data acquisition, turn of spray voltage, gases and then sheath-liquid, then finally the separation voltage could be switched off and washing / injection was initiated. To start an acquisition the above procedure was reversed, therefore there was an additional period of time between migration times registered in the mass spectrometer and actual migration times (*i.e.* the time from when the separation voltage was initially applied). This could be determined by noting the time between the application of separation voltage and initiation of mass spectral data acquisition. Unfortunately, this factor reduces migration time reproducibility and precludes the use of a contact closure start, thus requiring an operator to be present to start all analyses.

#### 4.2.6 Analysis of Cimetidine and Related Impurities by CZE/MS

The SIR mass electropherograms obtained for the separation of cimetidine and related impurities are shown in Figure 4.3, corresponding to an injection (10 mbar / 0.1 min) of approximately 46 pg of each analyte in column. All ions monitored correspond to the protonated molecule,  $[M+H]^+$ , with the exception of SK&F 92422. This analyte was monitored as a  $[M+H-NH_3]^+$  ion, due to the facile loss of ammonia from the precursor ion (determined by loop injection), Figure 4.4.



The separation integrity was maintained using mass spectrometry as the detection method when compared to UV absorption, that is the elution order was not altered.

The increase in effective column length (*i.e.* 1 m vs. 53 cm) did not increase the resolution of SK&F 92452 and 88958, in fact the resolution decreased to  $\sim 0.5$  (from 0.9). However, the analytes are of differing mass and therefore could be differentiated

on this basis. Table 4.2 summarises the analyte migration times, reproducibility and the number of theoretical plates generated (neutral marker not included, therefore effective mobilities could not be calculated).

On comparison with Table 4.1 (CZE/UV separation) it can be seen that the migration times have increased. This can be attributed to the increased column length and lower field strength. Migration time reproducibility was also slightly decreased, due to error in starting the analysis.

Table 4.2 Data from Separation of Cimetidine and Impurities

	Migration time / min	$t_m$ % RSD	Theoretical Plates /m
SK&F 91207	9.52	1.04	13 000
SK&F 92422	9.93	0.58	17 000
SK&F 92506	11.27	1.50	10 000
Cimetidine	12.79	0.96	98 000
SK&F 92452	13.16	1.03	189 000
SK&F 88958	13.25	1.04	68 000

In addition, the efficiency decreased; this could also be attributed to the increased column length. Efficiency is proportional to field strength and therefore inversely proportional to capillary length, *i.e.* as capillary length increases, efficiency decreases. Analyte zone dispersion also increases with longer columns due to additional longitudinal diffusion, therefore further decreasing efficiency.

The mass electropherograms obtained for full scan analyses are shown in Figure 4.5. For these experiments, an injection of 20 mbar / 0.2 minute from 100  $\mu\text{g/mL}$  samples (~350 pg of each analyte injected) was employed.

The signal-to-noise ratio has decreased compared to SIR data, which was expected owing to the enhanced sensitivity of SIR through the increased time spent analysing the masses of interest. The SIR electropherograms were generated from ~ 50 pg of analyte, whereas the full scan data from ~350 pg corresponding to approximately 7 times more analyte, demonstrating the increased sensitivity of SIR.

In both the full scan and SIR data SK&F 91207, 92422 and 92506 exhibit a severe tail compared with the remaining analytes. This was consistent throughout all analyses and as yet no adequate explanation can be suggested.

The corresponding mass spectra (Figure 4.6) feature peaks arising from the protonated molecules,  $[M+H]^+$  (Table 4.3). All other ions present are from the solvent.

Table 4.3 Protonated Molecule  $m/z$  Values

Analyte	Protonated molecule $m/z$
SK&F 91207	255
SK&F 92422	271 $[254 (M+H-NH_3)^+]$
SK&F 92506	393
Cimetidine	253
SK&F 92452	269
SK&F 88958	283

#### 4.2.7 Conclusions

The separation of cimetidine and related impurities has successfully been transferred from a CZE/UV method to a CZE/MS method, employing a volatile ammonium acetate buffer. No significant change in separation integrity was observed *cf.* CZE/UV. An increase in migration times and a decrease in peak efficiency were observed; these factors could be attributed to the increased column length required for the MS interface.

Data was obtained in both full scan and selected ion recording mode, which consumed ~350 pg and ~50 pg respectively, indicating the higher level of sensitivity obtained whilst using selected ion recording. However, SIR data acquisition requires knowledge of the sample prior to analysis, which can limit its suitability.

A reduction in the peak resolution (temporal separation) of SK&F 92452 and 88958 has been demonstrated to be less significant employing mass spectral detection *cf.* UV detection. The mass discrimination power of the mass spectrometer allows a further dimension of separation by mass.

### 4.3 Nanospray Interface Procedure

The development of a nanospray interface was based on the work of Gaskell *et al.*<sup>13</sup>.

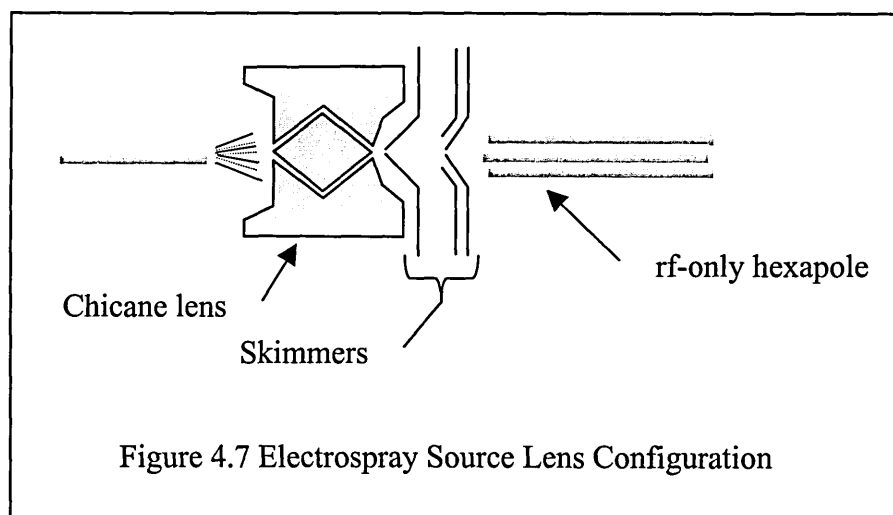
Two discrete interfaces were developed,

- Nanospray/MS for pressure flow
- Nanospray/MS for electrophoretic flow

Both interfaces employed similar source and experimental parameters, but different probe set-ups.

#### 4.3.1 Source Modification

The major modification required within the source was the removal of the high voltage counter-electrode, otherwise known as a 'chicane lens' (ESI lens configuration is shown in Figure 4.7). This was to accommodate the modified probe, which was approximately 42 mm longer than the standard probe set-up. Consequently, the first skimmer became the counter electrode during nanospray.



Because of the reduced flow rate, the droplets formed during the nanospray process are significantly smaller and thus require less desolvation (*cf.* traditional electrospray). Therefore the flow of bath gas was reduced to ~50 L/hr and the source temperature was ambient (thermocouple registered ~28°C).

### 4.3.2 Modification of Probe for Pressure Flow Nanospray

A Quattro I (Micromass, Manchester, UK) mass spectrometer equipped with an electrospray source was used throughout. The pressure flow nanospray was performed on a modified probe as representation in Figure 4.8. The liquid flow was provided by a Harvard Apparatus Model 11 (Edenbridge, UK) syringe pump, employing Hamilton Gastight syringes between 25 – 100  $\mu\text{L}$  (Supelco, Poole, UK).

Un-coated fused silica capillaries of various sizes (see below) were obtained from Composite Metal Services Ltd. (Hallow, UK). Coopers Needle Works (Birmingham, UK) supplied the stainless steel needles. All unions, ferrules and PEEK tubing were obtained from Supelco (Poole, UK) and silver conductive paint from RS (Loughborough, UK).

A 50  $\mu\text{m}$  i.d. x 375  $\mu\text{m}$  o.d. capillary was used between the syringe pump and the probe, with an in-line 100 nL Vici internal loop injector (IB-329, Thames Restek, Windsor, UK).

Various spray tips were investigated; these are summarised in Table 4.4.

Table 4.4 Summary of Spray Tips Used

Tip	Internal diameter / $\mu\text{m}$	Outer diameter / $\mu\text{m}$	Material
①	20	90	Fused silica
②	50	150	Fused silica
③	25	180	Stainless Steel
④	Drawn, gold coated fused silica		

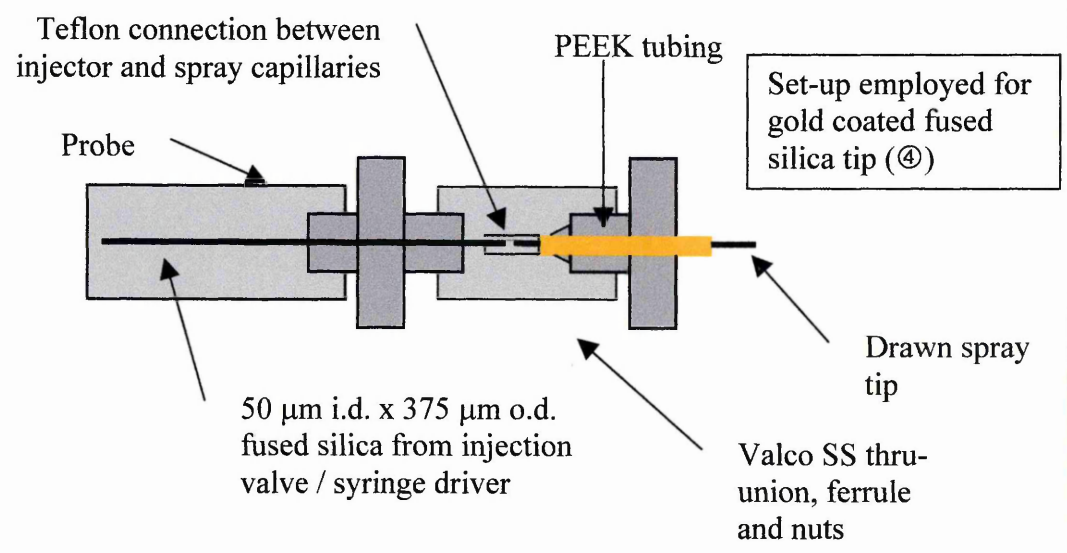
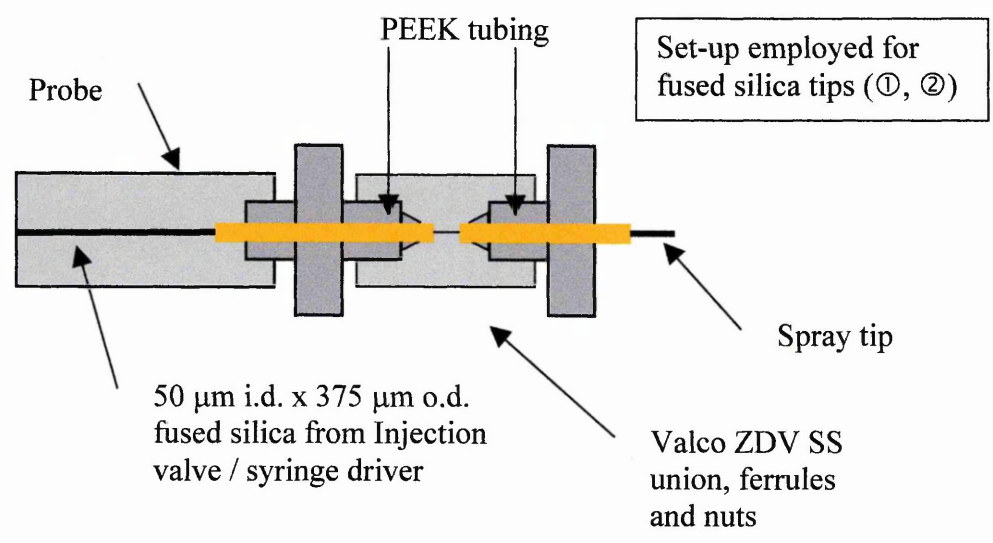
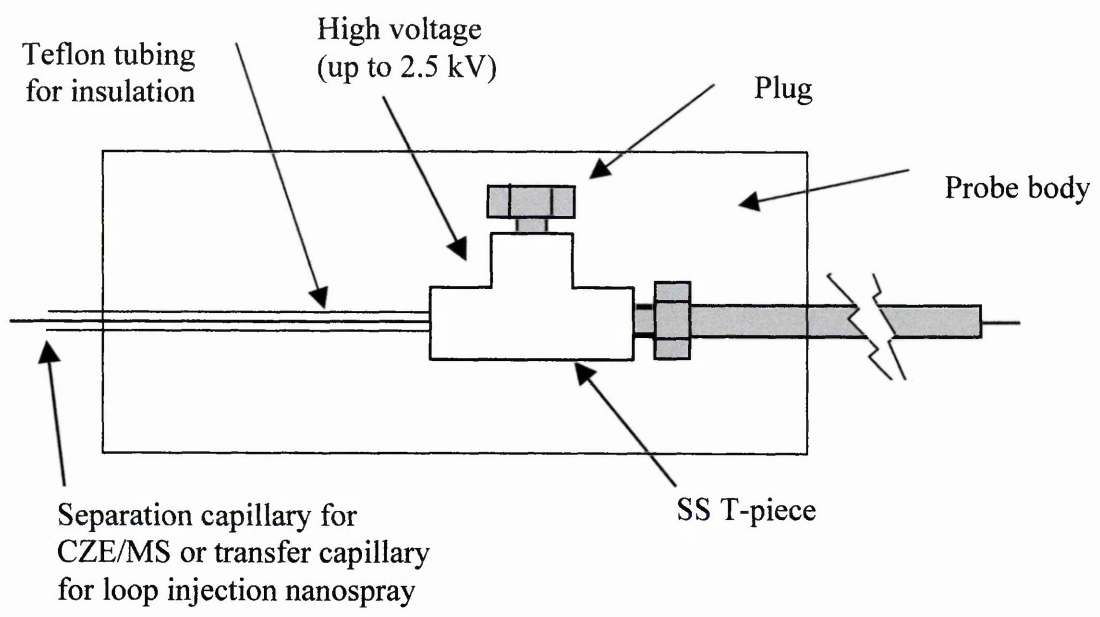


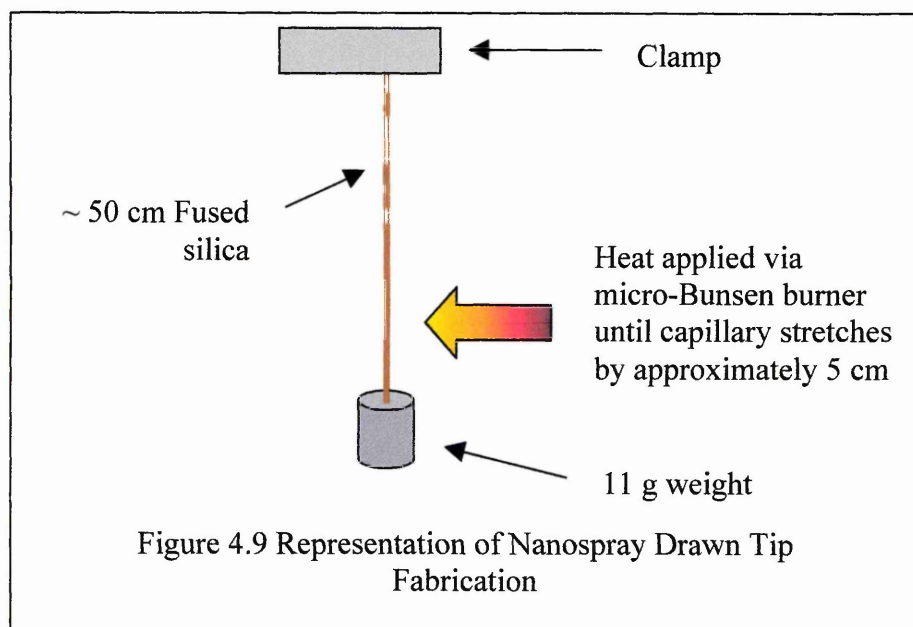
Figure 4.8 Nanospray Interface based on that of Gaskell *et al.*<sup>13</sup>

#### 4.3.2.1 Production of Drawn, Conductive Coated Spray Tips

In all cases, the tips were produced from 50  $\mu\text{m}$  i.d. x 375  $\mu\text{m}$  o.d. un-coated fused silica capillary.

Two methods were employed for drawing the capillary tips. These methods were:-

1. A piece of capillary was simply held in a micro-Bunsen burner flame until it softened and was then pulled apart.
2. An 11 g weight was attached to a 50 cm length of fused silica. The capillary was heated with a micro-Bunsen burner until the capillary stretched by  $\sim 5$  cm (Figure 4.9). Resulting in the production of two spray tips,  $\sim 10$  cm and  $\sim 40$  cm in length. The two tips were then separated at the desired point (using a sapphire cutting tool to ensure a smooth cut).

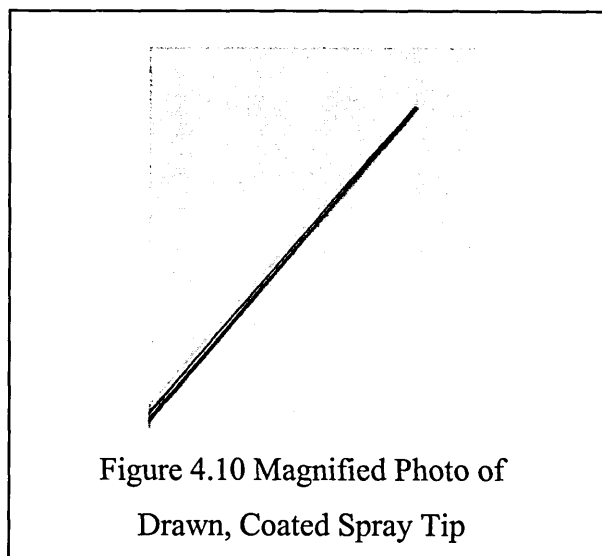


Two methods of gold coating were employed; the capillaries were washed then coated or derivatised then coated. Without derivatisation the gold coating was easily removed or damaged, especially by electrical discharge, thereby rendering the tip unusable.

The derivatisation procedure (based on the method of Kriger *et al.*<sup>10</sup>) could be separated into two steps, which were cleaning and reaction stages,

1. Cleaning step: the capillary tip was immersed in a beaker containing acetone in an ultrasonic bath for 1 minute, then flushed with several column volumes of methanol. To further remove any organic species from the capillary surface the tip was immersed in 'Piranha' solution (1:4 30 % H<sub>2</sub>O<sub>2</sub> : concentrated H<sub>2</sub>SO<sub>4</sub>) at 70°C for 20 minutes, then flushed with several column volumes of water. The capillary was then dried with argon and left in an oven at 105 °C for 10 minutes.
2. Reaction step: 5 g (3-mercaptopropyl)trimethoxysilane (Aldrich, Poole, UK) dissolved in 200 g 2-propanol and 5 mL water was brought to reflux. The capillary tip was immersed for ten minutes, then removed and washed with 2-propanol and cured in an oven at 105 °C for 10 minutes. This process was repeated a further two times.

The derivatised capillary was then ready for sputter coating, which was performed at a vacuum of 0.1 torr (~ 0.1 mbar), with an anode current of 20 mA for 2 minutes (employing an Emscope SC500 sputter coater). A magnified photo of a drawn, coated spray tip ready for use is shown in Figure 4.10.



The internal diameter at the tip was not determined owing to the irreproducible nature of production. A method of improving reproducibility was attempted. The tips were inserted into a stainless steel capillary of 100 µm i.d. and broken off, resulting in a tip

i.d. of  $\sim 15 \mu\text{m}$ . However, the tip had a jagged appearance (*cf.* when cut using the sapphire tool), which when employed resulted in poor spray stability. Cut tips were utilised; therefore, it was necessary to optimise the spray voltage employed for each tip prior to use.

#### 4.3.2 Pressure Flow Nanospray Mass Spectrometry

The mass spectrometer electrospray source and probe were modified as outlined above to perform nanospray MS. The four spray tips listed in Table 4.4 were investigated for stability at various flow rates and limit of detection (by a serial dilution of cimetidine).

Tips ① ② and ③ were connected to approximately 50 cm of fused silica (from the injection valve) via a stainless steel zero-dead-volume (ZDV) union. The tips were sleeved in a 2 cm length of PEEK tubing and held in place in the union by a Valco ferrule and nut. The capillary from the injection valve was also sleeved in PEEK tubing (2 cm) and held in the union with a Valco ferrule and male / male union, which connected the assembly to the electrospray probe. Table 4.5 summarises the PEEK tubing employed for the various tips. The spray voltage was applied to the union.

Table 4.5 Dimensions of PEEK Tubing Employed to Secure Spray Tips

	Tip o.d. / $\mu\text{m}$	PEEK tubing employed (i.d. / $\mu\text{m}$ )
①	90	Red (127)
②	150	Yellow (180)
③	180	Yellow (180)
④	375	Orange (500)

An alternative set up was employed for tip ④, enabling the spray voltage to be applied to the tip outlet rather than at the capillary junction. The spray tip was butted to approximately 50 cm of fused silica (from the injection valve) via a Teflon connector. The tip was then sleeved with 2 cm of orange PEEK tubing and secured in a 1/16" SS thru-union with a Valco ferrule and nut. The assembly was then connected to the probe via a male /male union. The electrical connection to the gold-coated tip was supplied via silver conductive paint.

These assemblies are shown in Figure 4.8.

To determine suitable flow rates for each of these spray tips cimetidine was infused at a concentration of 50 µg/mL in 1:1 MeCN : H<sub>2</sub>O + 0.1 % acetic acid. The flow rate was allowed to stabilise for at least 2 minutes after being altered. The data were plotted as the intensity of *m/z* 253 ion (cimetidine [M+H]<sup>+</sup>) vs. time. Table 4.6 summarises the flow rates for each tip.

Table 4.6 Flow Rates for Various Nanospray Tips

	Lower stability rate / nL/min	Higher stability rate / nL/min	Optimum rate / nL/min	Plot of <i>m/z</i> 253 intensity vs. time
①	150	>700	150	Figure 4.11
②	300	>800	300	Figure 4.12
③	400	>800	500	Figure 4.13
④ Method 1*	500	>800	500	Figure 4.14
Method 2†	150	>800	150	Figure 4.15

The optimum flow rate was determined as the rate that generated the highest ion current and least noise (*i.e.* the most stable spray). In each case, the upper limit was greater than 800 nL/min. This flow rate could be achieved with ‘traditional’ electrospray and therefore the true upper limit was not determined. The lower limit was established by reducing the flow until the spray became unstable (signified by a rapid decrease in ion current). In all cases (except ③) the lower limit also provided the optimum signal intensity, least noise and hence greatest sensitivity. A spray was obtained down to 300 nL/min using ③. However, at this flow rate the intensity trace was dominated by dropouts in the spray (signifying instability), whereas at higher flow rates (600 nL/min) the ion current was steadier. During use, the stainless steel tip (③) required careful manipulation especially in positioning to minimise discharges (to the counter electrode). Even when a current limiting resistor (47 MΩ) was used in line with the electrospray voltage, frequent discharges were observed. To minimise electrical damage to the

\* Pulled by hand, derivatised and Au coated.

† Drawn using weight, derivatised and Au coated.

instrumentation (*i.e.* source control circuitry *etc.*) the stainless steel capillaries were not employed any further.

For enhanced sensitivity, each tip was used at its optimum flow rate.

The limit of detection (LOD) for each tip was determined by a serial dilution of cimetidine, employing 100 nL loop injections of 100 µg/mL to 0.1 µg/mL at the optimum flow rate for the tips. These data are summarised in Table 4.7.

Table 4.7 Limit of Detection Data for Various Nanospray Tips

	Limit of Detection / µg/mL	Quantity injected / pg	Chromatogram
①	0.1	10	Figure 4.16
②	0.05	5	Figure 4.17
④ <sup>†</sup>	0.1	10	Figure 4.18
Co-axial sheath flow	1.0	100	Figure 4.19

The various tips gave similar sensitivities, ~ 0.1 µg/mL. Therefore, the most suitable tip for nanospray employing pressure flow was tip ②. This was due to the ease of fabrication *cf.* ④ and the wider i.d. (*cf.* ①) would result in a reduced incidence of blockage. In addition, the increased (optimum) flow rate would allow numerous samples to be rapidly analysed (especially *cf.* ①). There is also a large volume associated with the fused silica and sample loop / injector, thus a higher flow rate will minimise band broadening associated with dead volume.

To compare the relative sensitivities of nanospray and co-axial sheath flow interfaces the limit of detection was determined for each. The co-axial sheath flow interface was assembled as in CZE/MS analyses. The LOD was performed by injecting 100 nL of sample into the separation capillary, which was pumped at a flow rate of 1 µL/min, the sheath flow was delivered at 3 µL/min. The mobile phase and sheath liquid comprised 1:1 MeCN : H<sub>2</sub>O + 0.1 % acetic acid.

<sup>†</sup> Prepared by method 2, drawn using weight, derivatised and Au coated.

A LOD of 1  $\mu\text{g/mL}$  was obtained employing the co-axial sheath flow interface, whereas nanospray, using tip ②, gave a LOD of 0.05  $\mu\text{g/mL}$ . This suggests that in this system there is an order of magnitude decrease in sensitivity due to the dilution effects of the sheath flow, indicating that sensitivities could be affected in CZE/MS analyses. In this LOD investigation the dilution was at a ratio of 1:3 (sample : sheath), in CZE/MS this would more significant (due to the reduced velocity through the column and the reduced injection volume), approximately 0.2:3, therefore it would be desirable to develop a sheathless interface for CZE/MS.

#### 4.3.2.1 Conclusions

A nanospray interface based on the reported design of Gaskell *et al.*<sup>13</sup> has been successfully employed on a Quattro I mass spectrometer. In addition, the probe has been modified to use drawn, gold-coated fused silica tips, which could be developed into a CZE/MS interface.

A number of different tips have been investigated and it was determined that the best tip was a 50  $\mu\text{m}$  i.d. x 150  $\mu\text{m}$  o.d. fused silica capillary. This tip was able to accommodate flows of >800 to 200 nL/min and had a detection limit (for cimetidine) of 0.05  $\mu\text{g/mL}$ . The 20  $\mu\text{m}$  i.d. x 90  $\mu\text{m}$  o.d. fused silica tip was also useful. However, the capillary was difficult to cut owing to the narrow o.d., which lead to a jagged cut that resulted in the formation of split or poor sprays. The stainless steel tips were simple to use. However, extreme care was necessary to prevent electrical discharge within the source.

The detection limits of a nanospray (0.05  $\mu\text{g/mL}$ ) and co-axial sheath flow (1  $\mu\text{g/mL}$ ) interface were investigated. The nanospray source was an order of magnitude more sensitive than the co-axial sheath flow interface. This could be attributed to the dilution effects of the sheath liquid, suggesting that the dilution effects in CZE/MS could be significant.

### 4.3.3 Modification of Probe for Nanospray CZE/MS

#### 4.3.3.1 Instrumentation

A Quattro I mass spectrometer (Micromass, Manchester, UK), with an electrospray (ESI) source was used throughout. The source and electrospray probe were modified to perform nanospray as outlined in sections 4.3.1 and 4.3.2.

Data were acquired in either selected ion recording mode (SIR) with a 1 Da window across each mass with a 0.08s dwell time or by full scan mode across the  $m/z$  range of 250 – 400 Da in 0.4s.

Separations were performed on a PrinCE 560 (Prince Technologies, Emmen, The Netherlands) at a potential of + 30 kV (supplied to the inlet electrode). Capillaries were un-coated fused silica of 50  $\mu\text{m}$  i.d. x 375  $\mu\text{m}$  o.d. and a total length of 1 m (Composite Metal Services Ltd. (Harrow, UK)). Injections were performed hydrodynamically. The buffer comprised 1:1 MeCN : 10 mM ammonium acetate pH 3.7 (adjusted with glacial acetic acid), and was filtered through a 0.2  $\mu\text{m}$  pore syringe filter.

#### 4.3.3.2 Chemicals

Cimetidine and related compounds were obtained from SmithKline Beecham (Harlow, UK), the structures of which are shown in Table 3.1 (Chapter 3). Acetonitrile was of HPLC grade. Water was distilled and deionised by a Milli-Q RG purification system (Millipore, Fisons, Loughborough, UK). Ammonium acetate and acetic acid were of HPLC grade and were purchased from Aldrich (Poole, UK). All other materials were of reagent grade or better.

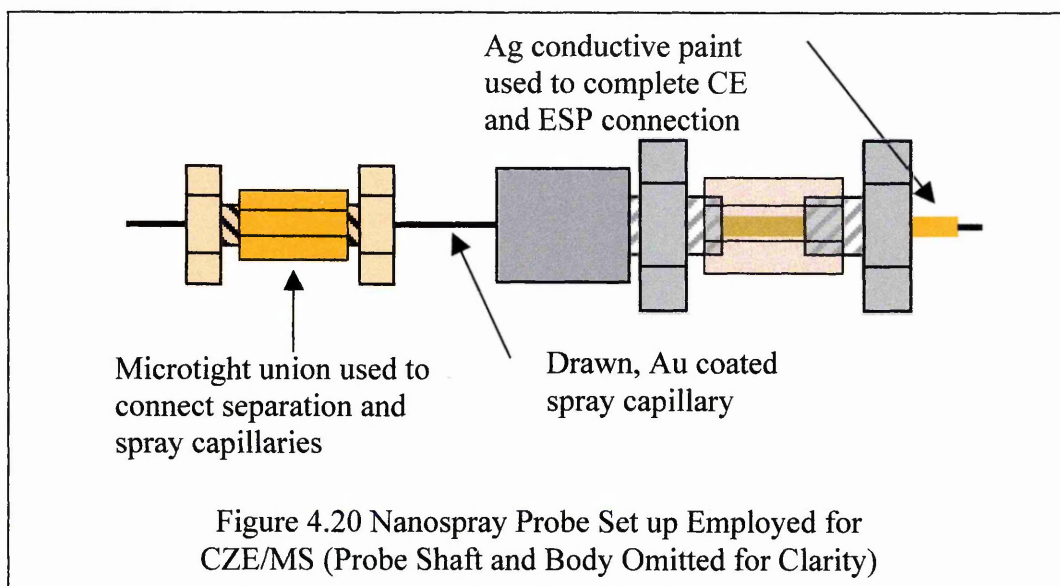
Individual stock solutions of each analyte (1000  $\mu\text{g}/\text{mL}$ ) were prepared in water and diluted to a working concentration of 50  $\mu\text{g}/\text{mL}$  (except SK&F 92506 100  $\mu\text{g}/\text{mL}$  owing to poor detection) with water.

#### 4.3.3.3 Development of CZE / Nanospray /MS

The fused silica tips (① and ②) were simple to implement, whereas the drawn, coated tips (④) were time consuming to prepare and fragile. Therefore, it would be advantageous to be able to perform nanospray CZE/MS using the simple fused silica tips. However, initial attempts employing a 20  $\mu\text{m}$  i.d. x 90  $\mu\text{m}$  o.d. tip painted with Ag conductive paint (to provide a conductive connection to the capillary tip) were unsuccessful. This was because the narrow tip was easily blocked. In addition, it was difficult to obtain a smooth cut tip, which would result in the formation of a poor spray. The 50  $\mu\text{m}$  i.d. x 150  $\mu\text{m}$  o.d. painted tips were more robust, but the conductive paint rapidly deteriorated, resulting in poor electrical contact.

Initially an analyte signal could be obtained during electrophoretic infusion employing the painted tips. However, the ion current rapidly decreased in conjunction with a decrease in CZE current. This was attributed to the formation of bubbles within the ZDV union (joining the separation and spray capillaries), which could be viewed under a magnifying lens when pressure was applied to the inlet electrode. The formation of bubbles at a metal / fused silica interface has been reported previously<sup>16</sup>. Therefore, drawn, gold-coated tips were seen as the method of choice for CZE/MS, whereas the fused silica tips were only useful for pressure flow nanospray.

The drawn, gold-coated tips were fabricated by Method 2 (*i.e.* weight drawn as outlined in section 4.3.2.1). Two sets of tips were prepared, one derivatised and coated (tip A), the other simply cleaned and coated (tip B). The tips employed were ~ 40 cm in length and passed straight through the probe and were connected to the separation capillary by a Microtight union. The capillary was therefore electrically isolated from the electrospray voltage, this connection was achieved through the use of Ag conductive paint between the gold coating and the stainless steel union (Figure 4.20).



Two types of tip were compared for robustness; the capillary was either cleaned then derivatised (A) or just cleaned (B) prior to gold coating. In both cases, the coating appeared to cover the whole of the outer surface, resulting in a conductive layer (tested with a digital voltmeter).

Application of 2.5 kV to both tips induced an electrospray (employing 1:1 MeCN : H<sub>2</sub>O + 0.1 % acetic acid pressure driven at 300  $\mu$ L/min) of comparable ion current. After an electrical discharge (induced by increasing the voltage to 3.2 kV) the electrospray could easily be re-initiated employing tip A. However, attempts to re-initiate the spray employing tip B were unsuccessful. When these tips were viewed under a microscope (x 50) the conductive layer of A remained intact, whereas the coating of B terminated approximately 1 mm from the outlet, this would no longer permit electrospray. In addition, the appearance of the conductive surface of A was unchanged from when it was produced, whereas the surface of B appeared flaky and discontinuous. Therefore, an electrical discharge had irreversibly damaged the coating on tip B, whereas the derivatised tip remained operational.

A derivatised tip (40 cm) was connected to a CZE separation capillary (60 cm) using a Microtight junction and flushed thoroughly with 1:1 MeCN : 10 mM ammonium acetate pH 3.7. The addition of organic solvent to the buffer has been suggested to be necessary for nanospray CZE/MS<sup>1,2</sup>, its function is to reduce the surface tension of the liquid,

which aids the electrospray process. Electrical connectivity was made through silver paint between the probe (ESP voltage) and the gold tip.

Electrophoretic infusion of cimetidine and SK&F 88958 (25  $\mu\text{g/mL}$ ) in the buffer was attempted to 'tune' the system. However, only solvent ions ( $\text{MeCN [M+H]}^+$  at  $m/z$  42, acetic acid  $[\text{M+H}]^+$  at  $m/z$  61) were observed. Application of supplementary pressure to the inlet vial (up to 250 mbar) resulted in weak analyte ions being observed. Improved stability and intensity could be achieved using no bath gas. This has been observed previously<sup>17</sup> using a co-axial sheath flow interface on a Quattro MS. The phenomenon was attributed to an elevated gas pressure within the source (through inadequate evacuation of the bath gas) leading to a reduction of linear velocity through the capillary. Unfortunately the use of no bath gas resulted in the generation of  $\text{H}_2\text{O}$  cluster ions (*i.e.*  $\text{H}^+[\text{H}_2\text{O}]_n$ , where  $n > 18$ ), known as unstable van der Waals polymers<sup>18</sup>. The cluster ions were eliminated when the gas flow rate was increased.

The analyte signal remained poor irrespective of tuning and probe positioning. The spray tip was exchanged for an underivatized tip. A strong signal was obtained for both cimetidine and SK&F 88958 with electrophoretic infusion with a supplementary pressure of 20 mbar.

The ease of operation of the underivatized tip compared to the derivatized could have been due to modification of the inner surface of the capillary (and thus EOF) during the derivatization process. The process was based on that of Kriger *et al.*<sup>10</sup>, in which they modify the capillary inner surface with (3-aminopropyl)triethoxysilane (APS), after the capillary outer surface was derivatized. Thus, a new surface was generated prior to use. In an attempt to regenerate the silanol surface of the fused silica the capillary was flushed with 0.1 M NaOH (commonly used to remove adherents from the surface). Unfortunately, this resulted in the narrow capillary tips becoming blocked. Therefore, underivatized tips were used for all further analyses. Between analyses the column and tip were flushed with buffer (1 bar, 2 minutes).

#### 4.3.3.4 Results / Discussion

Figure 4.21 shows the SIR mass electropherograms of the separation of cimetidine and impurities using CZE/MS corresponding to ~ 30 pg (~ 60 pg SK&F 92506) of each analyte in column (10 mbar / 0.07 min). Full scan data were also obtained (Figure 4.22) from a 10 mbar / 0.1 min injection, relating to ~ 50 pg in column (~ 100 µg/mL SK&F 92506), whereas approximately 50 pg was required to generate SIR data employing the co-axial sheath flow interface. This indicates the increase in sensitivity obtained using a sheathless interface. The reduced sensitivity of a co-axial sheath flow interface was a consequence of the dilution effects of the sheath liquid.

The mass spectra generated from the full scan data are shown in Figure 4.23, featuring the protonated ions,  $[M+H]^+$ , of the analytes.

Migration times, reproducibility and the efficiencies (as the number of theoretical plates per metre) are shown in Table 4.8. The most noticeable difference between the separation using the co-axial sheath flow and nanospray interface is the migration order.

Table 4.8 Nanospray CZE/MS Data (n= 4)

	Migration time ( $t_m$ ) / min	$t_m$ % RSD	Theoretical Plates /m
SK&F 92422	10.71	1.24	4 200
SK&F 91207	10.95	1.12	3 500
SK&F 92506	12.27	3.07	3 400
Cimetidine	15.02	1.67	7 200
SK&F 88958	16.07	2.13	10 500
SK&F 92452	19.43	2.60	10 800

The migration order using UV detection and the co-axial sheath flow interface was SK&F 91207; 92422; 92506; cimetidine; 92452 and 88958

Whereas, using the nanospray interface it was

SK&F 92422; 91207; 92506; cimetidine; 88958 and 92452.

The migration order has been inverted at two places *i.e.* SK&F 92422 migrates in front of 91207 and 88958 in front of 92452.

This change in selectivity has arisen through the change in buffer composition. The effect of organic solvents on CZE separations is difficult to predict, as demonstrated here. The inclusion of MeCN to the buffer will have reduced the viscosity and altered the degree of solvation of the analytes causing them to migrate at a different rate than previously observed. In addition, the effect of organic solvent on the surface charge of the capillary is unclear.

The migration times are longer due to the reduced EOF (caused by the addition of MeCN), the reproducibility has also decreased, this can be attributed to instabilities in the spray causing variations in the EOF and hence migration times. However, the reproducibility is better than 3 % RSD, this in conjunction with mass spectral detection would allow facile identification of analytes. The efficiencies (*cf.* CZE/UV) are significantly reduced. This was caused by increased zone dispersion within this system. The main contribution arising through the use of a union to join the spray and separation capillaries. The union employed was a Microtight junction (PEEK unions designed specifically for fused silica). However, these unions rely on a perfect cut end to produce a zero dead volume union, which in practise is difficult to achieve. Therefore, there would be dead volume within the system, which would contribute to zone dispersion.

Efficiencies would also be decreased because of the longer residence time in the capillary and the application of supplementary pressure to the inlet vial (generating a laminar flow profile).

#### 4.3.3.5 Conclusions

Cimetidine and related impurities have successfully being separated and detected using CZE/nanospray/MS, employing drawn, gold-coated spray tips manufactured from fused silica capillary.

Initial attempts employing derivatised spray tips (with 'molecular adhesive') were unsuccessful. This has been ascribed to an alteration of the inner surface of the capillary eradicating the EOF and thus flow through the capillary. Therefore, underderivatised capillaries were used for all subsequent analyses.

The overall sensitivity was improved compared to a co-axial sheath flow interface. Approximately 50 pg of each analyte was required to generate full scan data using a sheathless interface, whereas ~350 pg was necessary to obtain full scan data employing co-axial sheath flow. The signal-to-noise ratio of the nanospray SIR data suggests that the detection limits would be a further order of magnitude lower than employed in this study.

The separation selectivity (migration order) has altered, which can be attributed to the incorporation of MeCN in the buffer (reducing the surface tension, thus improving the electrospray process). In addition, migration times have increased; this can also be attributed to the addition of MeCN to the buffer. Organic solvents decrease the EOF and hence the apparent analyte mobility. A dead volume present at the capillary junction resulted in a reduction of efficiency (owing to increased zone dispersion). A single column / spray capillary would eliminate the dispersive effects of such a junction. In addition, the supplementary pressure applied to the inlet vial (to improve spray stability) would serve to induce a laminar flow profile within the capillary further increasing zone length.

This initial investigation of a nanospray CZE/MS interface has demonstrated the increase in sensitivity obtained when no sheath liquid is employed. However, further development is required to improve robustness and reproducibility.

#### 4.4 Electropherograms and Mass Spectra

DAX 6.0: Martin Palmer 15/08/99 16:01:48PM

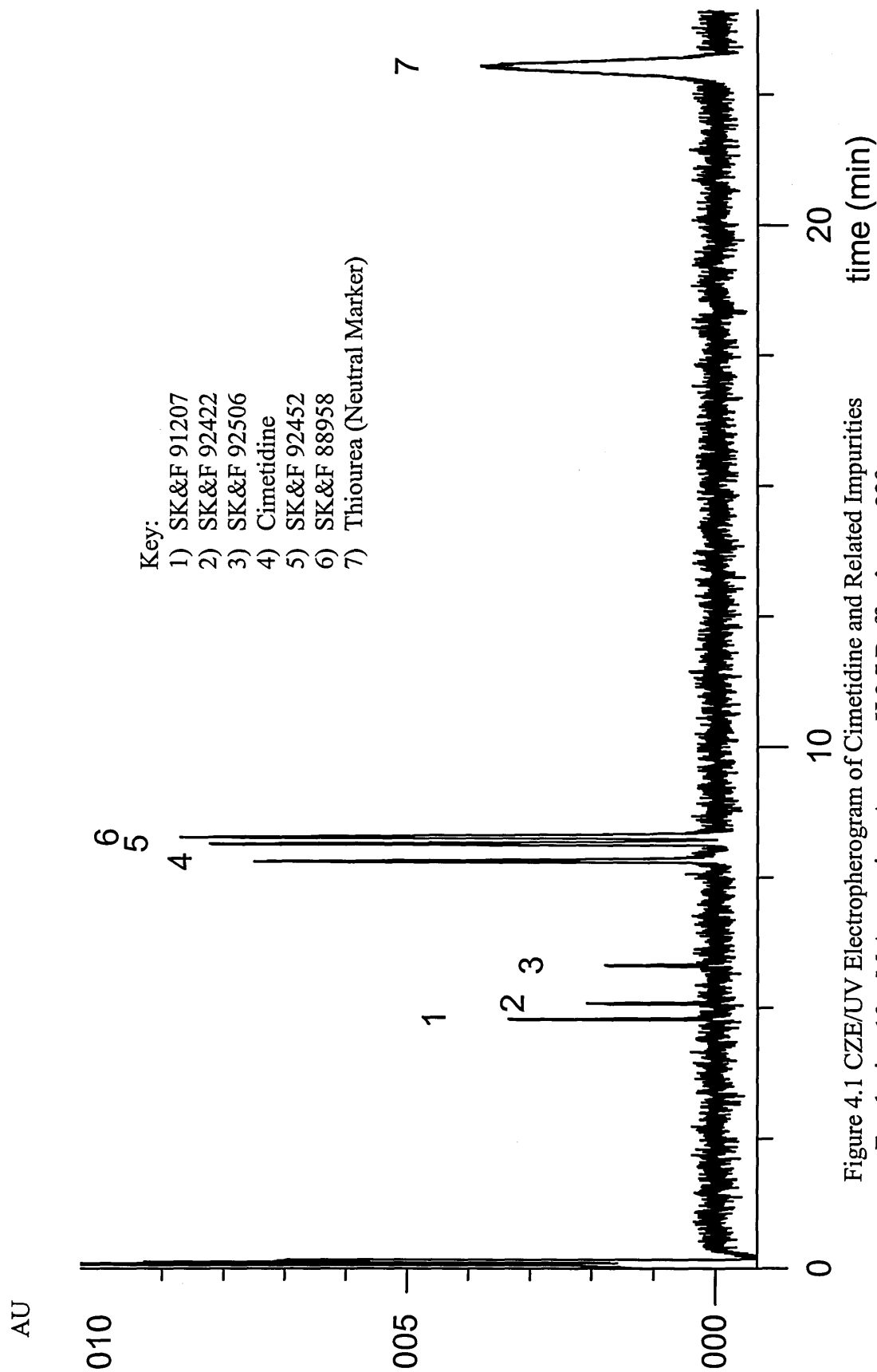


Figure 4.1 CZE/UV Electropherogram of Cimetidine and Related Impurities  
Employing 10 mM Ammonium Acetate pH 3.7 Buffer,  $\lambda_{\text{max}} = 230 \text{ nm}$

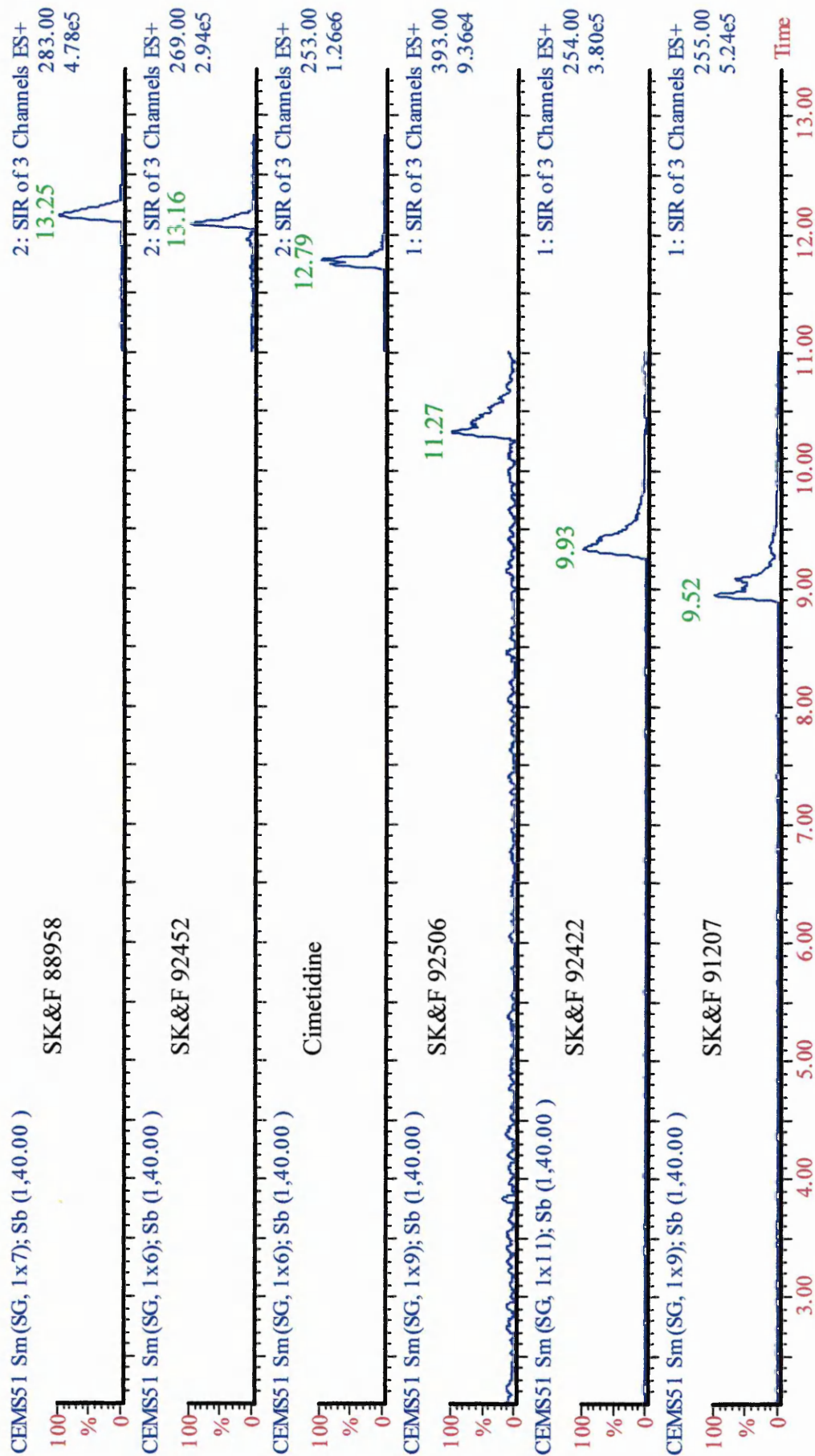


Figure 4.3 Co-axial Sheath-flow CZE/MS SIR of 50 pg each Analyte ( $t_m$  mean times)

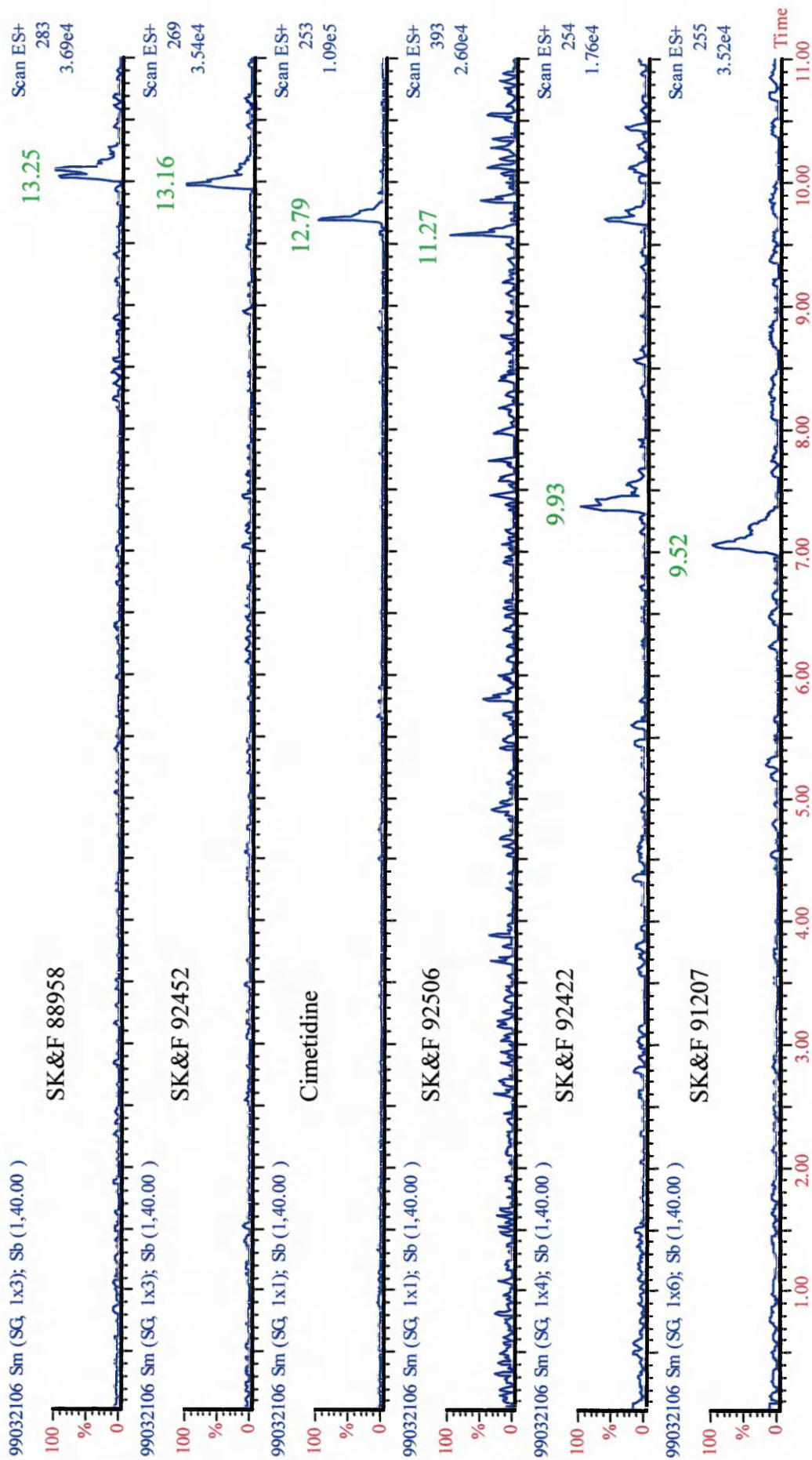


Figure 4.5 Co-axial Sheath-flow CZE/MS Full Scan of 350 pg each Analyte (t<sub>m</sub> mean times)

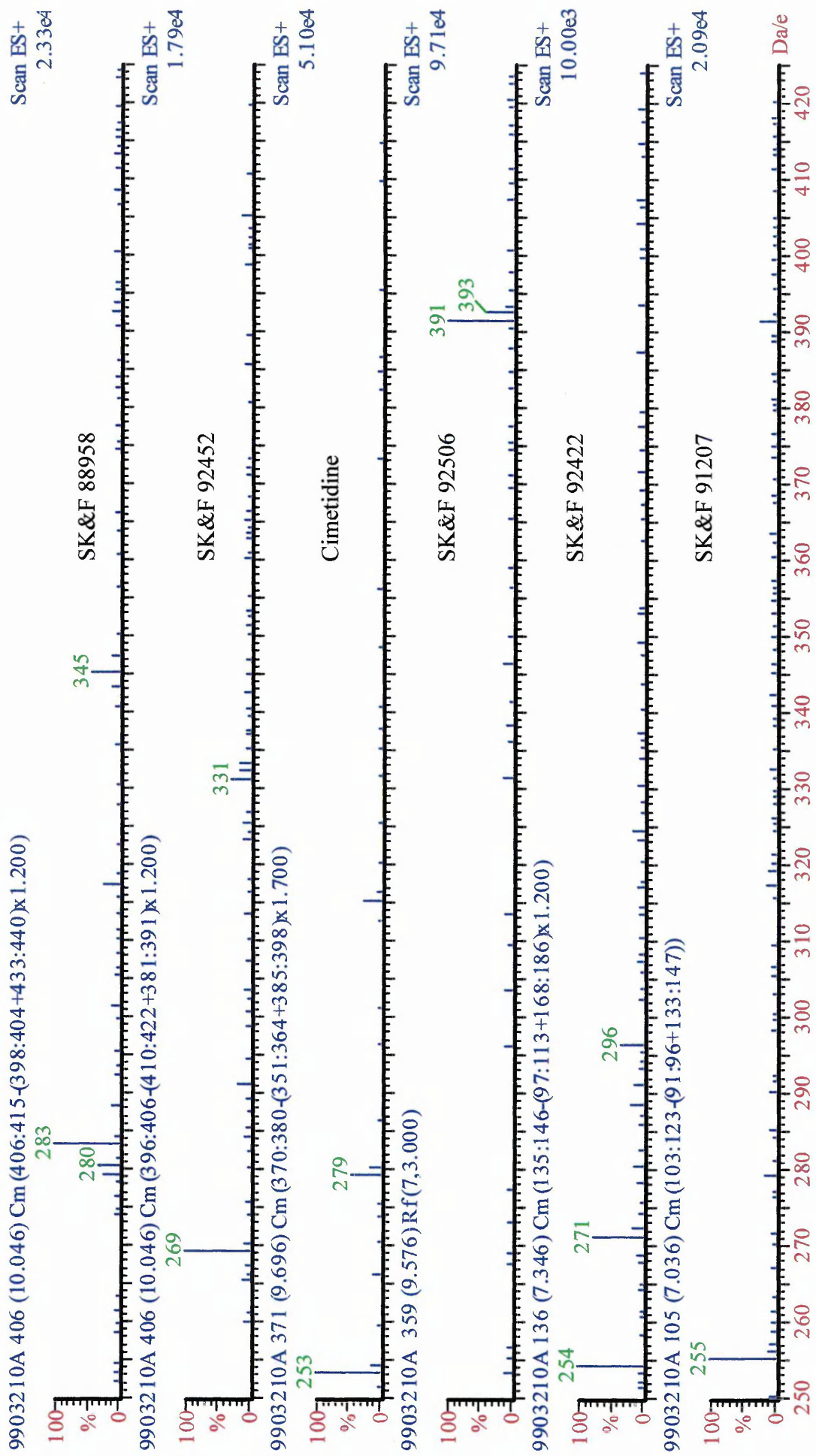


Figure 4.6 Co-axial Sheath-flow CZE/MS Mass Spectra Featuring [M+H]<sup>+</sup>

m/z corresponding to SK&F 91207 – 255; 92422 – 271 ([M+H-NH<sub>3</sub>]<sup>+</sup> - 254); 92506 – 393; Cimetidine – 253; 92452 – 269; 88958 – 283

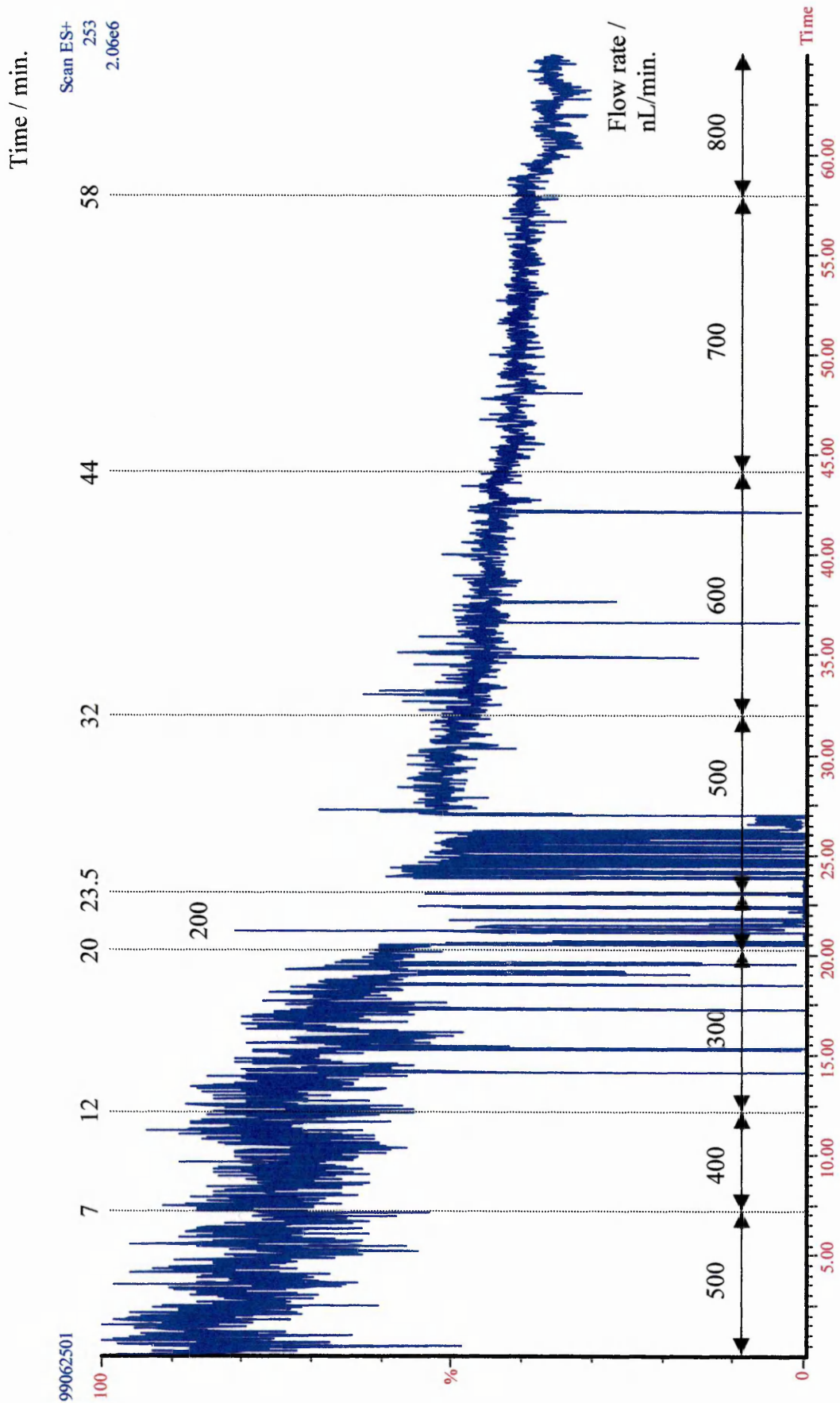


Figure 4.14 Spray Stability Dependence on Flow Rate – Hand Drawn, Au Coated Tip  
 (Time – minutes, flow rate – nL/min)

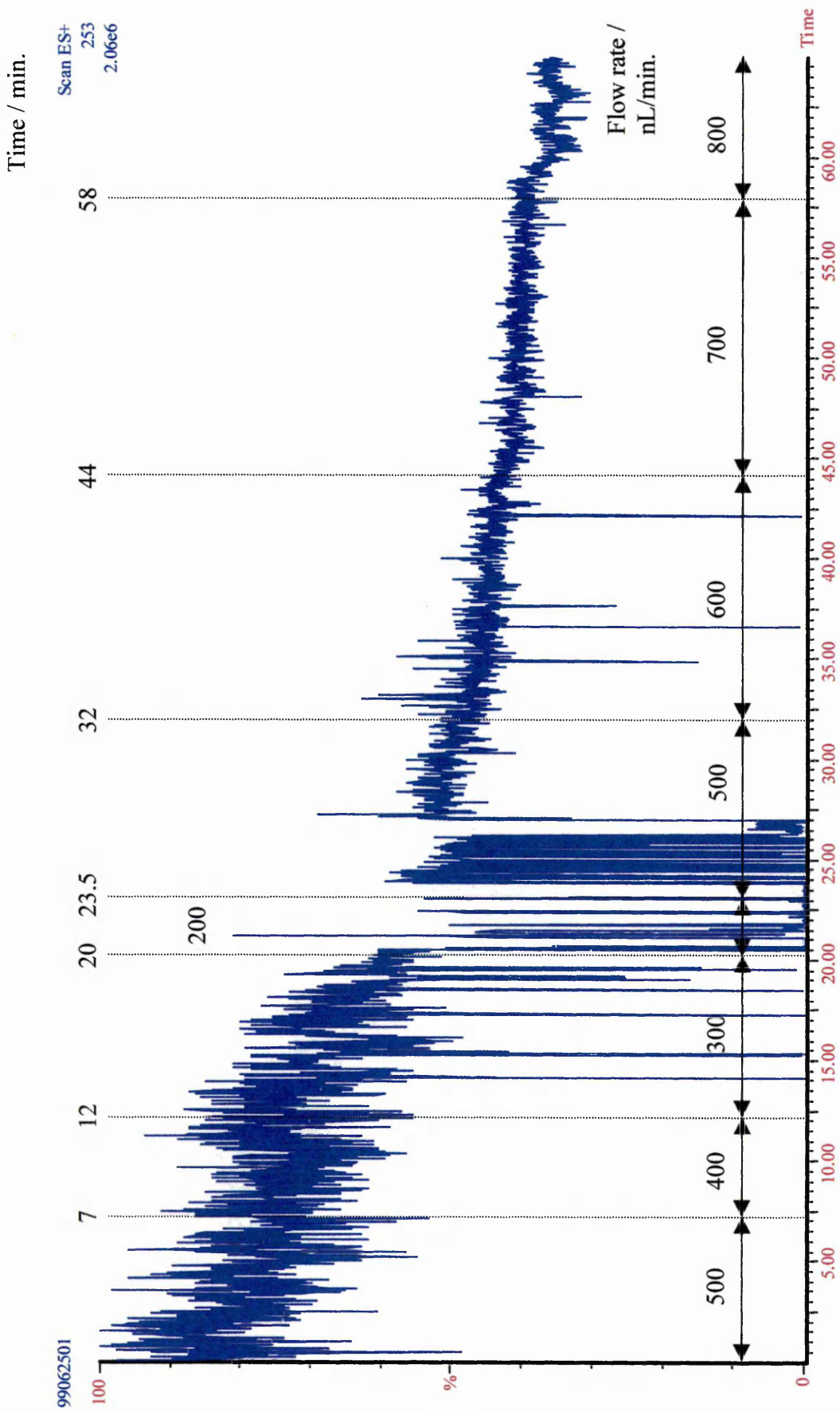


Figure 4.14 Spray Stability Dependence on Flow Rate – Hand Drawn, Au Coated Tip  
 (Time – minutes, flow rate – nL/min)

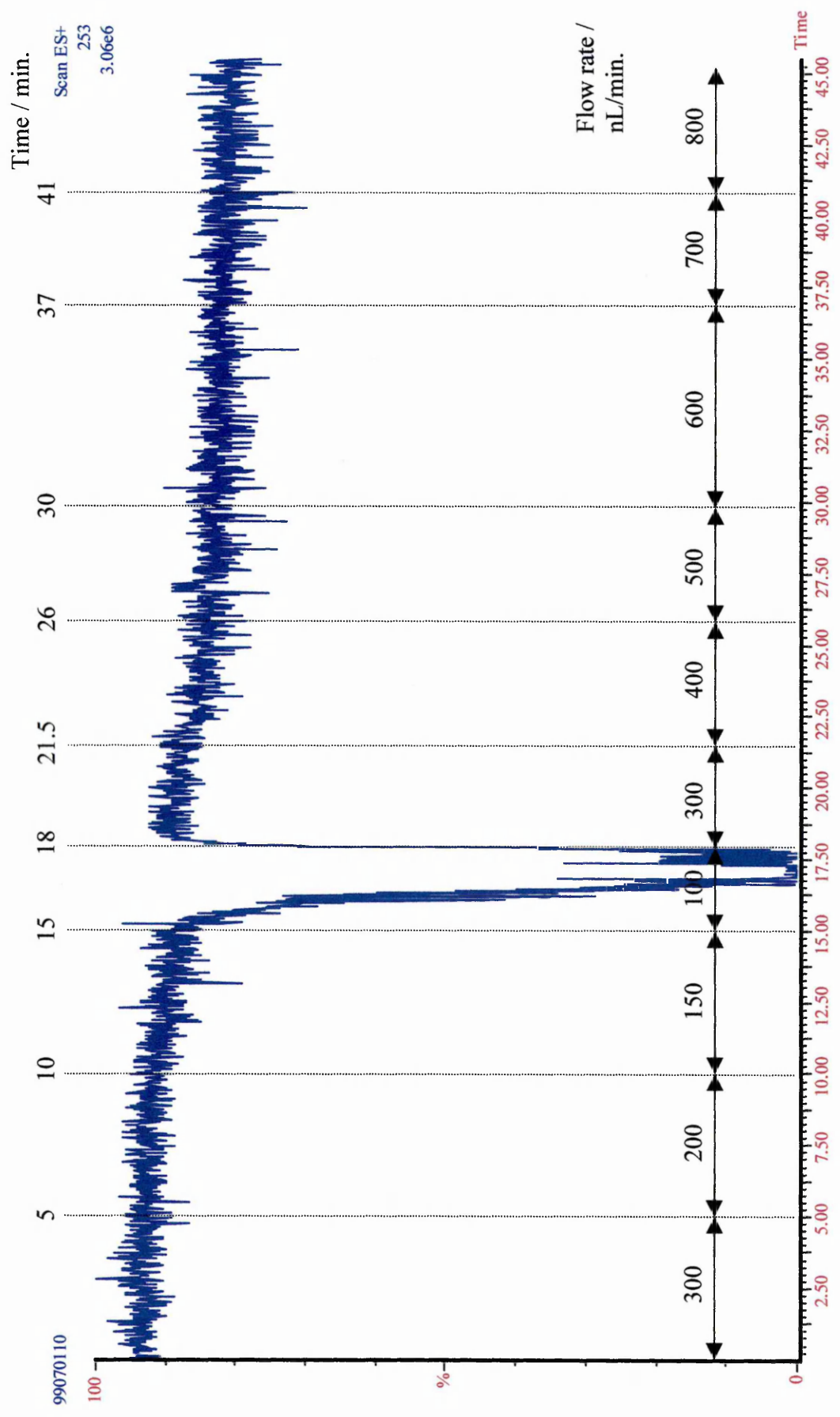


Figure 4.15 Spray Stability Dependence on Flow Rate – Au Drawn by Weight, Coated Tip  
(Time – minutes, flow rate – nL/min)

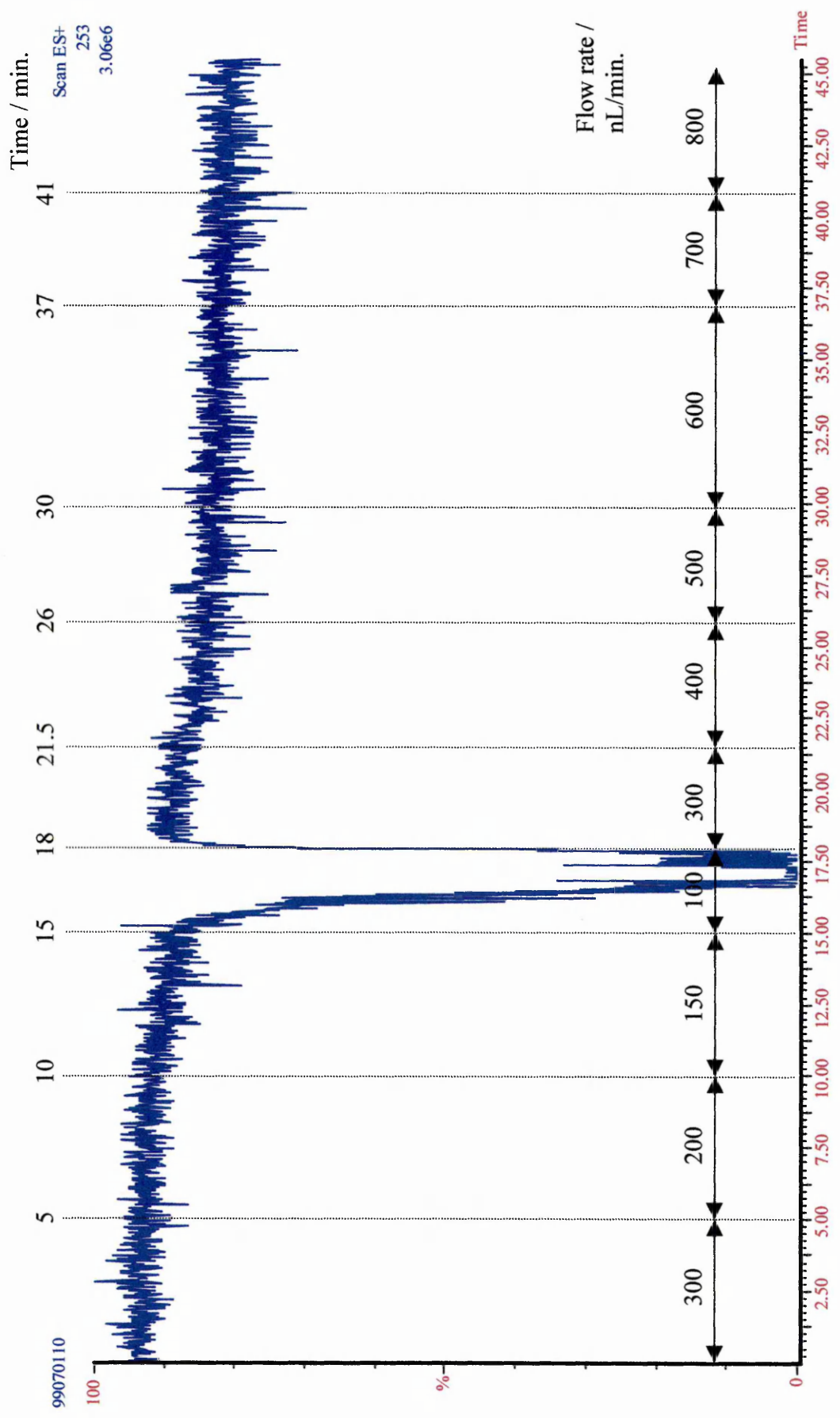


Figure 4.15 Spray Stability Dependence on Flow Rate – Au Drawn by Weight, Coated Tip  
(Time – minutes, flow rate – nL/min)

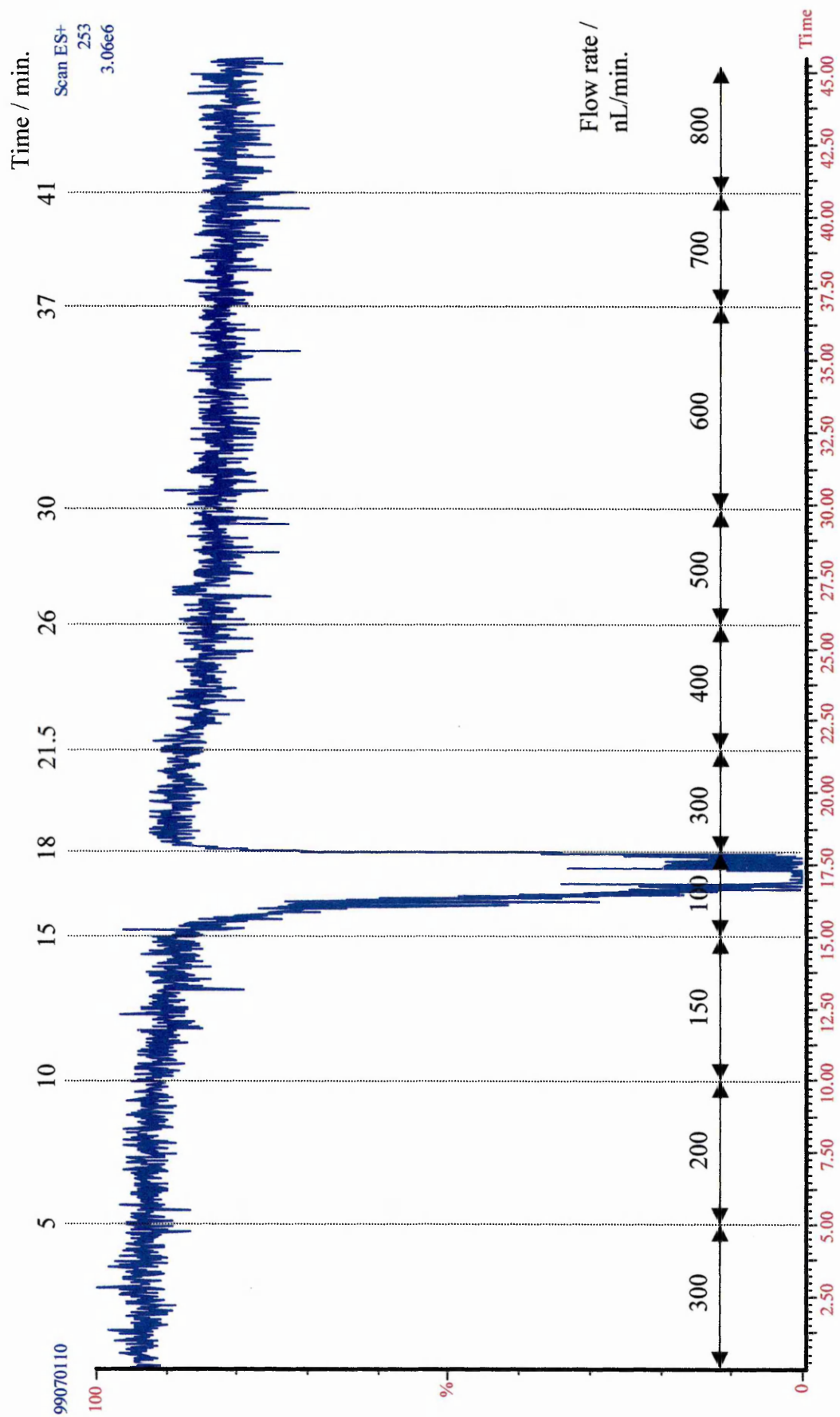


Figure 4.15 Spray Stability Dependence on Flow Rate – Au Drawn by Weight, Coated Tip  
(Time – minutes, flow rate – nL/min)

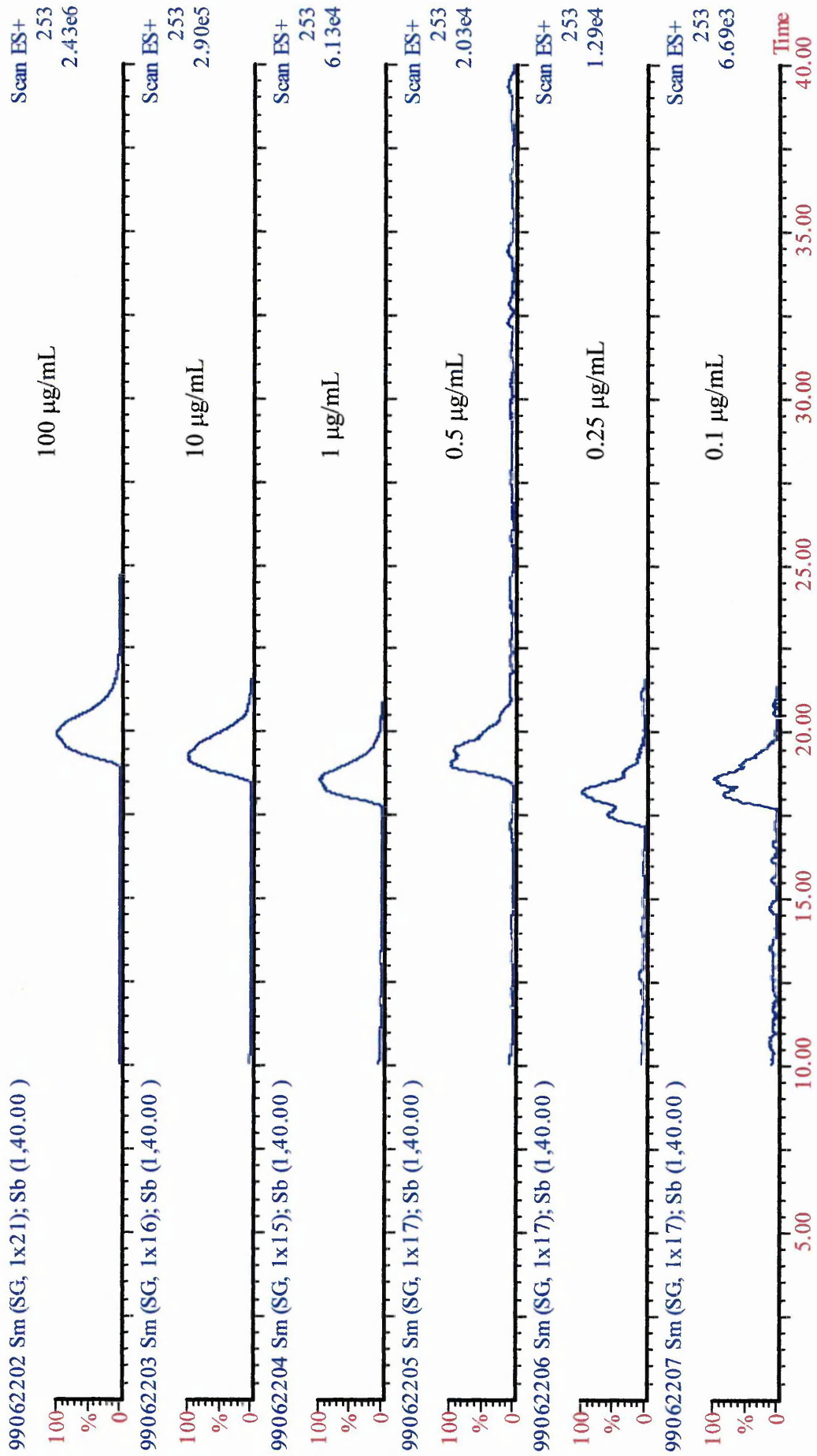


Figure 4.16 Serial Dilution of Cimetidine Employing Tip ①  
20 µm i.d. x 90 µm o.d. Fused Silica Nanospray Tip

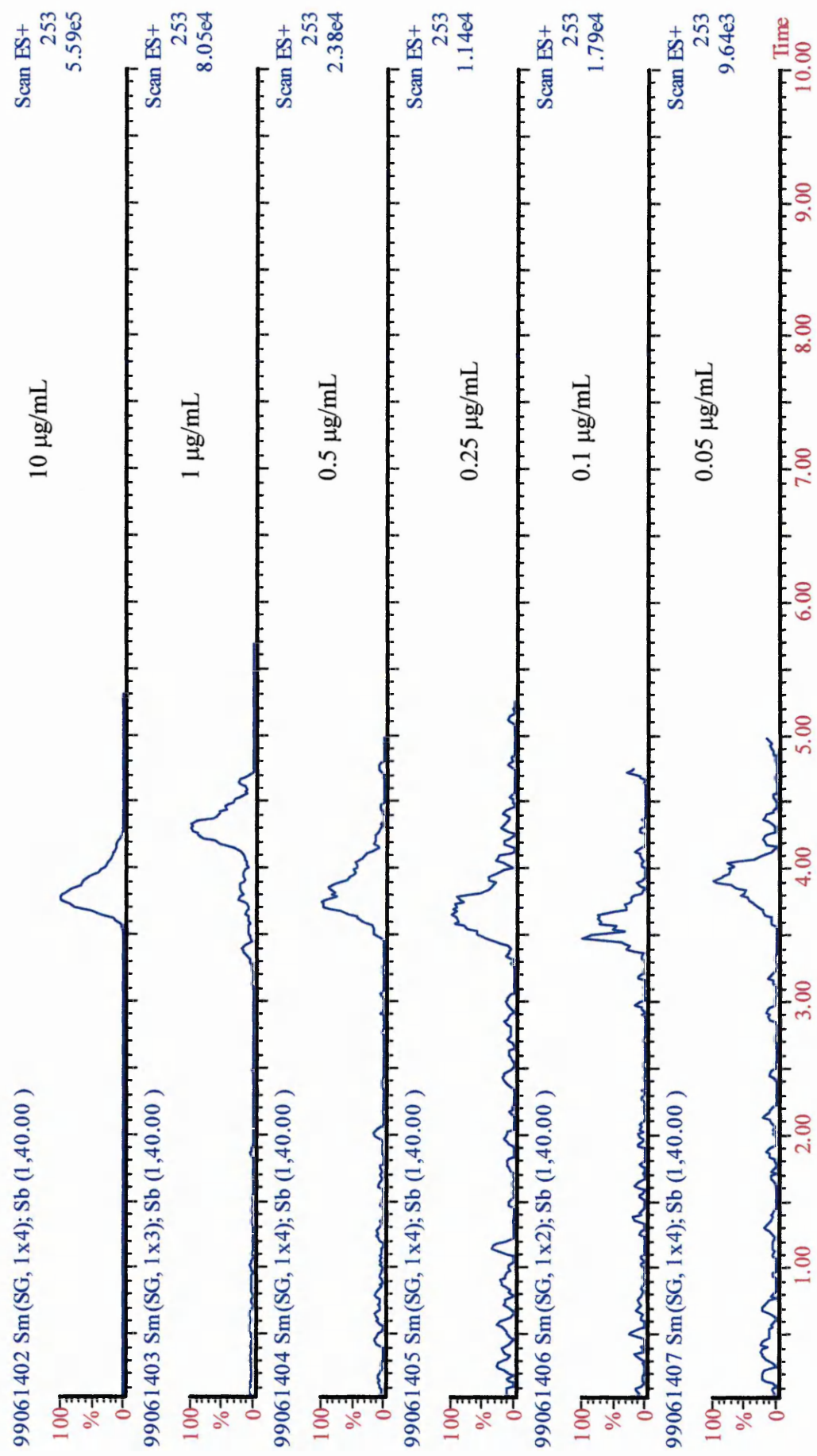


Figure 4.17 Serial Dilution of Cimetidine Employing Tip @  
50 µm i.d. x 150 µm o.d. Fused Silica Nanospray Tip

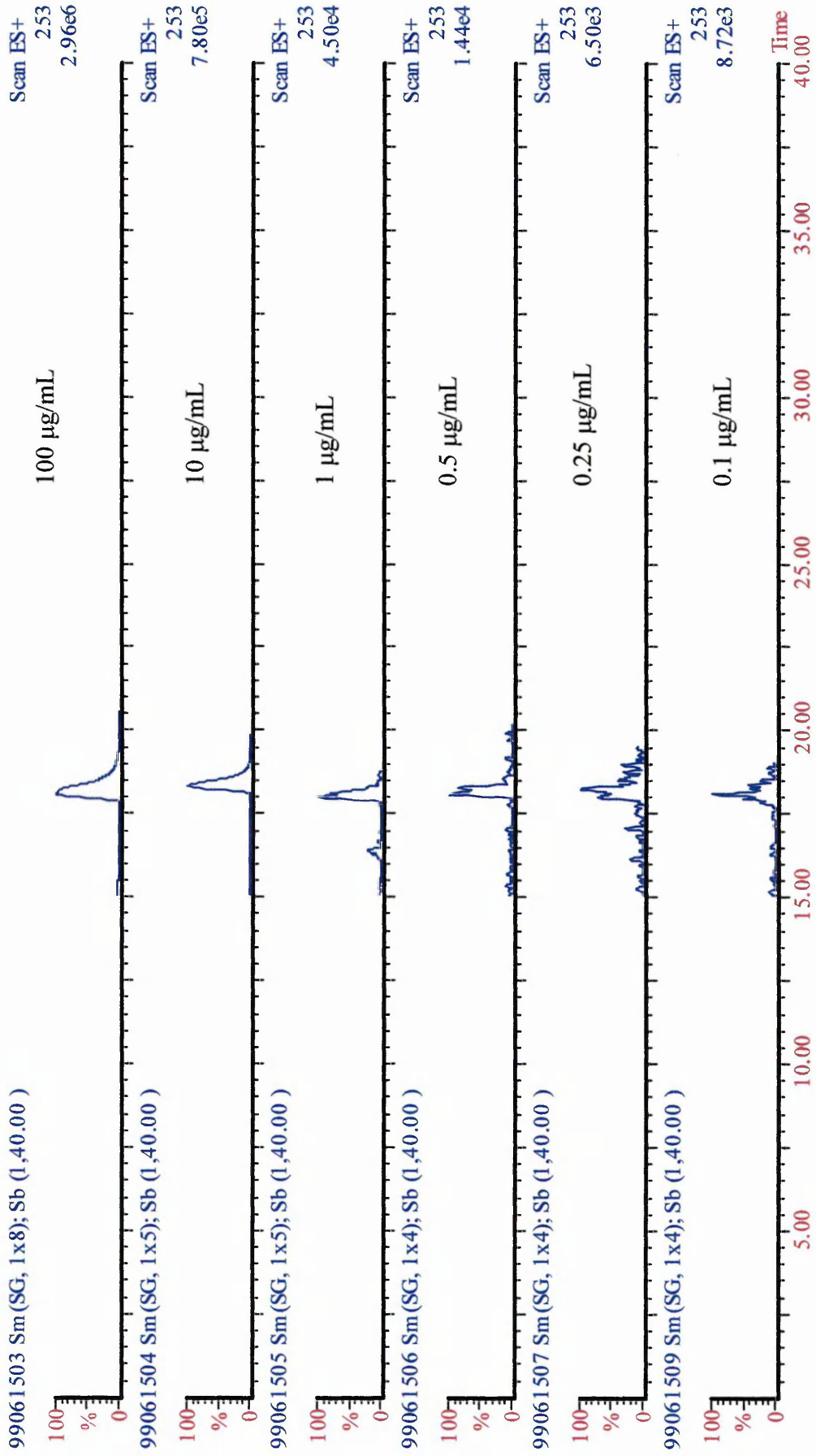


Figure 4.18 Serial Dilution of Cimetidine Employing Tip ④  
Method 2 Prepared Nanospray Tip

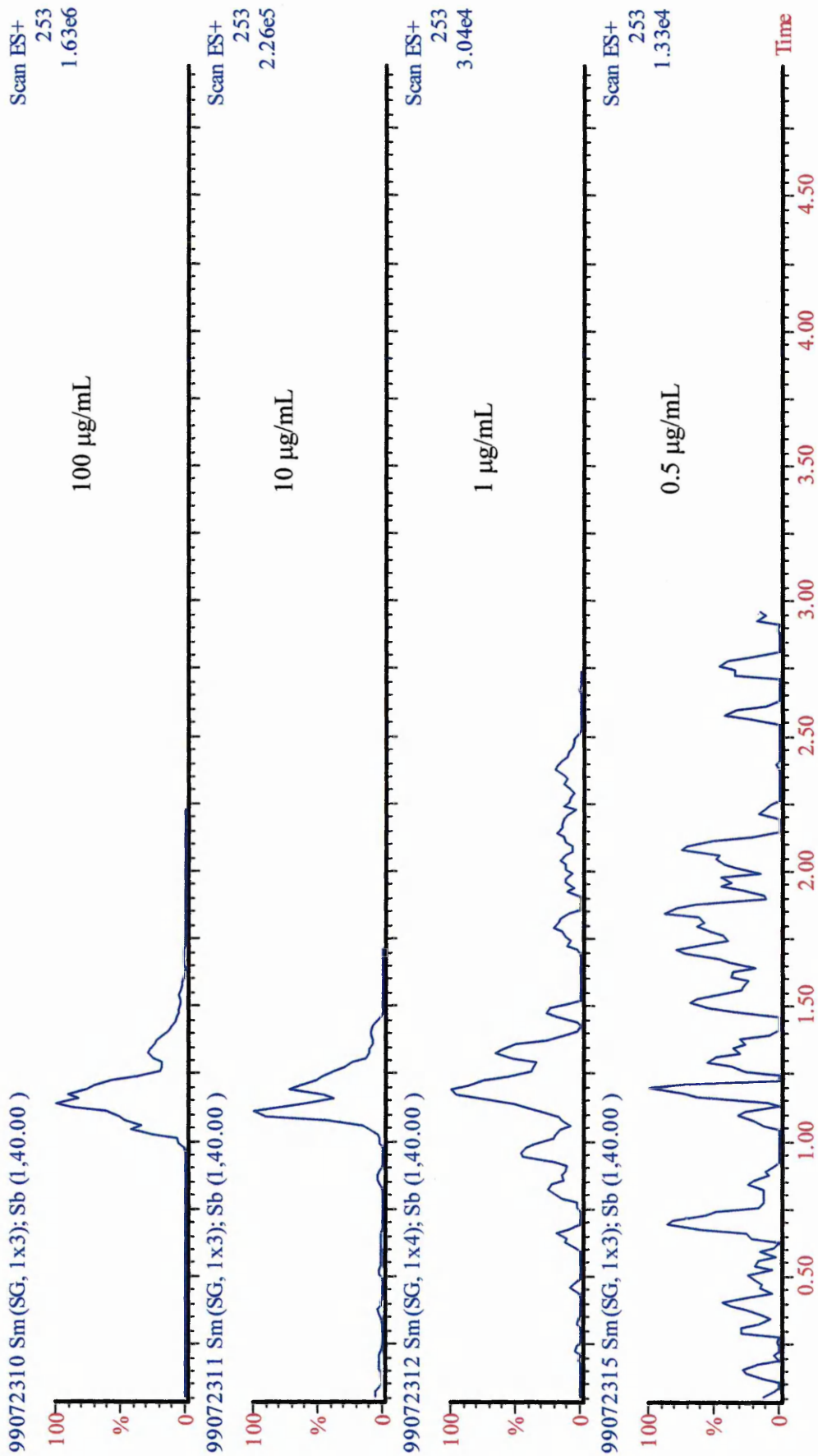


Figure 4.19 Serial Dilution of Cimetidine Employing Co-axial Sheath-flow Interface

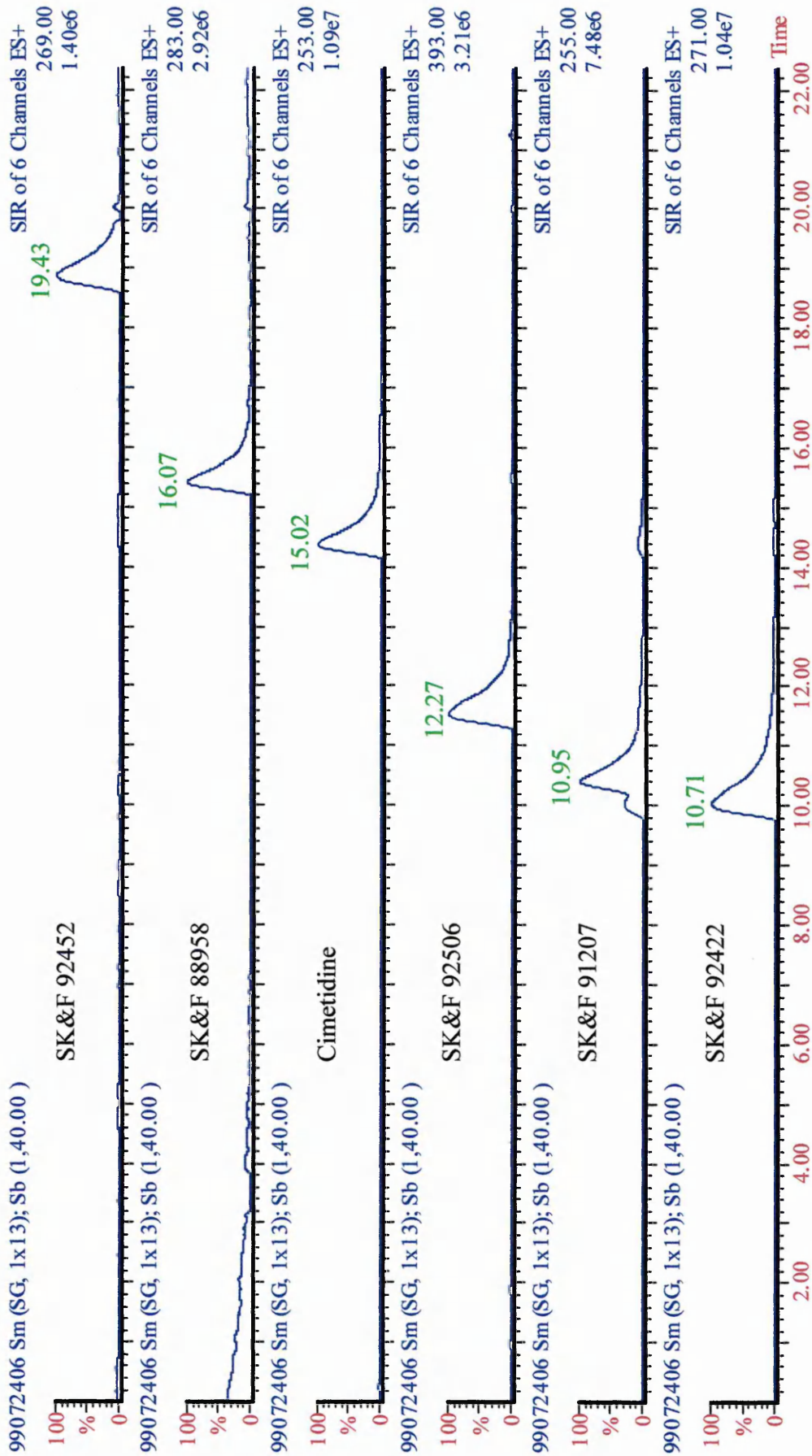


Figure 4.21 Nanospray CZE/MS SIR of 30 pg each Analyte (60 pg SK&F 92506)  
(Average Migration Times Given)

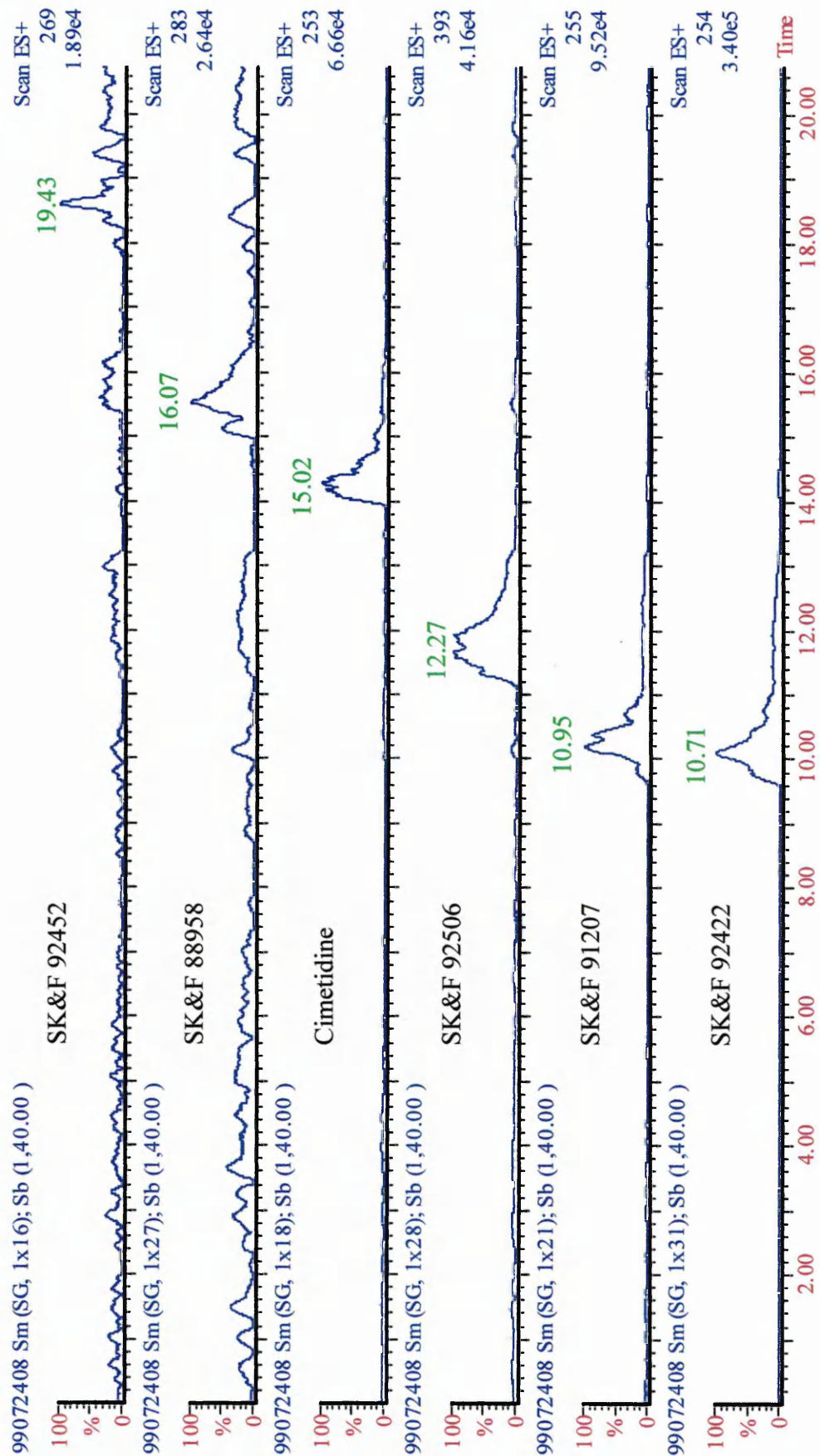


Figure 4.22 Nanospray CZE/MS Full Scan Data of 50 pg each Analyte (100 pg SK&F 92506) (Average Migration Times Given)

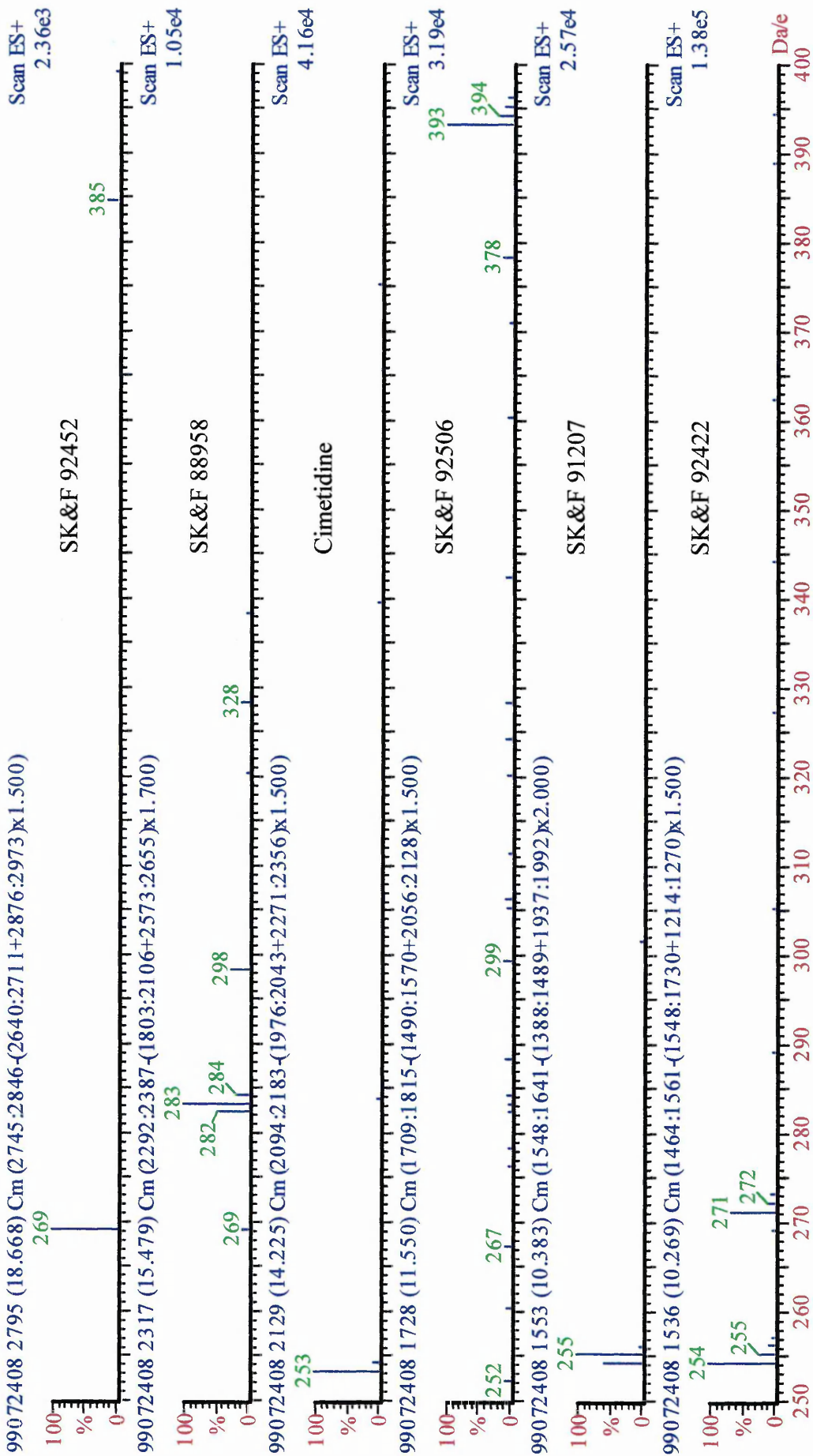


Figure 4.23 Nanospray CZE/MS Mass Spectra Featuring  $[M+H]^+$   
 $m/z$  correspond to SK&F 92422 – 271 ( $[M+H-NH_3]^+$  - 254) ; 91207 – 255; 92506 – 393;  
 Cimetidine – 253; 88958 – 283 and 92452 – 269

#### ***4.5 Overall Conclusions***

The separation of cimetidine and related impurities has been successfully transferred to CZE/MS employing a volatile buffer system.

The use of a co-axial sheath flow interface afforded a separation without any significant change in separation integrity compared to UV detection. Whereas, when a sheathless interface was employed the selectivity was altered, this could be attributed to the addition of organic solvent to the buffer (to aid the electrospray process).

An increase in migration times was observed for both interfaces, this could be directly linked to an increase in the column length (and hence a reduced electric field). In addition, decreases in peak efficiencies were observed for both interfaces, the co-axial sheath flow interface employs a longer capillary (*cf.* CZE/UV), which will increase zone dispersion. The increased zone dispersion in the nanospray interface could be attributed to the presence of dead volume within the union employed to link the separation and spray capillary.

Data was obtained for both full scan and selected ion recording modes, sensitivities were enhanced employing a sheathless interface. Only 50 pg of analyte was required to generate full scan data using the sheathless interface, compared to ~ 350 pg for the co-axial sheath flow system.

A reduction in the peak resolution (temporal separation) of SK&F 92452 and 88958 has been demonstrated to be less significant employing mass spectral detection rather than UV detection. This is because the mass discrimination power of the mass spectrometer allows separation by mass.

## References

---

- (1) Olivares JA; Nguyen NT; Yonker CR; Smith RD. *Analytical Chemistry* **59** (1987) 1232
- (2) Smith RD; Olivares JA; Nguyen NT; Udseth HR. *Analytical Chemistry* **60** (1988) 436
- (3) Smith RD; Barinaga CJ; Udseth HR. *Analytical Chemistry* **60** (1988) 1948
- (4) Loo JA; Udseth HR; Smith RD. *Analytical Biochemistry* **179** (1989) 404
- (5) Lord GA; Gordon DB; Myers P; King BW. *Journal of Chromatography A* **768** (1997) 9
- (6) Bateman KP; White RL; Thibault P. *Rapid Communications in Mass Spectrometry* **11** (1997) 307
- (7) Wahl JH; Gale DC; Smith RD. *Journal of Chromatography A* **659** (1994) 217
- (8) Barnidge DR; Nilsson S; Markides KE; Rapp H; Hjort K. *Rapid Communications in Mass Spectrometry* **13** (1999) 994
- (9) Valaskovic GA; McLafferty FW. *Journal of the American Society of Mass Spectrometry* **7** (1996) 1270
- (10) Kriger MS; Cook KD; Ramsey RS. *Analytical Chemistry* **67** (1995) 385
- (11) Goss CA; Charych DH; Majda M. *Analytical Chemistry* **63** (1991) 85
- (12) Lee ED; Mück W; Henion JD; Covey TR. *Biomedical and Environmental Mass Spectrometry* **18** (1989) 844
- (13) Jones RC; Ferro M; Summerfield SG; Gaskell SJ. *Journal of Mass Spectrometry* **33** (1998) 1261
- (14) Moseley MA; Jorgenson JW; Shabanowitz J; Hunt DF; Tomer KB. *Journal of the American Society of Mass Spectrometry* **3** (1992) 289
- (15) Banks JF. *Journal of Chromatography A* **712** (1995) 245
- (16) Herring CJ; Qin J. *Rapid Communications in Mass Spectrometry* **13** (1999) 1
- (17) Cooper PA. PhD Thesis, University of Manchester Institute of Science and Technology, 1996
- (18) Klots CE; Compton RN. *Journal of Chemical Physics* **69** (1978) 1644

## **Chapter 5**

*Accurate Mass Determination of Narrow Electrophoretic  
Peaks using an Orthogonal Acceleration Time-of-flight  
Mass Spectrometer*

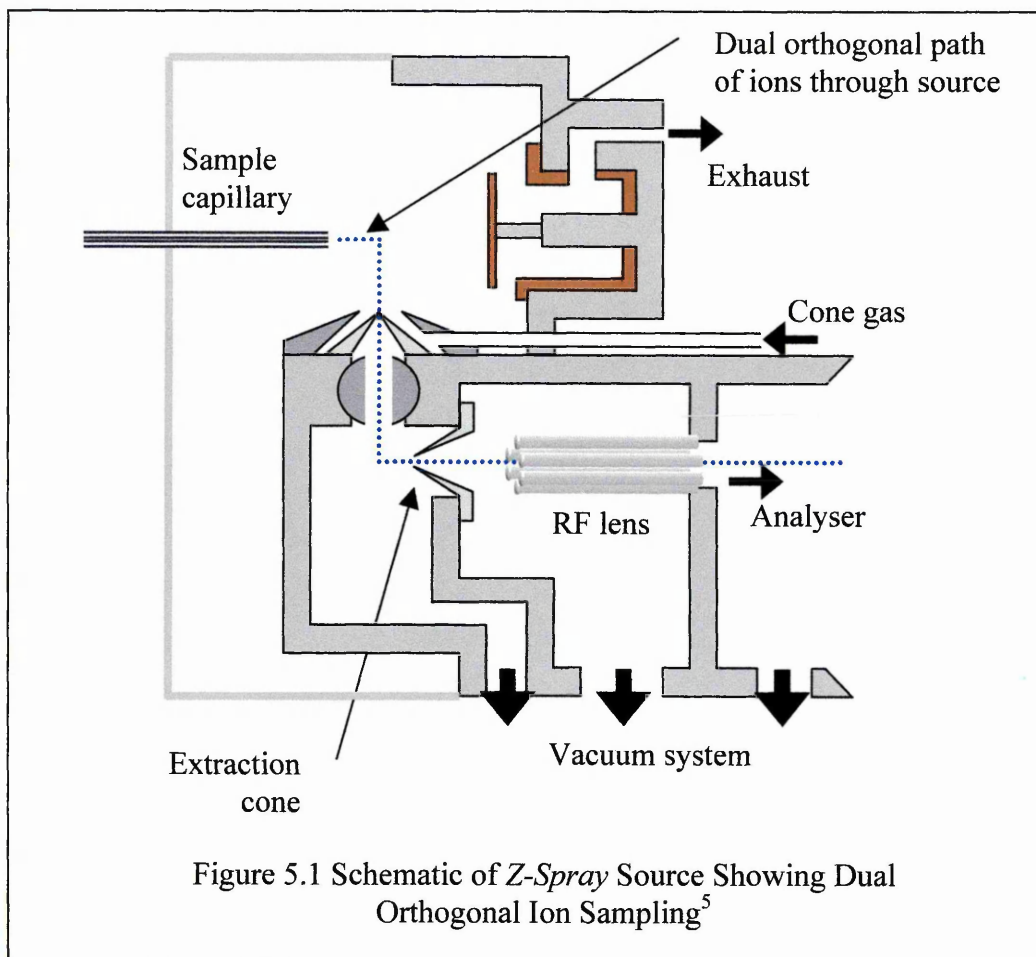
## 5.1 Introduction

Time-of-flight mass spectrometry (ToF MS) has recently enjoyed a resurgence of interest, mainly owing to the development of matrix assisted laser desorption / ionisation (MALDI) and the improvement of timing electronics. ToF MS has distinct advantages<sup>1</sup> over scanning instruments these include high duty factors (percentage of ions formed which are detected), (extremely) high acquisition rates, sensitivity and extensive mass range. Furthermore, the development of the ion mirror (reflectron)<sup>2</sup> and orthogonal acceleration<sup>3</sup> have increased the development and scope of ToF MS.

A reflectron corrects for positional and velocity discrepancies in the acceleration region of the instrument and removes neutral species, which may have resulted from in-flight decay. As a result of the reflectron, resolution in excess of 5000 (full width, half maxima, FWHM, *i.e.*  $m/\Delta m_{1/2}$ ) is now readily available. The development of orthogonal acceleration allows continuous ion sources (*e.g.* electrospray) to be coupled to time-of-flight mass spectrometers (oa-ToF MS). For more detail on oa-ToF MS, orthogonal acceleration and reflectrons see Chapter 1, Section 1.2.2.5b pt. ii.

oa-ToF MS seems ideally suited for coupling with high efficiency separation techniques, such as capillary zone electrophoresis. The EOF generated in CZE results in extremely efficient separations ( $> 1 \times 10^5$  plates / metre are common) and consequently peak widths of a few seconds, requiring very fast mass spectral acquisition rates and high sensitivities (usually  $10^{-9} - 10^{-12}$  g quantities injected in column). Scanning instruments are not able to obtain sufficient data points across such a peak resulting in peak skew, where the mass spectral data does not accurately represent the sample composition at any one time. Therefore the fast acquisition rates and sensitivities of oa-ToF MS make it ideal for CZE/MS.

The use of a Micromass *Z-spray*<sup>4</sup> source allows the use of involatile buffers without significant background interference and source contamination, due to its dual orthogonal sampling (Figure 5.1<sup>5</sup>).



The majority of involatile buffer and neutral species end up coating the source baffle, whereas analyte ions are sampled through the skimmer, where further desolvation occurs, analyte ions are then sampled through an extraction cone into the mass analyser.

## 5.2 Experimental

### 5.2.1 CZE Separation

A PrinCE Model 450 CE System (PrinCE Technologies, Emmen The Netherlands) was used throughout this study. The buffer comprised 10 mM sodium dihydrogen phosphate adjusted to pH 3.1 (using 0.1 M HCl). The column was washed between analyses with 0.1 M NaOH (1 bar, 30 s), Water (1 bar, 60 s) and buffer (1 bar, 120 s).

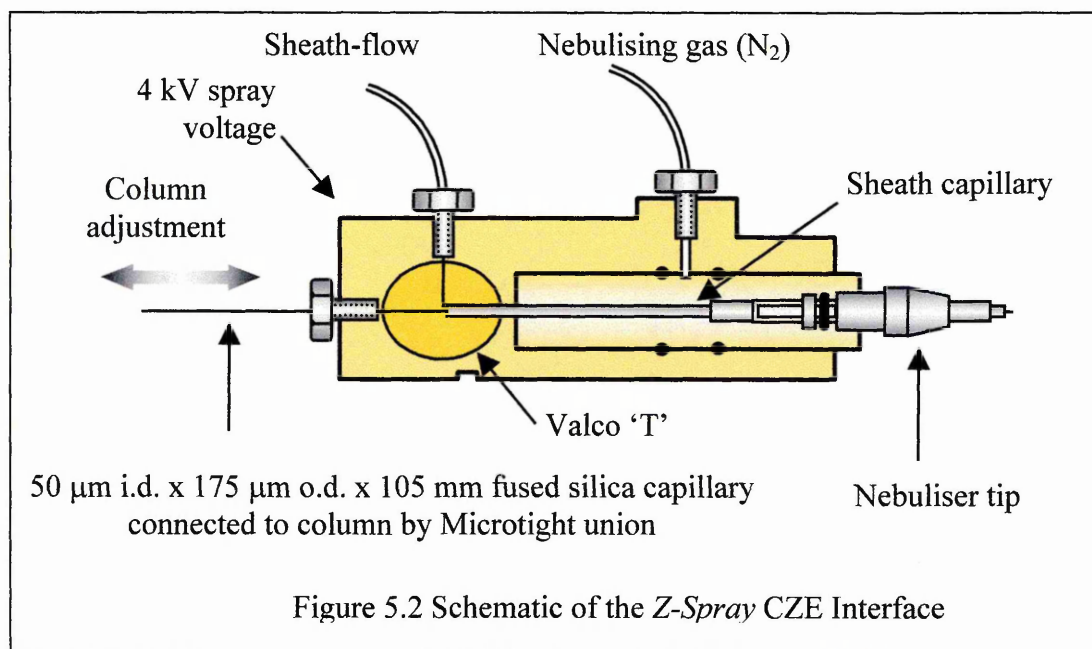
Separations were performed using an un-coated fused silica capillary (Composite Metal Services Ltd. Hallow, UK) of 50  $\mu\text{m}$  i.d. x 365  $\mu\text{m}$  o.d. and 60 cm in length. The

separation capillary was coupled to a 50  $\mu\text{m}$  i.d. x 175  $\mu\text{m}$  o.d. x 105 mm fused silica spray capillary by a Microtight junction.

Samples were injected hydrodynamically (1 bar, 0.05 min) with an injection volume corresponding to 65 nL. Separations were achieved with a field strength 370  $\text{Vcm}^{-1}$  (30 kV), with + 4.0 kV applied to the outlet (cathode) to generate electrospray.

### 5.2.2 Mass Spectrometry

An LCT oa-ToF MS (Micromass, Manchester UK), a reflectron time-of-flight mass analyser (effective path length of 1.2 m), was used. Positively charged ions were formed using a *Z-Spray*<sup>4</sup> co-axial sheath-flow CZE interface (Figure 5.2) operating in electrospray mode.



The ion source was operated with a probe voltage of 4.0 kV and a cone voltage of 25 V. The orthogonal sampling was operated at a frequency of 20 kHz. Mass data were acquired at a rate of 2 spectra / second over the  $m/z$  range 200 – 800. Instrument resolution was measured as 5600 (FWHM), using the sodiated molecule of cimetidine ( $[\text{M}+\text{Na}]^+$ ,  $m/z$  275). An instrument base mass calibration was generated using the ammoniated ions of a polyethylene glycol mixture. Any subsequent mass drift was corrected for using a single-point lock mass, on a per spectrum basis.

A make-up sheath-flow was used to aid the electrospray process, consisting of 0.5 µg/mL erythromycin (Sigma, Poole UK) in 1:1 MeCN : H<sub>2</sub>O at a flow rate of 2 µL/min. Nitrogen (5 psi) was used to assist electrospray nebulisation and desolvation.

The sodiated molecule of erythromycin (*m/z* 756.4510) provided the lock mass for exact mass measurement. Exact masses were measured using the mean of three consecutive scans from an electrophoretic peak following 'lock mass' correction.

### 5.2.3 Chemicals and Reagents

SmithKline Beecham Pharmaceuticals supplied cimetidine and impurities (Table 3.1, Chapter 3), 1000 µg/mL stock solutions were diluted with water to suitable concentrations. Sample concentrations were

1 µg/mL for cimetidine, SK&F 91207, 92422 and 88958;

2 µg/mL for SK&F 92452 and

4 µg/mL for SK&F 92506.

All solvents and reagents used were of reagent grade or better.

### 5.3 Results / Discussion

The CZE/UV separation developed in Chapter 3 was employed in this investigation\*, a typical UV electropherogram is shown in Figure 5.3. The total ion electropherogram (TIE) based on base peak intensities is shown in Figure 5.4. The presence of peaks of high signal-to-noise ratio in the TIE would allow CZE/oa-ToF to be a suitable separation / detection technique for the analysis of unknowns. Similar signal intensities have been obtained on a quadrupole instrument, but data acquisition was performed in selected ion recording mode, where prior knowledge of the sample is essential. The reconstructed ion electropherograms corresponding to the analytes are shown in Figure 5.5. The MS data are consistent with the separation obtained by CZE/UV. All of the analytes are well resolved, with the exception of SK&F 92452 and 88958, where

---

\* The CZE/UV buffer comprised 10 mM sodium dihydrogen phosphate adjusted to pH 3.1 (0.1 M HCl). Separations were performed with a field strength of 350 Vcm<sup>-1</sup> on an 85 cm column with detection at 230 nm at an effective length of 53 cm. For more information see Chapter 3.

$R = 0.38$  ( $R = 0.9$  for CZE/UV separation), however, the peaks could be resolved by mass discrimination.

Peak widths are between 6 and 10 seconds (at baseline) these values are consistent with those obtained by CZE/UV (4 – 10 seconds). Therefore, by employing oa-ToF between 12 and 20 spectra were obtained for each peak, allowing sufficient data points to be acquired for it to be accurately represented.

The mass spectra (shown in Figures 5.6 to 5.10) of the peaks contain sodiated molecules,  $[M+Na]^+$ , of very high S/N ratio. Sodiated species were observed rather than protonated molecules because of the high concentration of sodium in the separation buffer (*i.e.* sodium dihydrogen phosphate). This was in contrast with previous work employing a quadrupole mass spectrometer<sup>6</sup>, where protonated molecules were obtained, owing to an acidic sheath-flow (0.1 % formic acid) being employed. The protons provided by the acid successfully displaced any sodium ions associated with the analyte molecules. The spectra are clean featuring the ion of interest only. The isotope pattern of cimetidine (Figure 5.12a) demonstrates the elevated resolution obtained using oa-ToF MS, the theoretical isotope pattern of cimetidine (Figure 5.12b) being in close agreement with that obtained experimentally.

### 5.3.1 Migration Time Reproducibility

Replicate injections were performed to assess the reproducibility of migration times ( $t_m$ ). The  $t_m$  values observed (Table 5.1) are similar to those obtained by CZE/UV, although a longer apparent column length (*i.e.* distance from inlet to detector) was employed. This could be attributed to an induced laminar flow within the CZE/oa-ToF MS separation due to the electrospray process. Care was taken to minimise any additional laminar flow (*i.e.* inlet vial at the same level as the spray tip).

The reproducibility was reduced for CZE/oa-ToF MS; this could be attributed to manual start of data acquisition. A contact closure start signal would reduce this contribution. In addition, discrepancies in the spray could cause variations in the EOF and hence

reproducibility. However, the generation of exact mass data replaces the need for high reproducibility, as the predicted molecular formula can confirm the identity of analytes.

Table 5.1 Migration Time Data

	CZE/oa-ToF MS (n=6)		CZE/UV (n=5)	
	Migration Time / min	% RSD	Migration Time / min	% RSD
SK&F 91207	5.333	1.94	4.894	0.246
SK&F 92422	5.553	1.73	5.208	0.231
SK&F 92506	6.033	1.72	5.887	0.195
Cimetidine	7.243	1.59	7.829	0.139
SK&F 92452	7.422	1.63	8.128	0.172
SK&F 88958	7.497	1.53	8.275	0.152

### 5.3.2 Peak Efficiency

The peak efficiency is a measure of the extent of zone dispersion within a column. The higher the efficiency the narrower and sharper the peak shape. The peak efficiencies expressed as the number of theoretical plates (Table 5.2) can be calculated using Equation 5.1.

$$N = 16 \left( \frac{t_m}{w_b} \right)^2 \quad \dots(5.1)$$

$w_b$  = Peak width at base

Table 5.2 Peak Efficiencies

	Number of Theoretical Peaks (plates per m)	
	CZE/oa-ToF MS	CZE/UV
SK&F 91207	47 000	210 000
SK&F 92422	36 000	190 000
SK&F 92506	24 000	160 000
Cimetidine	33 000	140 000
SK&F 92452	32 000	130 000
SK&F 88958	35 000	110 000

Peak efficiencies are significantly decreased compared to CZE/UV. This is mainly due to the larger injection volume employed<sup>†</sup>, approximately 65 nL for CZE/oa-ToF MS and 3.8 nL for CZE/UV. An increased injection volume will reduce separation efficiency due to the increased analyte zone length and a proportionately higher degree of dispersion; in addition, the presence of a small dead-volume within the capillary junction would reduce efficiency. Optimisation of sample loading (*i.e.* fixing the pressure regulation unit of the CZE) and reduction in the dead-volume of the union would serve to lessen these effects. Alternatively the union could be removed and narrow o.d. capillary could be employed for separations, which would pass directly through the interface to the tip, thus resulting in no dead volume.

### 5.3.3 Exact Mass Data

The exact mass was assigned by the use of an internal lock mass (in this case sodiated erythromycin,  $m/z$  756.4510, present in the sheath liquid). Exact masses were measured for three consecutive scans from an electrophoretic peak and the mean calculated. Five replicated sample injections were performed resulting in a total of 15 measurements. These data are presented in Table 5.3.

Table 5.3 Exact Mass Data

	Formula of [M+Na] <sup>+</sup>	Calculated mass	Experimental mass	$\sigma$ n = 15	mmu <sup>‡</sup> error	ppm <sup>§</sup> error
91207	C <sub>10</sub> H <sub>14</sub> N <sub>4</sub> S <sub>2</sub> Na	277.0558	277.0579	±0.0012	2.1	7.4
92422	C <sub>10</sub> H <sub>18</sub> N <sub>6</sub> OSNa	293.1161	293.1167	±0.0016	0.6	1.9
92506	C <sub>16</sub> H <sub>24</sub> N <sub>8</sub> S <sub>2</sub> Na	415.1463	415.1491	±0.0015	2.8	6.8
Cimetidine	C <sub>10</sub> H <sub>16</sub> N <sub>6</sub> SNa	275.1055	275.1071	±0.0007	1.6	5.6
92452	C <sub>10</sub> H <sub>16</sub> N <sub>6</sub> OSNa	291.1004	291.1013	±0.0010	0.9	3.2
88958	C <sub>11</sub> H <sub>18</sub> N <sub>6</sub> OSNa	305.1161	305.1176	±0.0009	1.5	5.0

<sup>†</sup> An increased injection volume was employed for the CZE/oa-ToF MS analysis because of pressure stability problems within the CZE instrumentation.

<sup>‡</sup> Milli-mass unit

<sup>§</sup> Parts per million

All measured values are accurate to less than 8 ppm, which would allow prediction / confirmation of empirical formulae.

The standard deviation for these measurements shows good precision. A possible systematic error (all deviations from calculated mass are positive) may have been introduced as a result of non-linearity in the base calibration file.

#### 5.3.4 Preliminary Investigation of Quantification

The potential of using the LCT for CZE/oa-ToF MS quantification was investigated. A serial dilution was performed and the response factors calculated for the concentration ranges 50 – 1 ng/ $\mu$ L for cimetidine, SK&F 91207, 92422 and 88958; 100 – 2 ng/ $\mu$ L for SK&F 92452 and 200 – 4 ng/ $\mu$ L for SK&F 92506, injections were performed in triplicate (*i.e.*  $n = 3$ ). The quantification software supplied with the instrument was used to calculate the calibration curves. Cimetidine was used as an internal standard to correct for any variation in injection volume and spray efficiency. The calibration curves were linear across the concentration ranges used, with  $r^2$  values of  $\sim 0.99$ . The calibration curve obtained for SK&F 91207 is shown in Figure 5.13. A true blank was not included in this data; hence the curve does not intercept the origin at zero.

The dilution series resulted in a detection limit of 0.5 ng/ $\mu$ L for cimetidine, at a signal-to-noise ratio of  $\sim 5:1$ , which corresponds to  $\sim 35$  pg injected in-column. It may be possible to improve this limit, through variation of experimental parameters. A reduction in the flow rate and acidification of the sheath-flow would reduce dilution and enhance ionisation efficiency of the analyte. In addition, at lower analyte concentrations increasing the scan rate (*i.e.* reducing the number of pulses summed to form a spectrum) would allow enhanced sensitivity, due to an increased duty cycle.

Although similar levels of sensitivity may be obtained on a scanning instrument using selected ion recording, previous knowledge of the sample is required. Furthermore, the full scan data acquired would allow evidence of potential interferences to be obtained. Additional selectivity is provided by the enhanced resolution available to the oa-ToF instrument.

DAX 6.0: Martin Palmer 15/08/99 16:02:56PM

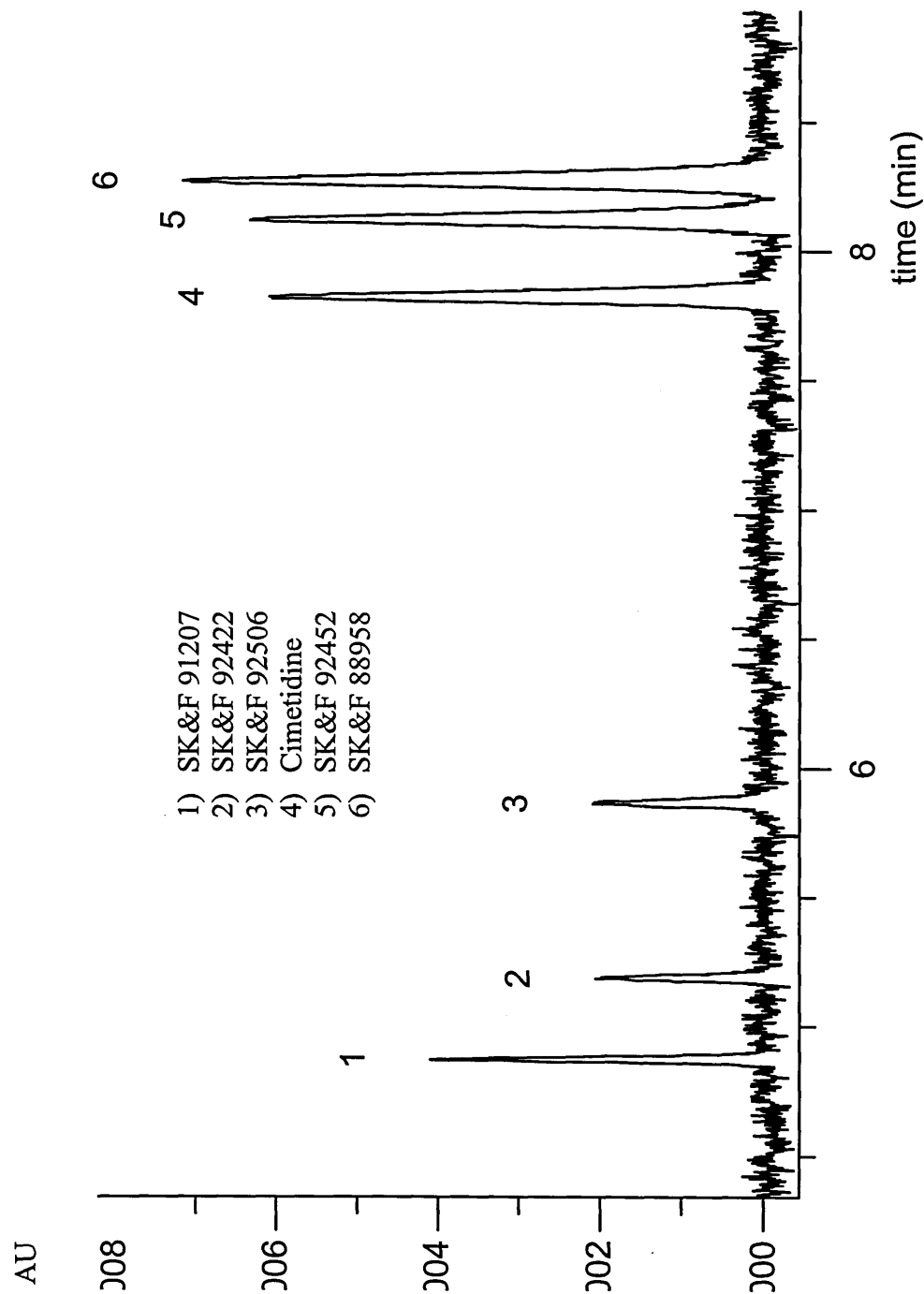


Figure 5.3 10 mM Sodium Dihydrogenphosphate pH 3.1, 30 kV,  $\lambda_{max} = 230$  nm, 10 mbar / 0.07 min Injection of 10  $\mu$ g/mL Cimetidine and Related Impurities

6 component mix (1 bar / 0.05 min) phos n/w  
CEMET30A Sm (Mn, 1x1)

TOF MS I

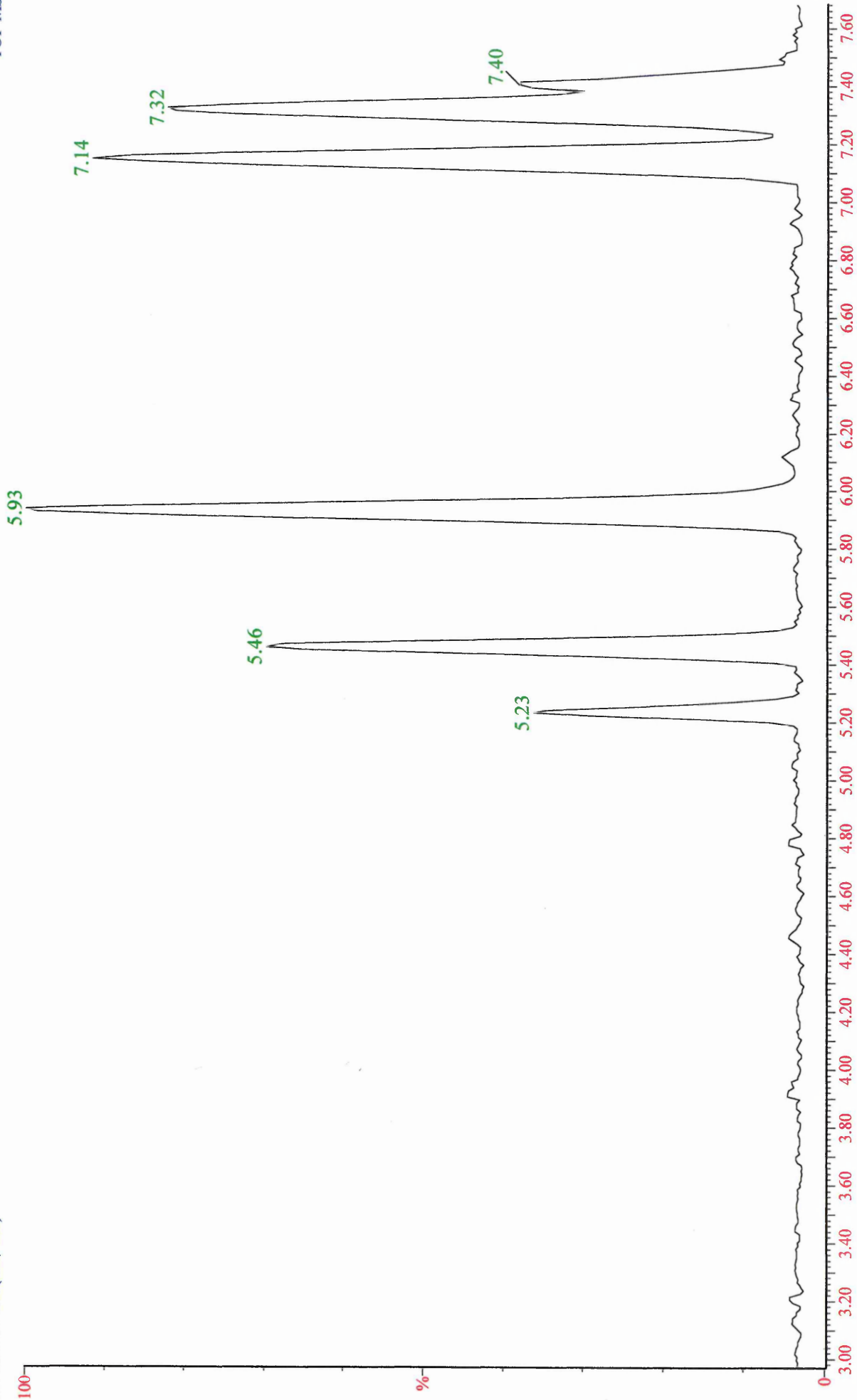


Figure 5.4 Total Ion Electropherogram of the Separation of Cimetidine and Related Impurities

**6 component mix (1 bar / 0.05 min) phos n/w**

CEMET30A Sm (Mn, 1x1)

TOF MS I  
305.248\_305



SK&F 88958

CEMET30A Sm (Mn, 1x1)

TOF MS I  
291.223\_291



SK&F 92452

CEMET30A Sm (Mn, 1x1)

TOF MS I  
275.229\_275



Cimetidine

CEMET30A Sm (Mn, 1x1)

TOF MS I  
415.322\_415



SK&F 92506

CEMET30A Sm (Mn, 1x1)

TOF MS I  
293.236\_293



SK&F 92422

CEMET30A Sm (Mn, 1x1)

TOF MS I  
277.178\_277



SK&F 91207

Figure 5.5 Reconstructed Mass Electropherograms of Cimetidine and Related Impurities

CEMET30A 505 (5.241) Cm (500:509-(483:495+518:536))

TOF MS ES+  
478

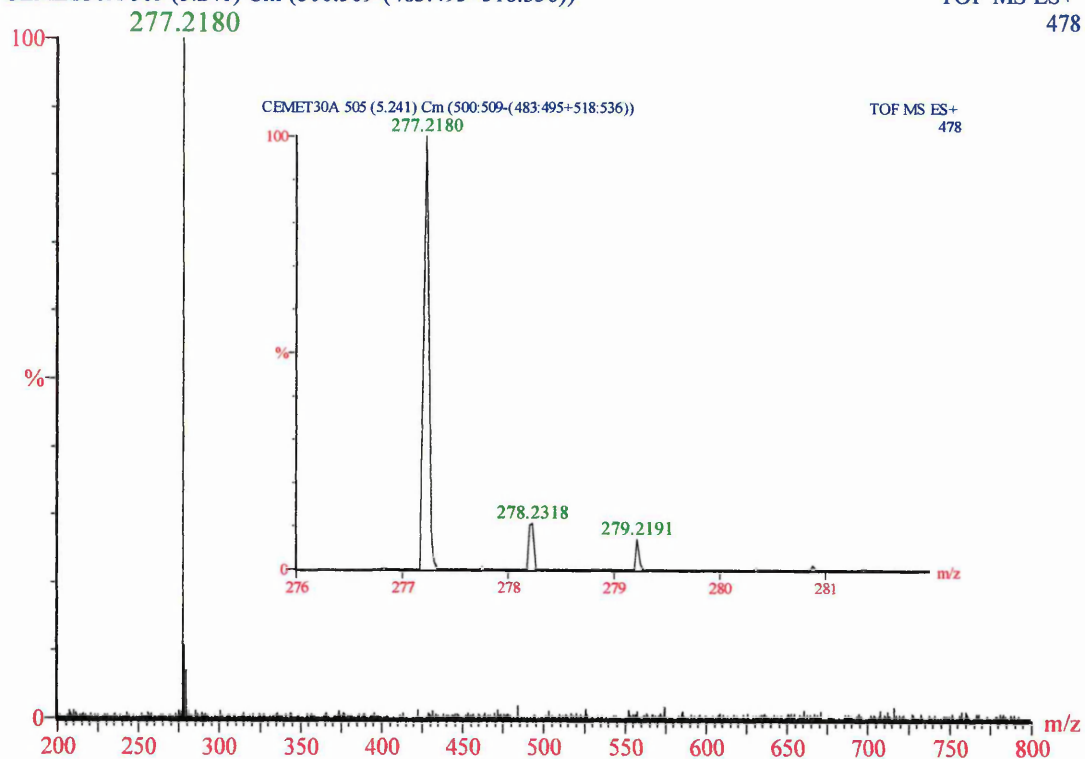


Figure 5.6 Mass Spectrum of SK&F 91207,  
[M+Na]<sup>+</sup> m/z 277

CEMET30A 522 (5.417) Cm (521:531-(542:551+507:516))

TOF MS ES+  
1.17e3

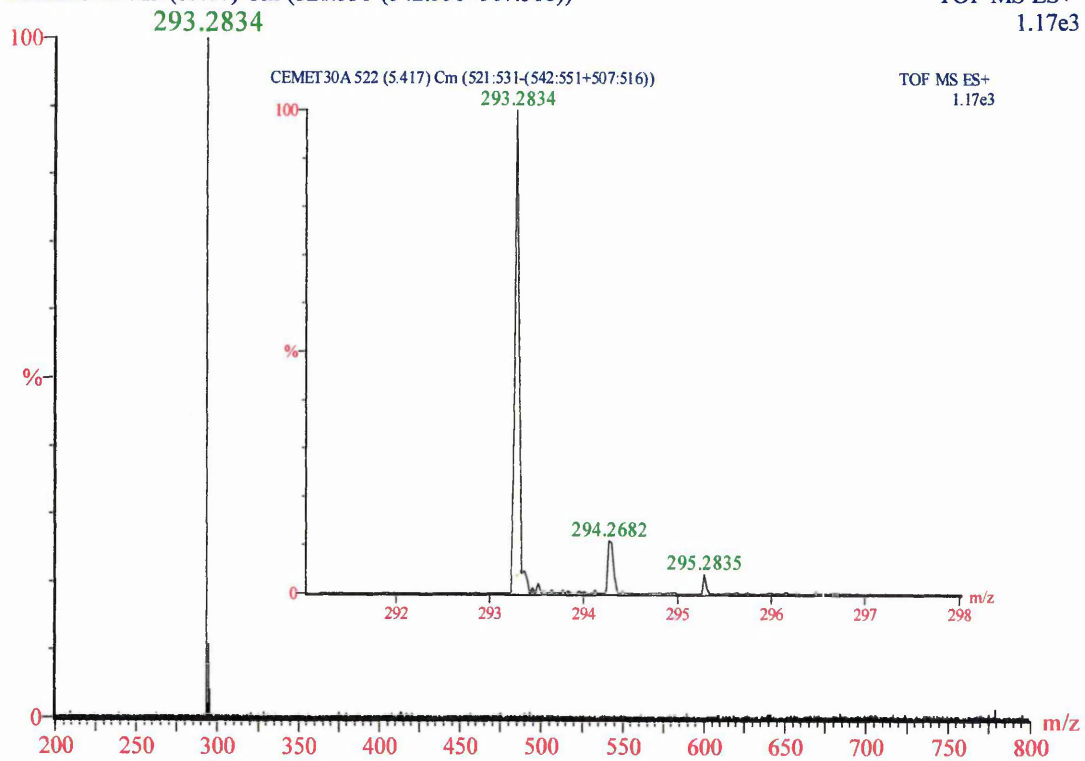


Figure 5.7 Mass Spectrum of SK&F 92422,  
[M+Na]<sup>+</sup> m/z 293

CEMET30A 573 (5.945) Cm (566:578-(551:560+583:591))

TOF MS ES+  
2.00e3

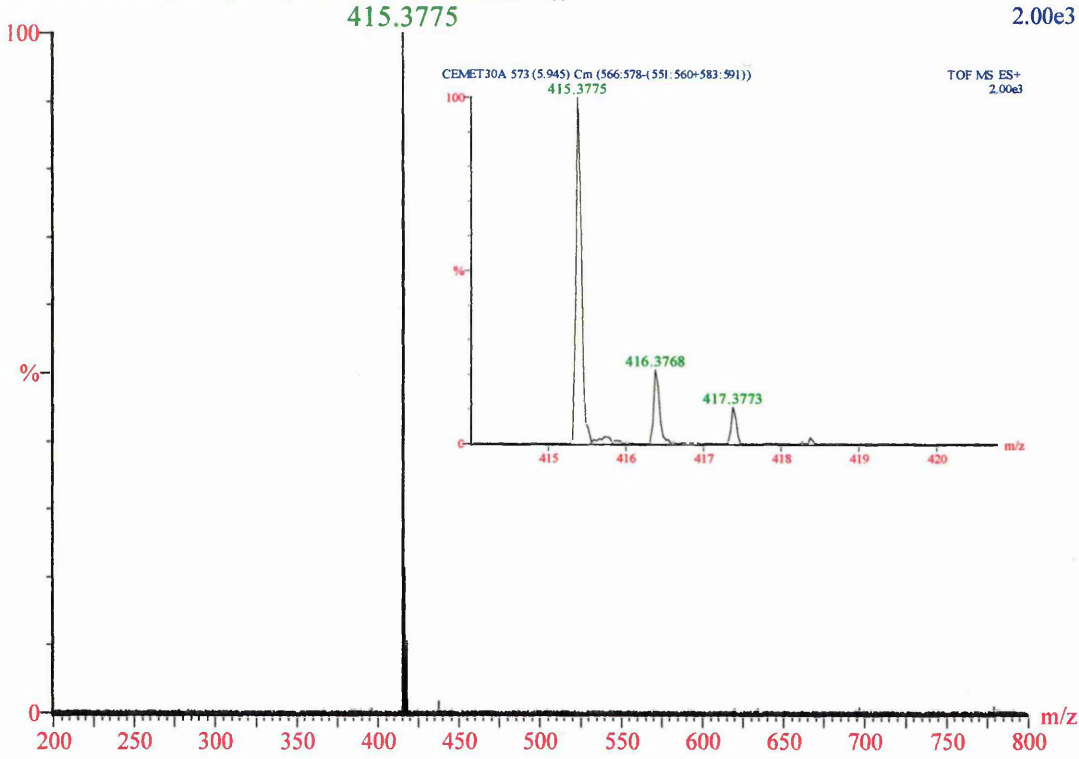


Figure 5.8 Mass Spectrum of SK&F 92506,  
 $[M+Na]^+$  m/z 415

CEMET30A 689 (7.144) Cm (684:695-(698:722+656:679))

TOF MS ES+  
1.88e3

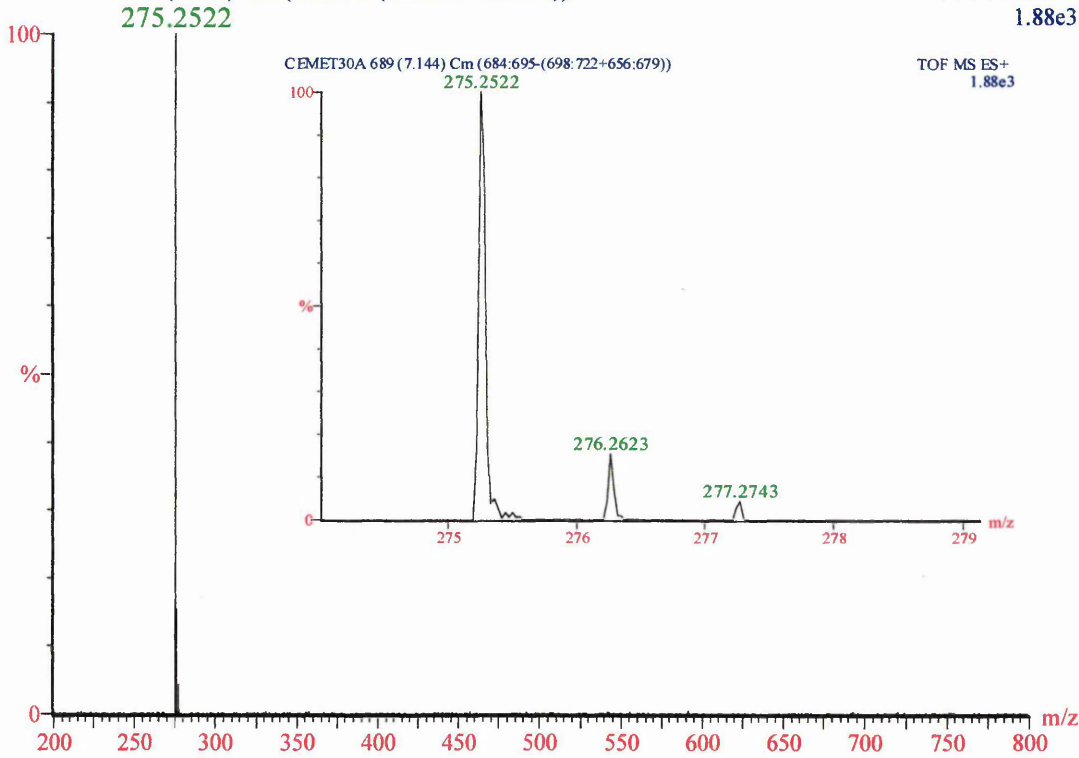


Figure 5.9 Mass Spectrum of Cimetidine,  
 $[M+Na]^+$  m/z 275

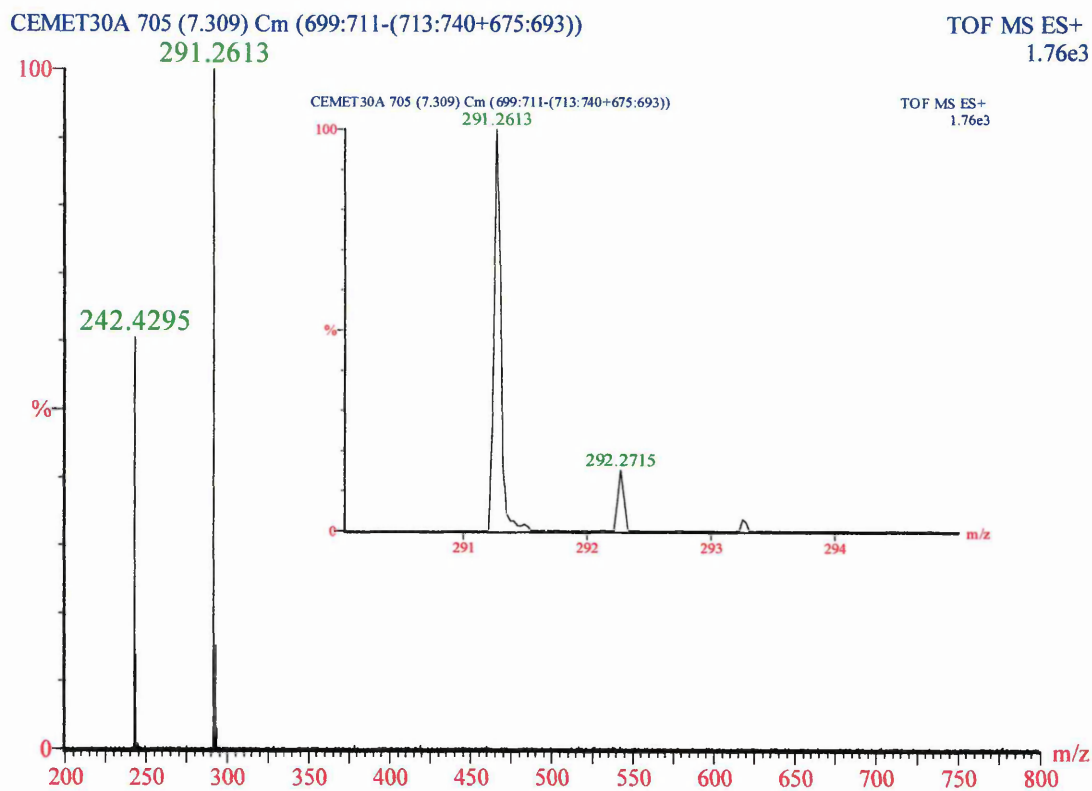


Figure 5.10 Mass Spectrum of SK&F 92452,  
 $[M+Na]^+$   $m/z$  291

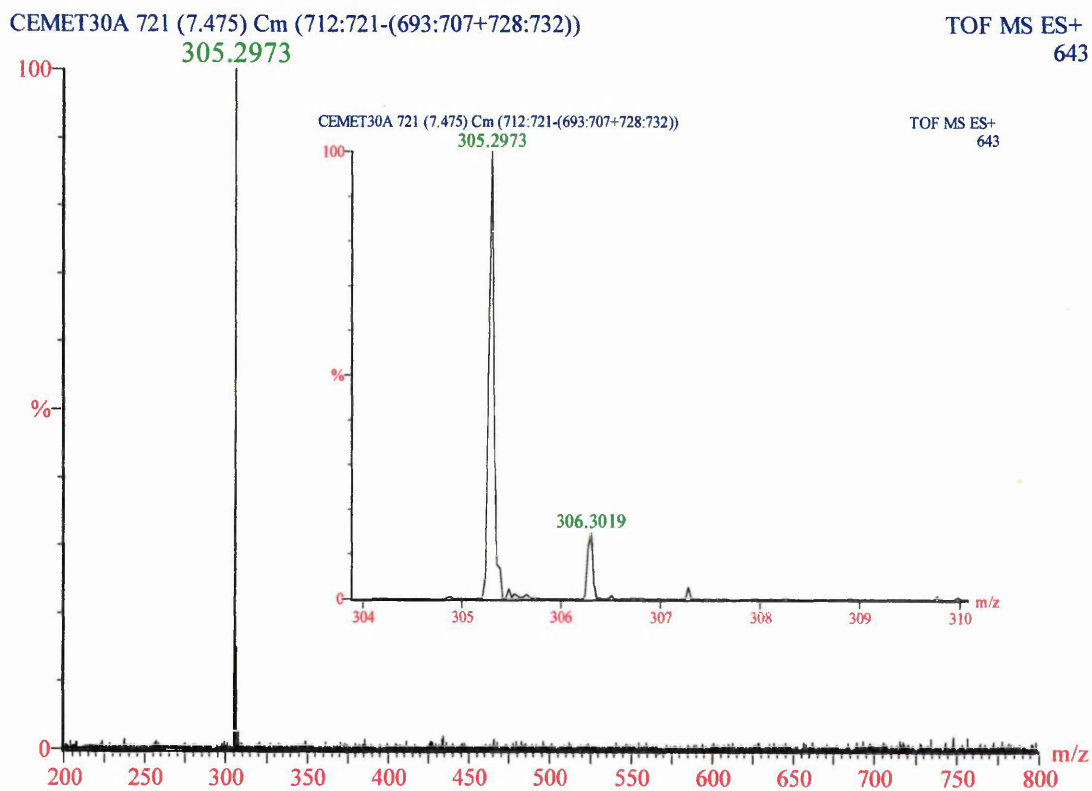


Figure 5.11 Mass Spectrum of SK&F 88958,  
 $[M+Na]^+$   $m/z$  305

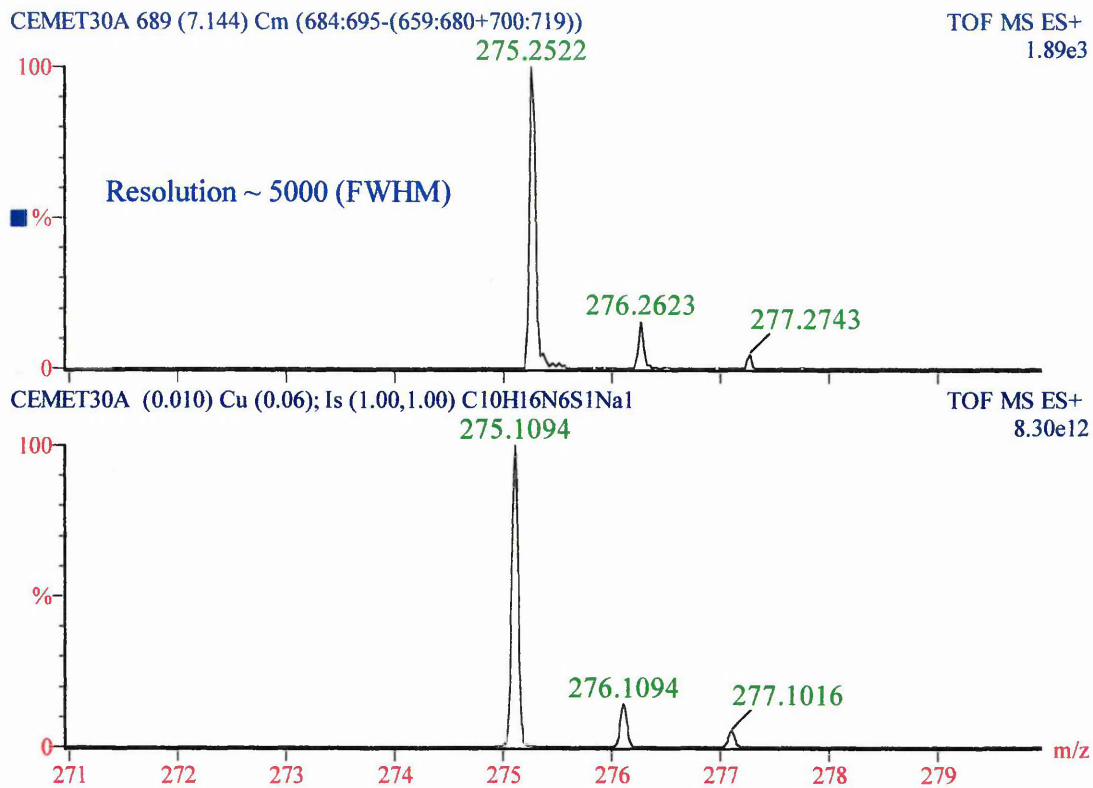


Figure 5.12 a) Mass Spectrum of Cimetidine Showing Isotope Pattern and Enhanced Resolution; b) Theoretical Isotope Pattern of Cimetidine

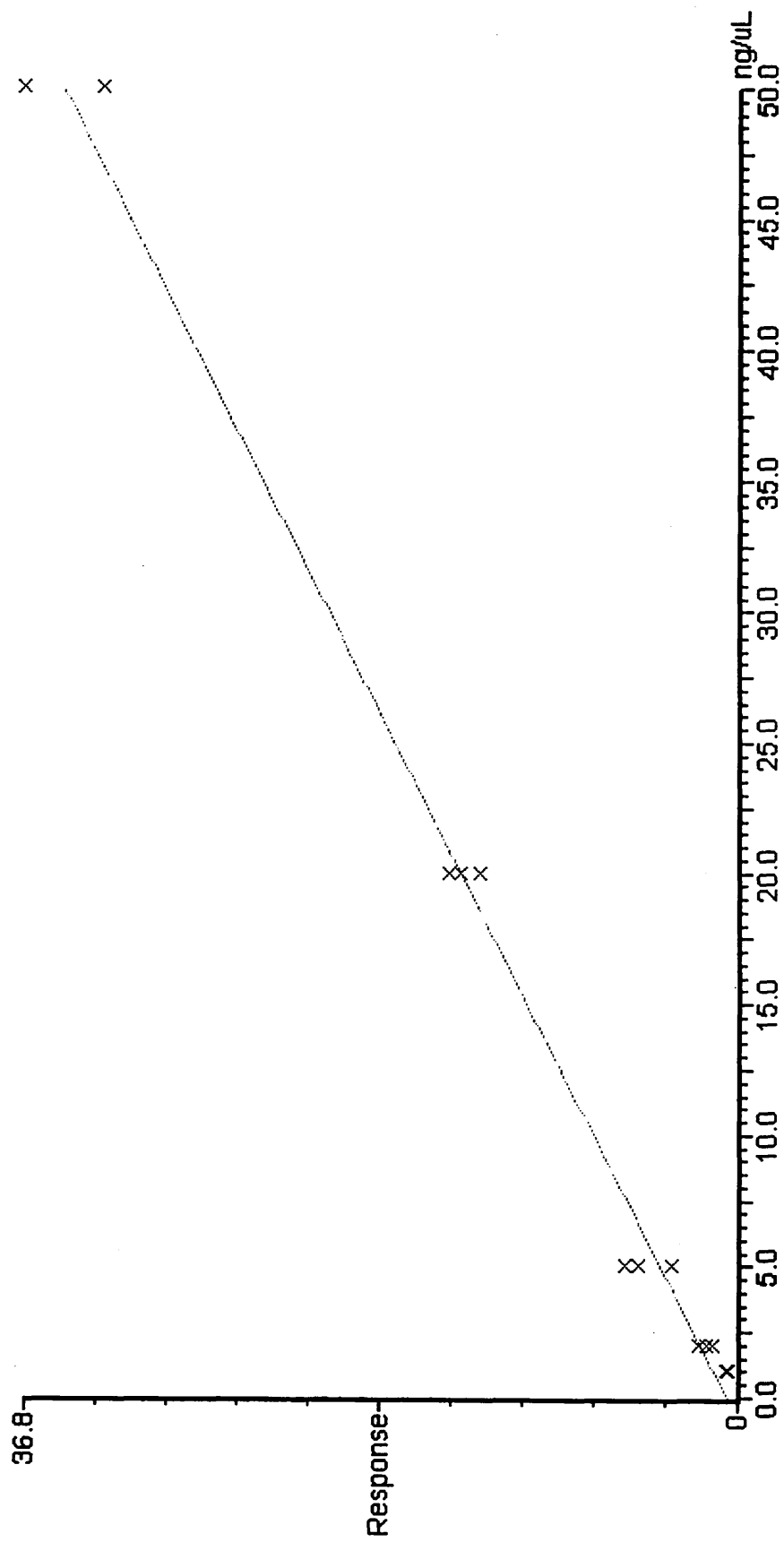


Figure 5.13 Calibration Curve Obtained for SK&F 91207,  $n = 3$ ,  $r^2 = 0.99$

## 5.5 Conclusions

Capillary zone electrophoresis has been successfully interfaced to an orthogonal acceleration time-of-flight mass spectrometer without any alteration in separation integrity compared to CZE/UV. Exact masses were obtained with less than 8 ppm error. Such accurate mass measurements would allow the confirmation / prediction of molecular formula. The use of a dual orthogonal entry system (*Z-Spray*) has permitted the use of an involatile buffer (*i.e.* phosphate) without significant source contamination.

The reconstructed mass electropherograms generated demonstrate the high sensitivity of oa-ToF MS. The mass spectra were generally clean, featuring the sodiated molecule of the compound of interest only. The oa-ToF MS generated data at an enhanced resolution of 5600 (FWHM).

The potential for CZE/oa-ToF mass spectrometric quantification has been demonstrated, with linear calibration curves generating a  $r^2$  values of  $\sim 0.99$ .

If a very narrow electrophoretic peak ( $< 3$  s) is analysed by a scanning mass analyser the peak intensity may change as an individual spectrum is detected, owing to the limited scan speed. This may result in a distortion of the relative intensities of the different mass peaks within the spectrum. Unlike scanning instruments, the oa-ToF MS performs parallel detection of all masses within the spectrum at very rapid acquisition rates. Therefore, each spectrum is representative of the sample composition at that point in time, irrespective of how rapidly the sample composition is changing.

The fast acquisition rates, high sensitivity and exact masses obtained indicate the advantages of oa-ToF MS over scanning techniques, such as quadrupole MS, for the analysis of narrow electrophoretic peaks.

## *References*

---

- (1) Guilhaus M; Mylynski V; Selby D. *Rapid Communications in Mass Spectrometry* **11** (1997) 951
- (2) Mamyrin BA; Schmikk DV. *Soviet Physics –JETP (English Translation)* **49** (1979) 762
- (3) Dawson JHJ; Guilhaus M. *Rapid Communications in Mass Spectrometry* **3** (1989) 155
- (4) US Patent, NO. 5 756 994, May 26 1998
- (5) Taken from LCT Users Manual, Micromass, Manchester UK
- (6) Collaboration with Dr Gwyn Lord, Manchester Metropolitan University, March 1998.

## **Chapter 6**

### ***The Incorporation of Reactive Species in the Sheath Flow for CZE/MS***

## 6.1 Introduction

The use of a sheath flow to manipulate the chemical nature of a sample has been well documented. Various applications exist; these include the sheath flow cuvette<sup>1</sup> for fluorescence detection and post-chromatographic modification of the mobile phase to produce favourable conditions for mass spectral analysis.

The sheath flow cuvette is employed in CZE / fluorescence detection, where a fluorescent compound is introduced via the sheath liquid and allowed to react with the (non-fluorescent) sample as it elutes from the capillary. This allows the separation of analytes based on their mobilities and not the mobility of the fluorescent-tagged moiety. Many forms of post-chromatographic manipulation exist; including halogenated make-up flow for improved sensitivity in negative ion LC/MS<sup>2,3</sup>, introduction of an organic solvent to reduce surface tension therefore aiding the electrospray process<sup>4,5</sup> or to affect charge distribution of multiply charged ions<sup>6</sup>. In addition, the sheath flow can be used to adjust the pH of an eluent<sup>7</sup> or increase the bulk flow of liquid, as in the co-axial sheath flow CZE interface<sup>7</sup>.

A novel ionisation technique based on co-axial electrospray has been developed by Bayer *et al.*<sup>8</sup>, which they have termed 'Co-ordination-ionspray' (CIS). The sheath flow comprises an aqueous solution of metal ions (lithium, palladium, silver), which in conjunction with pneumatic nebulisation at the probe tip results in the formation of a metal-analyte complex. CIS/MS was demonstrated to be especially useful for analytes that do not ionise well by electrospray (*i.e.* terpenes, sugars, alcohols, PAHs *etc.*).

The utility of hydrogen / deuterium (H/D) exchange reactions for confirming the presence of active hydrogens (*i.e.* hydrogens attached to heteroatoms O, N and S) in organic compounds was initially demonstrated by Hunt *et al.*<sup>9</sup>. They illustrated the use of deuterated reagent gases in chemical ionisation, resulting in the gas-phase exchange with protonated analytes.

H/D exchange reactions have proved to be useful in the interpretation of multiply charged peptides and protein ions generated by electrospray<sup>10</sup>. In addition, it can be

useful for structural confirmation<sup>11</sup> and differentiation of pseudo-molecular ions from fragments<sup>12</sup>. It can also be employed in the distinction of isomers<sup>13</sup>, based on different exchange rates between isomers and total number of hydrogens exchanged.

The purpose of this investigation was to determine whether CZE/MS data could be acquired employing H/D exchange via the sheath flow. Cimetidine and related impurities, propranolol and atenolol have been employed as model pharmaceutical products as they are structurally well characterised. For more information on cimetidine, see Chapter 3. Propranolol and atenolol are  $\beta$ -adrenoceptor blocking drugs (commonly known as  $\beta$ -blockers). Their uses include the treatment<sup>14</sup> of hypertension (abnormally high blood pressure), angina (pain associated with heart disease), reduction in recurrence rate of myocardial infarction (heart attack), arrhythmias (irregular heart beat), thyrotoxicosis (over production of thyroxine leading to autoimmune disease). In addition, they can be used to alleviate symptoms of anxiety (palpitations, tremor and tachycardia), prevention of migraine and topically in glaucoma (elevated fluid pressure within the eye). Atenolol is (relatively) water-soluble and therefore minimises certain side effects associated with  $\beta$ -blocker usage.

## ***6.2 Experimental***

### **6.2.1 Instrumentation**

#### ***6.2.1.1 Loop Injections***

A Quattro I (Micromass, Manchester, UK) mass spectrometer fitted with a home built nanospray interface (Chapter 4) was used for all loop injections. A probe voltage of 2.5 kV was used to effect electrospray with a cone voltage of 25 V. Desolvation was aided by a flow of nitrogen bath gas at a rate of ~50 L/hour. The source was typically operated at a temperature of 65 °C. Data was acquired in full scan mode over the  $m/z$  range 50 – 300 Da in 1.0 second.

Stock solutions of the analytes (dissolved in H<sub>2</sub>O) were diluted with either H<sub>2</sub>O or D<sub>2</sub>O to a concentration of 25  $\mu$ g/mL and injected via an internal loop Vici injection valve (100 nL, Thames Restek, Windsor, UK). The mobile phase was delivered by a Harvard

Apparatus Model 11 (Edenbridge, UK) syringe pump, at a flow rate of 500 nL/min. The mobile phase comprised 1:1 MeCN : H<sub>2</sub>O + 0.1 % acetic acid or 1:1 MeCN : D<sub>2</sub>O + 0.1 % acetic acid and was degassed by ultrasonification.

#### 6.2.1.2 Capillary Zone Electrophoresis / Mass Spectrometry

Separations were performed using a PrinCE Model 560 CE System (PrinCE Technologies, Emmen The Netherlands) at a potential of 30 kV (~ 300 Vcm<sup>-1</sup>). Uncoated fused silica capillaries were obtained from Composite Metal Services Ltd. (Hallow, UK) and were 50 µm i.d. x 375 µm o.d. x 90 cm in length. The CE was interfaced to the mass spectrometer via a home built co-axial sheath flow interface (Chapter 4). The probe was operated in the positive ion mode with 3.5 kV applied to the tip, and a source cone voltage of 25 V. Desolvation was assisted by nitrogen nebulising and bath gases (40 and 125 L/hr respectively). Data was acquired in the full scan mode over the *m/z* range 250 – 300 Da in 0.25 seconds.

Samples were injected hydrodynamically, 20 mbar for 0.1 minutes, which corresponds to an injection volume of 2.0 nL.

The running buffer employed throughout was 10 mM ammonium acetate adjusted to pH 3.8 with acetic acid. The capillary was conditioned prior to use and between analyses with 0.1 M HCl (2 bar for 120 s), H<sub>2</sub>O (2 bar for 60 s) and finally buffer (2 bar for 180 s) to preserve reproducibility.

The sheath liquid comprised 1:1 H<sub>2</sub>O / MeCN + 0.1 % acetic acid or 1:1 D<sub>2</sub>O / MeCN + 0.1 % acetic acid for deuterium exchange studies. Both systems employed a flow rate of 3 µL/min (Harvard Model 11 syringe pump, Harvard Apparatus, Edenbridge, UK).

#### 6.2.2 Chemicals and Reagents

Cimetidine and related impurities were supplied by SmithKline Beecham Pharmaceuticals (Harlow, UK). Propranolol and atenolol were supplied by AstraZeneca Pharmaceuticals (Macclesfield, UK).

D<sub>2</sub>O was a gift from AstraZeneca and was 99.9 % D atom. All other solvents and reagents used were of HPLC grade.

## **6.3 Results / Discussion**

### **6.3.1 Cimetidine and Related Impurities**

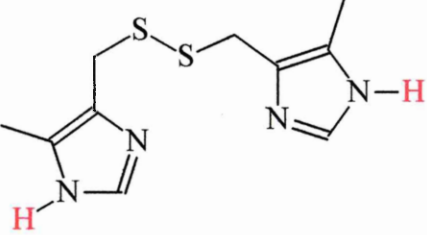
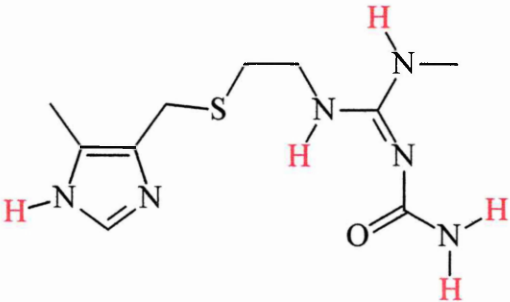
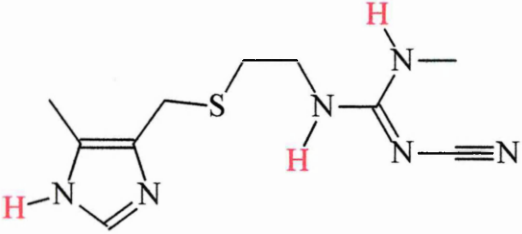
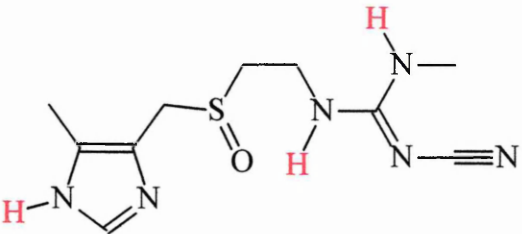
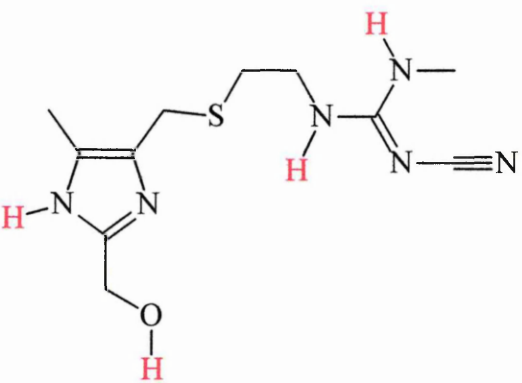
#### *6.3.1.1 Loop Injection to Determine the Extent of Exchange*

The structures of the analytes are shown in Table 6.1 (active hydrogens are hi-lighted in red).

The 25 µg/mL samples of cimetidine and related impurities were analysed to confirm the mass of the protonated molecule. The mass spectra obtained (Figure 6.1) feature the ions of interest, which correspond to the  $[M+H]^+$ . The mass spectrum for SK&F 92422 also features an ion at  $m/z$  254, this corresponds to the loss of NH<sub>3</sub> from the  $[M+H]^+$ , *i.e.*  $[M+H-NH_3]^+$ .

The D<sub>2</sub>O samples (25 µg/mL) were injected into a deuterated mobile phase to determine the extent of H/D exchange. The mass spectra obtained (Figure 6.2) exhibit ions that correspond to fully exchanged species (*i.e.* all hi-lighted hydrogens in Table 6.1 were exchanged for deuterium).

Table 6.1 – Structure of Cimetidine and Impurities

Structure	Name	[M+H] <sup>+</sup> m/z	([M <sub>EX</sub> +D] <sup>+</sup> ) <sup>*</sup> m/z for full exchange
	SK&F 91207	255	258
	SK&F 92422	271	277
	Cimetidine	253	257
	SK&F 92452	269	273
	SK&F 88958	283	288

\* Where [M<sub>EX</sub>+D]<sup>+</sup> corresponds to the fully exchanged deuterated analyte.

The molecular ion was a deuterated species, *i.e.*  $[M+D]^+$ , this could be attributed to the significantly higher concentration of  $D_2O$  present *cf.*  $H_2O$ . These data are summarised in Table 6.2.

Table 6.2 Extent of Exchange of Cimetidine and Related Impurities

	$[M+H]^+ m/z$	$[M_{EX}+D]^+ m/z$	H/D exchanged	Number of exchangeable sites
SK&F 91207	255	258	3	2
SK&F 92422	271	277	6	5
Cimetidine	253	257	4	3
SK&F 92452	269	273	4	3
SK&F 88958	283	288	5	4

The presence of ions corresponding to  $[M_{EX} + D-1]^+$  (*e.g.*  $m/z$  257 for SK&F 91207) indicates that the exchange is not complete. There are two possible reasons for this, if the active hydrogens are non-equivalent, exchange will be rate limited and only the most active will interchange. In addition, the presence of hydrogens from the buffer and the analytes could allow back-exchange to occur, leading to partially exchanged species (this must be the case for SK&F 91207 owing to the equivalence of all the active hydrogens).

#### 6.6.1.2 CZE/MS Employing $D_2O$ Sheath Flow

Cimetidine and related impurities have previously been analysed by CZE/UV and CZE/MS. The analytes were separated (Figure 6.3) employing the standard conditions described previously<sup>15,16</sup>. The migration order corresponds to SK&F 91207; 92422; cimetidine; 92452 and 88958, which was consistent to that obtained by CZE/UV<sup>15</sup>. The mass spectra (Figure 6.4) from these peaks were identical to those obtained by loop injection of the analytes, with a reduction in signal-to-noise ratio (owing to the reduced sample injection).

When the sheath-liquid was modified to the deuterated analogue, the appearance of the mass electropherograms was unchanged (Figure 6.5). Thus, the composition of the sheath liquid did not have any detrimental effects on the separation or the migration order. The corresponding mass spectra (Figure 6.6) were significantly more complex (*cf.* H<sub>2</sub>O experiments), exhibiting varying degrees of exchange. Only SK&F 91207 exhibited full exchange, these data are summarised in Table 6.3.

Table 6.3 Analysis of Cimetidine and Impurities using a D<sub>2</sub>O Sheath-liquid

	[M+H] <sup>+</sup>	Fully exchanged <sup>†</sup>	Base peak of molecular ion cluster	Number exchanged <sup>‡</sup>
SK&F 91207	255	258	258	2
SK&F 92422	271	277	274	2
Cimetidine	253	257	255	1
SK&F 92452	269	273	271	1
SK&F 88958	283	288	286	2

Each analyte has undergone exchange of active hydrogens. In addition, the molecular ion was charged with a deuterium ion (*i.e.* a [M+D]<sup>+</sup>) owing to the higher concentration of D<sub>2</sub>O *cf.* H<sub>2</sub>O. This conclusion was based on the data obtained for SK&F 91207, which only contains 2 active hydrogens, but exhibits a mass shift of 3 Da from the protonated molecule, thus a [M+D]<sup>+</sup> species was observed.

Therefore, taking the supposition that all of the other analytes carry a charge arising from a deuterium ion (*i.e.* [M+D]<sup>+</sup> species), the extent of exchange was reduced compared to loop injections which employed a completely deuterated system. This was because exchange was rate limited and only the most active hydrogens could exchange within the time scale of analyte / D<sub>2</sub>O mixing. This occurs at the capillary tip prior to spraying and in the gas phase prior to desolvation.

The fragment ion corresponding to the loss of ammonia from SK&F 92422 exhibits a complex exchange pattern. The fragment ion can exchange a maximum of 3 hydrogens (to *m/z* 257). The D<sub>2</sub>O loop injection experiment exhibits a fully exchanged species (*m/z*

<sup>†</sup> From loop injection using D<sub>2</sub>O diluted sample and D<sub>2</sub>O mobile phase.

<sup>‡</sup> Assuming charge-bearing species is a deuterium ion.

257), whereas a range of exchange is observed for CZE/MS employing a D<sub>2</sub>O sheath (between 0 – 2 H/D corresponding to  $m/z$  254 – 256), thus indicating the rate limitation of exchange.

The exchanged hydrogens of the molecular species can be assigned through study of the structures and spectra obtained. SK&F 91207 was the only analyte to undergo complete exchange under these conditions, suggesting that the imidazole-like hydrogens were readily exchanged. Therefore, the single hydrogen exchanged in SK&F 92452 and cimetidine corresponded to the imidazole-like hydrogen. Whereas SK&F 88958 and 92422 exchange two hydrogens each, one was likely to be the imidazole-like hydrogen. The other exchanged hydrogens would be determined by their relative acidity.

The remaining active hydrogens in SK&F 88958 correspond to hydroxyl and guanidino groups. Whereas SK&F 92422 contains an amide and guanidino group, which both contain two hydrogens, however, only one exchanges. Therefore, further investigation would be necessary to assign which hydrogens exchange; this could be achieved by MS/MS structural studies (*i.e.* product ion scanning).

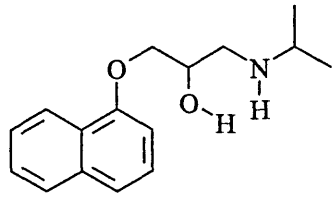
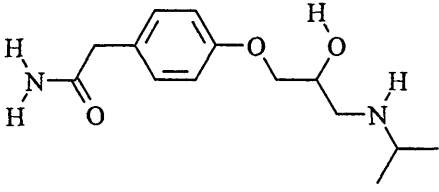
### **6.3.2 Propranolol and Atenolol**

#### *6.3.2.1 Loop Injection to Determine the Extent of Exchange*

The structures of Propranolol and atenolol are shown in Table 6.4 (the exchangeable hydrogens are hi-lighted in red).

The same analytical method (as the cimetidine analysis) was followed to determine the full extent of exchange. The mass spectra shown in Figure 6.7 were obtained from samples that had been diluted in water. The ion at  $m/z$  260 corresponds to the  $[M+H]^+$  of propranolol and the ion at  $m/z$  267 the  $[M+H]^+$  of atenolol.

Table 6.4 Structure of Propranolol and Atenolol

Structure	Name	$[M+H]^+$ <i>m/z</i>	$[M_{EX}+D]^+$ <i>m/z</i> for full exchange
	Propranolol	260	263
	Atenolol	267	272

When stock solutions were diluted with D<sub>2</sub>O (Figure 6.8, all possible hydrogens (highlighted in red in Table 6.4) exchanged, once more the charge bearing species was a deuterium ion ( $[M+D]^+$ ), these data are summarised in Table 6.5.

Table 6.5 Extent of Exchange of Propranolol and Atenolol

	$[M+H]^+$ <i>m/z</i>	$[M_{EX}+D]^+$ <i>m/z</i>	H/D Exchanged	Number of exchangeable sites
Propranolol	260	263	3	2
Atenolol	267	272	5	4

Therefore, both analytes exhibit exchange of all active hydrogens when diluted with D<sub>2</sub>O (as expected, H/D exchange is an equilibrium process and in this case, the equilibrium is pushed to one side). In addition, the charge bearing species was a deuterium ion, instead of the more familiar hydrogen, thus generating a deuterated molecule,  $[M_{EX}+D]^+$ .

Once more the presence of an ion at  $[M_{EX}+D-1]^+$  indicated that the exchange was not complete and the active hydrogens are non-equivalent.

### 6.3.2.1 CZE/MS Employing D<sub>2</sub>O Sheath Flow

Propranolol and atenolol were separated under the same conditions as employed for the analysis of cimetidine and related impurities, *i.e.* 10 mM ammonium acetate adjusted to pH 3.7 (with glacial acetic acid). The mass electropherograms obtained for the separation of the  $\beta$ -blockers are shown in Figure 6.9. The analytes were almost temporally resolved, but could be fully resolved by mass discrimination. Propranolol migrated in front of atenolol and both peaks were detected in less than 20 minutes employing these conditions. The mass spectra obtained (Figure 6.10) feature the protonated molecule at  $m/z$  260 and 267 (propranolol and atenolol respectively) and were similar to those obtained by loop injection.

The mass electropherograms obtained for propranolol and atenolol employing the deuterated sheath liquid are shown in Figure 6.11. The use of a deuterated sheath liquid had no effect on the separation or migration order. The corresponding mass spectra (Figure 6.12) display the effects of H/D exchange.

The active hydrogens in propranolol have fully exchanged along with the addition of a charge bearing deuterium ion, *i.e.* a mass shift of 3. Whereas atenolol does not exhibit full exchange, with only 2 out of the 4 active hydrogens exchanging (the charge bearing species being a deuterium ion). Atenolol contains the same active hydrogens as propranolol, with the addition of an amide group. Therefore, the 2 hydrogens exchanging in atenolol correspond to those which exchanged in propranolol, *i.e.* the hydroxyl and secondary amine.

Once more the presence of an ion at  $m/z$   $[M_{EX}+D-1]^+$  indicates that exchange is not complete and is rate limited.

### 6.3.3 Fully Deuterated CZE/MS

To simplify the identification of exchanged hydrogens it would be advantageous to be able to perform CZE/MS with a deuterated buffer and sheath-liquid, therefore obtaining fully exchanged analytes as in loop injections. This was investigated employing a buffer comprising 10 mM ammonium acetate adjusted to pH 3.7 in D<sub>2</sub>O, all other experimental conditions were the same as used for the separation based on a H<sub>2</sub>O buffer. Unfortunately, no analyte ions were observed in the mass spectrometer, even when electrophoretic infusion of cimetidine and SK&F 88958 was attempted. D<sub>2</sub>O and H<sub>2</sub>O do differ in their properties (Table 6.6). The ratio of dielectric constant to viscosity ( $\epsilon/\eta$ ) is less for D<sub>2</sub>O (63.46) than H<sub>2</sub>O (87.74), which will have the effect of reducing the EOF and hence apparent analyte mobility. However, this should not prevent the electrokinetic infusion of a sample through the capillary.

Table 6.6 Properties of H<sub>2</sub>O and D<sub>2</sub>O

	Dielectric Constant ( $\epsilon$ )	Viscosity ( $\eta$ ) \ cp	$\epsilon / \eta$
H <sub>2</sub> O	87.74	1.00	87.74
D <sub>2</sub> O	78.06	1.23	63.46

Therefore, to determine whether there was flow through the capillary CZE/UV<sup>§</sup> employing the deuterated buffer was performed. A typical electropherogram obtained is shown in Figure 6.13. The mean migration times ( $t_m$ , where  $n = 5$ ) are summarised in Table 6.7, which are similar to those obtained in H<sub>2</sub>O, with the latter three analytes migrating slightly faster in the D<sub>2</sub>O buffer. This does not correspond with the theoretical effect expected from the  $\epsilon/\eta$  ratio and as yet no adequate explanation can be suggested.

<sup>§</sup> The separation conditions were 10 mM ammonium acetate dissolved in D<sub>2</sub>O adjusted to pH 3.7. Separations were performed on a capillary of 50  $\mu\text{m}$  i.d. x 375  $\mu\text{m}$  o.d. of 85 cm in length with a field strength of 300  $\text{Vcm}^{-1}$ , detection was at 230 nm 53 cm from the inlet. Injections were performed hydrodynamically (25 mbar / 0.1 minutes) employing cimetidine and related impurities at a concentration of 10  $\mu\text{g/mL}$  diluted in D<sub>2</sub>O. An additional stage was added to the capillary conditioning, D<sub>2</sub>O was flushed through the capillary (1 bar for 30 s) prior to the buffer.

Table 6.7 Mean Migration Time Data for CZE/UV Separation Employing a D<sub>2</sub>O Buffer

	Mean $t_m$ / min (n = 5)	% RSD	Theoretical plates / m	$t_m$ using H <sub>2</sub> O buffer / min.
SK&F 91207	4.96	0.08	269 000	4.800
SK&F 92422	5.24	0.08	195 000	5.105
SK&F 92506	5.91	0.14	232 000	5.830
Cimetidine	7.59	0.43	242 000	7.835
SK&F 92452	7.85	0.51	262 000	8.172
SK&F 88958	7.97	0.53	282 000	8.304

Therefore, irrespective of anomalous migration times, the analytes should be observed by CZE/MS, but connectivity problems within the interface may prevent their migration. Further work must be undertaken to investigate this, *e.g.* the use of a sheathless interface.

## 6.4 Mass Electropherograms and Spectra

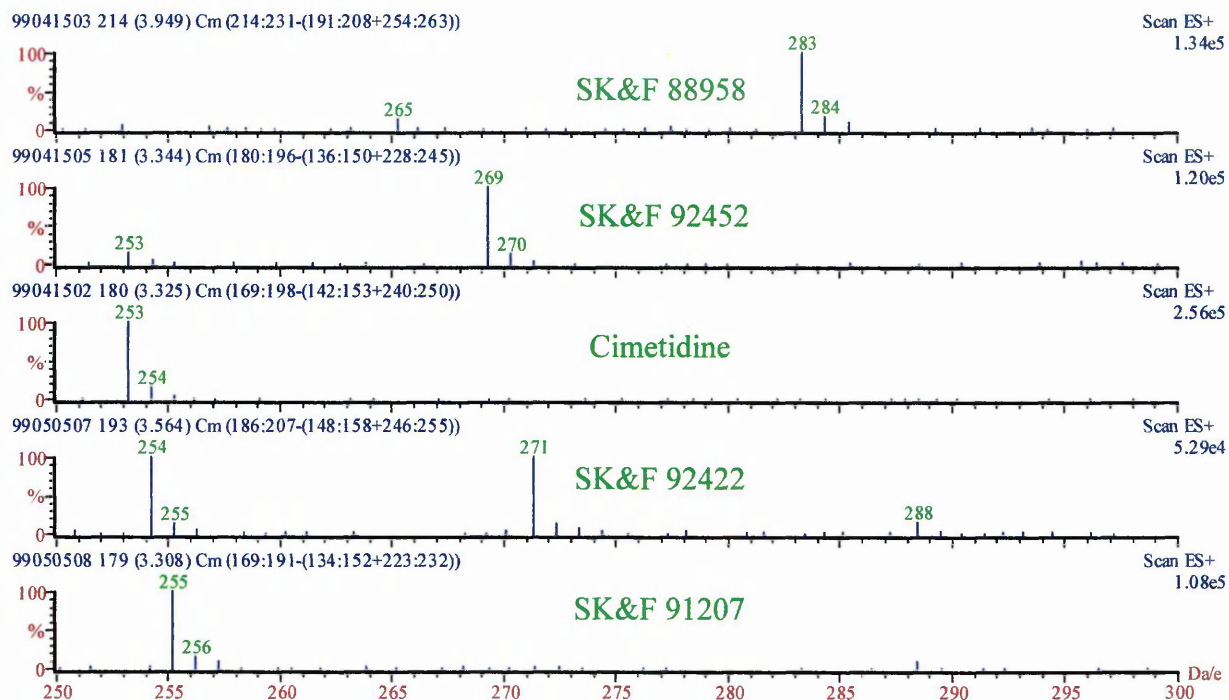


Figure 6.1 Loop Injection Mass Spectra of Cimetidine and Related Impurities using H<sub>2</sub>O Mobile Phase

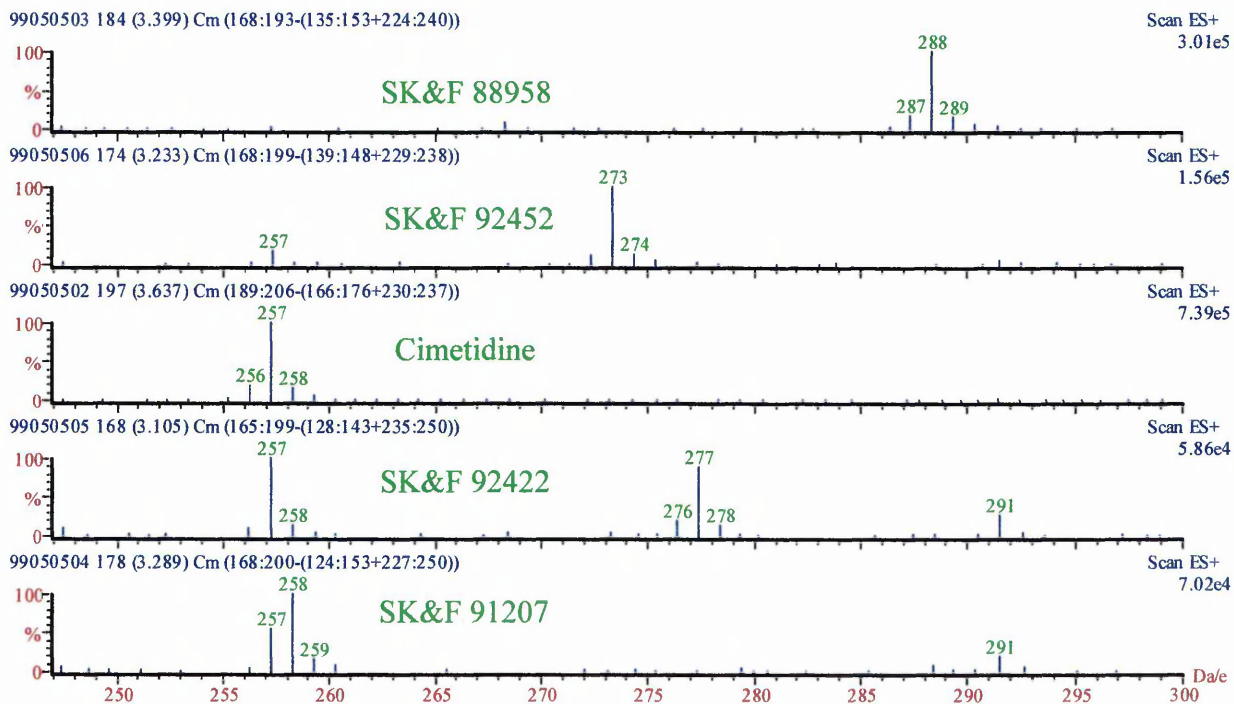


Figure 6.2 Loop Injection Mass Spectra of Cimetidine and Related Impurities using D<sub>2</sub>O Mobile Phase

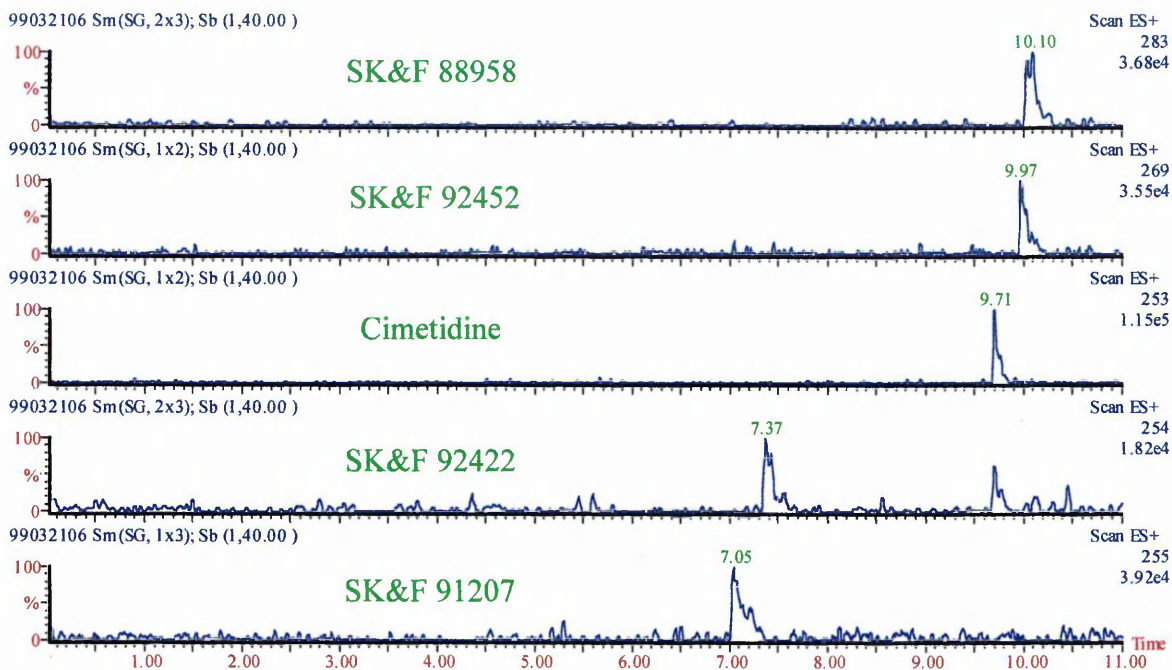


Figure 6.3 Mass Electropherograms of Cimetidine and Related Impurities using H<sub>2</sub>O Sheath-liquid

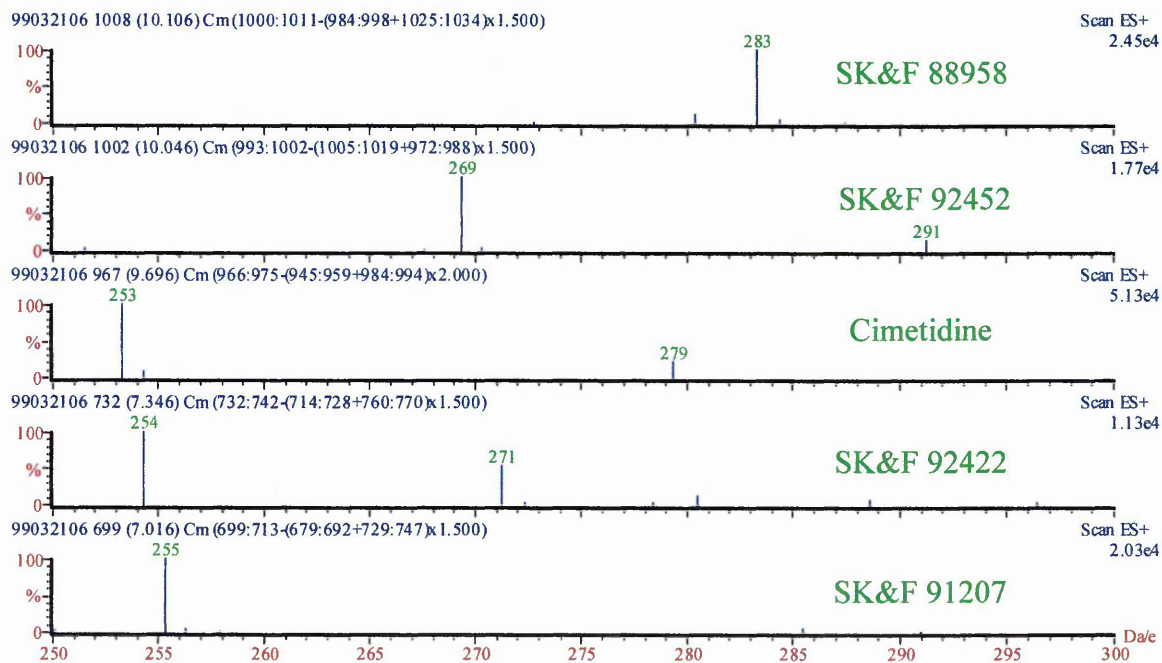


Figure 6.4 CZE/MS Mass Spectra of Cimetidine and Related Impurities using H<sub>2</sub>O Sheath-liquid

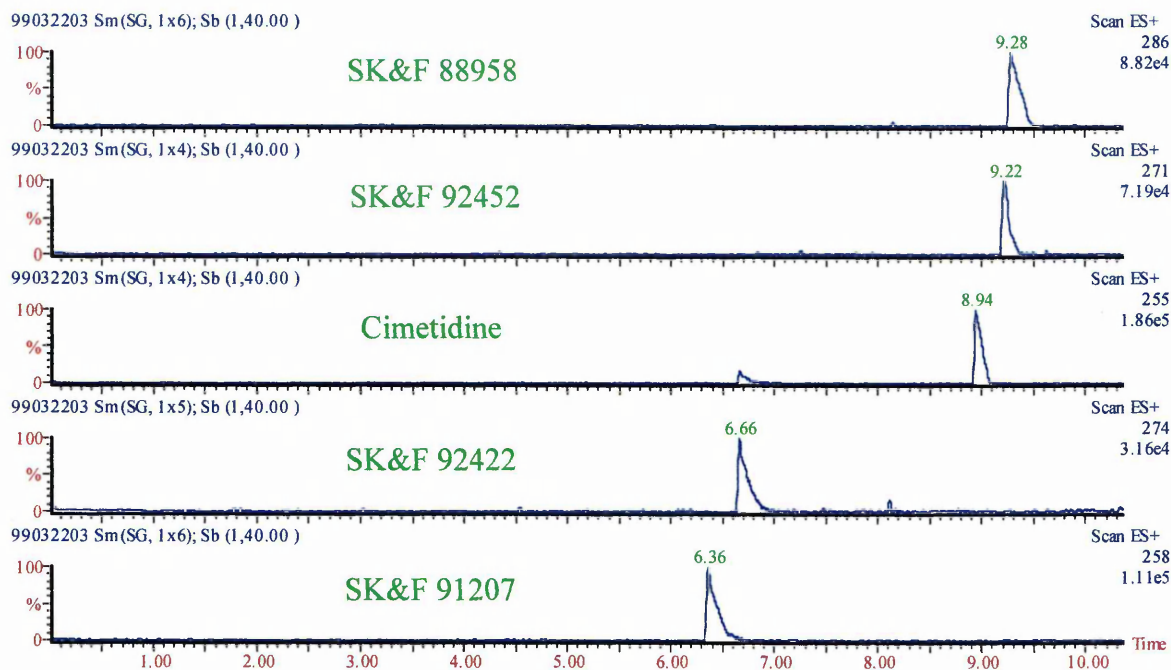


Figure 6.5 Mass Electropherograms of Cimetidine and Related Impurities using D<sub>2</sub>O Sheath-liquid

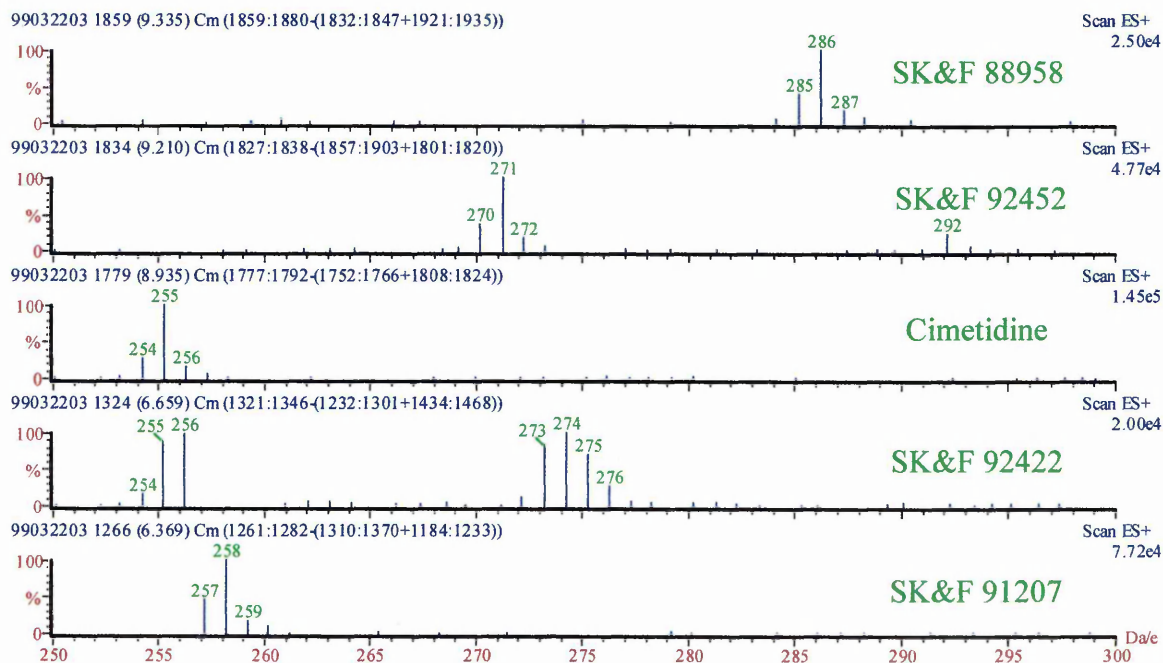


Figure 6.6 CZE/MS Mass Spectra of Cimetidine and Related Impurities using D<sub>2</sub>O Sheath-liquid

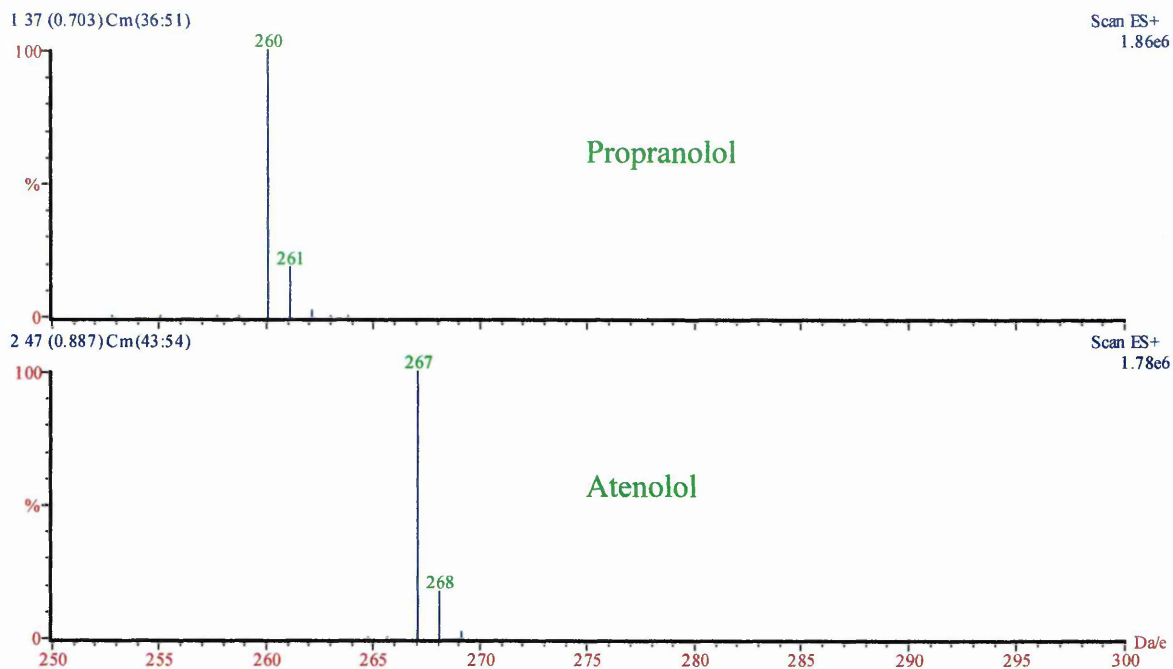


Figure 6.7 Loop Injection Mass Spectra of Propranolol and Atenolol using H<sub>2</sub>O Mobile Phase

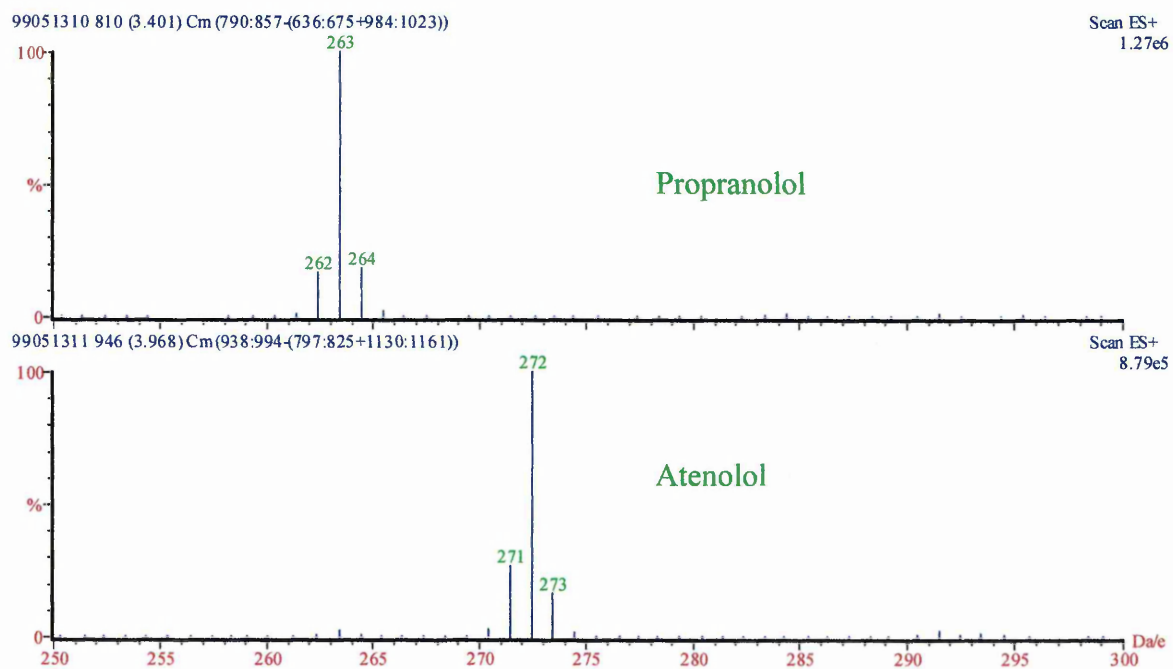


Figure 6.8 Loop Injection Mass Spectra of Propranolol and Atenolol using D<sub>2</sub>O Mobile Phase

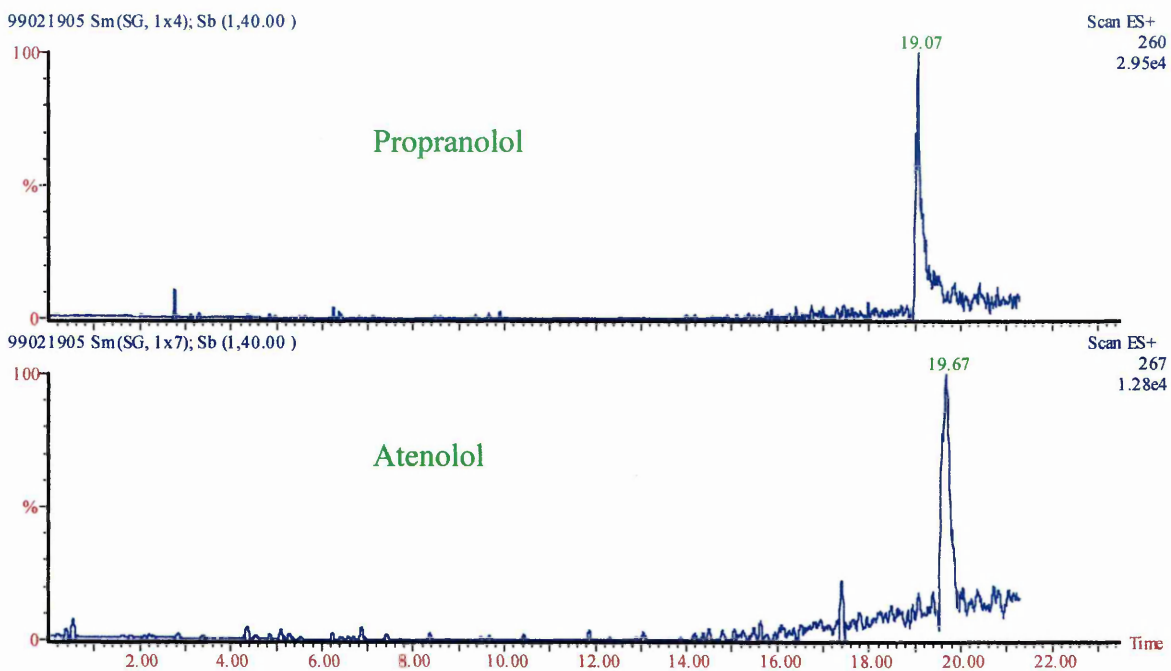


Figure 6.9 Mass Electropherograms of Propranolol and Atenolol using H<sub>2</sub>O Sheath-liquid

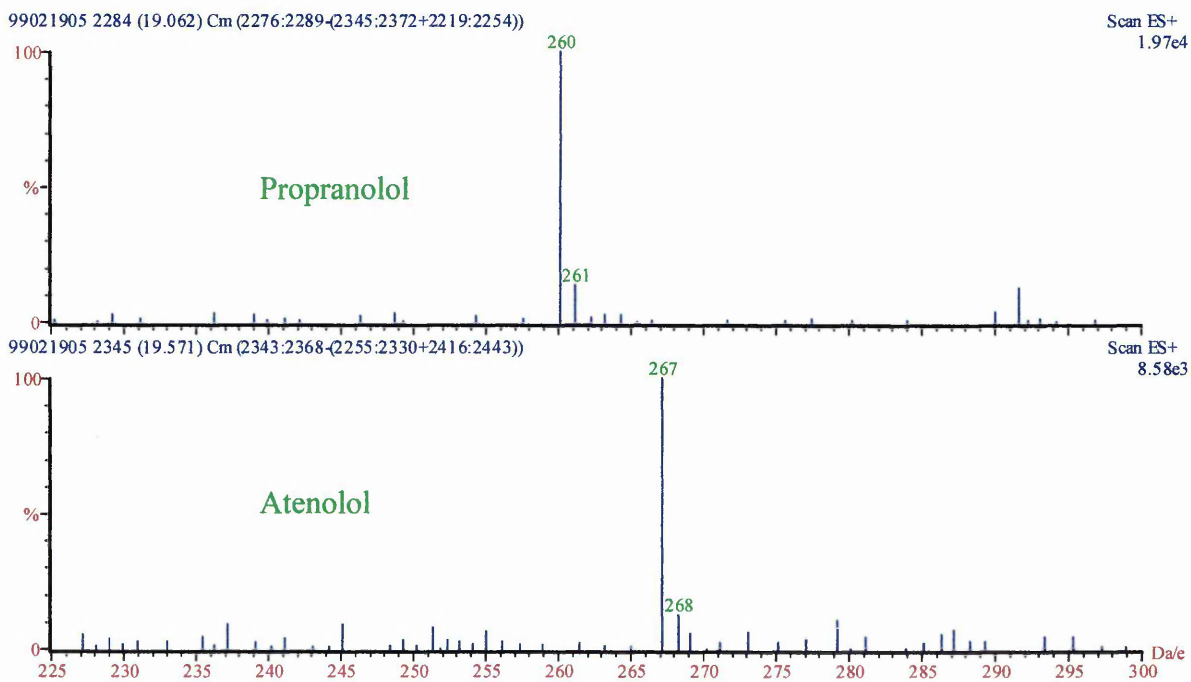


Figure 6.10 CZE/MS Mass Spectra of Propranolol and Atenolol using H<sub>2</sub>O Sheath-liquid

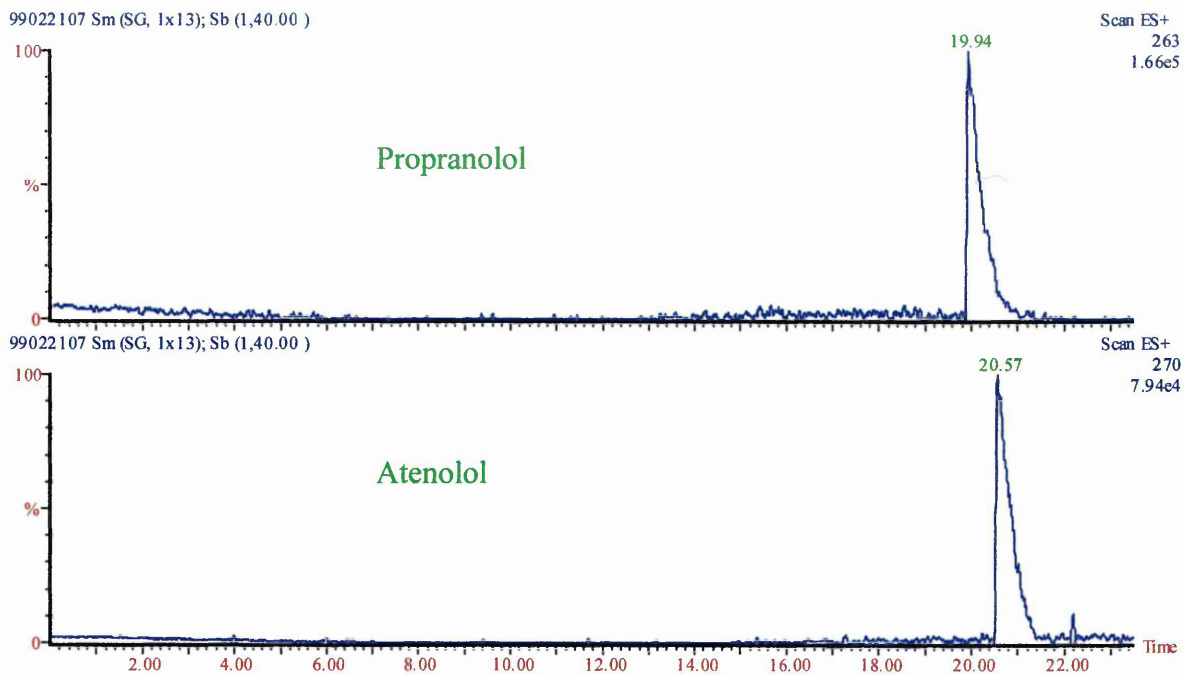


Figure 6.11 Mass Electropherograms of Propranolol and Atenolol using D<sub>2</sub>O Sheath-liquid

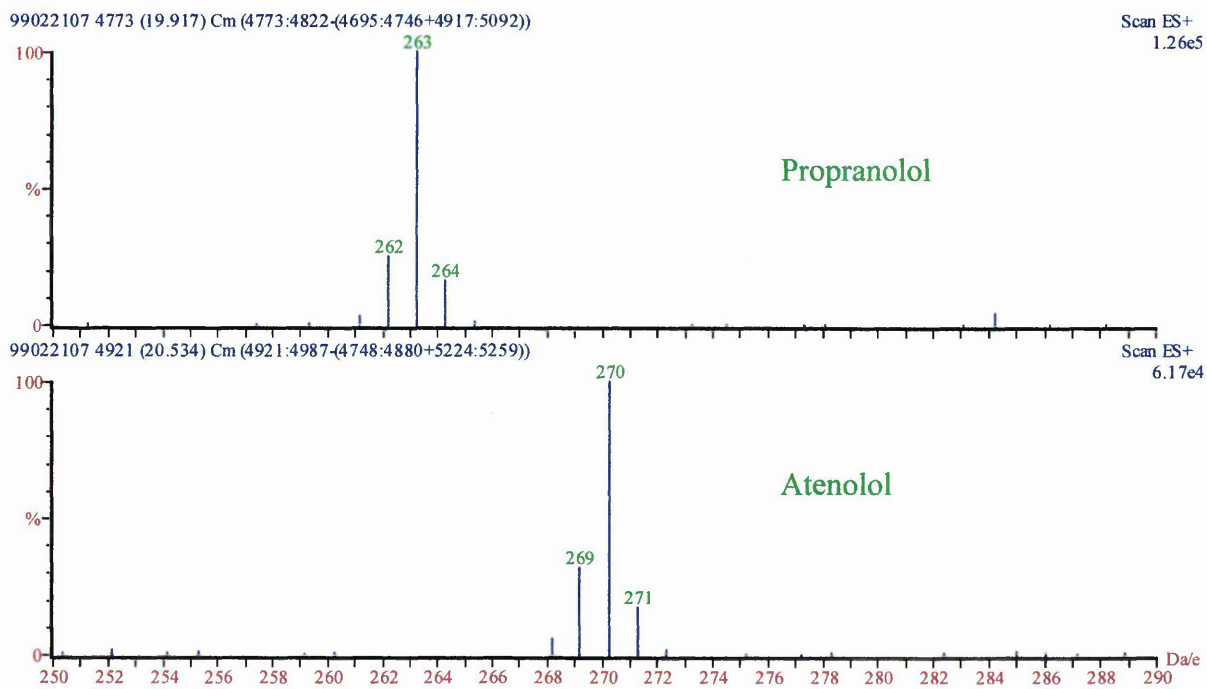


Figure 6.12 CZE/MS Mass Spectra of Propranolol and Atenolol using D<sub>2</sub>O Sheath-liquid

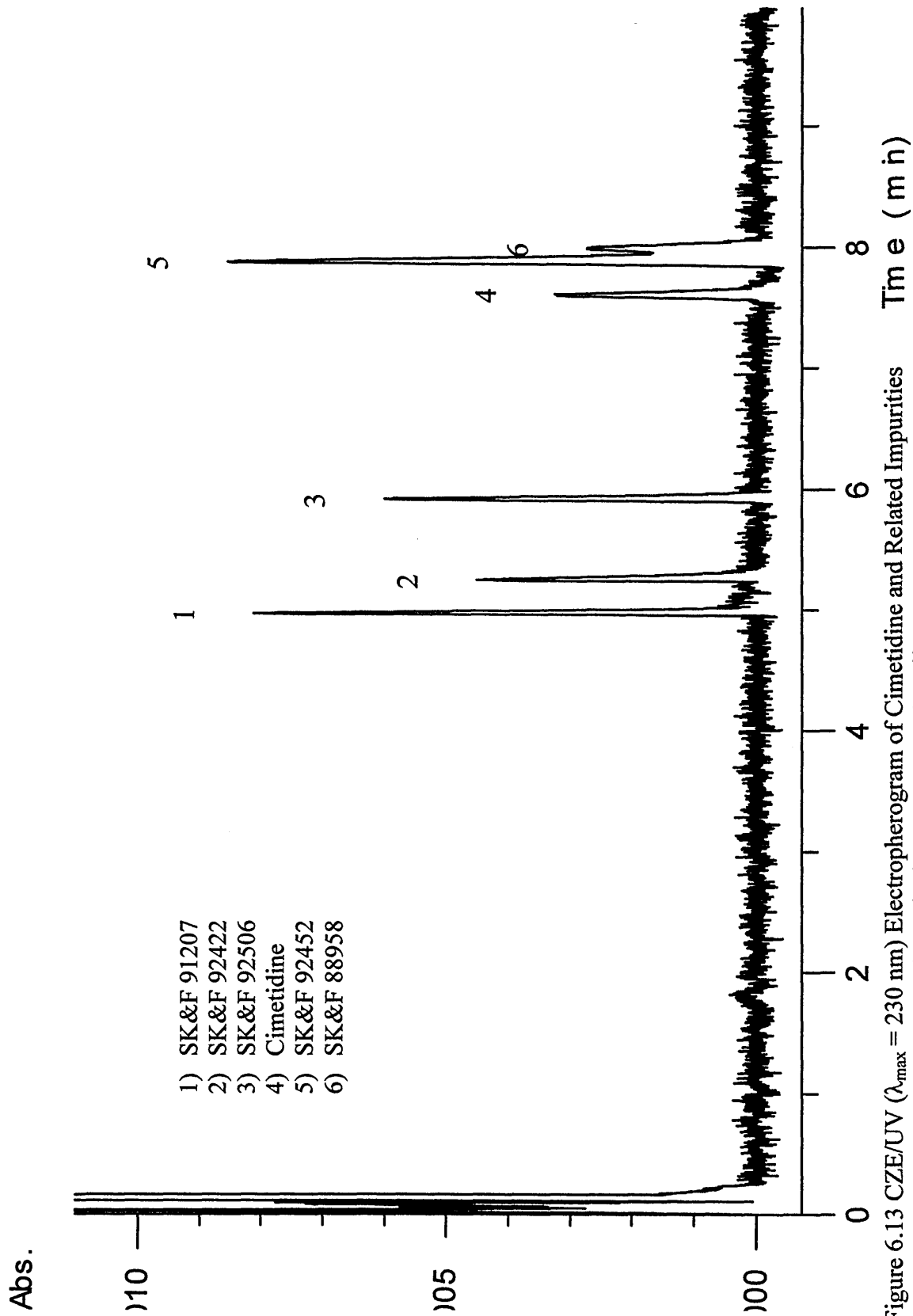


Figure 6.13 CZE/UV ( $\lambda_{\text{max}} = 230 \text{ nm}$ ) Electropherogram of Cimetidine and Related Impurities Separated Employing a Deuterated Buffer

## 6.5 Conclusions

A method has been developed that allows the post-separation H/D exchange of analytes, employing a co-axial sheath flow CZE interface. Thus indicating that fast scale reactions can be performed in the time scale of analyte / make-up flow mixing and analyte desolvation. Therefore, other fast reactions could be employed to determine functional groups or structural confirmation.

Initially to determine the extent of exchange, loop injection of the analytes (diluted in D<sub>2</sub>O) employing a D<sub>2</sub>O mobile phase was performed. The  $m/z$  of the ions generated corresponded to fully exchanged species. However, there was an ion present at an  $m/z$  corresponding to  $[M_{EX+D-1}]^+$ . The presence of this ion indicates that complete exchange does not occur. This could be attributed to non-equivalence of the hydrogens; *i.e.* the rate of exchange would be different for the non-equivalent hydrogens, resulting in only the most active hydrogens being exchanged. In addition, the presence of residual hydrogens could result in back-exchange occurring. The contribution of the latter situation could be reduced by employing a fully deuterated system *i.e.* by adjusting the pH with CD<sub>3</sub>CO<sub>2</sub>D *etc.*

The effect of a deuterated make-up flow on the CZE/MS separation of the pharmaceutical compounds was investigated. The extent of exchange was reduced compared to the deuterated loop injections. This could be attributed to the higher concentration of hydrogens present (in the buffer) affecting the H/D exchange equilibrium. Once more the presence of  $[M_{EX+D-1}]^+$  species indicated that non-equivalence / back-exchange was occurring. To simplify interpretation (*i.e.* the number of exchangeable hydrogens), a separation employing deuterated buffer and sheath liquid was investigated. Unfortunately, the analytes were not detected by the mass spectrometer. The feasibility of a D<sub>2</sub>O buffer was confirmed by CZE/UV employing an ammonium acetate buffer dissolved in D<sub>2</sub>O. It is believed that connectivity problems within the CZE/MS interface prevented the analytes from being detected. A sheathless interface may be able to alleviate this problem.

## References

---

- (1) Coble PG; Timperman AT. *Journal of Chromatography A* **829** (1998) 309
- (2) Geerdink RB; Maris FA; de Jong GJ; Frei RW; Brinkman UA Th. *Journal of Chromatography* **394** (1987) 51
- (3) Kato Y; Numajiri Y. *Journal of Chromatography* **562** (1991) 81
- (4) Perkins JR; Parker CE; Tomer KB. *Journal of the American Society of Mass Spectrometry* **3** (1992) 139
- (5) Hershberger LW; Callis JB; Christian GD. *Analytical Chemistry* **51** (1979) 1444
- (6) Loo JA; Udseth HR; Smith RD. *Biomedical and Environmental Mass Spectrometry* **17** (1988) 411
- (7) Loo JA; Udseth HR; Smith RD. *Analytical Biochemistry* **179** (1989) 404
- (8) Bayer E; Gfrörer P; Rental C. *Angewandte Chemie International Edition* **38** (1999) 992
- (9) Hunt DF; McEwan CN; Upham RA. *Analytical Chemistry* **44** (1972) 1292
- (10) Focus: H/D Exchange of Proteins in Solution. *Journal of the American Society of Mass Spectrometry* **10** (1999) 671; and references cited therein
- (11) Karlsson KE. *Journal of Chromatography* **647** (1993) 31
- (12) Adejare A; Brown PW. *Analytical Chemistry* **69** (1997) 1525
- (13) Nourse BD; Hettich RL; Buchanan MV. *Journal of the American Society of Mass Spectrometry* **4** (1993) 296
- (14) *British National Formulary* **31** (1996) 73
- (15) a) Chapter 3.  
b) Ellis DR; Palmer ME; Tetler LW; Eckers C. *Journal of Chromatography A* **808** (1998) 269
- (16) a) Chapters 4 – 5.  
b) Palmer ME; Clench MR; Tetler LW; Little DR. *Rapid Communications in Mass Spectrometry* **13** (1999) 256

## **Chapter 7**

### ***Separation of Nicotine Metabolites by CZE/MS***

## 7.1 Introduction

Smoking is the major cause of preventable mortality and morbidity in the western world, with an estimated half of all regular smokers dying as a consequence of their habit<sup>1</sup>. From a health point of view, the degree and duration of exposure to tobacco smoke is important, yet there are currently no measures of the dose of tobacco smoke absorbed in a population.

To assess the levels of exposure two methods can be employed, these are questionnaires and the determination of biological markers. A major drawback of a questionnaire is deception by the interviewee, individuals generally underestimate their true intake, and some deny smoking at all. In addition, it is difficult to ascertain the exposure to tobacco smoke, *i.e.* number and depth of inhalations. Questionnaires become useful when they are used in conjunction with biological markers. A number of biological markers can be used, these include breath carbon monoxide (CO), blood carboxyhaemoglobin (COHb), thiocyanate (a metabolic product of hydrogen cyanide, HCN) and nicotine along with its related metabolites. CO and COHb are not accurate markers of tobacco intake as CO is found abundantly as an environmental pollutant. Thiocyanate may be present in blood due to the intake of various green vegetables and nuts, so can not be easily employed as a marker for tobacco intake. Nicotine is the major component of the particulate phase of tobacco smoke, and its presence in biological fluids is due to exposure to tobacco smoke\*. However, nicotine is not suitable for estimating exposure, since external factors (such as pH) affect the observed concentration in biological matrices. Therefore, cotinine (which is the major metabolite of nicotine and undergoes further metabolic processes, see Scheme 7.1) is generally employed as a specific biological marker. Of the biological fluids that can be studied, urine is typically analysed. This is because urinary concentrations are approximately 5 – 10 times greater than the corresponding serum or saliva cotinine levels. So therefore, urinary cotinine levels are likely to be more sensitive as a measure of exposure to tobacco smoke.

---

\* Consumption of certain fruit (*e.g.* aubergines) can lead to the presence of nicotine in biological fluids. However, it is at such low levels that for practical purposes can be ignored.

Cotinine is the preferred marker of smoking status and tobacco smoke intake for both smokers and non-smokers. It is both more sensitive and specific than COHb or thiocyanate as a marker of smoking status. In addition, cotinine has a relatively long half-life. Therefore, cotinine can be employed as a reliable measure of average daily exposure and generally can be found in greater concentrations than the rapidly metabolised precursor, nicotine.

It is desirable to use the complete metabolic profile as a marker for tobacco smoke exposure, owing to the enhanced sensitivity of analysing all metabolites rather than a single metabolite. However, many problems have been associated with the separation and detection of nicotine and its related metabolites. Analytical techniques employed include GC (/MS), HPLC, immunoassay and colourimetric analyses.

Liquid chromatographic methods have been demonstrated<sup>2-4</sup> for the determination of nicotine and metabolites in biological fluids (and LC/MS employing particle beam<sup>5</sup>). However, HPLC is limited in the number of metabolites that can be separated, owing to the similarity of the analyte structures.

Gas chromatography has been extensively employed for the determination of nicotine<sup>6</sup>. Unfortunately, these analytes are polar and therefore require derivatisation prior to analysis by GC.

Immunoassay (both radioimmunoassay<sup>7,8</sup> (RIA) and enzyme-linked immunosorbent assay<sup>9</sup> (ELISA)) and colorimetric<sup>10</sup> analyses have also been developed. RIA and ELISA assays can be obtained that are highly selective for cotinine. However, cross-reactions can occur (for example with 3-hydroxycotinine), which could lead to falsely high results. Colorimetric assays are only quantitative (and not qualitative) for nicotine and its metabolites, *i.e.* the metabolites are detected as a whole, and information on which metabolites are present is not provided.

Capillary electrophoretic methods (CZE and MEKC) have been employed in the determination of nicotine in tobacco products (*i.e.* cigars, cigarettes *etc.*)<sup>11-14</sup>. However, capillary electrophoresis (CZE and MEKC) has not been employed for the determination of nicotine *and* its metabolites. Therefore, CZE (interfaced to mass

spectrometry) has been investigated for its suitability as a separation technique for these analytes.

## **7.2 Experimental**

### **7.2.1 CZE/UV Separation**

All separations were performed on a PrinCE Model 560 CE System (PrinCE Technologies, Emmen, The Netherlands). Fused silica capillaries of 50  $\mu\text{m}$  i.d. x 365  $\mu\text{m}$  o.d. and 85 cm in length were obtained from Composite Metal Services Ltd. (Hallow, UK). UV detection was performed on-column using a Bischoff Lambda 1010 UV/vis detector ( $\lambda = 260$  nm, time constant 0.2 s, range 0.1 Au) at a window burnt in the polyimide coating 53 cm from the inlet. Data acquisition and instrument control was performed using DAX v6.0 software (PrinCE Technologies).

Separations were achieved using a field strength of 350  $\text{Vcm}^{-1}$  (*i.e.* + 30 kV applied to the inlet) unless otherwise stated. Injections were performed hydrodynamically (25 mbar / 0.2 min) corresponding to an injection volume of 5.5 nL.

The capillary was initially conditioned and flushed between analyses with 0.1 M HCl (2 bar / 60 s) followed by water (2 bar / 30 s) and finally buffer (2 bar / 120 s) to regenerate the capillary surface.

### **7.2.2 CZE/MS Analysis**

A Quattro I (Micromass, Manchester UK) triple quadrupole mass spectrometer was used throughout, employing a home-built co-axial sheath-flow interface (Chapter 4) to couple the CE to the mass spectrometer. The sheath liquid comprised 1:1 MeCN : H<sub>2</sub>O + 0.1 % acetic or formic acid, and was supplied at a flow rate of 3 – 5  $\mu\text{L}/\text{min}$  by a Harvard Model 11 Syringe Pump (Edenbridge, UK).

Positive ions were generated through the application of 3.5 kV to the probe tip, with a source cone voltage of 25 V. Desolvation was aided by nitrogen nebulising gas

(~40 L/hr) and bath gas (~225 L/hr). The source was typically operated at a temperature of 65 °C. Capillaries employed for CZE/MS were 50 µm i.d. x 375 µm o.d. and 100 cm in length.

Data was either acquired by selected ion recording of the analyte protonated molecules with a 1 Da window for a dwell time of 0.08 s or in full scan mode from 70 – 200 Da in 0.5s.

### 7.2.3 Investigation of Isobaric Species

Mass spectral detection was performed on a Quattro I triple quadrupole mass spectrometer (Micromass, Manchester, UK) modified to operate with a nanospray source (as outlined in Chapter 4).

Positive ions were generated through the application of 2.5 kV to the probe tip. Desolvation was aided by bath gas (Nitrogen, 50 L/hr).

The analyte under investigation was infused at a concentration of 25 µg/mL in 1:1 MeCN : H<sub>2</sub>O + 0.1 % acetic acid at a flow rate of 500 nL/min (Harvard Model 11 Syringe Pump, Edenbridge, UK).

#### *a) Cone Voltage*

In-source fragmentation was performed at cone voltages of 25 V, 50 V and 100 V. Data was acquired over the mass range 50 – 200 Da in 0.6 s.

#### *b) Product Ion Scans*

The precursor ion was monitored in the final detector of the instrument and was reduced to 50 % height using argon collision gas. The product ions scans were acquired in MCA mode (*i.e.* signal summation) over the mass range  $m/z$  50 – 200 Da in 1.1 s employing a cone voltage of 25 V.

Collision energies employed were +35 eV for *Trans*-3'-hydroxycotinine, 5'-hydroxycotinine and  $\gamma$ -3-Pyridyl- $\gamma$ -oxo-N-methyl-butylamide; and +45 eV for cotinine-N-oxide

#### **7.2.4 Analytes and Reagents**

Nicotine and its metabolites were obtained from Biomedical Research Centre, SHU (RF Smith and K Chambers) their structures are shown in Scheme 7.1 (which is a reduced version of the metabolic pathway<sup>15</sup>). Stock solutions of analytes were diluted to 100  $\mu$ g/mL with water and analysed at this concentration. Acetonitrile was of HPLC grade, water was distilled and deionised by a Milli-Q RG purification system (Millipore, Fisons, Loughborough, UK). Ammonium acetate, ammonium formate, acetic acid and formic acid were of HPLC grade or better and were purchased from Aldrich (Poole, UK). All other materials were of reagent grade or better.

##### *7.2.4.1 Analysis of Biological Fluid*

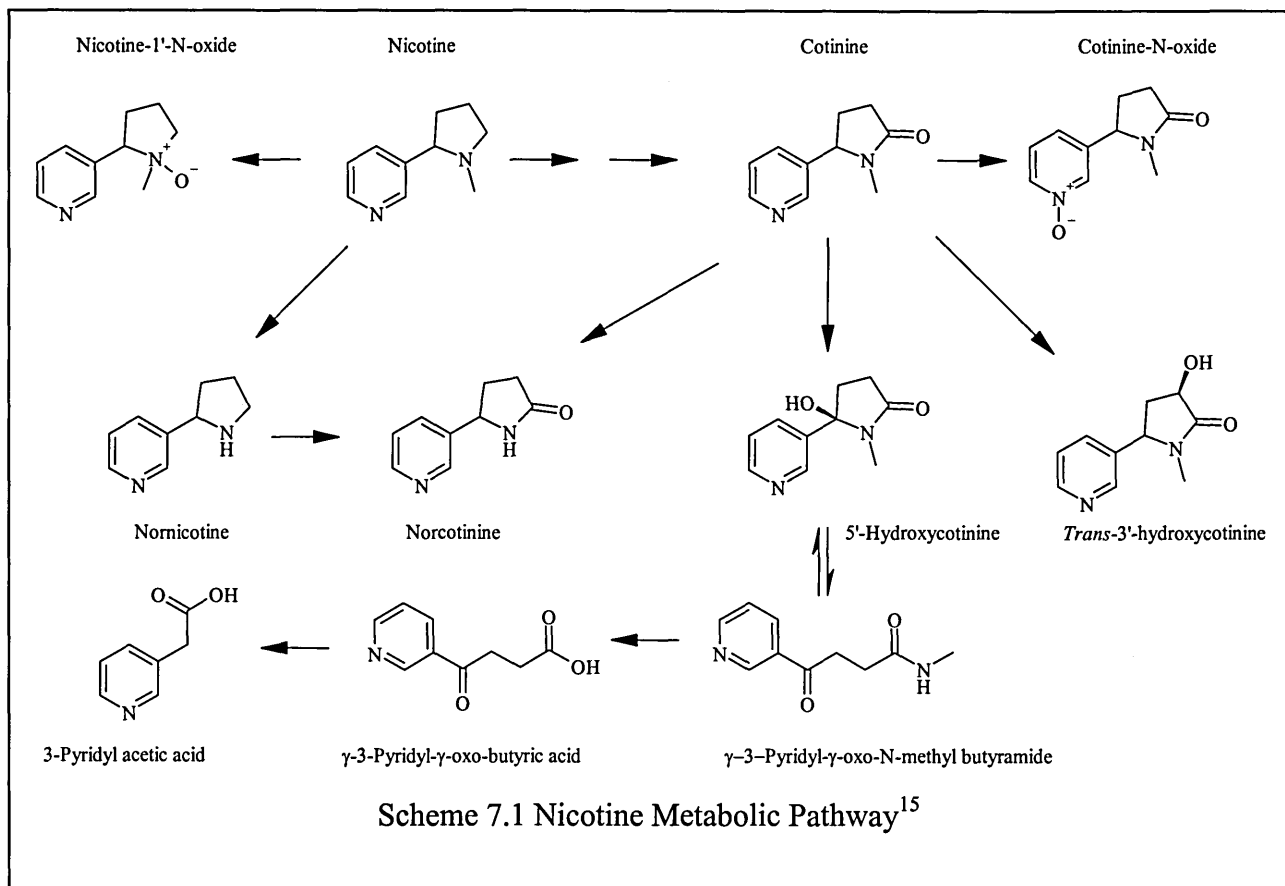
Urine samples were obtained from five smokers and pooled. CZE/MS was performed as above employing the buffer determined in section 7.3.2. The neat smokers' urine sample was injected hydrodynamically (25 mbar / 0.2 minutes). The spiked sample contained 100  $\mu$ g/mL nicotine and cotinine in the pooled smokers' sample.

#### **7.2.5 Buffer Preparation**

The buffers were prepared by dissolution of a suitable quantity of electrolyte in water; pH manipulation was achieved employing 0.1 M HCl (phosphate), glacial acetic acid (ammonium acetate) or formic acid (ammonium formate).

All samples and separation buffers were degassed prior to analysis employing a Branson 1210 ultrasonic bath and filtered through a 0.2  $\mu$ m syringe filter. pH measurements were determined using a Hanna Instruments Checker (Fisher, Loughborough, UK), which was calibrated with solutions of known pH.

The running buffers were prepared on a daily basis and replenished every five analyses to prevent electrolytic depletion and changes in pH.



### 7.3 Results / Discussion

#### 7.3.1 Development of CZE/MS Separation

A CZE/UV separation had previously been developed<sup>16</sup>, unfortunately the method employed a high concentration of an involatile buffer (phosphate), which would be incompatible with our mass spectrometer. Therefore a suitable separation was required that employs a volatile buffer system.

The separation shown in Figure 7.1 (Section 7.4 Electropherograms and Mass Spectra) corresponds to the original conditions<sup>16</sup>. These conditions were 100 mM disodium hydrogen phosphate pH 3.0 (using HCl), with the addition of 0.01 % triethylamine (TEA, interacts with capillary wall reducing analyte-wall interaction) and 10 % MeCN.

The EOF was not detected within 20 minutes and only 8 peaks from the 11 analytes were observed.

Substituting the phosphate for a volatile buffer (100 mM ammonium acetate, pH 3.7 0.01 % TEA and 10 % MeCN) resulted in an extremely unstable baseline, with only 3 peaks observed. Figure 7.2 shows the electropherogram of 100 mM ammonium acetate (pH 3.7) without additives, 6 analytes were observed within 20 minutes. Reduction of the buffer strength (50 mM, increasing the EOF velocity) allowed the separation of 7 peaks in less than 12 minutes. Further reduction in buffer strength to 10 mM (Figure 7.3) did not increase the speed of separation. However, the efficiency did significantly decrease (Nicotine efficiency, approximately 12 000 plates per metre employing 10 mM buffer *cf.* 70 000 plates per metre employing 100 mM buffer).

A reduction in buffer pH would result in a decreased EOF (reducing the  $\mu_{\text{EOF}}$  contribution to  $\mu_{\text{OBS}}$ ) and an increase in analyte charge. Figure 7.4 shows the separation obtained employing 25 mM ammonium formate adjusted to pH 2.8 (with formic acid). The baseline stability was poor, however 9 peaks could be observed. Increasing the buffer strength to 50 mM (Figure 7.5) improved peak shape allowing the identification of 9 peaks. The addition of 10 % MeCN to the buffer improved baseline stability and efficiency. Figure 7.6 shows the electropherogram obtained employing 50 mM ammonium formate at pH 2.8 including 10 % MeCN. When thiourea was added to the sample (to determine the EOF and mobilities) 11 peaks in total were observed, one analyte migrated closely to the EOF, indicating it was only weakly charged at this pH. Table 7.1 summarises the data obtained from this separation.

The migration time reproducibility was extremely high, *i.e.* 0.13 – 0.25 % RSD, this could allow the identification of analytes by migration time alone.

There is a range of efficiencies, between ~70 000 and 800 000 plates /m, with the analytes seeming to form two groups. Nicotine and cotinine seem to form broad peaks (and hence low efficiency). In addition, peak 8 was broad; this was because it corresponds to two analytes, 5'-Hydroxycotinine and  $\gamma$ -3-Pyridyl- $\gamma$ -oxo-N-methylbutyramide. These two analytes are in equilibrium, thus at this pH one of the isomers

would be dominant (it is not known which structure dominates), thus there will be twice as much of this analyte present in the column. The remaining analytes all form highly efficient narrow peaks.

The purpose of this analysis was to determine whether CZE could be employed to quantify these metabolites within biological matrices (*i.e.* urine). Therefore, reproducible peak areas were necessary. Under these conditions, peak area reproducibility was poor (between 3 – 22 %); this was likely to be caused by variations in sample injection. Reproducibility could be improved by employing an internal standard, such as nicotinic acid or deuterated nicotine or cotinine (if separable from the analytes).

These separation conditions (*i.e.* 50 mM ammonium formate, pH 2.8 10 % MeCN) will therefore be used for all further analyses.

Table 7.1 Nicotine Metabolites Separation Data (n = 7)

	Mean migration time / min	$t_m$ % RSD	Theoretical plates <sup>†</sup> / (m)	Mobilities / $10^{-9} \text{ m}^2 (\text{Vs})^{-1}$	Peak area % RSD
Normicotine	4.531	0.24	309 000	44.95	4.94
Nicotine	5.035	0.24	65 000	39.73	4.60
Nicotine-1'-N-oxide	5.443	0.24	381 000	36.21	3.43
Norcotinine	6.793	0.23	428 000	27.60	3.87
Cotinine	7.268	0.22	129 000	25.32	4.16
3-Pyridylacetic acid	7.963	0.19	405 000	22.49	4.97
<i>Trans</i> -3'- Hydroxycotinine	8.083	0.21	281 000	22.05	2.83
5'-Hydroxycotinine & $\gamma$ -3-Pyridyl- $\gamma$ -oxo- N-methylbutyramide	8.351	0.21	105 000	21.11	3.75
$\gamma$ -3-Pyridyl- $\gamma$ -oxo- butyric acid	13.379	0.13	783 000	10.49	21.89
Cotinine-N-oxide	34.772	0.25	216 000	0.01	18.46

<sup>†</sup> Calculated using  $N=5.54(t_m/w_{0.5})^2$ , where  $t_m$  = migration time (min.) and  $w_{0.5}$  = peak width at half height (min.).

### 7.3.2 Transfer of Analysis to CZE/MS Analysis

Loop injections of each analyte were performed to determine whether any fragmentation occurred, and to confirm the molecular mass. Each analyte was observed as the protonated molecule,  $[M+H]^+$ .

The co-axial sheath flow CZE/MS interface was set up as outlined in Chapter 4. The mass spectrometer was tuned for maximum sensitivity using electrophoretic infusion of nicotine and cotinine in the buffer (50 mM ammonium formate pH 2.8, 10 % MeCN) using a sheath liquid of 1:1 MeCN : H<sub>2</sub>O + 0.1 % acetic acid at 3  $\mu$ L/min. The column was then flushed with buffer. An injection of nicotine, cotinine and 3'-hydroxycotinine (100  $\mu$ g/mL of each for 25 mbar / 0.2 min, corresponding to ~ 450 pg of each analyte) was then performed. However, no peaks were observed, in addition the baseline and separation current were extremely erratic. The capillary was reconditioned and the analysis repeated, once more no peaks were observed. A mismatch in conductivities between the separation buffer and sheath-liquid was suspected to be the problem.

The buffer concentration was reduced to 25 mM ammonium formate pH 2.8 without MeCN. Analysis of nicotine, cotinine and 3'-hydroxycotinine was performed, which resulted in broad peaks. When the separation was repeated with the addition of 10 % MeCN, the peak widths improved. However, migration times were erratic, the addition of 50 mbar to the inlet vial improved reproducibility. The additional pressure served to induce a laminar flow within the capillary, which reduced migration times and peak resolution. However, most of the analytes could be discriminated by mass (there are 6 isobaric species, these will be dealt with in Section 7.3.3).

Replicate injections were performed of the separation of nicotine and metabolites with a supplementary pressure of 50 mbar. It has been suggested<sup>17</sup> that enhanced sensitivity can be obtained in CZE/MS by matching the sheath liquid and buffer compositions. In addition, it is often advantageous to use a high percentage of organic solvent in the sheath liquid (to aid the electrospray process), whereas its inclusion in the separation media can alter selectivity (*e.g.* Chapter 4 section 4.3.3). Therefore, the sheath liquid was modified to include formic acid (rather than acetic acid). This significantly

improved peak shapes and analyte signal-to-noise ratios. An increase in the flow rate to 5  $\mu\text{L}/\text{min}$  further improved the spray stability and sensitivity.

A representative separation based on these conditions (25 mM ammonium formate pH 2.8, 10 % MeCN with 5  $\mu\text{L}/\text{min}$  sheath liquid 1:1 MeCN : H<sub>2</sub>O + 0.1 % formic acid) is shown in Figure 7.7 with MS detection by selected ion recording (SIR). Data was also acquired in full scan mode (Figure 7.8), a reduction in signal-to-noise was observed when compared to SIR data, due to the decreased dwell time on the  $m/z$  of interest. The corresponding mass spectra (Figure 7.9) all feature protonated molecules, with little interference.

Replicate injections were performed employing SIR acquisition. These data are summarised in Table 7.2. The separation integrity has been maintained with the modification of the buffer system and the application of supplementary pressure.

The migration times were longer for the CZE/MS separation, because of the increased column length and reduced electric field strength. However, when the analyte electrophoretic mobilities for UV and MS detection were compared (Table 7.3), the mobilities were increased for CZE/MS. The increase in mobility can be attributed to the application of supplementary pressure (50 mbar) to the inlet vial, which would induce laminar flow through the capillary, thus increasing the linear velocity.

The migration time reproducibility is good (typically < 1.2 %), even though data acquisition was initiated manually.

Table 7.2 Nicotine Metabolites CZE/MS Separation Data (n = 6)

	Mean migration time / min	$t_m$ % RSD	Theoretical plates <sup>†</sup> / (m)	Mobilities <sup>§</sup> / $10^{-9} \text{ m}^2 (\text{Vs})^{-1}$	Peak area % RSD <sup>**</sup>
Normicotine	7.21	1.14	79 000	52.8	51.48
Nicotine	7.65	1.03	18 000	48.3	22.38
Nicotine-1'-N-oxide	8.11	1.06	87 000	44.3	17.70
Norcotinine	9.94	1.08	32 000	31.6	116.74
Cotinine	10.56	0.96	22 000	28.3	10.30
3-Pyridylacetic acid	10.91	0.89	25 000	26.7	20.65
<i>Trans</i> -3'- Hydroxycotinine	11.06	0.85	87 000	25.9	15.56
5'-Hydroxycotinine & $\gamma$ -3-Pyridyl- $\gamma$ -oxo- N-methylbutyramide	12.30	1.13	85 000	20.9	20.24
$\gamma$ -3-Pyridyl- $\gamma$ -oxo- butyric acid	12.36	0.32	76 000	20.7	11.94
Cotinine-N-oxide	22.74	0.25	69 000	0.16	32.39

<sup>†</sup> Calculated using  $N=16(t_m/w_b)^2$ , where  $t_m$  = migration time (min.) and  $w_b$  = peak width at base (min.).

<sup>§</sup> The effective mobilities quoted are not the true effective mobilities due to the supplementary pressure applied, but they allow comparison of analyte flow velocities within columns of differing lengths, i.e. CZE/UV and CZE/MS column.

<sup>\*\*</sup> Taken from SIR data only, therefore n = 5.

Table 7.3 Electrophoretic Mobilities of Analytes Employing CZE/UV and CZE/MS

	Electrophoretic mobilities / $\times 10^{-9} \text{ m}^2 (\text{Vs})^{-1}$		
	CZE/MS	CZE/UV	$\Delta$ mobility
Nornicotine	52.8	45.0	7.8
Nicotine	48.3	39.7	8.6
Nicotine-1'-N-oxide	44.3	36.2	8.1
Norcotinine	31.6	27.6	4.0
Cotinine	28.3	25.3	3.0
3-Pyridylacetic acid	26.7	22.5	4.2
<i>Trans</i> -3'-Hydroxycotinine	25.9	22.0	3.9
5'-Hydroxycotinine & $\gamma$ -3-Pyridyl- $\gamma$ -oxo-N-methyl-butylamide	20.9	21.1	-0.2
$\gamma$ -3-pyridyl- $\gamma$ -oxo-butylamide	20.1	10.5	9.6
Cotinine-N-oxide	0.16	0.01	0.15

Plate numbers were reduced for the CZE/MS separation; this could be attributed to an increase in column length and reduced field strength. In addition, the induced laminar flow within the capillary would disrupt the flat flow profile, increase zone length, and hence reduce efficiency.

The peak area reproducibility is extremely poor ( $\sim 10 - 120$  % RSD, where  $n = 5$ ), for quantification purposes an internal standard would be essential. The variation in peak area is too great to be due to deviations in injection volume; instrumental response (*i.e.* spray stability and efficiency) must be playing a role in the variability of peak areas. It has also been shown that variations in analyte velocity ( $v$ ) through the column can affect the peak area<sup>18</sup> as follows:

$$A = \frac{kn}{v} = \frac{knL}{\mu_{EOF}V} \quad \dots(7.1)$$

$A$  = Peak area;  $k$  = Constant<sup>††</sup>;  $n$  = Amount of analyte injected;  $L$  = Capillary length;  $\mu_{EOF}$  = Electroosmotic mobility;  $V$  = Applied voltage.

Thus, variation in analyte velocity / ionisation efficiency will affect peak area, the use of an internal standard could minimise these effects

<sup>††</sup> Dependant on ionisation efficiency.

### 7.3.3 Isobaric Species

A major advantage of using mass spectrometry over UV absorption is the increase in selectivity, temporally co-migrating or poorly separated peaks can be resolved by mass discrimination. However, isobaric species, *i.e.* compounds of the same nominal mass (usually isomers), cannot be resolved by mass alone. In this investigation there are two sets of isobaric species (*trans*-3'-hydroxycotinine; 5'-hydroxycotinine; cotinine-N-oxide and  $\gamma$ -3-Pyridyl- $\gamma$ -oxo-N-methyl-butylamide all with a mass of 192; norcotinine and nicotine both have a mass of 162).

Norcotinine and nicotine are well resolved and can be differentiated by their relative response. Nicotine gives a significantly higher response than norcotinine when present at the same concentration employing UV and MS detection.

Cotinine-N-oxide is well resolved from the other analytes (migrates close to the EOF) and could be identified by migration time. However, 3'-hydroxycotinine and 5'-hydroxycotinine (in equilibrium with  $\gamma$ -3-Pyridyl- $\gamma$ -oxo-N-methyl-butylamide) migrate close together and could not be differentiated by migration time or the corresponding mass spectra. It is important to differentiate between *trans*-3'-hydroxycotinine and 5'-hydroxycotinine, because the 3'-hydroxy form is a major urinary metabolite of nicotine (*ca.* 38 %) <sup>15</sup> and is used as a marker for smoking status, thus it requires quantification without interference.

The analytes may be discriminated by the use of tandem mass spectrometry or in-source fragmentation (via manipulation of cone voltage), which could provide structural-specific product ions.

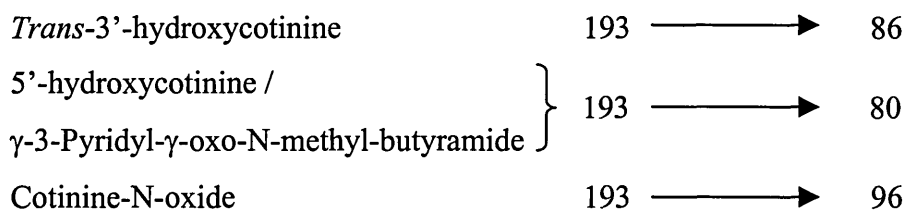
The effect of in-source fragmentation on the isobaric species is shown in Figure 7.10. Product ion scans of the analytes were also acquired (Figure 7.11). Employing elevated cone voltages and product ion MS/MS, fragment ions have been generated. The interpretation of these ions is given in Table 7.4.

Table 7.4 Interpretation of Isobaric Analyte Fragments

	Analyte structure	Product ions
Cotinine-N-oxide		 98 96
5'-hydroxycotinine		 80
$\gamma$ -3-Pyridyl- $\gamma$ -oxo-N-methyl-butyr- amide		
<i>Trans</i> -3'-hydroxy- cotinine	  86 58	

Based on these assigned structures it would be possible to differentiate between these analytes by monitoring specific fragment ions.

*i.e.*



Therefore a multiple reaction monitoring (MRM) analysis could be used<sup>††</sup>, which would allow identification of *Trans*-3'-hydroxycotinine and cotinine-N-oxide through the transition 193 → 86 and 193 → 96 respectively. Identification of 5'-hydroxycotinine /  $\gamma$ -3-Pyridyl- $\gamma$ -oxo-N-methyl-butyr-  
amide would not be possible as the sole product ion formed was common to all of the isobaric species. However, if the other two isobaric species were identified then the presence of an ion of  $[M+H]^+$   $m/z$  193, which formed a product ion at  $m/z$  80 would suggest the presence of 5'-hydroxycotinine (and  $\gamma$ -3-pyridyl- $\gamma$ -oxo-N-methyl-butyr-  
amide).

The presence of a common product ion at  $m/z$  80 could be employed in precursor ion scanning as a rapid identification (or screening employing MRM) method for these analytes within an unknown sample.

### 7.3.4 Analysis of Biological Samples for Nicotine Metabolites

The potential of this separation for the identification of nicotine metabolites has been demonstrated, however, an internal standard would be essential for quantification.

Biological matrices contain a large quantity of compounds (*i.e.* salts, peptides *etc.*), therefore there may be problems identifying target compounds within these matrices due to interferences. Urine contains the highest concentration of nicotine metabolites, for example it contains up to 1400 ng/mL cotinine (whereas saliva and plasma contain up to 300 ng/mL), therefore making detection easier. CZE unlike HPLC can tolerate neat urine without desalting, providing the columns are thoroughly conditioned between analyses (to remove any adhered material from the surface). Urine samples from smokers and non-smokers were analysed for nicotine and related metabolites.

Figure 7.12 shows the SIR total ion electropherogram obtained from the injection from a pool of five smokers' urine. Unfortunately, no peaks were observed, suggesting that the levels of analyte within the sample were below the detection limit<sup>§§</sup>. The sample was then spiked with 100 µg/mL of nicotine and cotinine and analysed (Figure 7.13). Two peaks were observed at the migration times that corresponded to the analytes, thus indicating that these analytes could be detected within this matrix.

In order to analyse urine for nicotine metabolites; sample preconcentration would be required prior to analysis. This could take the form of solid phase extraction (SPE) or transient-isotachopheresis (t-ITP). SPE is simple to use and is frequently employed in chromatography. In addition, SPE would have the advantage of removing salts from the sample decreasing its conductivity, therefore increasing sample stacking. Whereas t-ITP is more complex to implement, requiring two buffers of differing conductivity. However, t-ITP can significantly increase sample injection volumes and focus them into narrow zones, thus increasing the sample concentration within the column.

---

<sup>††</sup> The MRM analysis was not possible on our instrumentation due to a lack of MS/MS sensitivity.

<sup>§§</sup> As yet not determined for this system.

7.4 Electropherograms and Mass Spectra

DAX 6.0: Martin Palmer 15/08/99 17:16:06PM

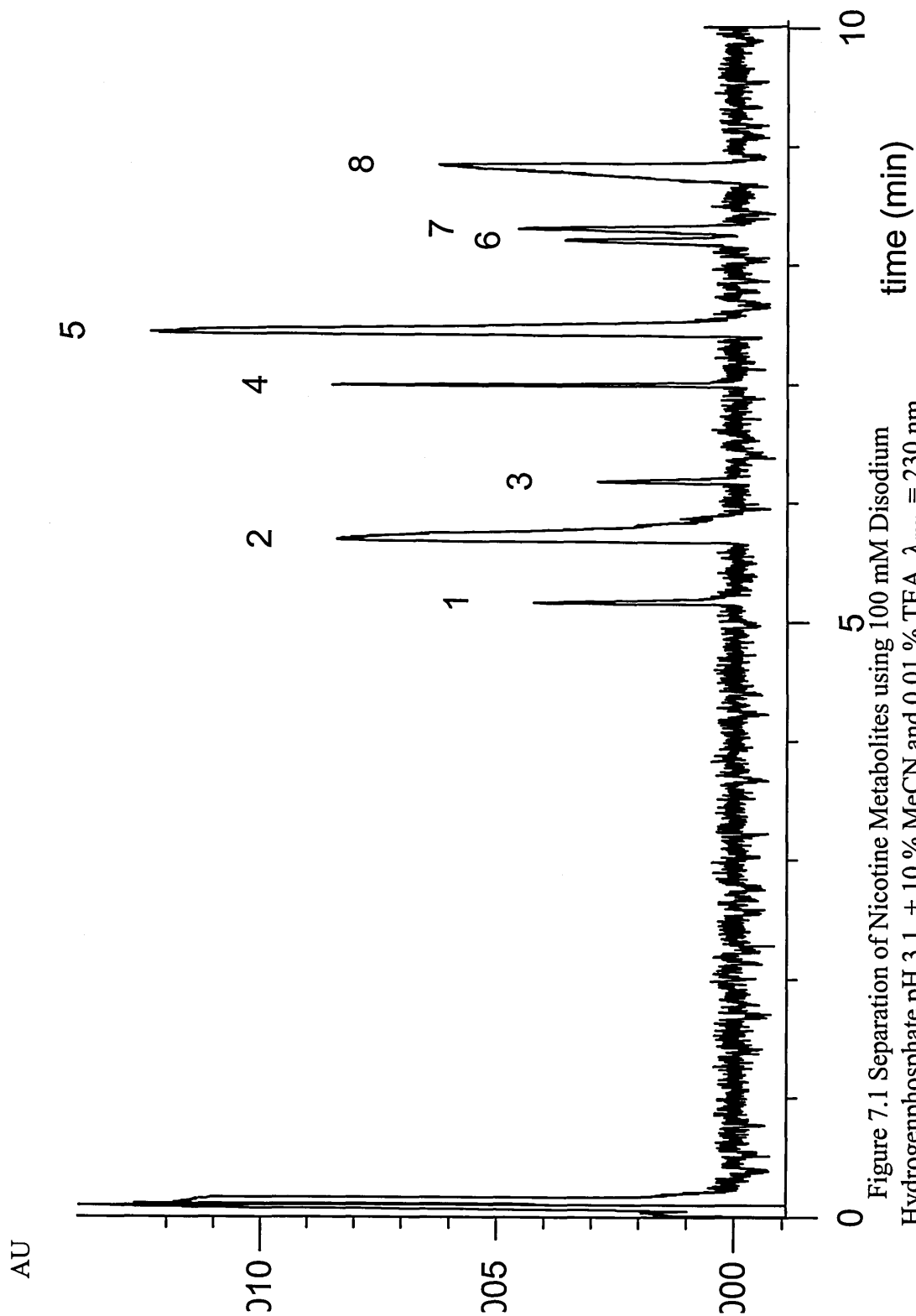


Figure 7.1 Separation of Nicotine Metabolites using 100 mM Disodium Hydrogenphosphate pH 3.1, + 10 % MeCN and 0.01 % TEA,  $\lambda_{max} = 230$  nm

DAX 6.0: Martin Palmer 15/08/99 17:14:27PM

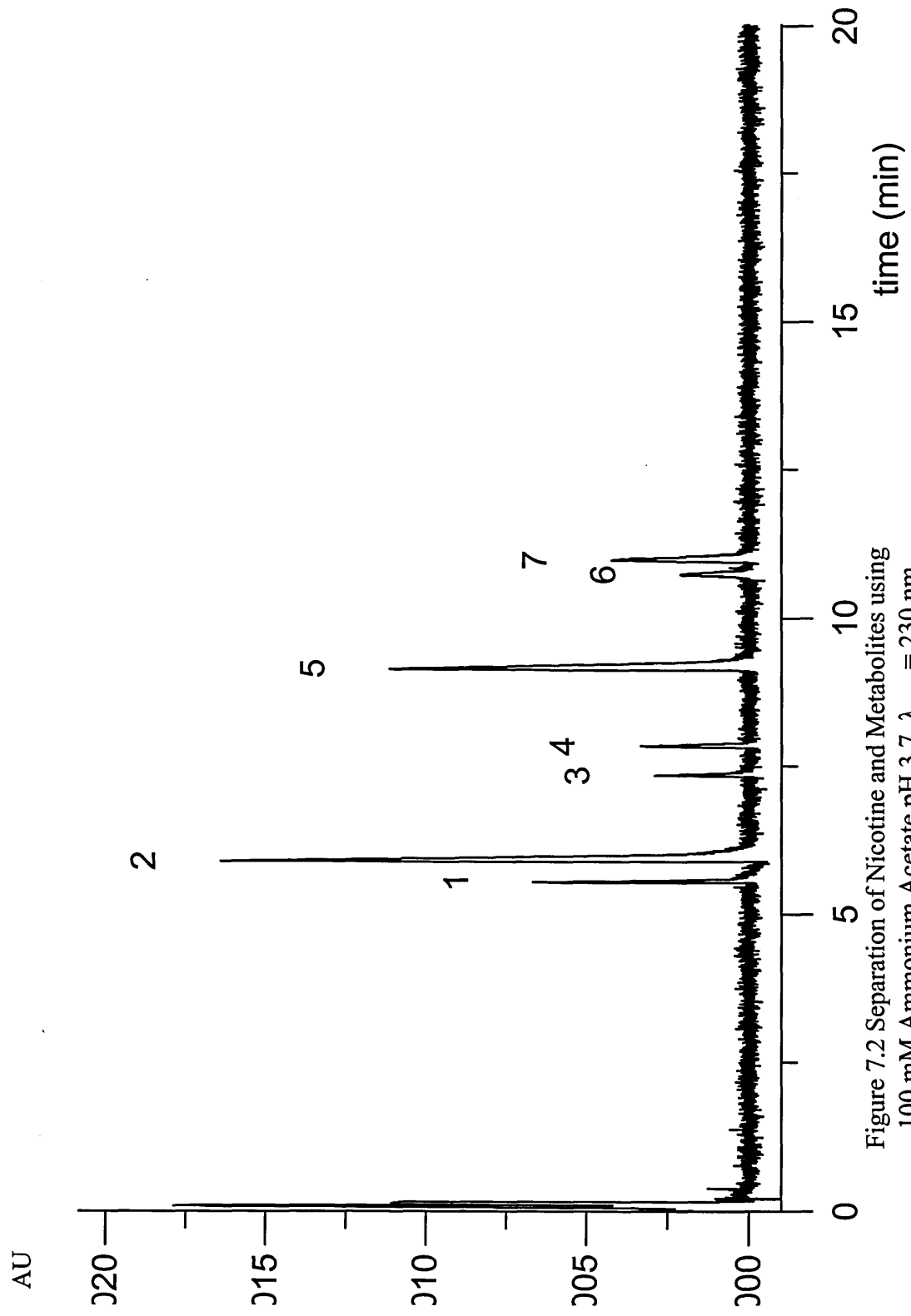


Figure 7.2 Separation of Nicotine and Metabolites using 100 mM Ammonium Acetate pH 3.7,  $\lambda_{\text{max}} = 230 \text{ nm}$

DAX 6.0: Martin Palmer 15/08/99 17:15:22PM

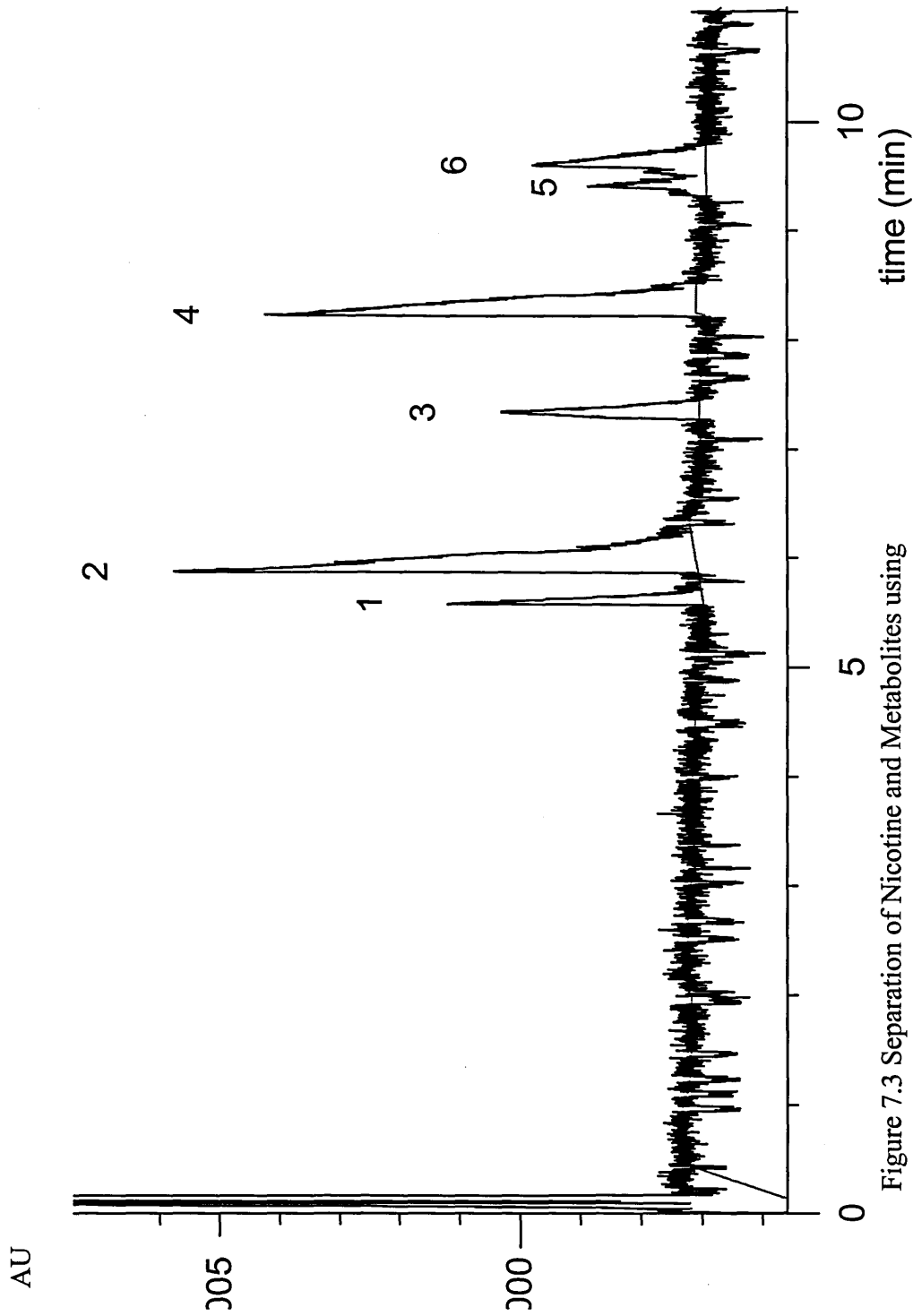


Figure 7.3 Separation of Nicotine and Metabolites using  
10 mM Ammonium Acetate pH 3.7,  $\lambda_{\text{max}} = 230 \text{ nm}$

DAX 6.0: Martin Palmer 15/08/99 17:14:47PM

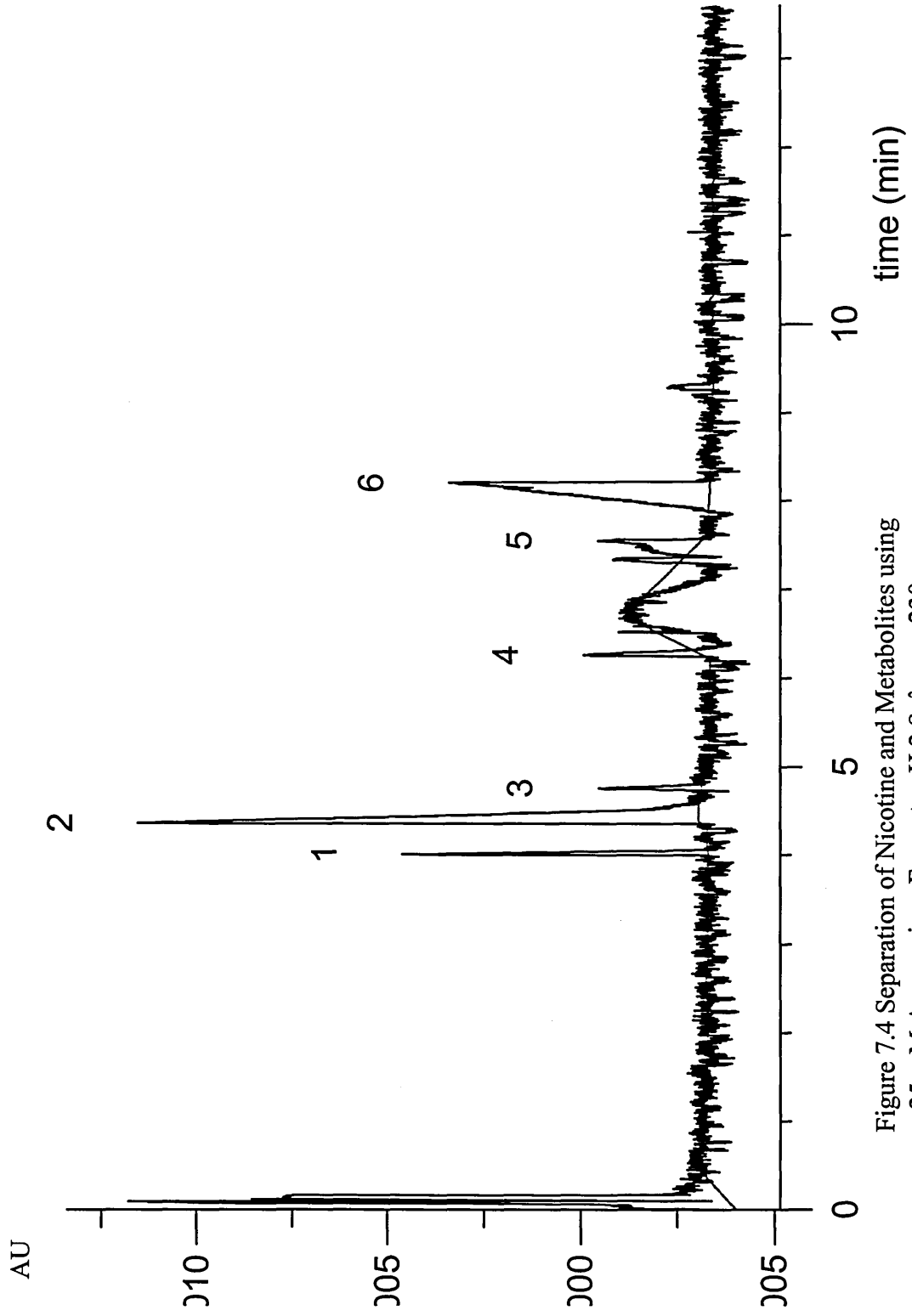


Figure 7.4 Separation of Nicotine and Metabolites using  
25 mM Ammonium Formate pH 2.8,  $\lambda_{\text{max}} = 230 \text{ nm}$

DAX 6.0: Martin Palmer 15/08/99 17:14:05PM

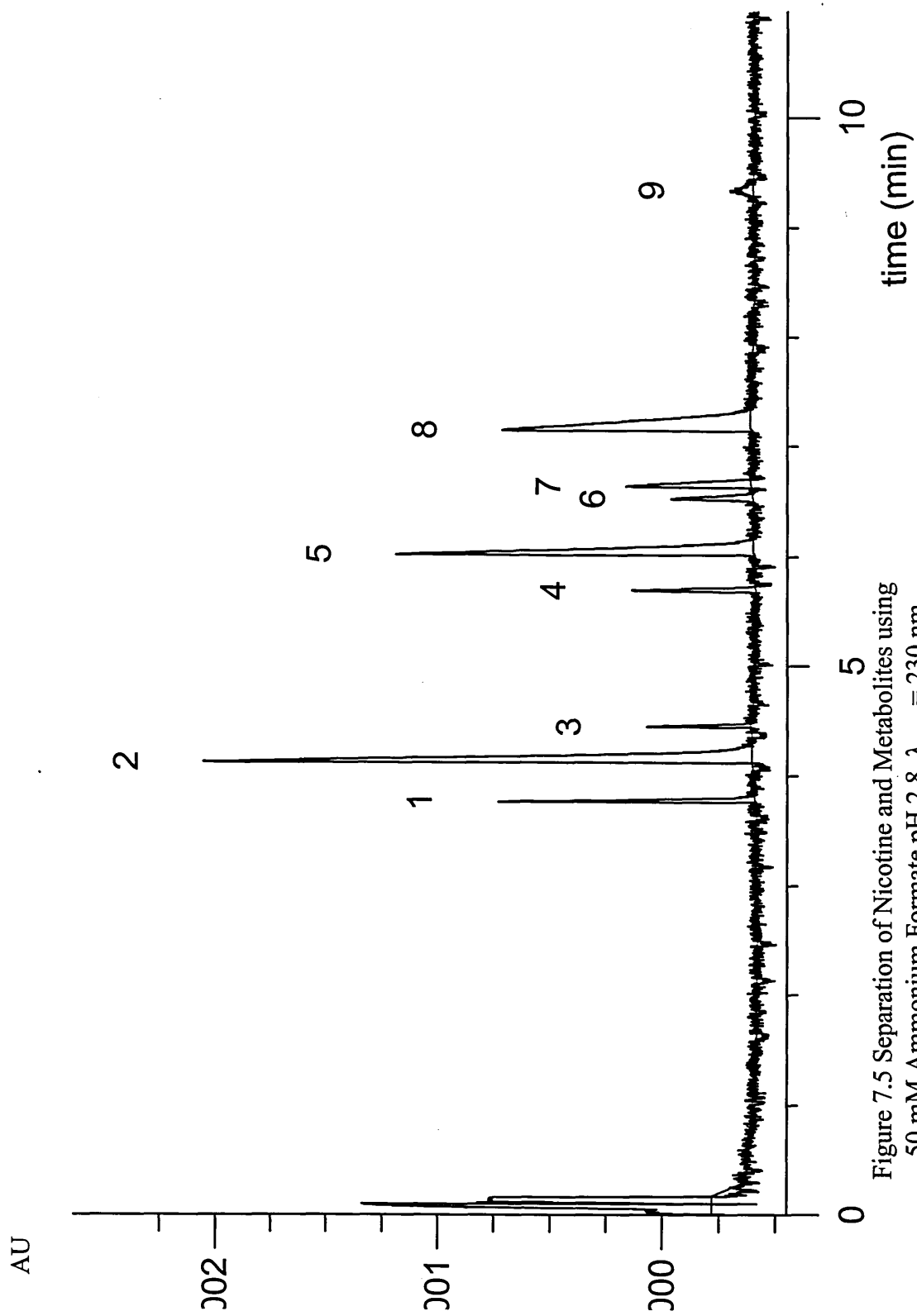


Figure 7.5 Separation of Nicotine and Metabolites using 50 mM Ammonium Formate pH 2.8,  $\lambda_{\text{max}} = 230 \text{ nm}$

DAX 6.0: Martin Palmer 22/07/99 18:22:24PM

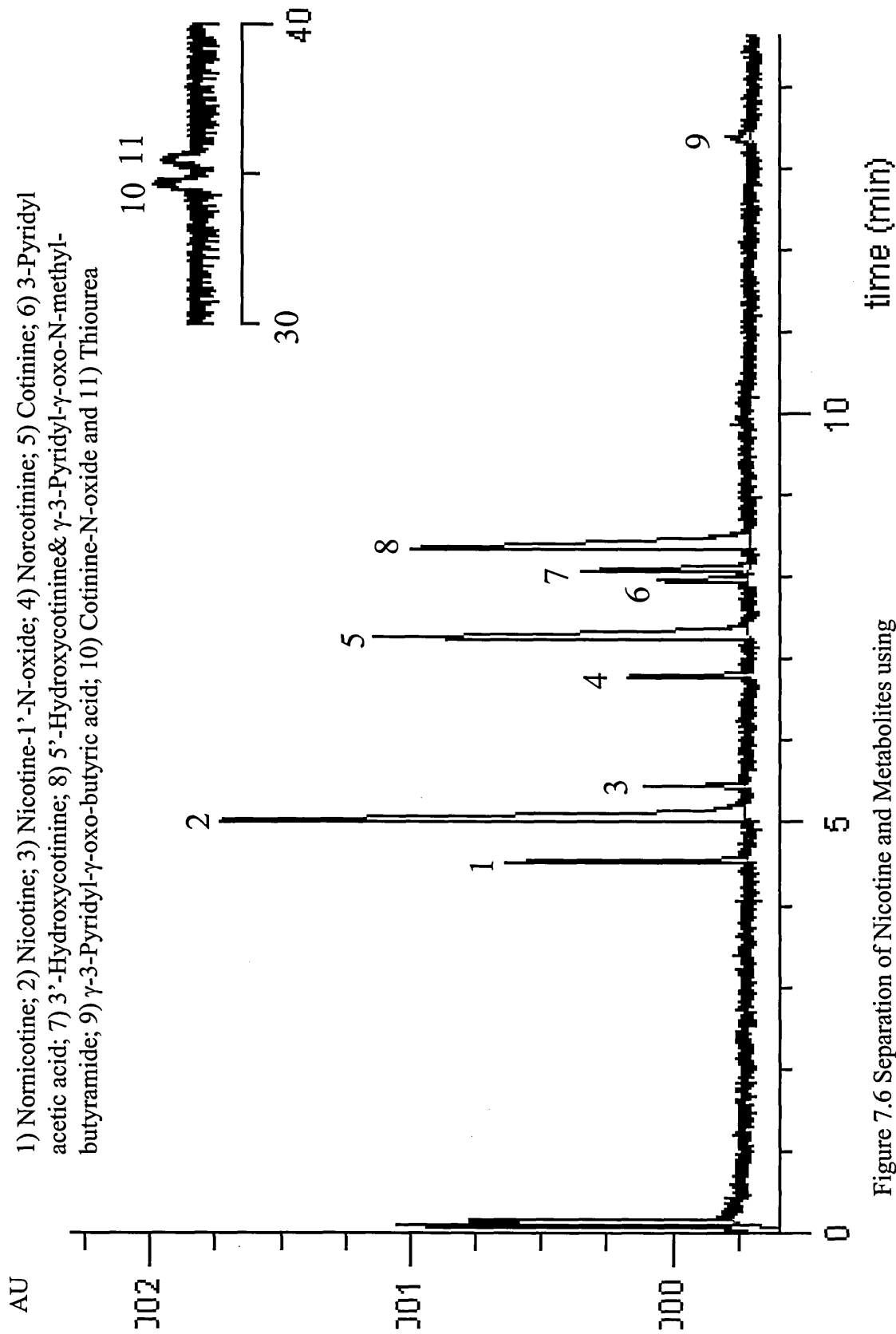


Figure 7.6 Separation of Nicotine and Metabolites using 50 mM Ammonium Formate pH 2.8 + 10 % MeCN,  $\lambda_{\text{max}} = 230 \text{ nm}$

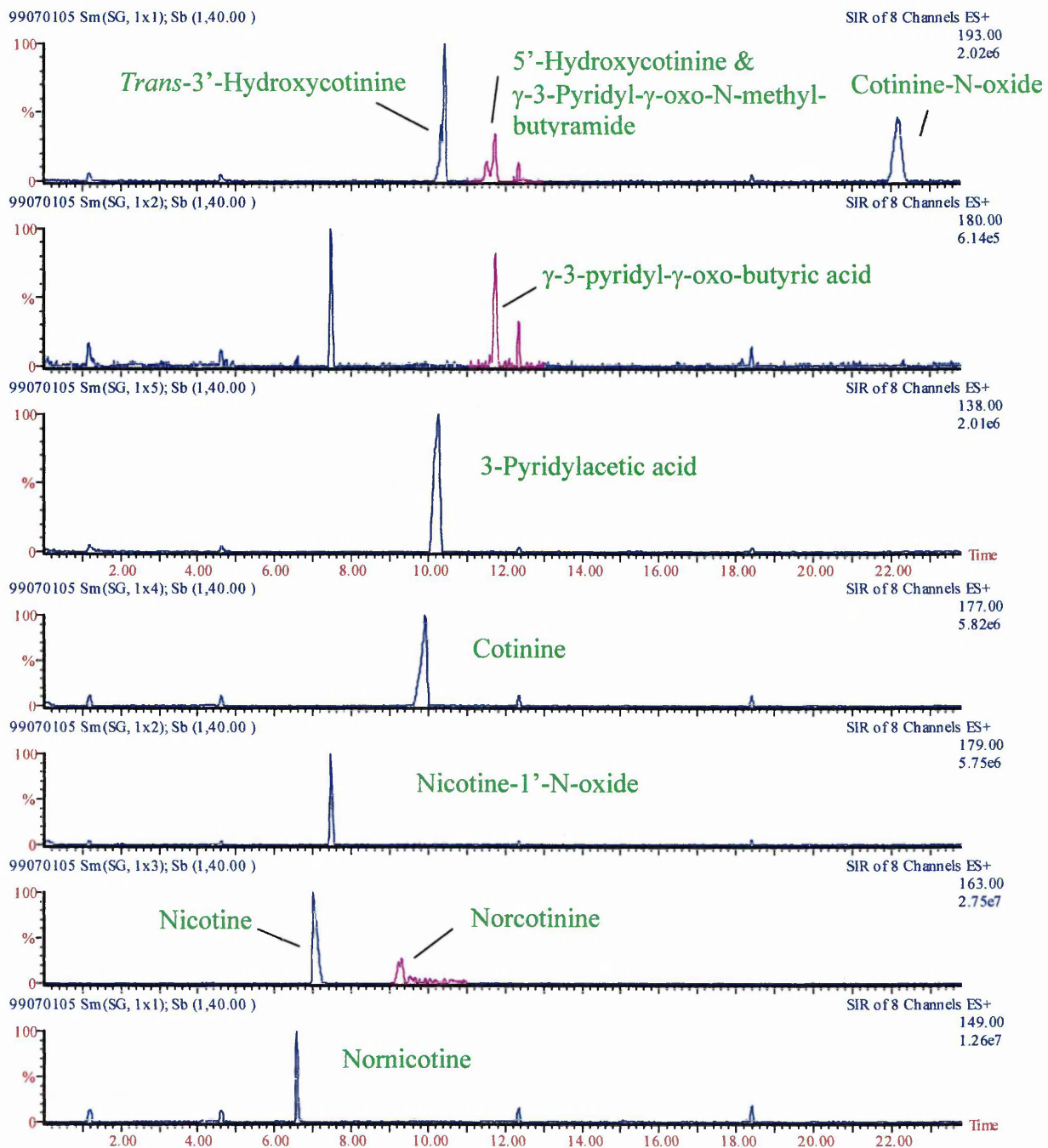


Figure 7.7 Selected Ion Recording Mass Electropherograms of Nicotine Metabolites

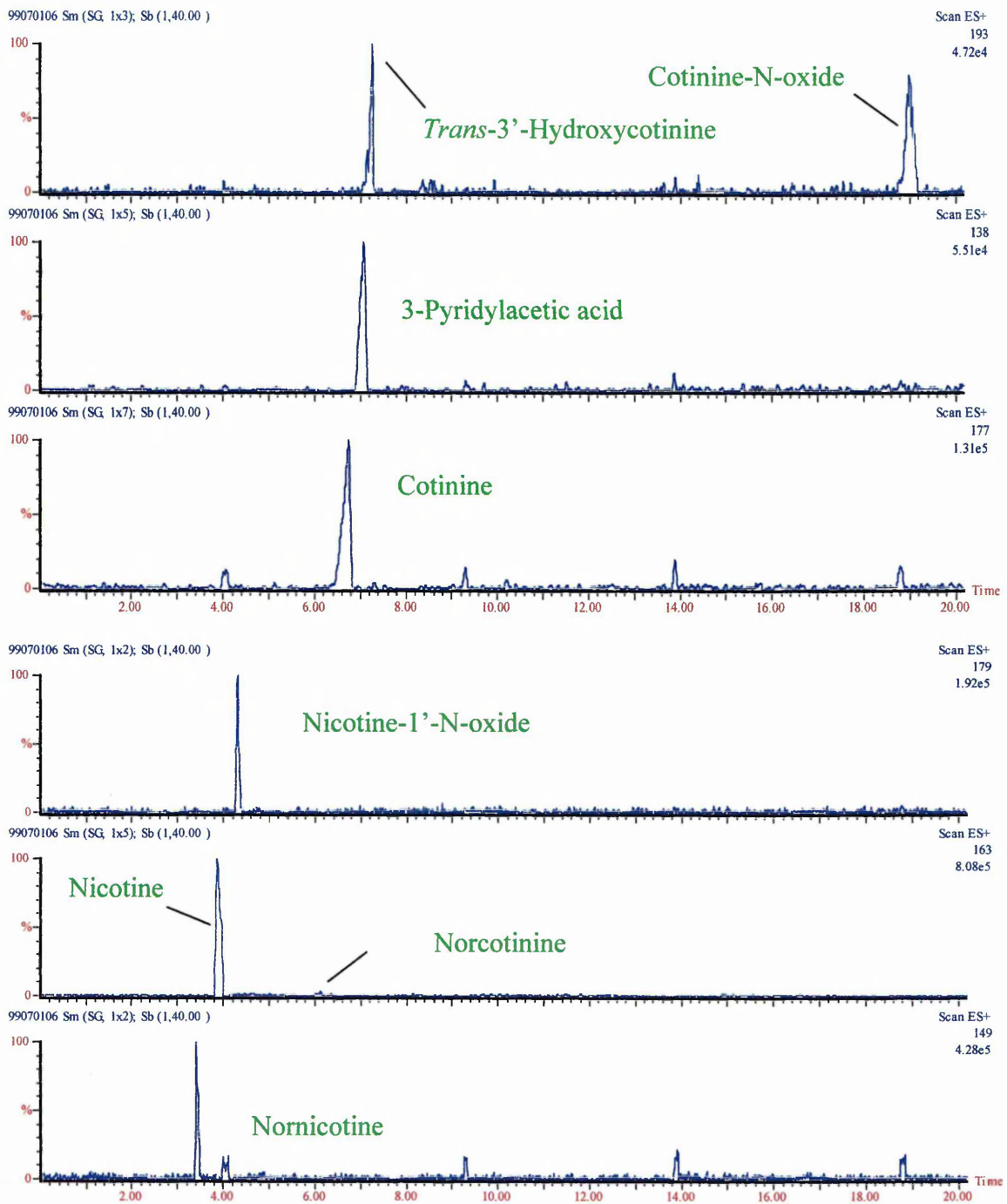


Figure 7.8 Full Scan Mass Electropherograms of Nicotine Metabolites

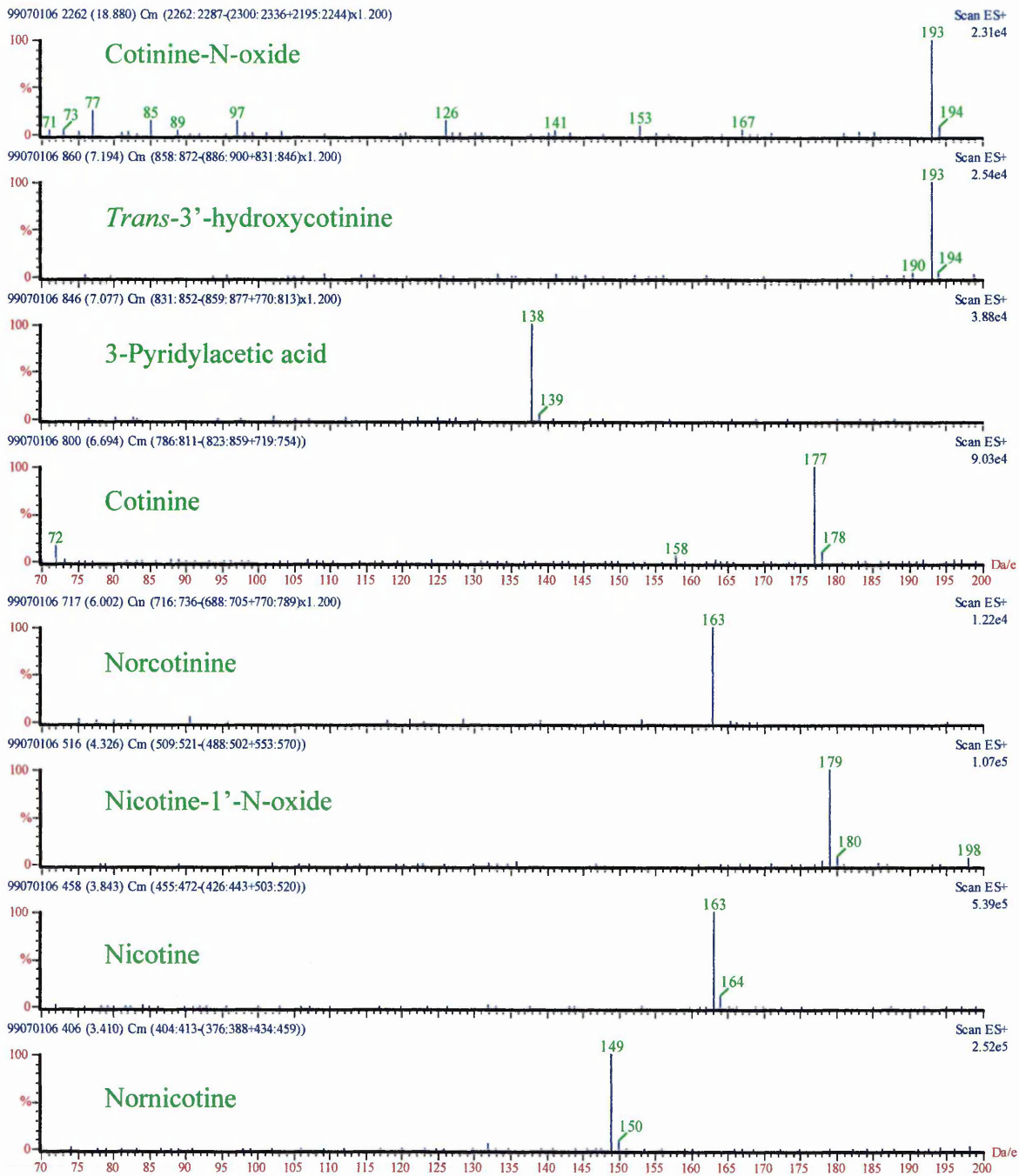


Figure 7.9 Mass Spectra of Nicotine Metabolites

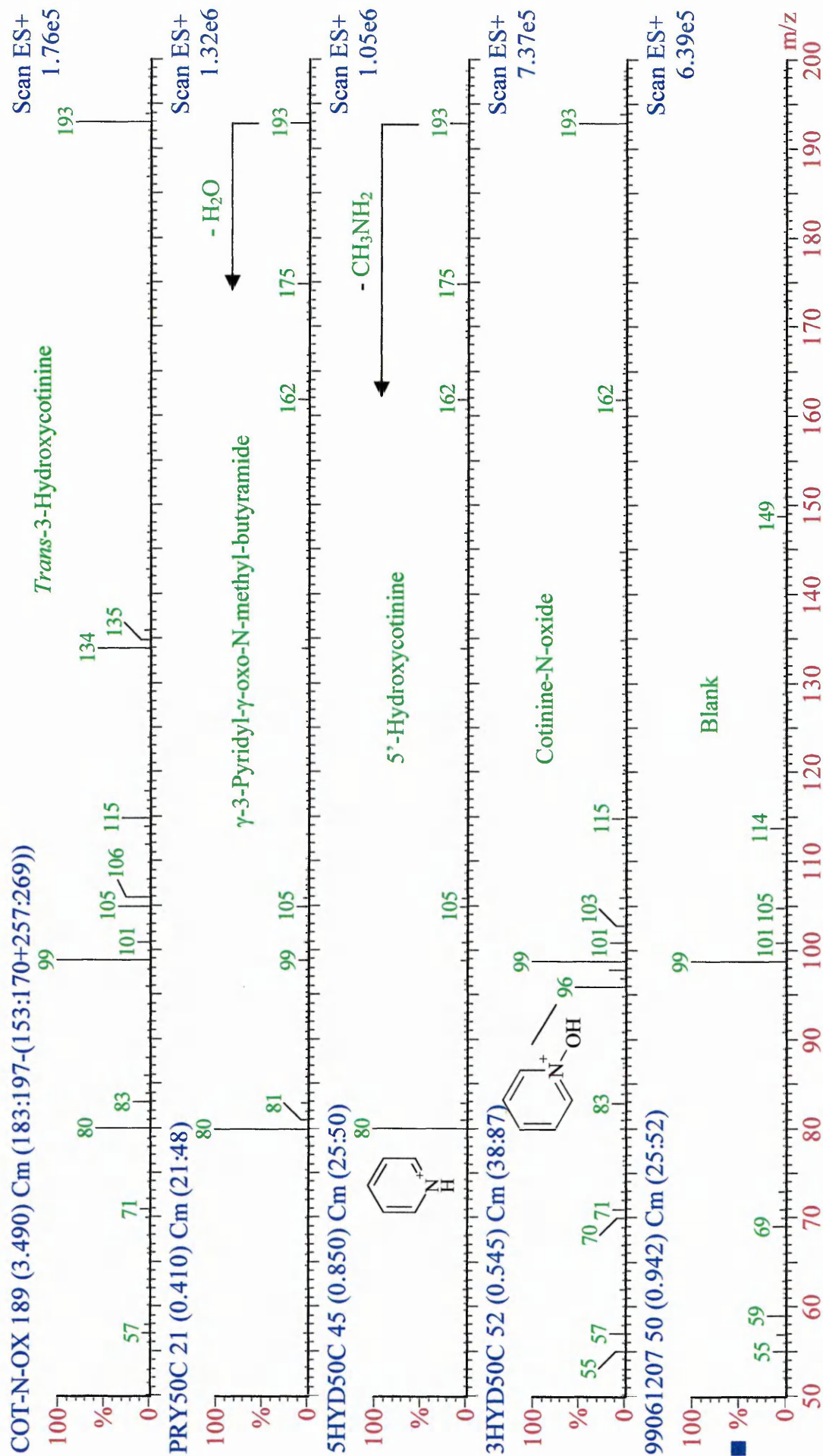


Figure 7.10 Mass Spectra of In-source Dissociation, using a Cone Voltage of 50 V

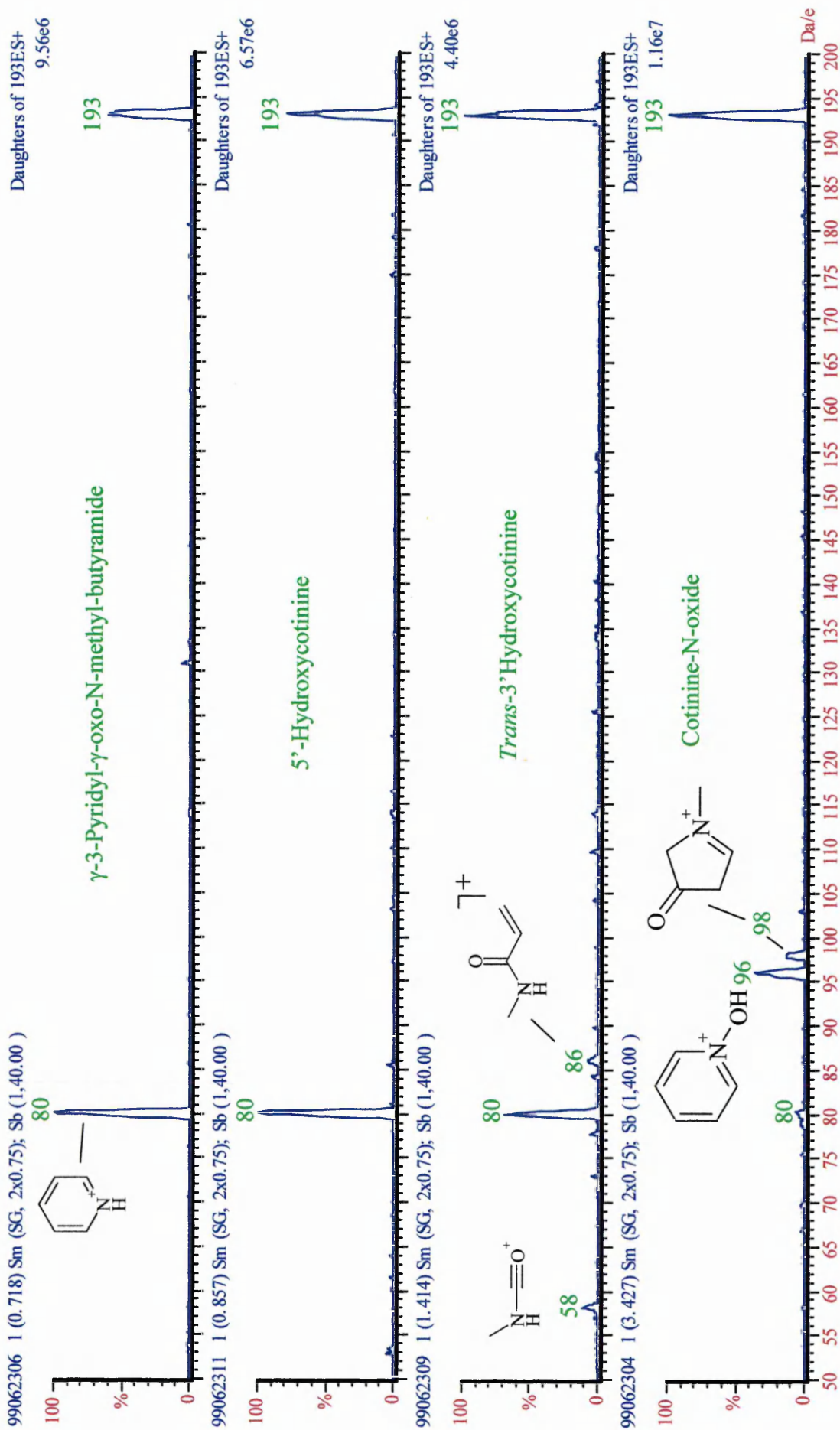


Figure 7.11 Product Ion Spectra of Isobaric Species with Predicted Fragment Ion Structures

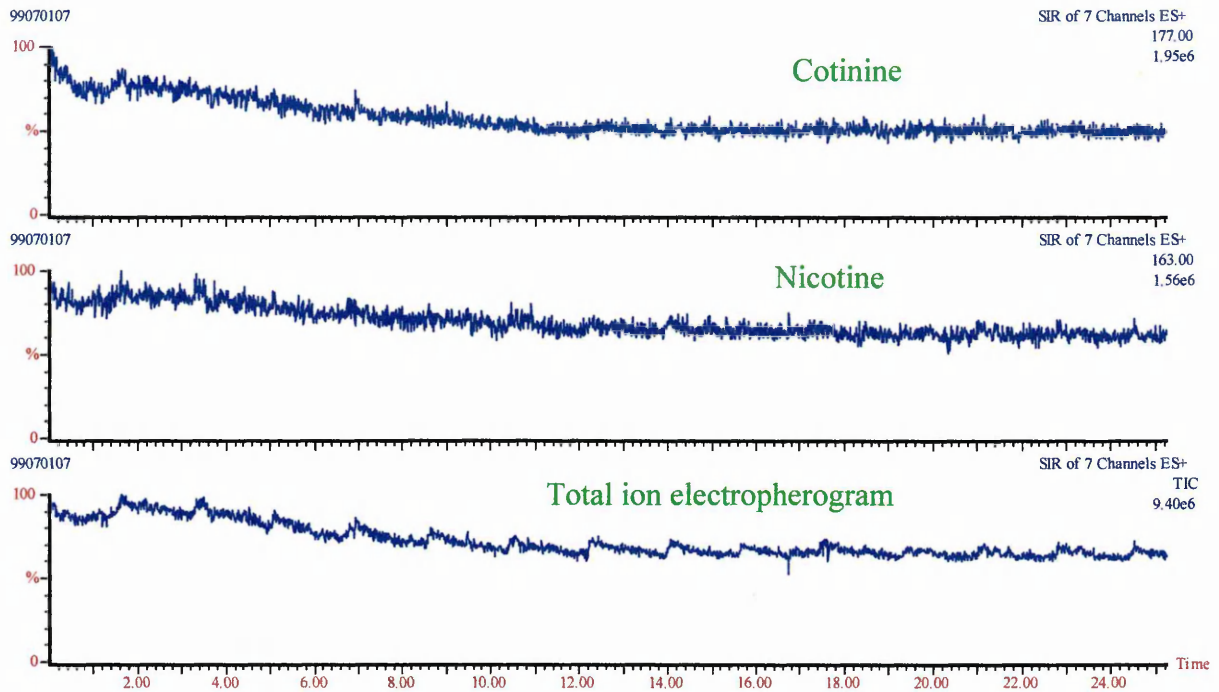


Figure 7.12 SIR Total Ion Electropherogram and Mass Electropherograms of Neat Smokers Urine

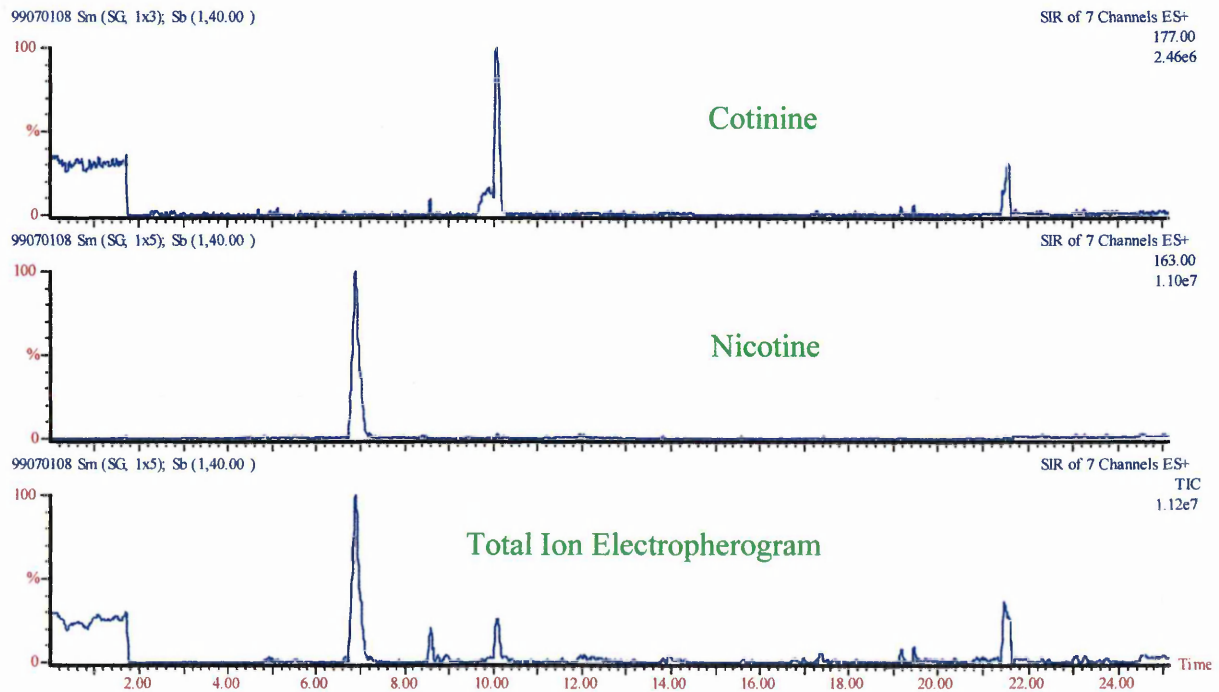


Figure 7.13 SIR Total Ion Electropherogram and Nicotine and Cotinine Mass Electropherograms of 100 µg/mL Spiked Urine

## ***7.5 Conclusions***

A CZE separation of nicotine and its metabolites has been developed that allows the detection of 10 out of 11 analytes. Two analytes co-migrated under these conditions, however, these species are in equilibrium, which could potentially be affected by pH, therefore producing only one analyte structure. Further investigation would be necessary to determine which isomer is dominant at this pH. This could be achieved through structural analysis by tandem mass spectrometry (product ion scan) employing an infusion of the analyte at different pH values.

The separation has been successfully transferred to mass spectral detection and data has been obtained in full scan and selected ion recording modes. Approximately 450 pg of each analyte was consumed generating the mass spectral data.

Nicotine and cotinine were successfully detected in a spiked urine sample without any matrix interferences employing SIR data acquisition. However, further orders of magnitude in sensitivity would be required to detect these analytes in non-spiked biological samples. To achieve this, sample preconcentration would be required prior to the separation. This could be accomplished by either solid phase extraction of the analytes or a transient-isotachophoretic stage during sample injection.

The metabolites contain two groups of isobaric species. One pair of isobaric species could be electrophoretically resolved, whereas the others were investigated employing MS/MS and in-source fragmentation (at elevated cone voltages), these analyses have led to the assignment of structural-specific product ions. Based on these ions a multiple reaction monitoring analysis could be used for quantification purposes.

## References

---

- (1) Doll R; Peto R; Wheatley K; Gray R; Sutherland I. *British Medical Journal* **309** (1994) 901
- (2) Barlow RD; Thompson PA; Stone RB. *Journal of Chromatography* **419** (1987) 375
- (3) Rop PP; Grimaldi F; Oddoze C; Viala A. *Journal of Chromatography* **612** (1993) 302
- (4) Zuccaro P; Altieri I; Rosa M; Passa AR; Pichini S; Ricciarello G; Pacifici R; *Journal of Chromatography* **621** (1993) 257
- (5) Pacifici R; Pichini S; Altieri I; Rosa M; Bacosi A; Caronna A; Zuccaro P. *Journal of Chromatography* **612** (1993) 209
- (6) Jacob P; Wilson M; Benowitz NL. *Journal of Chromatography* **222** (1981) 61
- (7) Langone JJ; Gjika HB; Van-Vunakis H. *Biochemistry* **12** (1973) 5025
- (8) Knight GJ; Wylie P; Holman MS; Haddow JE. *Clinical Chemistry* **31** (1985) 118
- (9) Abad A; Manclús JJ; March C; Montoya A. *Analytical Chemistry* **65** (1993) 3227
- (10) Smith RF; Mather H; Ellard GA. *Clinical Chemistry* **44** (1998) 275
- (11) Ralapati S. *Journal of Chromatography B* **695** (1997) 117
- (12) Yang SS; Smetena I; Goldsmith AI. *Journal of Chromatography A* **746** (1996) 131
- (13) Yang SS; Smetena I. *Chromatographia* **40** (1995) 375
- (14) Matysik F-M. *Journal of Chromatography A* **853** (1999) 27
- (15) Benowitz NL; Jacob P; Fong I; Gupta S. *Journal of Pharmacology and Experimental Therapeutics* **268** (1994) 296
- (16) Personal communication with Adrian King, SHU
- (17) Sample R. Seminar, Interfacing MS Detection with Capillary Electrophoresis, CE Method Development Seminar, Hewlett-Packard, Cheadle 21st June 1999
- (18) Lambert WJ; Middleton DI. *Analytical Chemistry* **62** (1990) 1585

## **Chapter 8**

### ***Conclusions***

## 8.1 Conclusions

The aims of this thesis were to develop a CZE/MS interface for our instrumentation and then to apply the interface to novel application areas.

ESI has been demonstrated on numerous occasions to be the most suitable ionisation interface for CZE/MS. However, an electrospray (ESI) interface was not initially available for our mass spectrometer, therefore we attempted to develop an ESI interface in-house. Conversion of commercial thermospray (TSP) sources for operation in ESI mode have been cited in the literature employing two distinct methodologies, an in-line and orthogonal entry system. The in-line system would be difficult to construct, whereas orthogonal entry was simple and cheap to implement. A Trio3 TSP source was successfully modified to operate as an ESI interface, with comparable sensitivity to other home built systems. Data was obtained on a low-mass pharmaceutical product and multiply charged proteins (up to 66 kDa for bovine serum albumin). Unfortunately the interface did not prove to be robust and the transfer capillary was easily blocked, further developments to remedy this were not successful. However, a commercially available electrospray instrument (Quattro I) was obtained and used for all further investigations.

A capillary zone electrophoresis separation of cimetidine and related impurities has been developed off-line using UV detection. The off-line separation employed a phosphate buffer system, which had to be substituted with ammonium acetate, owing to the involatile inorganic buffer would lead to source contamination, which would thus require regular cleaning. The conditions developed could successfully separate six analytes (two analytes proved to be insoluble in an aqueous phase and two co-migrated) in less than ten minutes with high efficiencies. Various separation parameters (buffer strength and pH, addition of organic modifier, temperature) were investigated to improve the resolution of two closely migrating analytes.

Mass spectral interfaces for CZE/MS fall into three major categories, co-axial sheath flow, liquid junction and nanospray, owing to instrumental constraints (*i.e.* the Quattro I MS employs a ~ 40 cm probe for ESI) only co-axial and nanospray systems could be investigated.

The ammonium acetate separation conditions for cimetidine were then applied to a home-built co-axial sheath flow CZE/MS interface. The separation integrity was maintained employing mass spectral detection rather than UV. The increased column length required for CZE/MS resulted in reduced efficiency and thus resolution. However, the mass discrimination power allowed resolution on a mass basis. As a further development, a nanospray CZE/MS interface employing drawn gold-coated fused silica tips was developed. A significant change in selectivity was observed utilising nanospray *cf.* co-axial interface, owing to the significant addition of organic modifier to the buffer (as recommended in the literature). The purpose of the organic modifier was to reduce the surface tension of the buffer and thus allow successful desolvation during the nanospray process.

The standard separation for cimetidine and related impurities was then applied to a time-of-flight (ToF) mass spectrometer operated at enhanced resolution. The instrumentation used allowed the analysis to be conducted under the original conditions (*i.e.* phosphate buffer) without significant source contamination. This resulted in the on-line accurate-mass determination of the analytes as they eluted from the capillary. Mass accuracies of less than 8 ppm were obtained for all analytes (where  $n = 15$ ). This investigation also demonstrated that ToF MS is the most suitable mass spectrometer for CZE detection, reducing the possibility of peak skew, owing to the inherent fast data acquisition times and high sensitivity over quadrupoles.

The purpose of the sheath liquid in a co-axial interface is to increase the bulk flow of liquid to a suitable rate for electrospray ionisation. Therefore, there is the possibility that the sheath liquid could be potentially used to chemically modify the analytes as they migrate from the capillary. This process has already been successfully applied to the sheath flow cuvette for fluorescence detection. Thus reactions that occur on a fast time scale could be employed to investigate the chemical structure / nature of the analytes on-line. Hydrogen / deuterium exchange is a rapid process that results in an equilibrium, the position of which is determined by the relative acidity of the analyte and the proportion of the H and D in the matrix. The standard CZE/MS separation conditions (ammonium acetate) for cimetidine and impurities were employed with a sheath liquid comprising D<sub>2</sub>O. The analytes exhibited exchange. Only one analyte was fully exchanged, with the others demonstrating various degrees of exchange, thus indicating

that the protons are non-equivalent or there is a rate limitation imposed by the CZE/MS interface. To simplify interpretation it would be advantageous to be able to perform analyses with a completely deuterated system, however this could not be achieved owing to possible connectivity problems within the interface preventing the migration of analytes within the capillary. Thus the sheath liquid has successfully been employed to chemically alter the analytes as they migrated from the column, therefore, other fast reactions could be utilised to determine functional groups or for structural confirmation.

As a further application of the CZE/MS interface, a separation of nicotine and its metabolites has been developed, which employs an ammonium acetate buffer in an aqueous : organic (acetonitrile) medium. The separation of eleven metabolites was achieved in less than 35 minutes. However, two of the analytes co-migrated, the metabolic pathway shows these analytes to be in equilibrium, it is possible that the equilibrium could therefore be affected by pH. A spiked sample of urine was analysed and nicotine and cotinine were successfully detected, thus indicating that this method would be suitable for the analysis of biological samples.

## ***8.2 Overall Conclusions***

The development and implementation of a co-axial sheath flow interface for the coupling of capillary zone electrophoresis and mass spectrometry has been successfully demonstrated with the analysis of pharmaceutical compounds. In addition, a nanospray probe has been used to generate a sheathless interface. The co-axial interface has also been employed for post-column hydrogen / deuterium exchange allowing the study of active hydrogens within the analytes.

Overall this author considers that CZE/MS continues to demonstrate its suitability as a separation technique, however, it appears unlikely that it will supersede HPLC (or GC) and will remain a complementary technique, especially useful in sample limited situations.

This author suggests that the production of dedicated CZE/MS instrumentation would simplify the technique and thus increase the popularity. Current technology requires that

(capillary) column lengths have to be significantly increased (*cf.* CZE/UV) to overcome physical constraints, thus increasing analysis time and reducing efficiency. If integrated instruments or probe systems (such as that developed by Lane *et al.*<sup>1</sup>) were further developed an increase in interest and consequently published work would be observed, enhancing and improving the technique.

### **8.3 Future Work**

The aims of this research were to develop a suitable interface for CZE/MS and attempt to improve the robustness and routine use of existing interface techniques. During this research a number of interesting areas have been highlighted that require further investigation. These include additional optimisation of the CZE separation parameters and instrumentation employed, to increase both selectivity and sensitivity. Once fully optimised the analyses / procedures could be applied to 'real' samples (*i.e.* biological samples, drug substances *etc.*) and problems.

The use of reactive species in the sheath-flow for CZE/MS has been demonstrated. The development of a fully deuterated system (*i.e.* buffer and sheath-liquid and employing modifiers such as CD<sub>3</sub>CO<sub>2</sub>D *etc.*) would prove to be advantageous in the prediction of the number of active hydrogen within a compound, making interpretation of spectra more facile *cf.* partially exchanged species.

Thus, post-separation reactions are feasible employing reactive species in the sheath liquid, further investigation of other reactive species could now be undertaken. For example, a specific reaction could be employed as a screen for a class of compounds in a mixture.

A major area of research that has not been investigated in this research is CZE coupled to tandem mass spectrometry (*i.e.* MS/MS) owing to poor instrumental transmission / sensitivity. These type of experiments could be employed to solve problems that cannot be resolved by normal scanning techniques *i.e.* the generation of structure-specific product ions for the determination of isobaric species in the nicotine metabolite study and increasing sensitivity employing MRM analyses. The increased sensitivity obtained

employing MRM analyses could potentially allow on-line quantification by CZE/MS/MS.

A major drawback of this research is that it focuses on CZE, a technique that can only separate charged analytes (neutral species co-migrate). Capillary electrochromatography (CEC) is a hybrid of CZE and HPLC, combining advantages of both techniques. Although the use of CEC is becoming more widespread, it is still not a routine technique, with packing procedures and bubble formation generating most of the problems. To date, we have not been able to successfully implement CEC/MS on our instrumentation, mainly due to current (and hence flow) instabilities within the packing material primarily caused by bubble formation. This is perhaps one of the most important areas to be investigated in the interfacing of electroseparation methods with mass spectrometry. The development of routine CEC/MS will enable a whole host of analytes and problems to be investigated that are not amenable to CZE or where sample quantity or poor resolution prohibits the use of HPLC.

Perhaps the most innovative (and interesting) areas of research in interfacing CZE (and related techniques) to mass spectrometry is the use of nanospray. Various research groups have suggested numerous methodologies, the most common being drawn, gold-coated fused silica capillaries. The major limitations of these tips are their time consuming preparation, poor reproducibility and fragility. Derivatizing the capillary prior to coating has been demonstrated to be desirable, enhancing the lifetime of the tip, but as illustrated by this work, this can have deleterious consequences on the inner surface of the capillary. Constant flushing of the capillary with water during coating procedures could reduce these effects, generating a stable, useful tip. It would also be advantageous to investigate the effects of the buffer composition on both spray and separation stability, in an attempt to optimise and preserve the separation integrity (*cf.* CZE/UV) whilst employing nanospray CZE/MS.

### *References*

---

(1) Lane SJ; Boughtflower R; Paterson C; Morris M. *Rapid Communications in Mass Spectrometry* **10** (1996) 733

#### ***8.4 Major Symposia and Meetings Attended***

BMSS LC/MS Symposium, Robinson College, Cambridge. December 1997

23<sup>rd</sup> Annual BMSS Meeting, University of Warwick, Coventry. September 1998

15<sup>th</sup> Montreux Symposium on Liquid Chromatography / Mass Spectrometry, Montroux, Switzerland. November 1998\*

24<sup>th</sup> Annual BMSS Meeting, Reading University, Reading. September 1999†

#### ***8.5 Publications***

(1) Ellis DR; Palmer ME; Tetler LW; Eckers C. *Journal of Chromatography A* **808** (1998) 269

‘Separation of Cimetidine and Related Materials by Aqueous and Non-aqueous Capillary Electrophoresis’

(2) Palmer ME; Clench MR; Tetler LW; Little DR. *Rapid Communications in Mass Spectrometry* **13** (1999) 256

‘Exact Mass Determination of Narrow Electrophoretic Peaks Using an Orthogonal-Acceleration Time-of-Flight Mass Spectrometer’

(3) Palmer ME; Tetler LW; Wilson ID. *Rapid Communications in Mass Spectrometry* **14** (2000) 808

‘Hydrogen / Deuterium Exchange using a Co-axial Sheath Flow Interface for Capillary Electrophoresis / Mass Spectrometry’

(4) Chambers K; Palmer ME; Smith RF; Tetler LW. In preparation.

‘Separation of Nicotine Metabolites by Capillary Zone Electrophoresis and Capillary Zone Electrophoresis / Mass Spectrometry’

---

\* Oral presentation: ‘Exact Mass Determination of Narrow Electrophoretic Peaks Using an Orthogonal-Acceleration Time-of-Flight Mass Spectrometer’

† Oral presentation: ‘Separation of Nicotine Metabolites by CZE/MS’